Investigating Functions of Human Group 2 Innate Lymphoid Cells in Health and Disease



Janina Nahler

Wadham College

A thesis submitted for the degree of

Doctor of Philosophy in Medical Sciences

Trinity Term 2021

Abstract

Group 2 innate lymphoid cells (ILC2) have emerged as important effectors of type 2 immune responses that contribute to protection against extracellular parasites and tissue repair. Dysregulated ILC2 responses have been implicated in allergic inflammatory disorders such as atopic dermatitis (AD), a chronic inflammatory skin disease associated with epidermal barrier defects and dysregulated type 2 inflammation. However, much remains to be understood regarding ILC2 effector functions, especially in the context of cutaneous inflammation.

Using an *in vivo* human skin blister model, extensive multianalyte profiling revealed significant differences in the protein expression profile of healthy and AD skin; and skin ILC2 were found to express a range of cytokine- and chemokine-encoding genes following intradermal allergen challenge. *In vitro* experiments confirmed secretion of a broad range of cytokines and chemokines, including granulocyte-macrophage colony-stimulating factor (GM-CSF) and the chemokines CCL22 and CCL17, by human ILC2 in response to activation by alarmin cytokines. Elevated levels of CCL22 and CCL17 were detected in both sera and skin blister fluids from individuals with AD compared to healthy controls, and increased surface expression of CCR4, the shared receptor for CCL22 and CCL17, was detected on blood ILC2 and T cells from individuals with AD. *In vitro,* ILC2 were found to promote recruitment of both ILC2 and T cells, directly and indirectly through induction of monocyte-derived dendritic cell (moDC) chemokine production, involving CCL22 and CCL17. Thus, ILC2 may contribute to AD pathogenesis by promoting the accumulation of $CCR4^+$ ILC2 and Th2 cells. Moreover, through GM-CSF secretion, human ILC2 were identified as inducers of monocyte differentiation into $CD1a^+$ moDC, resembling *in vivo* inflammatory moDC. ILC2-induced moDC were capable of activating CD1a-reactive T cells, resident in healthy skin and increased in abundance in AD skin.

Taken together, this study identified previously unrecognised roles of human ILC2 in the chemotactic recruitment of ILC2 and T cells and as inducers of moDC differentiation with implications for cutaneous inflammation.

Acknowledgments

The work of this thesis was made possible because of the guidance and support from many people who I would like to thank.

Firstly, I would like to express my deepest gratitude and appreciation to my supervisors Prof Graham Ogg and Dr Clare Hardman. I feel extremely fortunate to have had you as my supervisors and mentors, supporting, guiding and encouraging me at every step of my DPhil. Graham, thank you for always making time for me, supporting me and my academic career and importantly for sharing your enthusiasm for science with me. Every single meeting with you has made me feel more motivated and excited to continue with my research. Clare, I am endlessly appreciative of your scientific as well as personal support over the years. Over 4 years ago, you took me under your wings and provided me with the initial “wet” lab training. Since then, you have become a wonderful colleague and friend.

I would also like to thank other members of the lab, especially Dr Yi-Ling Chen, Dr Jeongmin Woo and Lea Nussbaum. Yi-Ling, thank you for sharing your vast scientific knowledge and your precious clones with me, for your continuously helpful advice and, on a personal note, your support and friendship. Thank you, Yi-Ling and Clare, for welcoming me into the ILC team and teaching me the ins and outs of growing our precious ILC2. Next, I would like to acknowledge Jeongmin for her immense help with the bioinformatic analysis. Lea, thank you for being a lovely colleague and friend, always checking up on me especially during the first lockdown and the thesis writing phase. I would also like to acknowledge Prof Luzheng Xue for his valuable scientific input, especially in regard to the chemotaxis assays.

I would like to extend my thanks to the WIMM flow cytometry facility staff, in particular Craig Waugh for his assistance with the ILC2 sorts; to the WIMM community for providing a research environment that encourages intellectual discussion and interlaboratory collaboration; to the MRC as my primary funding source and providing me with supplementary grants for conferences and training to further my academic career; to the Churchill Hospital Dermatology Department research nurses, and importantly to all the suction blister, skin and blood donors for generously donating samples for my research.

Special thanks go to my amazing friends in and out of Oxford. To my friends in Oxford, thanks for keeping me sane and making my experience here so special: Merve, Lucy, Hayley, Henry, Caitlin, Ed, Arthad and the Cat lovers – James, Miri, Maria, Miles, Eloise and Daan. I am immensely grateful for my long-distance friendships with Rachael and Steph – our several hour-long facetime/skype calls always put me in the best mood.

Finally, I would like to thank my wonderful boyfriend Tobias Schillings and my amazing family for always being there for me and believing in me. Thank you, Tobi, for your love, for being my rock, for always being so positive and passionate and importantly making the everyday life special. Thank you to my family for your unconditional love, for being my biggest supporters, and especially to my sister Caro for always making me laugh.

Table of Contents

List of Figures……...12

List of Tables……...16

List of Abbreviations……...17

Chapter 1: Introduction 21

1.1 Introduction to the immune system 21

1.1.1 First line of defence: the skin 21

1.1.2 Myeloid and lymphoid lineages of immune cells 23

1.1.3 Innate immunity 24

1.1.3.1 Dendritic cells 25

1.1.4 Adaptive immunity 26

1.1.4.1 T cells 26

1.2 Type 2 immunity 29

1.2.1 Initiation of type 2 immune responses by the epithelium 29

1.2.2 Type 2 immune effector cells 31

1.3 Innate lymphoid cells 34

1.3.1 ILC subsets 35

1.3.2 ILC development 37

1.3.3 ILC tissue residency and chemotaxis 39

1.3.4 Plasticity of ILC subsets 41

1.4 Group 2 innate lymphoid cells 41

1.4.1 Regulation of ILC2 activity 42

1.4.1.1 Signals stimulating ILC2 activity 42

1.4.1.1.1 IL-33, IL-25 and TSLP 43

1.4.1.1.2 Lipid mediators 44

1.4.1.1.3 Neuropeptides 45

1.4.1.1.4 Cell-to-cell interactions 45

1.4.1.2 Signals inhibiting ILC2 activity 46

1.4.1.2.1 Suppressive cytokines 47

1.4.1.2.2 Lipid mediators 48
1.4.1.2.3 Cell-to-cell interactions 49
1.4.2 Role of ILC2 in immune defence, maintenance of tissue homeostasis and allergic inflammation 49
1.4.2.1 Role of ILC2 in the defence against parasitic worms 50
1.4.2.2 Role of ILC2 in tissue repair 52
1.4.2.3 Role of ILC2 in the maintenance of skin homeostasis 53
1.4.2.4 Role of ILC2 in allergic inflammation 54
1.5 Overall aims 55
Chapter 2: Methods and Materials 57
2.1 Patients and samples 57
2.2 Skin suction blister technique 57
2.3 Cell isolation and culture 58
2.3.1 Peripheral blood mononuclear cell (PBMC) isolation 58
2.3.2 Mononuclear cell isolation from human skin biopsies 58
2.3.3 Magnetic-activated cell sorting (MACS) 59
2.3.4 ILC2 sorting and culture 60
2.3.5 T cell sorting and culture 60
2.3.6 CD1a-reactive T cell clones sorting and culture 61
2.3.7 MoDC differentiation 61
2.3.8 Cell counting 62
2.4 Antibodies and reagents 62
2.4.1 Antibodies for FACS and flow cytometry analysis 62
2.4.1.1 Antibodies for ILC2 sorting and flow cytometry analysis 62
2.4.1.2 Antibodies for $CCR4^+$ and $CCR4^-$ T cell sorting 63
2.4.1.3 Antibodies for flow cytometry analysis of CCR4 expression 63
2.4.1.4 Antibodies for flow cytometry analysis of monocyte/moDC cell surface marker expression 63
2.4.1.5 Antibodies for flow cytometry analysis of CD1a-reactive T cell clones .64

2.4.2 Recombinant proteins....64
2.4.3 Buffers and cell culture media....65
2.5 Analysis of gene expression....66
2.5.1 RNA-sequencing....66
2.5.2 Real-time quantitative reverse transcription PCR (qRT-PCR)....66
2.6 Analysis of protein expression....67
2.6.1 SOMAscan assay....67
2.6.2 Luminex multiplex assay....67
2.6.3 Enzyme-linked immunosorbent assay (ELISA)....68
2.6.4 FACS and flow cytometry....69
2.6.4.1 FACS....69
2.6.4.2 Flow cytometry....69
2.7 Stimulation of primary immune cells....69
2.7.1 Stimulation of ILC2....69
2.7.2 MoDC culture in ILC2 supernatants....70
2.7.3 Monocyte culture in ILC2 supernatants....70
2.8 Chemotaxis assay....71
2.8.1 Titration studies....71
2.8.2 ILC2 and T cell chemotaxis to recombinant proteins....72
2.8.3 ILC2 or T cell chemotaxis to ILC2 supernatants....72
2.8.4 ILC2 chemotaxis to moDC supernatants....72
2.9 Co-culture of ILC2-induced moDC and CD1a-reactive T cell clones....73
2.10 Bioinformatic analysis....73
2.11 Statistical analysis....74
2.12 Illustrations....74
Chapter 3: Investigation of cutaneous and systemic immune responses in AD and the potential contribution of ILC2....75
3.1 Introduction....75
3.1.1 Cytokines....75

3.1.2 Chemokines 75
3.1.3 The pathogenesis of AD 77
3.1.3.1 Role of dysfunctional skin barrier in AD pathogenesis 77
3.1.3.2 Role of dysregulated immune responses in AD pathogenesis 78
3.1.4 Role of ILC2 in AD inflammation 80
3.1.5 Hypothesis and aims 81
3.2 Results 84
3.2.1 Comparison of the protein signature of healthy and AD skin 84
3.2.1.1 SOMAscan analysis of the skin proteome of individuals with AD and healthy volunteers 84
3.2.1.1.1 Study design and participants 84
3.2.1.1.2 Comparison of healthy, atopic asymptomatic and AD cutaneous protein expression profiles 86
3.2.1.1.3 Investigation of factors responsible for separate clustering of AD_1 and AD_2 blister fluid SOMAscan data 90
3.2.1.1.4 Effect of intradermal allergen challenge on cutaneous protein expression 92
3.2.1.1.5 Comparison of cytokine and chemokine expression in healthy and AD skin 93
3.2.1.2 Luminex multianalyte profiling of chemokine and cytokine levels in healthy and AD skin 96
3.2.1.2.1 Analysis of overall cutaneous cytokine/chemokine profiles 96
3.2.1.2.2 Analysis of skin-specific cytokine levels during sterile allergic skin inflammation 99
3.2.1.2.3 Analysis of skin-specific chemokines levels during sterile allergic skin inflammation 100
3.2.2 Analysis of serum cytokine and chemokine profiles of individuals with AD and healthy volunteers 102
3.2.2.1 Differences in the overall serum cytokine/chemokine expression patterns 102
3.2.2.2 Analysis of pro-inflammatory serum cytokine levels 103

3.2.2.3 Analysis of serum chemokine levels 105
3.2.2.4 Serum chemokine levels as predictors of AD.....107
3.2.3 Tissue-specific chemokine and cytokine profiles.....109
3.2.4 Potential contribution of ILC2 in cutaneous inflammation.....110
3.2.4.1 RNA-sequencing analysis of cutaneous human ILC2 upon *in vivo* allergen challenge 110
3.2.4.2 Isolation and expansion of human ILC2.....114
3.2.4.3 Investigation of cytokine and chemokine production by activated human ILC2……116
3.2.4.4 Analysis of cytokine and chemokine levels secreted by stimulated human ILC2 122
3.3 Discussion 128
3.3.1 AD skin shows an altered proteome signature in an *in vivo* human skin blister model 128
3.3.2 AD patients are characterised by an altered systemic cytokine and chemokine signature with CCL17, CCL22 and CCL27 positively correlating with disease severity.....131
3.3.3 Human ILC2 may perform functions beyond their role as potent type 2 cytokine producers with implications for allergic inflammation.....133
Chapter 4: ILC2 amplify type 2 immune responses by promoting the recruitment of CCR4$^+$ ILC2 and T cells.....139
4.1 Introduction.....139
4.1.1 Regulation of T cell homing 139
4.1.2 Role of CCL22 and CCL17 in the recruitment of CCR4$^+$ T cells.....141
4.1.3 Role of CCR4 and its chemokine ligands in the maintenance of skin homeostasis 142
4.1.4 Role of CCR4 and its chemokine ligands in AD pathogenesis 143
4.1.5 ILC2 homing 144
4.1.6 Hypothesis and aims 145
4.2 Results 147
4.2.1 CCL22 and CCL17 expression by human ILC2 147

4.2.1.1 Transcriptional expression of *CCL22* and *CCL17* in human ILC2 147
4.2.1.2 CCL22 and CCL17 secretion by human ILC2 148
4.2.1.3 CCL22 and CCL17 secretion by skin ILC2.....149
4.2.1.4 CCL22 and CCL17 secretion by ILC2 from individuals with AD 152
4.2.2 ILC2 promote moDC CCL22 and CCL17 production.....153
4.2.3 CCR4 expression on human ILC2 156
4.2.3.1 Comparison of CCR4 expression on *ex vivo* blood and skin ILC2 and T cells from healthy donors and individuals with AD 156
4.2.3.2 CCR4 expression on *in vitro* cultured ILC2 159
4.2.3.3 CCR4 downregulation by CCL22 and CCL17 160
4.2.3.4 Activation-induced upregulation of surface CCR4 on human ILC2.....163
4.2.4 Chemotactic responsiveness of $CCR4^{+}$ ILC2 and ILC2-mediated recruitment of ILC2 and T cells.....166
4.2.4.1 Optimisation of *in vitro* chemotaxis assay 166
4.2.4.2 Chemotactic recruitment of *ex vivo* T cells to skin-tissue levels of CCL22 and CCL17.....170
4.2.4.3 Recruitment of T cells by ILC2-derived CCL22 and CCL17 172
4.2.4.4 ILC2 chemotaxis to CCL22 and CCL17 173
4.2.4.5 ILC2 can induce ILC2 recruitment indirectly through induction of chemokine production by moDC.....176
4.3 Discussion 178
4.3.1 Human ILC2 produce the chemokines CCL22 and CCL17 178
4.3.2 ILC2 express functional CCR4 that enables ILC2 homing to CCL22 and CCL17……180
4.3.3 ILC2 promote recruitment of ILC2 and T cells.....183
4.3.4 Functional implications of ILC2-mediated chemotaxis in homeostasis and inflammation 185
Chapter 5: ILC2 orchestrate innate and adaptive immune responses 188
5.1 Introduction.....188
5.1.1 Role of ILC2 in the induction of adaptive immune responses.....188

5.1.2 Monocyte-derived dendritic cells....189
5.1.2.1 *In vitro* differentiated monocyte-derived dendritic cells....189
5.1.2.2 *In vivo* monocyte-derived dendritic cells....189
5.1.3 CD1a and the activation of CD1a-restricted T cells....190
5.1.4 Hypothesis and aims....192
5.2 Results....193
5.2.1 Effect of ILC2 on fully differentiated moDC....193
5.2.1.1 Effect of ILC2 on the survival and phenotype of fully differentiated moDC....193
5.2.1.2 Effect of ILC2 on the surface expression of CD1a on fully differentiated moDC....196
5.2.1.3 Effect of ILC2 on the surface expression of DC-SIGN on fully differentiated moDC....197
5.2.2 Effect of ILC2 on the differentiation process of moDC....199
5.2.2.1 Effect of ILC2 on the survival of differentiating moDC....199
5.2.2.2 Effect of ILC2 on the expression of CD1a on differentiating moDC....202
5.2.2.3 Effect of ILC2 on the expression of DC-SIGN on differentiating moDC....203
5.2.2.4 Effect of ILC2 on the expression of MHC and co-stimulatory molecules on differentiating moDC....205
5.2.3 Effect of ILC2 on the survival and phenotype of ex vivo monocytes....207
5.2.3.1 Effect of ILC2 on the survival of monocytes/monocyte-derived cells....207
5.2.3.2 Expression of CD1 molecules on ILC2-induced moDC....210
5.2.3.3 Expression of DC-SIGN on ILC2-induced moDC....212
5.2.3.4 Expression of MHC and co-stimulatory molecules on ILC2-induced moDC....213
5.2.4 Identification of ILC2-secretory factors that contribute to the induction of moDC differentiation....215
5.2.4.1 IL-4 and GM-CSF production by ILC2....215
5.2.4.2 Contribution of ILC2-secreted IL-4 and GM-CSF to the induction of moDC differentiation....216

5.2.4.3 Contribution of ILC2-secreted IL-4 and GM-CSF to the upregulation of CD1a on ILC2-induced moDC 218

5.2.4.4 Contribution of ILC2-secreted IL-4 and GM-CSF to the upregulation of DC-SIGN on ILC2-induced moDC 220

5.2.4.5 Contribution of ILC2-secreted IL-4 and GM-CSF to the expression of CD1b and CD1c on ILC2-induced moDC 221

5.2.4.6 Contribution of ILC2-secreted IL-4 and GM-CSF to the expression of MHC molecules and CD86 on ILC2-induced moDC 223

5.2.5 Lipid antigen presenting capacity of $CD1a^+$ ILC2-induced moDC 225

5.3 Discussion 228

5.3.1 ILC2 support the survival and differentiation of moDC 228

5.3.2 ILC2 induce the differentiation of monocytes into functional moDC 229

5.3.3 Functional implications of ILC2-induced moDC differentiation 232

Chapter 6: Final Discussion and Future Directions 236

6.1 Main findings and functional implications 236

6.2 Final conclusion and future directions 241

References 243

Appendix 283

List of Figures

Figure 1.1 Structure and immune cell composition of healthy skin. 23
Figure 1.2 Developmental pathways of myeloid and lymphoid lineages. 24
Figure 1.3 Helper T cell differentiation. 28
Figure 1.4 Type 2 immunity. 34
Figure 1.5 ILC subsets resemble T helper cell lineages. 36
Figure 1.6 Progressive differentiation of cytotoxic and helper ILC. 39
Figure 1.7 Ligand-receptor interactions stimulating ILC2 activity. 43
Figure 1.8 Ligand-receptor interactions inhibiting ILC2 activity. 47
Figure 1.9 Central role of ILC2 in type 2 immunity. 50
Figure 3.1 Study design. 83
Figure 3.2 Distribution of skin blister fluid SOMAscan data. 85
Figure 3.3 Two-dimensional PCA of SOMAscan skin proteomic data. 87
Figure 3.4 Comparison of proteomic data of HC, AA and AD skin. 89
Figure 3.5 Comparison of AD_1 vs AD_2 clusters. 91
Figure 3.6 Comparison of protein expression profiles of HC, AA and AD skin following intradermal allergen challenge. 93
Figure 3.7 Comparison of chemokine and cytokine expression profiles in HC, AD and AA skin. 95
Figure 3.8 Overall comparison of Luminex cytokine/chemokine expression data of HC, AA and AD skin blister fluids. 98
Figure 3.9 Cytokine levels in HC and AD skin blister fluids following intradermal allergen challenge. 100
Figure 3.10 Chemokine levels in HC and AD skin blister fluids following intradermal allergen challenge. 101
Figure 3.11 Comparison of cytokine/chemokine expression profiles of HC and AD sera. 103
Figure 3.12 Levels of pro-inflammatory cytokines in HC and AD sera. 104
Figure 3.13 Levels of chemokines in HC and AD sera. 106
Figure 3.14 Analysis of serum chemokine levels as predictors of AD. 108
Figure 3.15 Analysis of cutaneous and serum cytokine/chemokine profiles. 110
Figure 3.16 RNA-sequencing analysis of human ILC2 and T cells. 113
Figure 3.17 Human ILC2 isolation and *in vitro* expansion. 115
Figure 3.18 Two-dimensional PCA of cytokine/chemokine expression profiles of human ILC2. 117

Figure 3.19 Cytokine/chemokine expression profile of human ILC2 following stimulation. 119
Figure 3.20 Cytokine/chemokine expression profile of human AD ILC2. 121
Figure 3.21 ILC2 cytokine and chemokine production in response to alarmin stimulants. 123
Figure 3.22 ILC2 cytokine production in response to stimulation with IL-33, IL-25 and TSLP. 125
Figure 3.23 ILC2 chemokine production in response to stimulation with IL-33, IL-25 and TSLP. 127
Figure 3.24 Potential contribution of ILC2 to protective immunity and allergic inflammation through cytokine- and chemokine-mediated mechanisms. 138
Figure 4.1 T cell homing is regulated by chemokine receptors and their ligands. 140
Figure 4.2 *CCL22*, *CCL17* and *CCR4* expression in ILC2 and T cells upon *in vivo* allergen challenge. 147
Figure 4.3 *CCL22* and *CCL17* mRNA expression in human ILC2. 148
Figure 4.4 CCL22 and CCL17 secretion by human ILC2. 149
Figure 4.5 Comparison of CCL22 and CCL17 secretion by skin- and blood-derived ILC2. 151
Figure 4.6 Comparison of CCL22 and CCL17 secretion by HC- and AD-derived ILC2...153
Figure 4.7 ILC2-induced secretion of CCL22 and CCL17 by moDC. 155
Figure 4.8 CCR4 surface expression on *ex vivo* human ILC2 and T cells. 158
Figure 4.9 CCR4 expression on *in vitro* cultured ILC2.....160
Figure 4.10 Analysis of CCL22- and CCL17-mediated downregulation of surface CCR4 on ILC2 and T cells. 162
Figure 4.11 Regulation of CCR4 surface expression on ILC2 by alarmins. 165
Figure 4.12 Migration of $CCR4^+$ T cells to recombinant CCL22 and CCL17. 168
Figure 4.13 Inhibition of CCR4-mediated T cell chemotaxis. 170
Figure 4.14 Migration of T cells to skin-tissue levels of CCL22 and CCL17. 171
Figure 4.15 Migration of T cells to ILC2 supernatants. 173
Figure 4.16 ILC2 migration to skin-tissue levels of CCL22 and CCL17 and to ILC2 supernatants. 175
Figure 4.17 Migration of ILC2 to ILC2-treated moDC supernatants. 177
Figure 4.18 Potential role of ILC2 in the recruitment of ILC2 and T cells during homeostasis and inflammation. 187
Figure 5.1 Experimental design – effect of ILC2 supernatants on fully differentiated moDC. 193

Figure 5.2 Effect of ILC2 supernatants on the survival and phenotype of moDC.....195
Figure 5.3 Effect of ILC2 supernatants on the expression of CD1a on moDC. 196
Figure 5.4 Effect of ILC2 supernatants on the expression of DC-SIGN on moDC. 198
Figure 5.5 Experimental design – effect of ILC2 supernatants on the differentiation process of moDC. 199
Figure 5.6 Survival of moDC following treatment with ILC2 supernatants during differentiation. 201
Figure 5.7 Expression of CD1a on moDC following treatment with ILC2 supernatants during differentiation. 203
Figure 5.8 Expression of DC-SIGN on moDC following culture in ILC2 supernatants during differentiation. 204
Figure 5.9 Expression of MHC and co-stimulatory molecules on moDC following culture in ILC2 supernatants during differentiation.....206
Figure 5.10 Experimental design – effect of ILC2 supernatants on monocytes. 207
Figure 5.11 ILC2 supernatants induce differentiation of monocytes into moDC.....209
Figure 5.12 Expression of CD1 molecules on ILC2-induced moDC. 211
Figure 5.13 DC-SIGN expression on ILC2-induced moDC.....212
Figure 5.14 Expression of MHC and co-stimulatory molecules on ILC2-induced moDC.214
Figure 5.15 ILC2 upregulate IL-4 and GM-CSF secretion following stimulation with alarmin cytokines.....215
Figure 5.16 Experimental design – testing the contribution of ILC2-secreted IL-4 and GM-CSF on the induction of moDC differentiation. 216
Figure 5.17 ILC2-derived GM-CSF contributes to the induction of moDC differentiation. 218
Figure 5.18 ILC2-derived GM-CSF contributes to the upregulation of CD1a on ILC2-induced moDC. 219
Figure 5.19 ILC2-derived GM-CSF contributes to the upregulation of DC-SIGN on ILC2-induced moDC. 221
Figure 5.20 ILC2-derived GM-CSF contributes to the induction of CD1b and CD1c on ILC2-induced moDC. 222
Figure 5.21 Contribution of ILC2-derived IL-4 and GM-CSF to the expression of MHC and CD86 on ILC2-induced moDC. 224
Figure 5.22 Activation of CD1a-restricted T cell clones by ILC2-induced moDC. 226
Figure 5.23 Proposed mechanism of ILC2-mediated moDC differentiation at barrier sites and its contribution to homeostasis and inflammation. 235
Figure 6.1 Proposed model of ILC2 involvement in AD skin inflammation. 240

Figure A.1 FMO controls for gating strategy of ILC2 analysis……283
Figure A.2 FMO controls for gating strategy of moDC analysis…… 284
Figure A.3 Luminex data distribution……285
Figure A.4 Comparison of cutaneous protein expression profiles of AD and HC subjects following intradermal allergen challenge measured by SOMAscan and Luminex……...286
Figure A.5 Posterior distribution of multivariate logistic regression model……288
Figure A.6 Effect of ILC2 stimulants on the phenotype on moDC……..289
Figure A.7 Effect of ILC2 stimulants on the differentiation process of moDC……...290
Figure A.8 Effect of ILC2 stimulants on monocytes……291
Figure A.9 CD80 expression on ILC2-induced moDC……292
Figure A.10 IFN-γ levels in ILC2-induced moDC……..293

List of Tables

Table 1 ILC2 antibody panel. 62
Table 2 MoDC antibody panel.....64
Table 3 Recombinant proteins 64
Table 4 Buffers and media.....65
Table 5 Chemokine receptors and their cognate ligands and target cells.....76
Table 6 Study participants 84

Table A.1 Skin suction blister fluids analysed by Luminex multianalyte profiling…….287

List of Abbreviations

AA	Atopic asymptomatic
AAM	Alternatively activated macrophage
AD	Atopic dermatitis
Adj	Adjusted
AHR	Airway hyperreactivity
AHR	Aryl hydrocarbon receptor
ALT	Alternaria alternata
ALX	Lipoxin A4 receptor
APC	Antigen presenting cell
ATP	Adenosine triphosphate
AUC	Area under the curve/ Accuracy score
BAL	Bronchoalveolar lavage
BCR	B cell receptor
BH	Benjamini-Hochberg
BSA	Bovine serum albumin
CCL	CC chemokine ligand
CCR	CC chemokine receptor
cDC	Classical/conventional dendritic cell
CHILP	Common helper innate lymphoid progenitor
CILCP	Common ILC progenitor
CLA	Cutaneous lymphocyte-associated antigen
CLP	Common lymphoid progenitor
CMP	Common myeloid progenitor
CRTH2	Chemoattractant receptor–homologous molecule expressed on T helper 2 cells
Ct	Cycle threshold
CXCL	C-X-C chemokine ligand
CXCR	C-X-C chemokine receptor
CysLTR1	Cysteinyl leukotriene receptor 1
d3	Day three
d5	Day five
DAMP	Damage-associated molecular pattern
DC	Dendritic cell
DC-SIGN	Dendritic-specific intercellular adhesion molecule-3-grabbing non-integrin
DEP	Differentially expressed protein

DF	Dilution factor
DMSO	Dimethyl sulphoxide
EGF	Epidermal growth factor
ELISA	Enzyme-linked immunosorbent assay
EOMES	Eomesodermin
EP	Prostaglandin E receptor
ERK	Extracellular signal-regulated kinase
ETS1	ETS Proto-Oncogene 1
FACS	Fluorescence activated cell sorting
FCS	Fetal calf serum
FcεRI	Fc-ε receptor 1
FMO	Fluorescence minus one control
FPR2	Formyl peptide receptor 2
FSC	Forward scatter
Foxp3	Forkhead box P3
GATA3	GATA binding protein 3
GITR	Glucocorticoid-induced TNFR-related protein
GM-CSF	Granulocyte-macrophage colony-stimulating factor
GO	Gene ontology
h	Hour
HC	Healthy control
HDM	House dust mite
HLA	Human leukocyte antigen
HRP	Horseradish peroxidase
HSC	Haematopoietic stem cell
HTA	Human Tissue Authority
ICAM	Intercellular adhesion molecule
ICOS	Inducible co-stimulator
ICOSL	Inducible co-stimulator ligand
ID2	Inhibitor of DNA-binding 2
IFN	Interferon
IGA	Investigator's global assessment
IgE	Immunoglobulin E
IGF1	Insulin-like growth factor 1
iILC2	Inflammatory ILC2
IL	Interleukin
IL-17RB	IL-25 receptor
ILC	Innate lymphoid cell
ILC1	Group 1 innate lymphoid cell

ILC2	Group 2 innate lymphoid cell
ILC3	Group 3 innate lymphoid cell
ILCP	Innate lymphoid cell precursor
KLRG1	Killer-cell lectin like receptor G1
LFA-1	Lymphocyte function-associated antigen 1
Limma	Linear models for microarray data
Lin	Lineage
LPS	Lipopolysaccharide
LT	Leukotriene
LTi	Lymphoid tissue inducer
LXA4	Lipoxin A4
MACS	Magnetic-activated cell sorting
MAIT	Mucosal-associated invariant T cell
MAPK	Mitogen-activated protein kinase
MFI	Mean fluorescence intensity
MHC	Major histocompatibility complex
MHCI	MHC class I
MHCII	MHC class II
mins	Minutes
moDC	Monocyte-derived dendritic cell
MR1	MHC class I-related protein
mRNA	Messenger RNA
NCR	Natural cytotoxicity receptor
NF-κB	Nuclear factor-κB
NFIL3	Nuclear Factor, Interleukin 3 regulated
NK	Natural killer
NKP	NK precursor
NKp30	Natural cytotoxicity receptor p30
NMU	Neuromedin U
NOD	Nucleotide-binding oligomerization domain-containing protein
PAMP	Pathogen-associated molecular pattern molecule
PAR	Protease-activated receptor
PBMC	Peripheral blood mononuclear cell
PBS	Phosphate buffered saline
PCA	Principal component analysis
PD-1	Programmed cell death protein 1
pDC	Plasmacytoid dendritic cell
PLZF	Promyelocytic leukaemia zinc finger protein
PGD2	Prostaglandin D2

PRR	Pattern recognition receptor
qRT-PCR	Real-time quantitative reverse transcription PCR
RAG	Recombination activating gene
RFU	Relative fluorescence unit
rh	Recombinant human
RM	Repeated-measures
ROR	Receptor-related orphan receptor
RPKM	Reads per kilobase of transcript per million mapped reads
RT	Room temperature
RUNX3	RUNX family transcription factor 3
SOMAmer	Slow off-rate modified DNA aptamer
SSC	Side scatter
ST2	IL-33 receptor
STAT	Signal transducer and activator of transcription
T-bet	T-box expressed in T cells
Tc2	Type 2 CD8+ T cells
TCF-1	T cell factor 1
TCR	T cell receptor
TF	Transcription factor
TGF-β	Transforming growth factor beta
Th	T helper cell
TL1A	Tumour necrosis factor-like cytokine 1A
TLR	Toll-like receptors
TMB	Tetramethyl benzidine
TNF	Tumour necrosis factor
TNFRSF	TNF receptor superfamily member
TOX	Thymocyte selection-associated high mobility group box factor
Treg	Regulatory T cell
TSLP	Thymic stromal lymphopoietin
VEGF	Vascular endothelial growth factor
VIP	Vasoactive intestinal peptide
VPAC2	Vasoactive intestinal peptide receptor 2

Chapter 1: Introduction

1.1 Introduction to the immune system

The immune system is a complex network of structures and immune cells that provide defence against threats to host viability. A key characteristic of the immune system is the ability to distinguish between self and non-self. Traditionally, the immune system has been divided into two subsystems: the innate and the adaptive immune system. The innate immune system provides immediate and non-specific immune responses following immunological recognition of infection and danger signals. In contrast, the adaptive immune system provides finely tuned, antigen-specific immune responses and develops immunological memory generating long-lasting immunity to pathogens. However, it has become evident that the innate and adaptive arms of the immune system are highly interconnected and cooperate to provide adequate protection against a wide range of pathogens whilst simultaneously limiting self-damage (1–3).

1.1.1 First line of defence: the skin

The skin forms a physical, chemical and immunological barrier that protects against the entry of pathogens and environmental agents, prevents the loss of water and mediates thermoregulation (4).

The skin is made up of two distinct layers: the epidermis and the dermis. While the epidermis consists primarily of keratinocytes, the dermis is highly vascular and made up of the extracellular matrix and fibroblasts (5). The epidermis consists of four layers: the stratum corneum, the stratum granulosum, the stratum spinosum and the stratum basale (Fig. 1.1). The outermost layer of the epidermis, the stratum corneum, provides a physical permeability barrier to the external environment. It is

composed of flattened denucleated keratinocytes, called corneocytes, and intercellular lipids. During keratinocyte differentiation, keratinocytes release structural proteins and lipids into the stratum corneum that form intercellular layers. In the stratum corneum, corneocytes, intercellular lipids (ceramides, free fatty acids and cholesterol) and intracellular components (such as filaggrin, loricrin and keratin filaments) form a hydrophobic barrier that counteracts water and salt loss and prevents the penetration of water-soluble molecules while providing a degree of fluidity and flexibility (6, 7). The stratum granulosum provides a second-line epidermal barrier. Neighbouring keratinocytes in the stratum granulosum are sealed by tight junctions, consisting of transmembrane proteins, such as claudins and occludins, and cytosolic scaffold proteins, that control paracellular movement of molecules (7). In addition to forming a physical barrier, the skin provides immunological defence against infectious agents. Cutaneous immune cells perform important immunosurveillance functions thereby contributing to the maintenance of skin homeostasis and barrier integrity (4, 8–11).

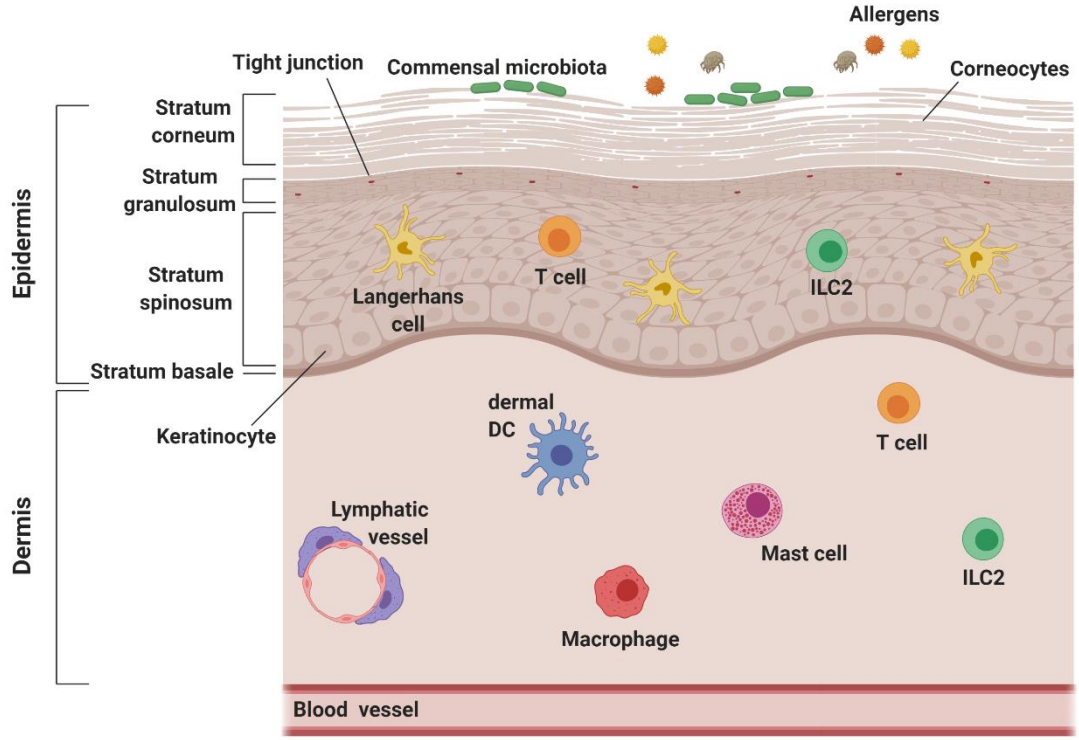


Figure 1.1 Structure and immune cell composition of healthy skin.
The skin forms a physical and immunological barrier preventing entry of harmful pathogens and allergens. There are fundamental differences between mouse and human skin. At steady state, the human epidermis is populated by Langerhans cells as well as group 2 innate lymphoid cells (ILC2) and CD8+ resident memory T cells. In mice, most T cells/ dendritic epidermal T cells in the epidermis are γδ T cells, while γδ T cells are rare in human skin. The dermis is populated by a range of innate and adaptive immune cells. Adapted from (4, 12).

1.1.2 Myeloid and lymphoid lineages of immune cells

Both innate and adaptive immune cells originate from pluripotent self-renewing haematopoietic stem cells (HSC) in the bone borrow. HSC have the potential to differentiate into red and white blood cells of all lineages by a process called haematopoiesis (Fig. 1.2), which is regulated by master transcription factors (TF) (13, 14).

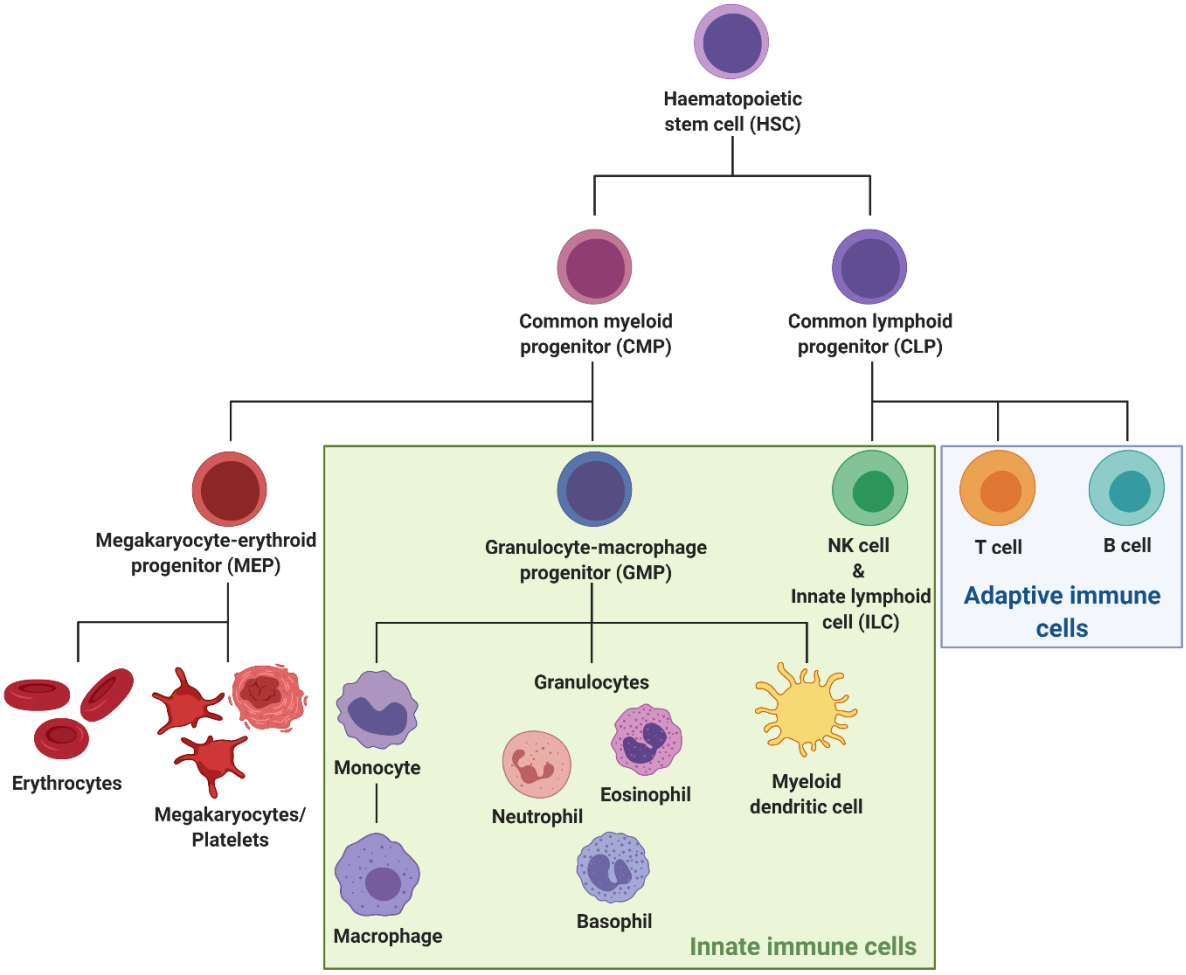


Figure 1.2 Developmental pathways of myeloid and lymphoid lineages.
HSC give rise to progenitor cells that are committed to either the myeloid or lymphoid lineage, common myeloid progenitors (CMP) or common lymphoid progenitors (CLP), respectively. CMP eventually differentiate into the myeloid lineage, including erythrocytes, megakaryocytes, granulocytes, monocytes/macrophages, and myeloid dendritic cells. Of note, dendritic cells (DC) can also develop from a lymphoid progenitor. CLP mature into the lymphoid lineage, which comprises adaptive T and B lymphocytes and innate natural killer (NK) cells and ILC. Adapted from (14, 15).

1.1.3 Innate immunity

Innate immune cells are characterised by the ability to rapidly sense and respond to invading pathogens and endogenous danger signals. Several mechanisms discriminate between self and non-self and activate immune effector functions

accordingly. Pattern recognition receptors (PRRs), such as Toll-like receptors (TLRs), recognise highly conserved motifs of microorganisms referred to as pathogen-associated molecular patterns (PAMPs) (16). Additionally, tissue or cell damage is signalled to immune cells by endogenous danger signals, collectively called damage-associated molecular patterns (DAMPs) (17). Recognition of PAMPs and DAMPs initiates innate effector responses such as the phagocytosis and destruction of pathogens and/or infected or damaged cells, activation of the complement system which results in opsonisation and lysis of foreign microorganisms, and the generation of inflammatory responses (18). In addition, innate immune cells play a critical role in instructing relevant adaptive effector responses and inducing T cell differentiation and activation (2).

1.1.3.1 Dendritic cells

Dendritic cells (DC) are professional antigen-presenting cells (APC) that are critical for the initiation of T cell-mediated responses, thereby bridging innate and adaptive immune responses. Following recognition of PAMPs and DAMPs, DC take up antigens and home to draining lymph nodes where they present processed antigens to naïve T cells, which initiates and guides T cell differentiation into discrete functional subsets. It has emerged that there are several DC subsets displaying functional and phenotypic heterogeneity, including conventional/classical DC (cDC), plasmacytoid DC (pDC), monocyte-derived DC (moDC) and Langerhans cells (2, 19). While cDC have been found to most efficiently prime naïve T cells, pDC are functionally specialised in the production of type I interferons (IFN) and promote activation of natural killer (NK) cells, effector $CD8^+$ T cells and $CD4^+$ T cell differentiation into T helper (Th) 1 cells (20). Langerhans cells, characterised by the expression of the surface markers CD1a and the C-type lectin langerin, reside in the

epidermis of the skin and are critically involved in immunosurveillance and the maintenance of skin homeostasis (8). MoDC expand significantly during inflammation (21) and will be discussed in detail in chapter 5.

1.1.4 Adaptive immunity

The adaptive immune system is comprised of B and T lymphocytes and is characterised by antigen specificity and immunological memory. Both B and T cells originate in the bone marrow, but while B cells mature in the bone marrow, T cell precursors migrate to and mature in the thymus. A distinguishing feature of adaptive immune cells is the expression of a repertoire of somatically rearranged antigen receptors, B-cell receptors (BCR) and T-cell receptors (TCR) on B and T cells, respectively, that mediate recognition of specific antigens (1). Terminally differentiated B cells, referred to as plasma cells, secrete high-affinity antibodies with a vast range of antigen specificities that mediate humoral immunity (22). An important feature of adaptive immunity is immunological memory mediated by memory B and T cells that provides long-lasting immunity and the rapid generation of specialised secondary immune responses (23).

1.1.4.1 T cells

Maturation of T cell precursors takes place in the thymus where they mature into distinct T cell lineages (αβ and γδ T cells) and undergo positive and negative selection ensuring self-major histocompatibility complex (MHC) restriction and self-tolerance. αβ T cells develop further into $CD4^+$ and $CD8^+$ T cells, referred to as helper and cytotoxic T cells, respectively. Activation of naïve T cells takes place in peripheral lymphoid tissues and is mediated by the interaction of TCRs with peptide-MHC complexes on APC, $CD8^+$ T cells with peptide-MHC class I (MHCI) complexes

and $CD4^+$ T cells with peptide-MHC class II (MHCII) complexes, which initiates the formation of the immunological synapse focused around a cluster of TCR-associated molecules. Naïve T cell activation induces clonal expansion and differentiation of naïve T cells into effector T cells (1, 24). Naïve $CD4^+$ T cells differentiate into several effector subsets characterised by subset-specific expression of TFs and effector cytokines (Fig. 1.3). Through subset-specific effector cytokine production Th subsets mediate specialised effector functions. In simplified terms, IFN-γ-producing Th1 cells mediate protection against intracellular bacteria and viruses, type 2 cytokine-producing Th2 cells against helminth parasites (25–27) and Th17 cells against extracellular bacteria and fungi (28, 29). In contrast, anti-inflammatory cytokine-producing regulatory T cells (Tregs) are critically involved in the maintenance of self-tolerance and homeostasis (30). It has become evident that Th cell subsets display a degree of flexibility in cytokine production and master regulator expression (31, 32).

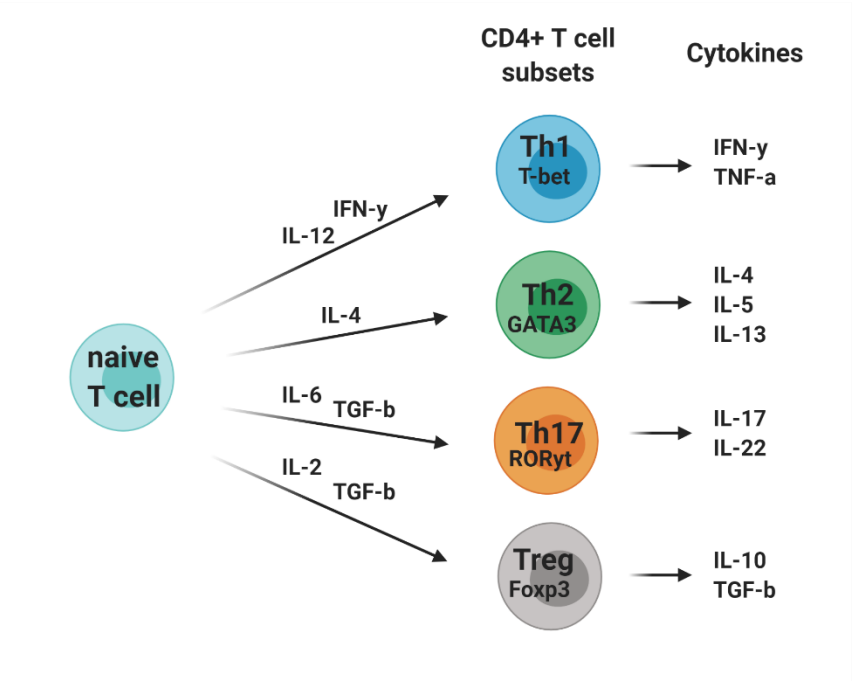


Figure 1.3 Helper T cell differentiation.

Following activation, naïve $CD4^+$ T cells differentiate into T helper cell subsets, characterised by subset-specific cytokine production, driven by specific cytokine signalling pathways and the activation of lineage-specific master TFs. T follicular helper cells, Th9 and Th22 cells are not depicted here. IL, interleukin; TGF-β, transforming growth factor beta. Adapted from (1).

In addition to conventional T cells dependent on classical MHC molecules for their activation, T cells with innate-like properties have been discovered that are characterised by the expression of restricted or semi-invariant antigen-recognition receptors, enrichment in mucosal tissues and rapid activation-induced cytokine production (33). Invariant natural killer T cells (iNKT) and mucosal-associated invariant T cells (MAIT) express semi-invariant αβ TCRs and recognise antigens presented by non-polymorphic MHC class I-like molecules CD1d and MHC class I-related protein (MR1), respectively (34, 35). A small number of γδ T cells exist that might not be dependent on a specific presentation molecule and instead might recognise antigens in an antibody-like manner (36). Moreover, it has become

evident that a proportion of the αβ T cell repertoire is capable of recognising lipids and small molecules presented by non-polymorphic antigen-presentation molecules such as CD1 and MR1 (37). CD1a-reactive T cells will be discussed in more detail in chapter 5.

1.2 Type 2 immunity

Type 2 immune responses play an important role in the protection against extracellular helminth parasites and the repair of associated tissue damage. By doing so, type 2 immune responses promote the maintenance of tissue homeostasis. However, dysregulation or inappropriate activation of type 2 immune responses is thought to underlie the pathogenesis of allergic inflammation (38).

Type 2 immune responses are characterised by the differentiation of naïve CD4+ T cells into Th2 cells and subsets of $CD8^+$ T cells into type 2-cytokine producing $CD8^+$ T cells (Tc2), the accumulation of innate immune cells and the production of cardinal type 2 cytokines IL-4, IL-5, IL-9 and IL-13. Type 2 cytokines initiate type 2 effector functions including B cell class switching to immunoglobulin E (IgE), recruitment and activation of granulocytes, epithelial cell hyperplasia, excessive mucus secretion and smooth muscle constriction (Fig. 1.4) (39–41).

1.2.1 Initiation of type 2 immune responses by the epithelium

Type 2 immune responses are believed to be initiated following recognition of products, enzymatic activity and tissue damage associated with the presence of helminths or allergens. Barrier epithelial cells play an important role during this initiation phase by sensing immune insults and releasing alarmin cytokines (Fig. 1.4a)

In the context of helminth infection, tissue damage caused by invading parasites has been identified as the primary trigger for the initiation of type 2 immunity. Such damage induce the release of alarmins IL-33, IL-25 and thymic stromal lymphopoietin (TSLP) (42). IL-33, IL-25 and TSLP have been found to be highly expressed by intestinal epithelial cells in mouse models of helminth infection (43–46). During infection with helminth parasites *Trichuris muris* or *Nippostrongylus brasiliensis,* mice lacking either IL-33 or IL-25 failed to induce an efficient type 2 immune response, unable to induce intestinal smooth muscle hypercontractility, goblet cell hyperplasia and mucus production, and consequently failed to clear infection (47, 48). During *T.muris* infection, TSLP was found to contribute to the initiation of a protective type 2 immune response, in part by inhibiting the production of proinflammatory type 1 cytokines thereby creating a type 2-permissive microenvironment (46).

In the context of allergic inflammation, several factors have been identified that contribute to the induction of type 2 immunity. Epithelial barrier integrity is essential in preventing the entry of and sensitisation to environmental allergens. Many allergens, such as fungi, house dust mite (HDM) and pollens, have been shown to possess intrinsic proteolytic activity. The HDM allergen *Der p 1* has been shown to directly disrupt epithelial barrier function by proteolytic cleavage of tight junction proteins occludin and claudin-1, enabling barrier permeability (49). Barrier epithelial cells express several innate receptors, such as PRRs and protease-activated receptors (PARs), that sense the presence of invading pathogens and allergens. The HDM allergen *Der p 2* has been found to be recognised by the PRR TLR4 due to its structural resemblance to the TLR4 ligand MD-2 (50), while the fungal allergen *Alternaria alternata* (ALT) is detected by airway epithelial cells through binding to

PAR2 (51, 52). Barrier epithelial cells respond to the recognition of allergens by producing an array of cytokines, in particular the type 2 immune response-inducing alarmins IL-33, IL-25 and TSLP (52–54). The critical involvement of alarmins in allergic inflammation is supported by data from mouse models that demonstrate resolution of allergic airway inflammation following blockade of IL-25 (55) and IL-33 signalling (56).

1.2.2 Type 2 immune effector cells

Following sensing of helminth parasites or allergens, the release of epithelial cell-derived alarmins results in the activation of a spectrum of innate immune cell types including ILC2, basophils, mast cells, eosinophils and DC. By providing early sources of type 2 cytokines and promoting Th2 differentiation and activation, local innate immune cells cooperate to perform and amplify type 2 effector functions (Fig. 1.4b) (39).

ILC2 have emerged as having a key role in type 2 immunity, which will be discussed in detail in section 1.4.2. Following helminth infection or allergen exposure, tissue-infiltrating basophils provide an important innate source of IL-4 (57) and are able to act as APC promoting Th2 differentiation and proliferation in an MHCII-dependent manner (58, 59). Mast cells populate barrier tissues and have been shown to be activated by epithelial-derived TSLP and IL-33, resulting in the release of type 2 cytokines and chemokines (60, 61). Mast cell-deficient mice failed to respond effectively to gastrointestinal helminth infection (62). Moreover, activated mast cells have been identified as a source of IL-33 during intestinal helminth infection (63) and cutaneous anaphylaxis (64). Eosinophilia is a cardinal feature of type 2 inflammation. IL-5 and eotaxin (CC chemokine ligand [CCL] 11), expressed at high

levels following helminth infection or allergen challenge, promote and facilitate eosinophil differentiation and selective recruitment into tissues (65, 66). Eosinophil activation by local signals, such as IL-33 (67), or inflammatory cytokines, such as IL-5, results in rapid secretion of preformed cytokines, including IL-4 and IL-13 (68). Following allergen challenge, eosinophils have been found to upregulate the expression of MHCII and co-stimulatory molecules and migrate to draining lymph nodes, where they might act as APC processing and presenting antigens to CD4+ T cells (69, 70). In vitro, eosinophils were capable of presenting antigens to T cells and polarising CD4+ T cells into IL-5-producing Th2 cells (71) implying involvement of eosinophils in Th2 differentiation. DC play a central role in the initiation of adaptive Th2 responses as professional APC, inducing differentiation of naïve T cells into Th2 cells through production of Th2-polarising cytokines (41). In models of allergic inflammation or helminth infection, DC depletion resulted in a failure to orchestrate adaptive Th2 cell responses, demonstrating the critical role of DC in Th2 cell differentiation and activation (72–74). Helminth- and allergen-derived products have been demonstrated to promote DC maturation resulting in increased Th2 cell polarising capacity (75, 76), while human Langerhans cells appear to have an intrinsic capacity to preferentially induce Th2 polarisation (77). Following lymph node egress and migration into affected tissues, mature Th2 cells produce type 2 cytokines (39) (Fig. 1.4c). Type 2 cytokines produced by both activated innate immune cells and adaptive Th2 cells orchestrate a broad range of downstream effector mechanisms, that are amplified by positive feedback loops (Fig. 1.4d). This is exemplified by IL-4/IL-13-induced B cell class switching to IgE, which further amplifies mast cell and basophil responses by binding to Fc-ε receptor 1 (FcεRI) and inducing the release of preformed and de novo mediators, including histamine

and prostaglandin D2 (PGD2), and pro-inflammatory cytokines (78). Downstream effector mechanisms of type 2 cytokines include the induction of epithelial cell hyperplasia, smooth muscle contraction, mucus production and increased vascular permeability that collectively mediate expulsion of mucosal helminth parasites as part of the “weep and sweep” response or cause symptoms of allergic inflammation, such as airway hyperresponsiveness, mucus hypersecretion and airflow obstruction in asthma (79, 80) (Fig. 1.4e).

In addition to providing protection against helminth parasites and causing allergic inflammation, some aspects of type 2 immunity have been linked to tissue remodelling and wound repair (38, 42). IL-4Rα-alternatively activated macrophages (AAM) are critically involved in the resolution and repair of tissue injury associated with helminth infection and allergic inflammation (81). AAM have been found to promote tissue regeneration by producing several wound healing factors such as arginase 1 (82), Ym1, Fizz1 (83), insulin-like growth factor 1 (IGF1), vascular endothelial growth factor (VEGF) and TGF-β (84). Together, these factors limit type 2 inflammation and instead facilitate tissue repair by promoting myofibroblast activation, angiogenesis, epithelial cell turnover and extracellular matrix deposition (38) (Fig. 1.4f).

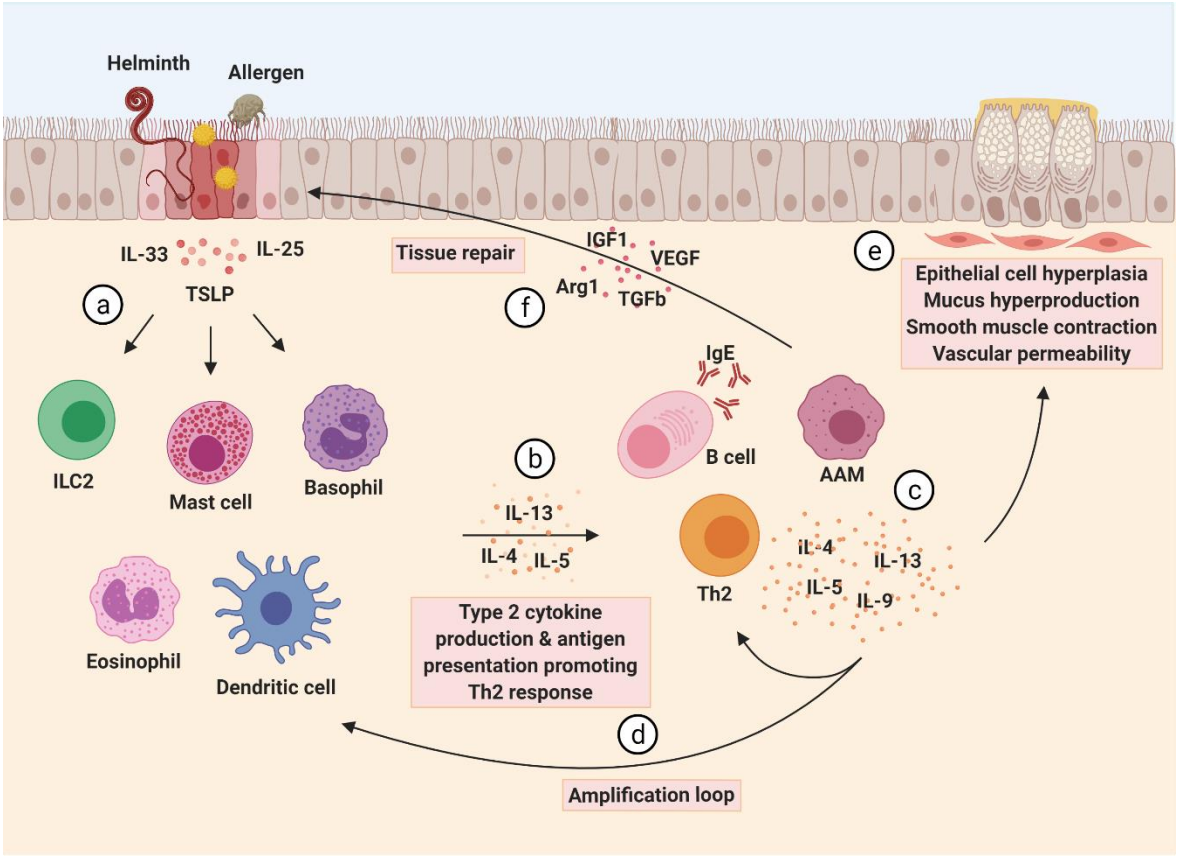


Figure 1.4 Type 2 immunity.

(**a**) Following release of alarmins by epithelial cells in response to helminth infection-associated tissue damage or allergen exposure, innate immune cells are rapidly activated and accumulate within the affected tissue site. (**b**) Innate immune cells produce type 2 cytokines and promote Th2 differentiation and recruitment (**c**) Type 2 cytokines promote IgE class switching and AAM differentiation. (**d**) Type 2 cytokines further amplify both innate and adaptive type 2 immune responses. (**e**) Type 2 cytokines promote epithelial cell hyperplasia, mucus hyperproduction, smooth muscle contraction and increased vascular permeability. (**f**) Type 2 immune responses also facilitate wound healing. Adapted from (38).

1.3 Innate lymphoid cells

Innate lymphoid cells (ILC) are part of the innate immune system and are particularly abundant at barrier and mucosal sites. ILC are characterised by a classic lymphoid cell morphology, but unlike adaptive T and B lymphocytes, ILC lack the expression of recombination activating gene (RAG)-dependent rearranged antigen receptors. Thus, ILC do not respond in an antigen-specific manner and instead are regulated

by environmental cues. Following activation, ILC respond rapidly by proliferating and producing an array of effector cytokines (85). ILC have been implicated in a range of physiological processes, such as protection against pathogens (10, 86, 87), maintenance of tissue integrity (88–90) and metabolic homeostasis (91). However, dysregulated ILC responses contribute to inflammatory disorders such as allergies (92–94) and autoimmune diseases (95). ILC exhibit a transcriptional and functional diversity resembling that of T cells and are therefore often referred to as the innate counterpart of adaptive T cells. The ILC family has been divided into cytotoxic and non-cytotoxic/helper ILC. Conventional NK cells are considered cytotoxic ILC and represent the innate counterpart of CD8+ T cells. Non-cytotoxic ILC are characterised by expression of the IL-7Rα (CD127) and have been grouped into three subsets, ILC1, ILC2 and ILC3, that represent the innate counterparts of Th1, Th2 and Th17 cell subsets, respectively (96) (Fig. 1.5).

1.3.1 ILC subsets

Non-cytotoxic ILC have been grouped into three subsets based on the production of signature cytokines, the differential requirements for TFs and the expression of phenotypic markers (96) (Fig. 1.5). ILC1 typically produce type 1 cytokines, notably IFN-γ and tumour necrosis factor (TNF), and are dependent on the TF T-box expressed in T cells (T-bet) for their development (97). ILC2 typically secrete type 2 cytokines, predominantly IL-5 and IL-13, and are developmentally dependent on GATA binding protein 3 (GATA3) and receptor-related orphan receptor alpha (RORα) (87, 98–101). ILC3 typically produce IL-17A, IL-22, granulocyte-macrophage colony-stimulating factor (GM-CSF) and TNFα and require RORγt for their development (86, 102). In humans, ILC3 can be further divided into three subpopulations, lymphoid tissue inducer cells (LTi) and natural cytotoxicity receptor

(NCR)$^+$ and NCR$^-$ ILC3 based on the expression of the NCR NKp44. LTi cells facilitate the formation of secondary lymphoid organs, including lymph nodes and Peyer`s patches, during embryogenesis (103, 104), NCR$^+$ ILC3 mainly produce IL-22 and NCR$^-$ ILC3 predominantly express IL-17A (105).

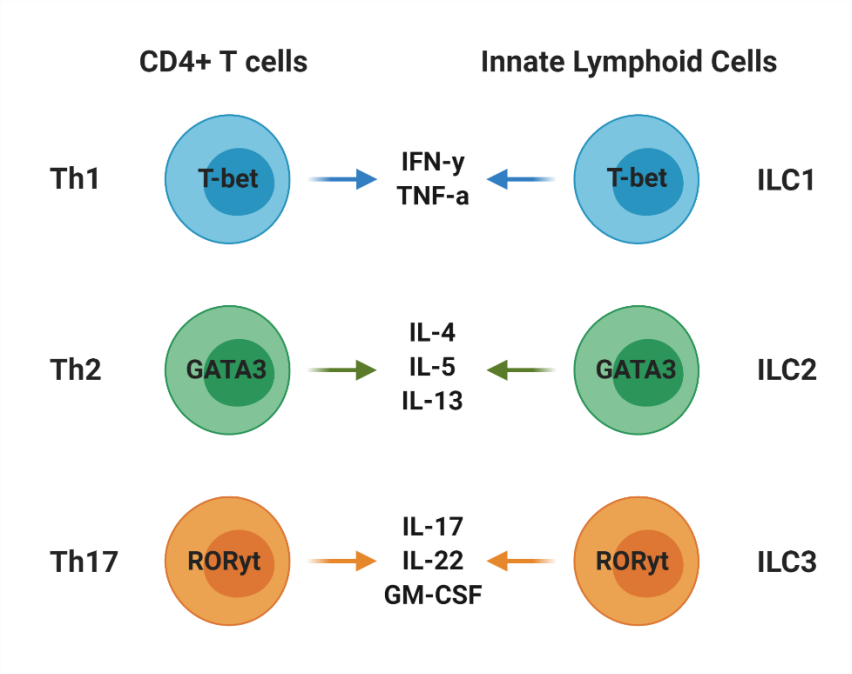


Figure 1.5 ILC subsets resemble T helper cell lineages.
ILC subsets resemble Th cell subsets in terms of master TFs and effector cytokine expression.

Functionally, ILC contribute to immune defence against invading pathogens. While ILC1 have been implicated in the protection against intracellular pathogens (106), ILC2 are critically involved in the expulsion of helminth parasites and tissue repair following viral infection (87, 88, 98, 100). Further detailed discussion of ILC2 follows below. In contrast, ILC3 are involved in the maintenance of intestinal homeostasis by interacting with the commensal microbiota and protecting against extracellular bacterial and fungal pathogens (107–109). To date, it is unclear whether an innate counterpart of Tregs exists. While a number of studies have reported the existence

of IL-10-producing ILC2 (110–113), ILC expressing the Treg master TF forkhead box P3 (Foxp3) have not yet been identified. An IL-10- and TGF-β-producing ILC population, referred to as regulatory ILC, was found to contribute to the resolution of murine innate intestinal inflammation by suppressing the activation of ILC1 and ILC3 (111). During allergic airway inflammation, IL-4-induced IL-10 production by murine ILC2 was reported to downregulate ILC2 activity and ameliorate airway hyperreactivity (AHR) (113). It remains to be established whether regulatory ILC and/or IL-10-producing ILC2 populations represent distinct ILC subsets or an alternative activation state of known ILC subsets.

1.3.2 ILC development

Developmentally, ILC are derived from the common lymphoid progenitor (CLP). While the developmental process of human ILC is beginning to be unravelled, the current models of ILC development are primarily based on data from mouse experiments (Fig. 1.6). ILC arise from multi-potent CLP in the bone marrow by progressive differentiation, first into common ILC progenitors (CILCP) and subsequently into common helper innate lymphoid progenitors (CHILP), under the control of specific TFs (114, 115). Differentiation of CILCP into CHILP is believed to depend on the transcriptional repressor ID2 and the TFs GATA3 and TCF-1 expression (106). ID2 expression has been demonstrated to block T cell development and promote murine and human ILC development (116). Differentiation of CHILP into innate lymphoid cell precursors (ILCP), under the influence of PLZF, gives rise to all IL-7Rα-expressing helper ILC subsets (117). While T-bet expression is essential for ILC1 development (106), differentiation of ILCP into ILC2 has been found to depend on GATA3 (101), RORα (118) and BCL11b (119, 120). In contrast, ILC3 development has been demonstrated to

depend on RORγt and aryl hydrocarbon receptor expression (121). Human ILCP, identified as lineage marker-negative $CD7^+$ IL-$7R\alpha^+$ $CD117^+$ cells, have been identified in the circulation and both lymphoid and non-lymphoid tissues and have been proposed to represent naïve ILC. Human ILCP were found to contain both unipotent cells, able to differentiate into either ILC1, ILC2 or ILC3, and multipotent populations that could give rise to two or all three helper ILC subsets. Interestingly, human ILCP appeared to retained the capacity to generate both cytotoxic NK cells and helper ILC (122). The presence of human ILCP in the circulation and tissues suggests that ILC subsets may be generated outside of the bone marrow in response to local environmental signals, providing a mechanism for ILC replenishment within tissues and the ability to adapt to changes in the microenvironment (114, 123).

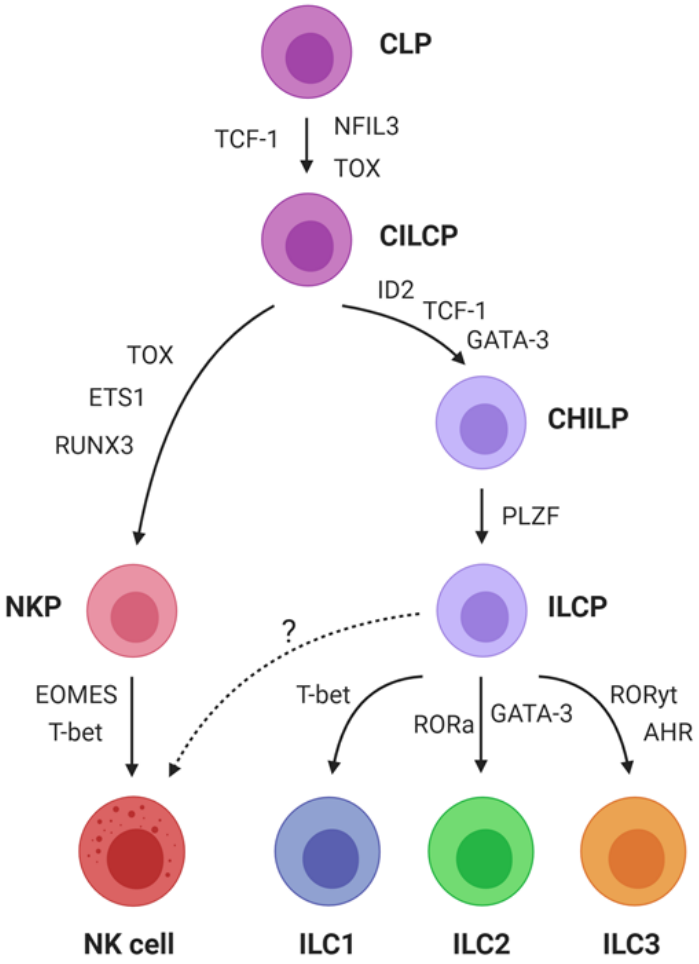


Figure 1.6 Progressive differentiation of cytotoxic and helper ILC.
ILC arise from the CLP in the bone marrow by progressive differentiation under the influence of specific TFs. AHR, aryl hydrocarbon receptor; CLP, common lymphoid progenitor; CHILP, common helper innate lymphoid progenitor; CICLP, common ILC progenitor; ILCP, innate lymphoid cell precursor; EOMES, eomesodermin; ETS1, ETS proto-oncogene 1; GATA3; GATA binding protein 3; ID2, inhibitor of DNA-binding 2; NFIL3, nuclear factor, interleukin 3 regulated; NKP, NK precursor; PLZF, promyelocytic leukaemia zinc finger protein; ROR, receptor-related orphan receptor alpha; RUNX3, RUNX family transcription factor 3; T-bet, T-box expressed in T cells; TCF-1, T cell factor 1; TOX, thymocyte selection-associated high mobility group box factor. Adapted from (114).

1.3.3 ILC tissue residency and chemotaxis

ILC populate a wide range of lymphoid and non-lymphoid tissues, in particular barrier and mucosal sites, with different ILC subsets being enriched in specific

tissues in a way that relates to their function in the maintenance of immune homeostasis (124). Initially, it was believed that ILC progenitors populate various tissues during fetal development, where they undergo multiple stages of development (125). Parabiotic mouse experiments supported the hypothesis that ILC were primarily tissue-resident cells maintained by self-renewal and expanded locally in response to immune challenge. However, during the chronic phase of helminth infection, recruitment of ILC2 from haematogenous sources into the gut was observed, which raised the possibility of ILC re-distribution and migration (126). Recent data indicates that mature ILC, distinguishable from ILC progenitors by high expression of subset-specific markers, can traffic between tissue sites. During the early stage of nematode infection, inflammatory ILC2 were found to chemotactically migrate from the intestine to the lymphatics, blood circulation and eventually to the lungs, which was crucial for worm clearance, tissue repair and host survival (127). Mature ILC have been proposed to develop diverse trafficking potentials due to the up- and downregulation of homing receptors. Murine ILC1 and ILC3 in gut-associated lymphoid tissues were shown to upregulate the expression of the CC chemokine receptor (CCR) 9 and integrin α4β7 in an retinoic acid-dependent manner, enabling the migration into the intestine (128). ILC3 homing from the intestine into draining mesenteric lymph nodes was found to be dependent on the expression of CCR7 (129). In contrast to ILC1 and ILC3, ILC2 appeared to constitutively express the gut-homing receptor CCR9 and did not express CCR7 (128). ILC2 migration will be discussed in more detail in chapter 4. While it has become evident that ILC have the potential to migrate between tissues, much remains to be understood regarding migratory patterns of ILC subsets and their functional implications.

1.3.4 Plasticity of ILC subsets

Evidence for ILC plasticity has emerged in recent years. Human IFN-γ-producing T-bet$^+$ ILC1 have been shown to differentiate into IL-22-producing NKp44$^+$ RORγt$^+$ ILC3 in response to *in vitro* treatment with IL-23 and IL-1β (130). Conversely, conversion of human NKp44$^+$ RORyt$^+$ ILC3 into IFN-γ-producing T-bet$^+$ ILC1 has been observed in response to IL-12 *in vitro* (92). Similarly, exposure of human and murine ILC2 to IL-1β and IL-12 *in vitro* gives rise to a hybrid ILC1-ILC2 phenotype with simultaneous expression of GATA3 and T-bet as well as type 1 and type 2 cytokines (131–133). IL-4 was shown to reverse the IL-12-induced trans-differentiation of ILC2 into ILC1 (132). Considering both the rarity and the predominant tissue-residency of ILC, functional plasticity might be critical for generating a prompt and appropriate immune response to changes in the microenvironment. However, ILC plasticity has also been suggested to contribute to immunopathology and the accumulation of specific ILC subsets in inflamed tissues, such as ILC1 in inflamed intestine in individuals with Crohn`s disease (92) and in lungs of individuals with chronic obstructive pulmonary disease (132, 133). Moreover, human ILC2 have been demonstrated to produce a broad range of cytokines, dependent on specific environmental cues (134–136).

1.4 Group 2 innate lymphoid cells

ILC2 were initially discovered in the context of helminth infection. In 2006, an IL-25-responding, type 2 cytokine-producing non-B/non-T cell population was described that appeared to be critically involved in *N.brasiliensis* worm expulsion (100). In 2010, several reports identified lineage (Lin)-negative ILC2 as an innate source of IL-13, important for effective helminth expulsion in mice (87, 98, 99). A human

equivalent of mouse ILC2 was identified in 2011, present in human lung, gut, nasal tissue and peripheral blood and characterised by lack of known lineage markers and the surface expression of IL-7Rα and chemoattractant receptor–homologous molecule expressed on T helper 2 cells (CRTH2) (94). ILC2 have since emerged as key initiators of type 2 immune responses, contributing to protection against helminth parasites, tissue repair and allergic inflammation (see below).

1.4.1 Regulation of ILC2 activity

ILC2 activity is tightly regulated by microenvironmental signals, such as cytokines, lipid mediators, neuropeptides and direct cell-to-cell interactions. The microenvironment is composed of tissue-resident non-haematopoietic sentinels, including epithelial cells such as bronchial epithelial cells in the lung (137), tuft cells in the gut (138) and keratinocytes in the skin (93), endothelial cells, smooth muscle cells, stromal cells, fibroblasts as well as sensory neurons, the extracellular matrix and tissue-resident and infiltrating immune cells (41). Cues derived from the microenvironment guide the activity and function of immune cells, such as ILC2, thereby shaping an ensuing immune response (41). Dysregulated ILC2 responses have been implicated in the development of allergic inflammatory disorders (section 1.4.2.4), highlighting the importance of mechanisms that regulate ILC2 activity.

1.4.1.1 Signals stimulating ILC2 activity

ILC2 are predominately activated by local environmental cues. Moreover, it is increasingly being recognised that ILC2 engage in direct interactions with other immune and tissue cells, of which some induce ILC2 stimulation. ILC2 respond to activation with increased proliferation and type 2 cytokine production (139) (Fig. 1.7). In addition, it is becoming evident that ILC2 can sense and respond to innate

signals involving both extracellular and intracellular PRRs, such as TLR2, TLR4 (10) and nucleotide-binding oligomerisation domain-containing protein 2 (NOD2) (135), respectively.

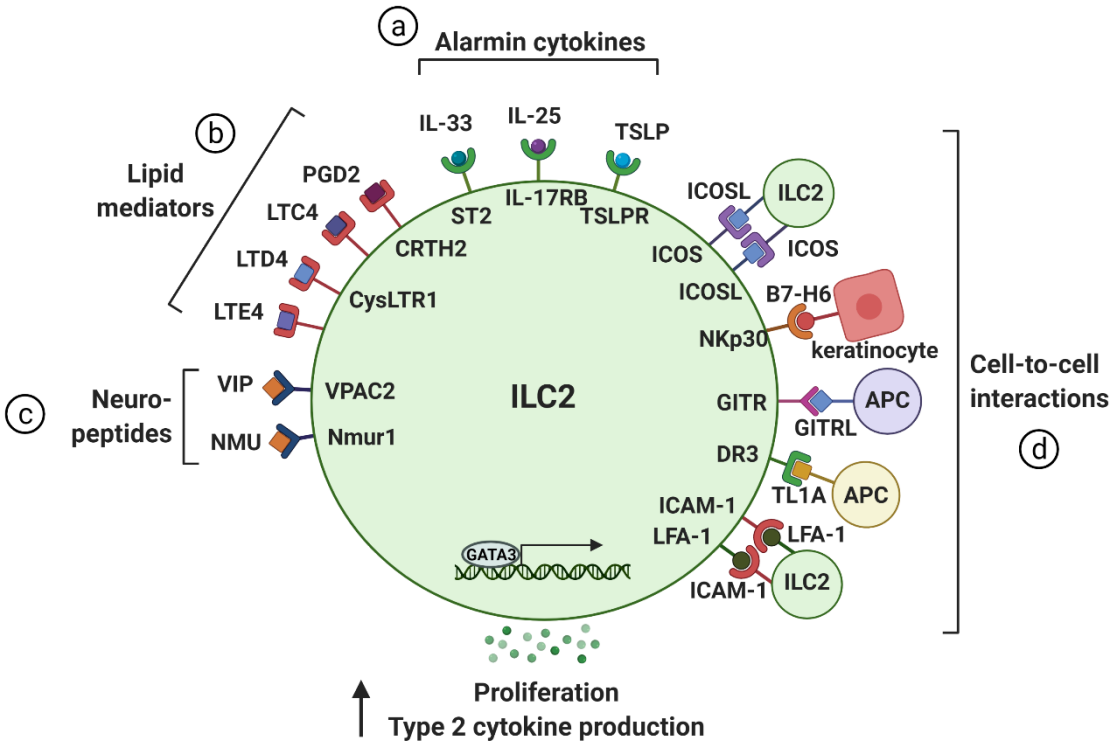


Figure 1.7 Ligand-receptor interactions stimulating ILC2 activity.
ILC2 are activated by a broad range of environmental signals and cell-to-cell interactions. ILC2 activation is accompanied by upregulated GATA3 expression and increased ILC2 proliferation and type 2 cytokine production. CysLTR1, cysteinyl leukotriene receptor 1; GITR, glucocorticoid-induced TNFR-related protein; ICOS, inducible co-stimulator; ICAM, intercellular adhesion molecule; LT, leukotriene; LFA-1, lymphocyte function-associated antigen 1; NKp30, natural cytotoxicity receptor p30; NMU, neuromedin U; TNFRSF, TNF receptor superfamily members; TL1A, tumour necrosis factor-like cytokine 1A; VIP, vasoactive intestinal peptide; VPAC2, vasoactive intestinal peptide receptor 2. Adapted from (139).

1.4.1.1.1 IL-33, IL-25 and TSLP

Alarmins IL-33, IL-25 and TSLP, predominately derived from epithelial cells, have been identified as potent ILC2 activators (Fig. 1.7a) (90, 93, 94, 98, 100, 140–142).

ILC2 are characterised by surface expression of receptors for IL-33 (ST2), IL-25 (IL-17RB) and TSLP (TSLPR). ILC2 responsiveness to alarmins has been suggested to be determined by tissue-residency, with lung-resident ILC2 predominately responding to IL-33, intestinal ILC2 to IL-25 and cutaneous ILC2 to TSLP (124). Consistently, in mouse models of allergic airway inflammation, ILC2 were most potently activated by IL-33 (140, 142), while tuft cell-derived IL-25 was found to be essential for intestinal ILC2 activation following helminth infection (138). An IL-25-responsive ILC2 cell population, referred to as inflammatory ILC2 (iILC2), has been reported in the context of *N. brasiliensis* infection. iILC2 proliferated in response to IL-25 but not IL-33 and displayed a degree of plasticity, expressing both GATA3 and RORγt and acquiring the ability to produce IL-17 (143). Controversy exists about whether TSLP alone can induce ILC2 activation or whether it functions as a co-stimulatory signal. Contrasting results have been reported regarding TSLP-mediated *in vitro* stimulation of human ILC2 (134, 144). In a murine model of AD-like inflammation, TSLP appeared to be critically involved in the induction of cutaneous ILC2 responses (141). IL-33, IL-25 and TSLP appear to have synergistic effects on ILC2 activation (93, 134, 144–146), potentially due to reciprocal upregulation of alarmin receptors (144, 147). Reported discrepancies in ILC2 responsiveness to IL-33, IL-25 or TSLP may be due to isolation method and *in vitro* culture conditions, but also heterogeneity within the ILC2 population. Environmental cues, such as tissue-specific signals, have been proposed to contribute to phenotypic and functional heterogeneity within the ILC2 population (124, 142, 148).

1.4.1.1.2 Lipid mediators

Lipid mediators, such as leukotrienes and prostaglandins, have been identified as activating signals for ILC2 (Fig. 1.7b). PGD2, predominantly produced by activated

mast cells (149), has been found to activate human and murine ILC2 through binding to CRTH2, inducing proliferation and type 2 cytokine production (136, 150). *In vitro* CRTH2-mediated ILC2 activation resulted in upregulated expression of surface ST2 and IL-17RB, suggesting that PGD2 increases ILC2 responsiveness to alarmins (136). Additionally, PGD2 was found to act as a potent ILC2 chemoattractant (136), contributing to ILC2 accumulation in the inflamed lung (151). Cysteinyl leukotrienes, including LTC4, LTD4 and LTE4, generated by activated inflammatory immune cells, have been identified as ILC2 activating signals and can act synergistically with PGD2 and alarmins to induce ILC2 activation (152–155).

1.4.1.1.3 Neuropeptides

The immune system and the nervous system closely interact to monitor tissue integrity and respond to tissue perturbances. ILC2 activity can be influenced by neuropeptides produced by peripheral neurons (Fig. 1.7c). The neuropeptide NMU has been demonstrated to induce ILC2 proliferation and type 2 cytokine production by signalling through the neuropeptide receptor Nmur1, contributing to helminth expulsion and allergic inflammation (156–158). The neuropeptide VIP has been reported to stimulate production of IL-5 by intestinal and pulmonary ILC2 (159, 160). Within the intestine, VIP has been suggested to link ILC2-mediated eosinophil recruitment to central circadian and metabolic rhythms (159). In the lung, VIP-mediated ILC2 activation appears to contribute to amplification of type 2 allergic airway inflammatory responses (160).

1.4.1.1.4 Cell-to-cell interactions

It has become evident that ILC2 interact with a diverse range of innate and adaptive immune cells with some of those interactions directly stimulating ILC2 activity (Fig.

1.7d). ILC2 have been found to express both ICOS and its ligand. ICOS:ICOSL interactions appear to provide survival signals to ILC2 and were shown to be required for efficient ILC2 function in the context of airway inflammation (161, 162). Similarly, both ICAM-1 and its ligand LFA-1 were detected on ILC2. Signalling through ICAM-1 via the extracellular signal-regulated kinase (ERK) pathway was found to be important for ILC2 development, homeostasis and function *in vitro* and during airway inflammation (163). Interaction of the natural cytotoxicity receptor NKp30 on human ILC2 with its activatory ligand B7-H6, expressed on tumour cells and pro-inflammatory monocytes and neutrophils, resulted in the induction of IL-13 production by ILC2 through nuclear factor-κB (NF-κB) signalling (164). In the context of malignancy, increased ILC2 activity, as a result of elevated expression of tumour-derived B7-H6 and PGD2, has been implicated in a tumour immunosuppressive axis through IL-13-mediated activation of monocytic-myeloid-derived suppressor cells (165). Several TNF receptor superfamily members (TNFRSF) have been implicated in ILC2 survival and activation. During intestinal helminth infection and allergic airway inflammation, binding of TL1A on APC to the TNFRSF member DR3 on ILC2 appeared to be required for efficient ILC2 function (166, 167). Interaction of the TNFRSF member GITR on ILC2 with its ligand GITR-L, predominantly expressed on APC, has been identified as a co-stimulatory signal for ILC2, upregulating IL-9 production synergistically with IL-33 (168).

1.4.1.2 Signals inhibiting ILC2 activity

ILC2 activity is negatively regulated by suppressive signals, including cytokines, lipid mediators and cell-to-cell interactions (Fig. 1.8), which is essential for the maintenance of immune homeostasis and the prevention of type 2

immunopathology. In addition, these are thought to be relevant to potential immune escape, for example in the setting of malignancy (169, 170).

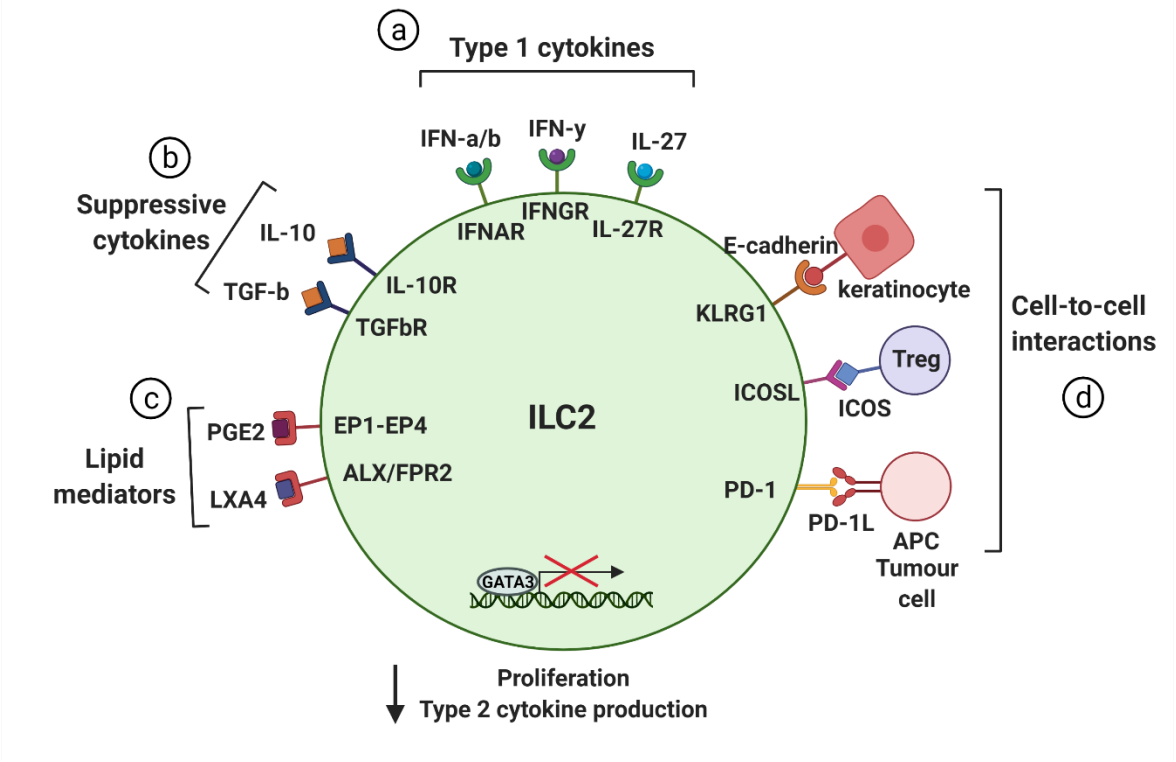


Figure 1.8 Ligand-receptor interactions inhibiting ILC2 activity.
ILC2 activity is negatively regulated by a broad range of environmental signals and cell-to-cell interactions. ILC2 negative regulation is accompanied by downregulated GATA3 expression and reduced ILC2 proliferation and type 2 cytokine production. ALX, lipoxin A4 receptor; EP, prostaglandin E receptor; RPR2, formyl peptide receptor-2; IFN, interferon; KLRG1, killer cell lectin-like receptor G1; LXA4, lipoxin A4; PD-1, programmed cell death protein 1. Adapted from (139).

1.4.1.2.1 Suppressive cytokines

Counterregulation exists between type 1 and type 2 immune responses (171). Consistent with this, ILC2 activity has been found to be negatively regulated by cytokines associated with type 1 immune responses (Fig. 1.8a). Type I interferons (IFN-α/β), IFN-γ and IL-27 have been demonstrated to reduce proliferation, type 2 cytokine production and GATA3 expression of IL-33-activated mouse and human

ILC2 in a signal transducer and activator of transcription 1 (STAT1)-dependent manner (172, 173). During helminth infection, activated T cells were found to produce IFN-γ several days after infection. By suppressing ILC2 function, T cells have been proposed to induce the switch from an antigen-independent to an antigen-dependent immune response (173). Moreover, the importance of terminating ILC2 responses has been demonstrated in the context of influenza virus infection. By suppressing ILC2 activity, type I interferons prevented the onset of infection-induced airway inflammation (172). In addition to type 1-associated cytokines, immunosuppressive cytokines IL-10 and TGF-β1 have been shown to inhibit alarmin-mediated activation of human ILC2 *in vitro* (Fig. 1.8b). However, while TGF-β1 *in vitro* treatment of ILC2 resulted in reduced IL-4, IL-5 and IL-13 production, it was accompanied by upregulated IL-9 secretion (174). *In vivo*, TGF-β1, released by pulmonary epithelial cells upon allergen or IL-33 exposure, was identified as a chemoattractant for ILC2 (137), questioning the role of TGF-β1 as an ILC2 suppressant.

1.4.1.2.2 Lipid mediators

Lipid mediators including PGE2, PGI2 and LXA4 have been demonstrated as negative regulators of ILC2 activity (Fig. 1.8c). The lipid mediator PGE2, abundantly expressed in the lung, has been found to suppress ILC2 proliferation and type 2 cytokine production by signalling through EP1-EP4, accompanied by downregulated GATA3, CD25 and ST2 expression (175, 176). Using a mouse model of acute allergic airway inflammation, the role of the lipid mediator PGI2 as an ILC2 suppressant was demonstrated, showing that both endogenous and exogenous PGI2 diminishes pulmonary accumulation of IL-5- and IL-13-producing ILC2 (177).

Moreover, signalling of the pro-resolving mediator LXA4 through receptors ALX/FPR2 on ILC2 has been shown to negatively regulate ILC2 activity (150).

1.4.1.2.3 Cell-to-cell interactions

While many cell-to-cell interactions appear to stimulate ILC2, there have been two reports of cell contact-dependent negative ILC2 regulatory mechanisms (Fig. 1.8d). Binding of the cell adhesion molecule E-cadherin, highly expressed on keratinocytes, to KLRG1 on human ILC2 prevented stimulation-induced ILC2 proliferation and type 2 cytokine production (93). Human induced Tregs were found to suppress ILC2 activity by engaging in ICOS-ICOSL interactions while simultaneously producing IL-10 and TGF-β1 (178). Immune checkpoint proteins, including PD-1, on ILC2 have been implicated in negative ILC2 regulation (169, 170, 179, 180). In the setting of malignancy, tumour-associated ILC2 expressed increased levels of PD-1 (169) and PD-1 blockade promoted tumour ILC2 expansion and anti-tumour effectors (170). During *N. brasiliensis* infection and IL-33-induced lung inflammation, PD-1 deficiency or blockade resulted in enhanced ILC2 activity and subsequent efficient worm clearance (179) and AHR exacerbation (180), respectively.

1.4.2 Role of ILC2 in immune defence, maintenance of tissue homeostasis and allergic inflammation

Through type 2 cytokine production and interactions with surrounding immune and tissue cells, ILC2 play a central role in type 2 immune responses (Fig. 1.9).

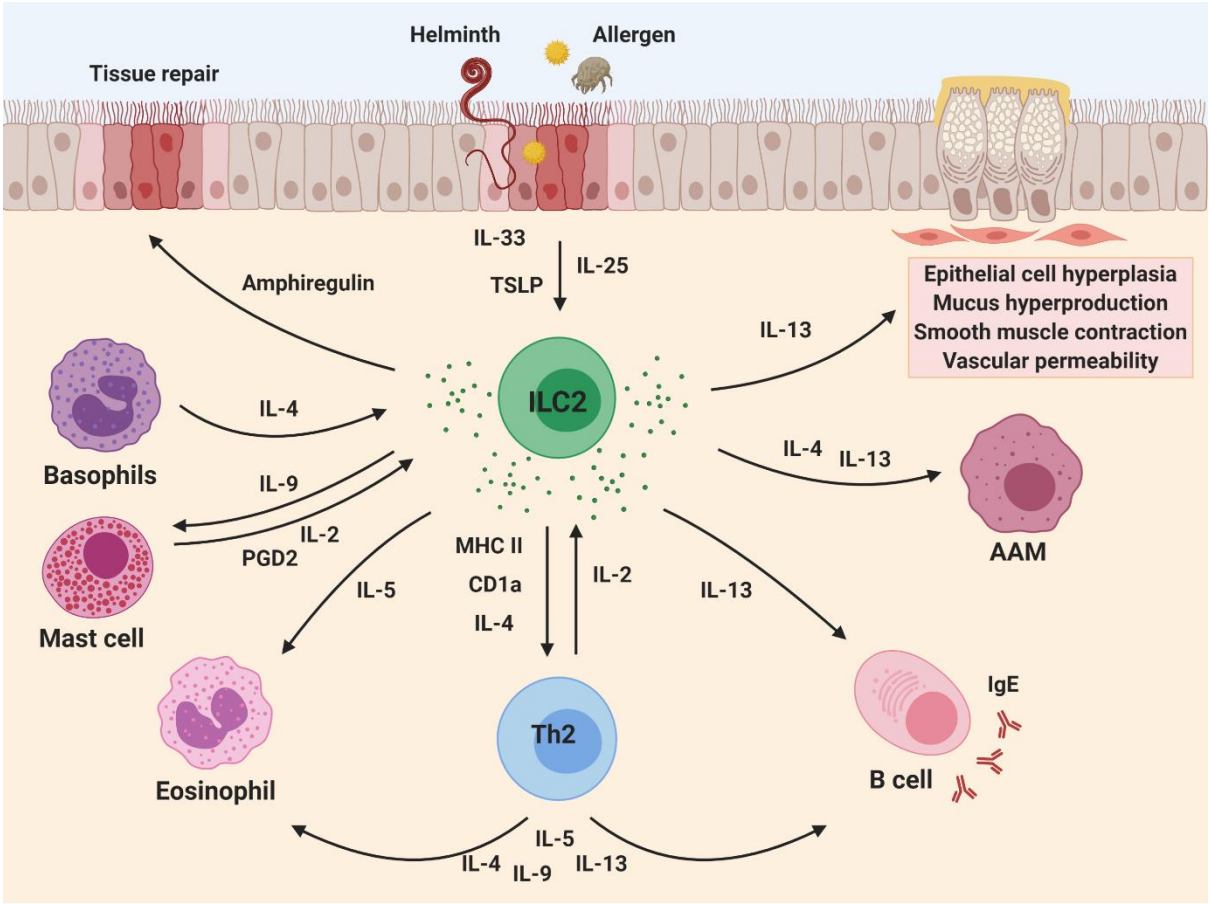


Figure 1.9 Central role of ILC2 in type 2 immunity.
Following activation, ILC2 induce type 2 immune effector functions through type 2 cytokine production and interactions with innate and adaptive immune cells. Adapted from (181).

1.4.2.1 Role of ILC2 in the defence against parasitic worms

As discussed in section 1.2, type 2 immune responses provide defence against helminth parasites by inducing a “weep and sweep” response. IL-13 is critically involved in the generation of type 2 effector functions, highlighted by the finding that IL-13-deficient mice were unable to clear worms (182), and ILC2 have been identified as a critical innate source of IL-13 during helminth infection (87, 98–100, 138). During *N.brasiliensis* infection of RAG knockout mice, activation of ILC2 through exogenous IL-25 or IL-33 was found to be sufficient for worm clearance independently of adaptive immunity (98–100). ILC2 may provide an early source of

IL-13, while Th2 cells may be involved during the later phase of type 2 immune response in part by providing ILC2 survival signals (87). Consistently, ILC2 and $CD4^+$ T cells were found to cooperate during *N.brasiliensis* infection, with ILC2 activating T cells via MHCII and T cells supporting ILC2 survival through IL-2 production (183). In the context of helminth infection, IL-25 and IL-33 have been identified as key activators of ILC2. A failure of IL-33- or IL-25-deficient mice to clear *N. brasiliensis* infection has been found to be accompanied by reduced IL-13 production by ILC2 (48, 138). A positive feedback loop between intestinal tuft cell-derived IL-25 and activated ILC2-derived IL-13 has been proposed to promote epithelial hyperplasia during helminth infection (138). During infection with the hookworm *Heligmosomoides polygyrus*, intestinal mast cells released IL-33 in response to damaged intestinal epithelium-derived adenosine triphosphate (ATP) and activated ILC2. ILC2-induced goblet cell hyperplasia and mucin secretion were found to be particularly important during the early phase of *H. polygyrus* infection by inhibiting settlement of adult worms (63). In addition to promoting worm expulsion, ILC2 appear to play a critical role during the recovery phase after helminth infection by promoting tissue repair (184) (section 1.4.2.2).

While the role of ILC2 in murine worm defence has been well studied, little is known about the involvement of ILC2 in natural human helminth infection. The frequency of peripheral blood ILC2 was reported to be decreased in young children infected with *Schistosoma haematobium* compared to uninfected children and was restored following anti-helminth treatment. Whether the reduction in peripheral ILC2 frequency is reflective of diminished ILC2 maintenance or increased ILC2 infiltration to sites of infection is currently unknown (185). Additional studies are required to decipher the role of ILC2 in human helminth infection.

1.4.2.2 Role of ILC2 in tissue repair

The maintenance of epithelial barrier integrity is essential for restricting entry of invading pathogens, commensal bacteria and allergens. The wound healing response, initiated by DAMPs such as alarmin released by damaged epithelial cells, involves leukocyte infiltration, clearance of damaged tissue and debris, antimicrobial activity, re-epithelialisation and tissue remodelling (186). Because of their abundance at barrier sites, ILC2 are strategically located to perform immunosurveillance and respond to tissue damage. In the lung, ILC2 have been found to play a critical role in pulmonary tissue repair and restoration of airway epithelial integrity after influenza virus infection by secreting the epidermal growth factor-like molecule amphiregulin (88). Amphiregulin signals through the epidermal growth factor receptor to induce the proliferation and differentiation of tissue precursors contributing to tissue remodelling (187). In a mouse model of chemically-induced colitis, amphiregulin production by IL-33-activated intestinal ILC2 promoted goblet cell mucus production and tight junction protein expression in the colon, resulting in the restoration of normal colonic architecture, epithelial barrier function and intestinal tissue homeostasis (188). Moreover, IL-33-activated ILC2 have been implicated in cutaneous wound healing following acute skin injury. In the absence of IL-33 or ILC2, wound healing and re-epithelialisation were impaired, demonstrating a critical role of the IL-33/ILC2 axis in cutaneous tissue repair (90). In addition to amphiregulin secretion, ILC2-secreted type 2 cytokines, such as IL-5 and IL-13, have been implicated in the wound healing response. ILC2-derived IL-13 has been shown to support macrophage polarisation to an alternatively activated phenotype (91). As mentioned in section 1.2, AAM contribute to tissue repair by producing wound healing factors that promote wound angiogenesis and

myofibroblast differentiation (189). During the resolution phase of influenza virus infection, pulmonary ILC2 were found to promote the accumulation of eosinophils through increased production of IL-5 (190). Eosinophils have been implicated in pulmonary tissue repair by producing the epidermal growth factor TGF-α (191). Following *N.brasiliensis* infection, ILC2-derived IL-9 was revealed to be important for successful restoration of tissue integrity, which appeared to be mediated through IL-9-dependent autocrine amplification of ILC2 type 2 cytokine and amphiregulin production (184). However, chronic/excessive wound healing responses can result in loss of tissue integrity and development of tissue fibrosis. Indeed, dysregulated ILC2 activity has been implicated in the development of pulmonary (192) and hepatic (193) fibrosis.

1.4.2.3 Role of ILC2 in the maintenance of skin homeostasis

ILC2 have been identified in both murine and human skin, at a greater abundance than in peripheral blood (93). In mice, dermal ILC2 have been proposed to perform cutaneous immunosurveillance at steady state, involving interactions with skin-resident mast cells and constitutive IL-13 production (11). IL-18 appeared to contribute to steady-state production of IL-13 by skin ILC2, and transcriptional profiling revealed increased IL-18 responsiveness of skin-derived compared to blood-derived ILC2 (124). In humans, epidermal ILC2 were found to express significant levels of the lipid antigen presenting molecule CD1a, implying a role of ILC2 in epidermal lipid surveillance (10). Moreover, human skin ILC2 were characterised by increased transcriptional expression of amphiregulin compared to blood ILC2 at both steady state and following activation (93), which suggests a role of cutaneous ILC2 in the maintenance of skin homeostasis.

1.4.2.4 Role of ILC2 in allergic inflammation

Dysregulated ILC2 activity has been implicated in the development of allergic inflammatory disorders. The role of ILC2 in atopic dermatitis (AD) pathogenesis is discussed in detail in chapter 3. Increased ILC2 frequency and activity have been detected in nasal polyps of individuals with chronic rhinosinusitis (94, 194), in blood, sputum and bronchiolar lavage fluid from asthmatic subjects (195–198), and in lesional AD skin (93, 141). High-dose systemic steroid treatment of children with severe therapy-resistant asthma resulted in a reduction of airway ILC2 numbers (198). Genome-wide association studies have identified several loci associated with allergic pathology that are linked to ILC2 activity, such as activating signals (IL-33, TSLP), type 2 cytokines (IL-4, IL-13) and TFs (GATA3, RORα) (199). Consistently, increased expression and elevated levels of ILC2 stimulatory signals, including IL-33 (200), PGD2 (201) and LTC4 (202), have been detected in endobronchial biopsies and bronchoalveolar lavage (BAL) fluid from subjects with severe asthma, respectively. In addition, the expression of ILC2 suppressive signals, such as LXA4 (203), appears to be downregulated in individuals with severe asthma. Preventative IL-27 treatment of OVA-challenged mice prevented the development of allergic airway inflammation (204). This implies that increased expressed of ILC2 stimulators coupled with loss of negative ILC2 regulation contributes to unrestrained ILC2 activity in asthmatic lungs.

Evidence from mouse models of allergen-induced airway inflammation demonstrates the critical involvement of alarmin-activated ILC2 in the initiation of type 2 lung inflammation (145, 205–207). Following allergen challenge, IL-5- and IL-13-secreting pulmonary ILC2 were found to promote the accumulation of eosinophils and AAM and induce goblet cell hyperplasia and excessive mucus

production (145, 208). Basophil-derived IL-4 appeared to be required for ILC2-mediated eosinophil recruitment (209). Moreover, ILC2 have been found to interact with mast cells in the context of lung inflammation with ILC2-derived IL-9 promoting mast cell expansion and mast cell-derived IL-2 in turn stimulating ILC2 proliferation (210). A feed-forward circuit between IL-33-producing epithelial cells and IL-13-producing ILC2 has been proposed to sustain chronic airway inflammation and hyperreactivity even in the absence of allergen challenge (196). ILC2 were found to be critically involved in the induction of a robust allergen-specific Th2 response during both allergen sensitisation and re-challenge. ILC2-derived IL-13 induced migration of activated lung DC to draining lymph nodes for Th2 cell priming (211) and stimulated CCL17 secretion by pulmonary DC resulting in the recruitment of $CCR4^+$ memory Th2 cells into the lung following allergen re-challenge (212).

1.5 Overall aims

The overall aim of this thesis was to expand our understanding of human ILC2 functions in health and disease, with a particular focus on cutaneous inflammation. Increased ILC2 frequency and activity have been implicated in allergic inflammation, such as AD (93, 141), and are accompanied by infiltration of both innate and adaptive immune cells to inflamed sites. Thus, I hypothesised that ILC2 may contribute to local inflammatory responses through pro-inflammatory effector functions that go beyond the production of type 2 cytokines and may involve regulation of leukocyte tissue homing, phenotype and activity. To gain insight into the cutaneous microenvironment in AD, protein expression profiles of healthy and AD skin were analysed using a human *in vivo* skin blister allergen model (chapter 3). To investigate the response of human ILC2 to alarmin stimulation with implications for the role of ILC2 in allergic inflammation, secretion of pro- and anti-

inflammatory cytokines and chemokines by human ILC2 was assessed *in vitro* (chapter 3). Relatively little is known about the role of ILC2 in the direct recruitment of immune cells. Thus, chemokine production by human ILC2 and its functional relevance in type 2 immunity was investigated (chapter 4). Furthermore, the interaction of ILC2 with myeloid cells has largely remained unexplored. Therefore, I aimed to evaluate the effect of human ILC2 on myeloid cell survival and differentiation (chapter 5).

Chapter 2: Methods and Materials

2.1 Patients and samples

All study participants gave fully informed written consent and samples were stored anonymously and under compliance with Human Tissue Authority (HTA) standards. Healthy blood and skin biopsies, blood from individuals with AD and skin suction blister fluids were collected under local ethics approval (Oxford C, 09/H0606/71, National Research Ethics Service Committee South Central). Blood samples were collected from healthy adult donors under WIMM HTA licence number 12433. Healthy controls included individuals of differing age, gender, ethnicity and medical history. Leukocyte cones were obtained from NHSBT Oxford Blood Donor Centre. Blood samples from individuals with AD, diagnosed according to validated diagnostic criteria, were collected in the department of Dermatology, Churchill Hospital, Radcliffe Hospitals NHS Trust, Oxford, UK. AD disease severity was determined according to Investigator's Global Assessment (IGA) scores (213). Human skin tissue samples were obtained from healthy donors undergoing plastic surgery under NHS ethics REC 14.NW.1153. Human healthy skin biopsies were taken with ethical approval of the NRES Committee South Central in the department of Dermatology, Churchill Hospital, Radcliffe Hospitals NHS Trust, Oxford UK.

2.2 Skin suction blister technique

Skin suction blister technique was performed by Prof Graham Ogg as previously described (10, 93, 214). Saline solution, HDM extract or ALT extract were injected intraepidermally by skin prick tests to the upper arms of healthy, AD and atopic asymptomatic volunteers. Suction blisters were formed approximately 30 minutes (mins) after intradermal challenge, by applying suction blister cups to the site of

injection at a vacuum pressure of 250mmHg. 24 hours (h) later, blister fluid was aspirated using a 30-gauge needle. Blister fluids were centrifuged at 1500rpm for 5mins at 4°C, cells stained for flow cytometry analysis or fluorescence-activated cell sorting (FACS) and the blister fluid phase stored at -80°C.

2.3 Cell isolation and culture

2.3.1 Peripheral blood mononuclear cell (PBMC) isolation

PBMC were isolated from blood samples by density gradient centrifugation. Peripheral blood was diluted 1:1 with R10 medium (Table 4) and carefully layered on top of Lymphoprep density gradient solution (Stemcell Technologies). Following centrifugation at 2000rpm at room-temperature (RT) for 20mins with the brake off, the PBMC layer was collected and washed twice in R10 medium, first for 10mins at 1800rpm and then for 5mins at 1500rpm, resuspended in R10 medium and used in experiments.

2.3.2 Mononuclear cell isolation from human skin biopsies

Human whole thickness skin samples were processed as previously described (10) by first removing subcutaneous fat with scissors. Using a scalpel, residual fat cells were scraped off the underside and hair from the upper side of the skin. Explants were cut into < 0.5mm pieces in petri dishes using scissors and scalpels and digested in collagenase P (1 mg/ml diluted in R10 medium, Roche) in petri dishes at 37°C overnight for no more than 16h. Following overnight digestions, DNase I (200 Kunitz unit/ml, Roche) was added for 15mins at RT before digestions was stopped by the addition of cold 10mM EDTA (Ambicon) solution. Then, the digested tissue was homogenised through 70µm cell strainers, washed with cold 10mM EDTA solution and centrifuged at 1800rpm for 10mins. The cell pellet was

resuspended in cold R10 medium and passed through 40µm cell strainers before centrifugation at 1500rpm for 5mins and resuspension in R10 medium. In the case of small skin biopsies, cell suspensions were stained with cell surface marker antibodies for flow cytometry analysis (Table 1). In the case of larger skin tissue samples, cell suspensions were layered carefully on top of Lymphoprep density gradient solution and mononuclear cells isolated by density gradient centrifugation.

2.3.3 Magnetic-activated cell sorting (MACS)

MACS bead cell separation system was used for isolation of $CD3^+$ T cells and $CD14^+$ monocytes from PBMC. PBMC were isolated from whole blood and resuspended in 80µl MACS buffer (Table 4) per 10^7 cells. 20µl CD3 (Miltenyi Biotec) or CD14 (Miltenyi Biotec) microbeads per 10^7 cells were added and incubated for 15mins at 4°C, with gentle agitation every 5mins. 2ml MACS buffer per 10^7 cells was added and centrifugated at 1200rpm for 10mins at 4°C. Cells were resuspended in 500µl MACS buffer per 10^8 cells. LS columns (Miltenyi Biotec) were attached to a QuadroMACS Separator (Miltenyi Biotec) and prepared by rinsing with 3ml MACS buffer. Cell suspensions were applied to 30µm pre-separation filters (Miltenyi Biotec), passed through columns and washed 3 times with 3ml MACS buffer. CD3- and/or CD14-depleted cell suspensions were purified further by passing through an LD column (Miltenyi Biotec) and the collected cell suspension kept for ILC2 isolation, either frozen in freezing solution (Table 4) for future use or resuspended in R10 medium for immediate use. Columns were removed from the separator, 6ml MACS buffer added to columns and the magnetically labelled cells eluted by pushing plungers into the columns. The $CD3^+$ cell fraction was frozen or used in functional T cell experiments and $CD14^+$ cells were differentiated into moDC (section 2.3.7) or cultured in ILC2 supernatant (section 2.7.3).

2.3.4 ILC2 sorting and culture

ILC2 were isolated and cultured as previously described (93). PBMC were depleted of T cells by CD3 MACS separation and surface stained with anti-human antibodies (Table 1). Lineage marker (CD4, CD8, CD14, CD19, CD16, CD56, CD11b, CD11c, CD123, FcεRI)-negative, $CD45^+$, $CD3^-$, $IL\text{-}7R\alpha^+$, $CRTH2^+$ ILC2 were FACS sorted at 100 cells/well into 96-well round-bottom plates and resuspended in a mixed lymphocyte reaction of γ-irradiated PBMC from three healthy donors ($2x10^6$ cells/ml) in ILC2 medium (Table 4) supplemented with IL-2 (100 IU/ml) and phytohemagglutinin-L solution (2.5 µg/ml) (eBioscience). Following cell sorting, ILC2 were cultured in ILC2 medium supplemented with IL-2 (200 IU/ml) at 37ºC and 5% CO2 for 6-8 weeks with half of the culture medium being replaced every 2-3 days. Approximately 2 weeks after the sort, expanding ILC2 lines were transferred from 96-well round-bottom plates to 96-well flat-bottom plates, and after a further 2 weeks expanding ILC2 lines were transferred to 48-well plates. After approximately 4-6 weeks of *in vitro* expansion, the purity of the expanded ILC2 lines was assessed by flow cytometry (section 2.4.1.1)

2.3.5 T cell sorting and culture

$CCR4^+$ and $CCR4^-$ T cells were sorted and cultured in a similar way to ILC2. PBMC were surface stained with anti-human antibodies (section 2.4.1.2) and $CD3^+$ $CCR4^+$ and $CD3^+$ $CCR4^-$ cells FACS sorted at 100 cells/well into 96-well round-bottom plates and resuspended in a mixed lymphocyte reaction of γ-irradiated PBMCs from three healthy donors ($2x10^6$ cells/ml) in ILC2 medium supplemented with IL-2 (100 IU/ml) and phytohemagglutinin-L solution (2.5 µg/ml). T cells were cultured in ILC2 medium in the presence of IL-2 (200 IU/ml) at 37ºC and 5% CO2 for 3-4 weeks with

half of the culture medium being replaced every 2-3 days. Expanding T cells were first transferred to 96-well flat-bottom and then to 48-well plates. CCR4 expression on expanded T cells was confirmed by flow cytometry (section 2.4.1.2).

2.3.6 CD1a-reactive T cell clones sorting and culture

CD1a-reactive T cell clones were kindly provided by Dr Yi-Ling Chen and a detailed methodology will be described in an upcoming publication. Briefly, polyclonal T cells were co-cultured with CD1a-transfected K562 cells and CD1a-reactive IFN-γ-producing T cells were labelled using an IFN-γ secretion assay (Miltenyi Biotec) according to manufacturer's instructions. The live responder T cells, secreting IFN-γ in a CD1a-dependent manner, were sorted by single-cell FACS into a 96-well round-bottom plate and were expanded for 2-3 weeks in a mixed lymphocyte reaction in the presence of IL-2 (200 IU/ml). CD1a-reactivity and functionality of expanded CD1a-reactive T cell clones was confirmed prior to use in co-culture experiments (section 2.9).

2.3.7 MoDC differentiation

Monocytes were isolated from PBMC by CD14-positive MACS separation. $0.5x10^6$ or $1x10^6$ monocytes/well were plated in 48- or 24-well non-coated plates (ThermoFisher), respectively, and cultured for 5 days in moDC medium supplemented with IL-4 (10 ng/ml) and GM-CSF (100 ng/ml). On day 3 (d3) of culture, half of the medium was replaced with fresh moDC medium supplemented with IL-4 (10 ng/ml) and GM-CSF (100 ng/ml). On day 5 (d5) of culture, differentiated moDC were collected, cell surface marker expression assessed by flow cytometry (section 2.4.1.4) and used in functional experiments (section 2.7.2).

2.3.8 Cell counting

Cells were collected, 10µl cell suspension combined with 10µl 0.4% trypan blue solution (ThermoFisher) and counted using the Countess Automated Cell Counter (ThermoFisher).

2.4 Antibodies and reagents

2.4.1 Antibodies for FACS and flow cytometry analysis

Staining was performed as described in 2.5.4.

2.4.1.1 Antibodies for ILC2 sorting and flow cytometry analysis

For ILC2 FACS and flow cytometry analysis, PBMC or ILC2 were labelled with Live/Dead violet cell stain (1:1000 dilution, Invitrogen) and anti-human antibodies for cell surface markers (Table 1). ILC2 were identified by gating on $CD3^-$, Lineage marker negative, $CD45^+$, IL-$7R\alpha^+$, $CRTH2^+$ cells. Fluorescence minus one (FMO) controls are shown in Fig. A.1.

Table 1 ILC2 antibody panel.

Target	Fluorochrome	Dilution	Clone	Company
CD3	BV650	1:100	OKT3	Biolegend 317324
CD4	PerCP	1:100 (FACS) 1:200 (flow cytometry)	OKT4	Biolegend 317432
CD8	PerCP	1:100 (FACS) 1:200 (flow cytometry)	RPA-T8	Biolegend 301030
CD11b	PerCP	1:100 (FACS) 1:200 (flow cytometry)	M1/70	Biolegend 101230
CD11c	PerCP	1:100 (FACS) 1:200 (flow cytometry)	BU15	Biolegend 337234
CD14	PerCP	1:100 (FACS) 1:200 (flow cytometry)	HCD14	Biolegend 325632
CD19	PerCP	1:100 (FACS) 1:200 (flow cytometry)	HIB19	Biolegend 302228

FcεRI	PerCP	1:100 (FACS) 1:200 (flow cytometry)	CRA-1	Biolegend 334616
CD123	PerCP	1:100 (FACS) 1:200 (flow cytometry)	32703	Bio-Techne FAB301C
CD16	PerCP	1:100 (FACS) 1:200 (flow cytometry)	B73.1	Biolegend 302030
CD56	PerCP	1:100 (FACS) 1:200 (flow cytometry)	5.1H11	Biolegend 362526
CD16	BV605	1:100	3G8	Biolegend 302040
CD56	BV605	1:100	HCD56	Biolegend 318334
CD45	AF700	1:200	2D1	Biolegend 368514
CRTH2	PE	1:50	BM16	Miltenyi Biotec 130-113-600 Biolegend 350106

2.4.1.2 Antibodies for CCR4$^+$ and CCR4$^-$ T cell sorting

For CCR4$^+$ and CCR4$^-$ T cell FACS and flow cytometry analysis, PBMC were labelled with Live/Dead violet cell stain (1:1000 dilution, Invitrogen) and anti-human CD3 (BV650, 1:100 dilution, OKT3, Biolegend: 317324) and CCR4 (APC, 1:100 dilution, LC291H4, Biolegend: 359408) antibodies.

2.4.1.3 Antibodies for flow cytometry analysis of CCR4 expression

CCR4 expression was analysed using the ILC2 antibody panel (Table 1), Live/Dead violet cell stain (1:100 dilution, Invitrogen) and anti-human CCR4 antibody (APC, 1:100 dilution, LC291H4, Biolegend 359408).

2.4.1.4 Antibodies for flow cytometry analysis of monocyte/moDC cell surface marker expression

Cells were labelled according to the moDC antibody panel (Table 2) and with the Zombie Red Fixable Viability Kit (Biolegend). FMO controls are shown in Fig. A.2.

Table 2 MoDC antibody panel.

DC-SIGN, dendritic-specific intercellular adhesion molecule-3-grabbing non-integrin; HLA, human leukocyte antigen

Target	Fluorochrome	Dilution	Clone	Company
CD1a	APC	1:100	HI149	Biolegend 300110
CD1b	FITC	1:100	SN13 (K5-1B8)	Biolegend 329106
CD1c	BV510	1:100	L161	Biolegend 331534
CD11c	PerCP	1:100	BU15	Biolegend 337234
CD14	APC/Cy7	1:100	63D3	Biolegend 367108
CD80	BV650	1:100	2D10	Biolegend 305227
CD86	BV421	1:100	BU63	Biolegend 374212
HLA-DR	AF700	1:100	L243	Biolegend 307626
HLA-ABC	PeCy5	1:100	W6/32	Biolegend 311430
DC-SIGN	PeCy7	1:100	9E9A8	Biolegend 330114

2.4.1.5 Antibodies for flow cytometry analysis of CD1a-reactive T cell clones

CD1a-reactive T cell clones were labelled with Live/Dead violet cell stain (1:1000 dilution, Invitrogen) and anti-human CD69 antibody (PE, 1:200 dilution, FN50, Biolegend 310906).

2.4.2 Recombinant proteins

Table 3 Recombinant proteins

rh, recombinant human

Experiment	Cytokine	Company
ILC2 stimulation	rhIL-33	Biolegend 581804
	rhIL-25	Biolegend 598904
	rhTSLP	Biolegend 582404
	rhIL-2	Biolegend 589108
moDC differentiation	rhIL-4	Biolegend 574004
	rhGM-CSF	Biolegend 572903

CD1a-reactive T cell clone experiments	rhIL-12	Biolegend 573004
	rhIL-18	Biolegend 592104
	rhIL-2	Biolegend 589108
Chemotaxis assay	rhCCL22	Biolegend 584904
	rhCCL17	Biolegend 573804

2.4.3 Buffers and cell culture media

Table 4 Buffers and media

FCS, fetal-calf serum; PBS, phosphate buffered saline; DMSO, dimethyl sulphoxide; BSA, bovine serum albumin;

Buffer/Media	Components	Company
R10 medium	RPMI medium 1640	Sigma-Aldrich
	10% FCS	Sigma-Aldrich
	L-glutamine (2 mM)	Sigma-Aldrich
	Penicillin (100 IU/ml)	Sigma-Aldrich
	Streptomycin (100 µg/ml)	Sigma-Aldrich
ILC2 medium	RPMI medium 1640	Sigma-Aldrich
	10% heat-inactivated human serum	Sigma-Aldrich
	L-glutamine (2 mM)	Sigma-Aldrich
	Penicillin (100 IU/ml)	Sigma-Aldrich
	Streptomycin (100 µg/ml)	Sigma-Aldrich
	Non-essential amino acids (1x)	Gibco
	Sodium pyruvate (100 µM)	Gibco
	HEPES (10 mM)	Gibco
	β-mercaptoethanol (50 µM)	Gibco
moDC medium	RPMI medium 1640	Sigma-Aldrich
	10% FCS	Sigma-Aldrich
	L-glutamine (2 mM)	Sigma-Aldrich
	Penicillin (100 IU/ml)	Sigma-Aldrich
	Streptomycin (100 µg/ml)	Sigma-Aldrich
	Non-essential amino acids (1x)	Gibco
	Sodium pyruvate (100 µM)	Gibco
	HEPES (10 mM)	Gibco

	β-mercaptoethanol (50 µM)	Gibco
MACS buffer	PBS 2% FCS EDTA (2 mM)	ThermoFisher Sigma-Aldrich Ambicon
Flow cytometry staining buffer	PBS 3% FCS	ThermoFisher Sigma-Aldrich
Flow cytometry fixation buffer	PBS 4% formaldehyde solution	ThermoFisher Sigma-Aldrich
Freezing solution	FCS 10% dimethyl sulphoxide	Sigma-Aldrich Sigma-Aldrich
ELISA reagent diluent	PBS 1% BSA	ThermoFisher Sigma-Aldrich
ELISA wash buffer	PBS 0.05% Tween20	ThermoFisher

2.5 Analysis of gene expression

2.5.1 RNA-sequencing

The RNA-sequencing dataset of skin suction blister- and blood-derived ILC2 (Lineage$^-$ CD45$^+$ IL-7Rα$^+$ CRTH2$^+$) and T cells (CD3$^+$) was generated by Dr. Maryam Salimi and analysed as previously described (10).

2.5.2 Real-time quantitative reverse transcription PCR (qRT-PCR)

Messenger RNA (mRNA) extraction was performed using a TurboCapture 96 mRNA kit (Qiagen, 72251) according to the manufacturer's instructions. Complementary DNA was synthesis by reverse transcription PCR using M-MLV reverse transcriptase (Invitrogen). qPCR was performed in duplicates on a QuantStudi7 Flex

real-time PCR machine using the TaqMan PCR Master Mix (Applied Biosystems) and the following TaqMan probes (Applied Biosystems): *GAPDH* (Hs02786624_m1), *IL-13* (Hs00174379_m1), *CCL22* (Hs01574247_m1), *CCL17* (Hs00171074_m1), *CCR4* (Hs00747615_s1). *GAPDH* was used as a housekeeping gene and *IL-13* was used a positive control for ILC2 stimulation. Cycle threshold (C_t) values over 32 were excluded from the analysis.

2.6 Analysis of protein expression

2.6.1 SOMAscan assay

SOMAscan proteomic assay of skin suction blister fluids was performed by SomaLogic, Inc., as previously described (215). A dataset of the expression of 1305 proteins in relative fluorescence units (RFU) was provided and analysed as described in section 2.10.

2.6.2 Luminex multiplex assay

Luminex multianalyte profiling of skin suction blister fluids was performed using a customised 26-plex magnetic Luminex assay (R&D). The panel included CCL21, CCL27, C-X-C chemokine ligand (CXCL) 11, Galectin-1, GM-CSF, IL-10, IL-17C, IL-21, IL-3, IL-5, CXCL8, CCL2, CXCL9, CCL17, CXCL10, CX3CL1, Galectin-3, Granzyme B, IL-13, IL-2, IL-22, IL-4, IL-6, M-CSF, CCL22, CCL18. Luminex multianalyte profiling of ILC2 supernatants and sera was performed using the 40-plex Bio-Plex Pro Human Chemokine Panel (Bio-Rad 171AK99MR2). Serum samples, stored at -80°C, had previously been obtained by centrifuging fresh peripheral blood at 3000rpm for 10mins. Luminex assays were performed according to the manufacturers' instructions. Prior to Luminex assays, skin suction blister fluids were thawed at 4°C and centrifuged at 10 000xg for 10mins. ILC2 supernatants

(section 2.7.1) and serum samples were thawed at 4°C and centrifuged at 1000xg for 15mins. Serum samples and ILC2 supernatants were diluted 1/4 and ½ in assay standard diluent, respectively,. Microplates were washed between steps using a magnetic microplate holder. Results were obtained using a Bio-Plex 200 System (Bio-Rad). Prior to data acquisition, the instrument was calibrated using the Bio-Plex Calibration Kit (Bio-Rad 171203060). Protein concentrations were calculated by standard curve interpolation of analyte fluorescence intensity values minus the background fluorescence intensity.

2.6.3 Enzyme-linked immunosorbent assay (ELISA)

Cell culture supernatants (section 2.7.1) were thawed at 4°C and analysed by sandwich ELISA. CCL22 concentrations were determined using the Human CCL22/MDC DuoSet ELISA kit (R&D DY336), CCL17 concentrations by the Human CCL17/TARC DuoSet ELISA kit (R&D DY364), IFN-γ concentrations by the Human IFN-γ DuoSet ELISA kit (R&D DY285B) and IL-13 concentrations by the Human IL-13 ELISA Ready-Set-Go kit (Invitrogen). For IFN-γ or IL-13 ELISA, supernatants were diluted 1/10-1/50 and 1/100-1/200, respectively. ELISA was performed according to manufacturer's instructions. Tetramethyl benzidine (TMB) substrate solution (Invitrogen) was used as a substrate for horseradish peroxidase (HRP)-labelled antibodies. Plates were incubated for 5-20mins in the dark at RT before the reaction was stopped with stop solution (H_2SO_4). Absorbance was measured at 450nm using a Clariostar microplate reader. Concentrations were determined by standard curve interpolation.

2.6.4 FACS and flow cytometry

2.6.4.1 FACS

Cells were labelled with antibodies in MACS buffer for 30mins at 4°C. Labelled cells were washed in MACS buffer at 1500rpm for 5mins, passed through 30µm pre-separation filters and resuspended in MACS buffer at approximately $40x10^6$ cells/ml. Single-stain control PBMC were used for compensation. FACS was performed on the FACSAria III cell sorter (BD) by Craig Waugh.

2.6.4.2 Flow cytometry

Cells were labelled with antibodies in flow cytometry staining buffer (Table 4) for 30mins at 4°C. Labelled cells were washed in staining buffer at 1500rpm for 5mins, fixed in fixation buffer (Table 4) for 10mins at RT and washed twice in staining buffer before being run on the LSR Fortessa cell analyser (BD). Single-stain compensation beads (BD) were used for compensation. Data was acquired using FACSDiva software and analysed in FlowJo_V10.

2.7 Stimulation of primary immune cells

2.7.1 Stimulation of ILC2

For stimulation studies, ILC2 were cultured in the presence or absence of IL-33 (50 ng/ml), IL-25 (50 ng/ml) and TSLP (50 ng/ml) individually or in combination in ILC2 medium or moDC medium (for moDC studies) in the presence of IL-2 (200 IU/ml) for 6-72h at 37°C and 5% CO2. Cell suspensions were centrifuged at 1500rpm for 5mins and cells were used for qRT-PCR analysis or flow cytometry. Supernatants were frozen at -80°C or used immediately for functional experiments.

2.7.2 MoDC culture in ILC2 supernatants

To assess the effect of ILC2-derived soluble factors on moDC survival, phenotype and differentiation, moDC were collected on d3 or d5 of differentiation, careful only to collect non-adherent cells, and cultured at $0.5x10^6$ cells/well in unstimulated or IL-33, IL-25, TSLP-stimulated ILC2 supernatants in a 48-well non-coated plate for 48h. Cell surface marker expression was assessed by flow cytometry.

To assess the effect of ILC2-derived soluble factors on moDC CCL22 and CCL17 secretion, d5 moDC were collected, cultured in moDC medium without IL-4/GM-CSF for 24h. MoDC were pre-treated for 1h with anti-IL-4Rα antibody (10 µg/ml, clone 25463, R&D MAB230) and anti-IL-13Rα2 (10 µg/ml, polyclonal goat IgG, R&D AF146) or isotype controls (10 µg/ml, goat IgG and mouse IgG2a, R&D) before being cultured in 1000µl unstimulated or IL-33, IL-25, TSLP-stimulated ILC2 supernatants in a 48-well non-coated plate for 24h. Cell culture supernatants were collected and CCL22 and CCL17 concentrations measured by ELISA.

2.7.3 Monocyte culture in ILC2 supernatants

Monocytes were isolated from PBMC by CD14 positive MACS separation. To assess the effect of ILC2-derived soluble factors on monocyte survival and differentiation, $0.5x10^6$ monocytes/well were cultured for 5 days in 1000µl unstimulated or IL-33, IL-25, TSLP-stimulated ILC2 supernatants, moDC medium alone or supplemented with IL-4 (10 ng/ml) and GM-CSF (100 ng/ml) in a 48-well non-coated plate. On d5 of culture, cells were collected, counted and analysed by flow cytometry.

To assess the effect of ILC2-derived IL-4 and/or GM-CSF on monocyte survival and differentiation, monocytes were resuspended in moDC medium and pre-treated for

1h with anti-IL-4Rα antibody (10 µg/ml, clone 25463, R&D: MAB230) or isotype controls (10 µg/ml, mouse IgG2a, R&D) or left untreated. Supernatants from unstimulated or IL-33, IL-25, TSLP-stimulated ILC2 were incubated for 1h with neutralising anti-GM-CSF antibody (50 µg/ml, BVD2-21C11, Biolegend: 502320) or isotype control (50µg/ml, rat IgG2aκ, Biolegend). $0.2x10^6$ monocytes/well were cultured for 5 days in 200µl ILC2 supernatants in the presence or absence of anti-IL-4Rα blocking antibody, anti-GM-CSF neutralising antibody or isotype controls in a 96-well non-coated plate, and half of the ILC2 supernatants ± antibodies/isotypes replaced on d3 of culture. On d5 of culture, cells were collected, counted and analysed by flow cytometry.

2.8 Chemotaxis assay

Chemotaxis assays were performed using HTS Transwell 96-well plates with 5µm pore filters (Corning Costar 3388). Migration after 1h was assessed by live imaging microscopy (IncuCyteS3 Live-Cell Analysis System, Sartorius). The confluency of the cells in the lower chamber, after removal of the upper chamber, was determined using the IncuCyte S3 Software (Sartorius) and calculated against the confluence of cells of known cell counts. Migration index was determined as the number of migrated cells relative to the random migration.

2.8.1 Titration studies

$0.15x10^6$ sorted $CCR4^+$ T cells in 100µl R10 medium were applied to the upper chamber and incubated for 1h at 37°C, 5% CO2. 3-fold serial dilutions (top concentration: 1500 ng/ml in R10 medium) of CCL22 and CCL17 were applied to the lower chamber. R10 medium was used as a negative control (random migration). For inhibition studies, CCL22 (10 ng/ml) and/or CCL17 (10 ng/ml) were

incubated for 1h with 2-fold serial dilutions (starting concentration 10 µg/ml) of neutralising anti-CCL22 (clone A15083D, Biolegend 694403) and/or anti-CCL17 (clone 54026, R&D MAB364).

2.8.2 ILC2 and T cell chemotaxis to recombinant proteins

Migration of $0.15x10^6$ ILC2 or T cells (MACS purified and rested for 3 days in ILC2 medium with 200 IU/ml IL-2) in 100µl R10 medium in the upper chamber was assessed to CCL22 (10 ng/ml) or CCL17 (10 ng/ml) in the absence or presence of anti-CCL22 (10 µg/ml), anti-CCL17 (10 µg/ml) or mouse IgG2aκ (10 µg/ml, R&D) and mouse IgG1 (10 µg/ml, R&D) isotype controls in the lower chamber. R10 medium in the absence or presence of neutralising antibodies or isotypes was used as the negative control.

2.8.3 ILC2 or T cell chemotaxis to ILC2 supernatants

Migration of $0.15x10^6$ ILC2 or T cells in 100µl ILC2 medium in the upper chamber was assessed to supernatants from unstimulated or stimulated ILC2 in the presence of anti-CCL22 (10 µg/ml), anti-CCL17 (10 µg/ml) or isotype controls (10 µg/ml) in the lower chamber. ILC2 medium in the presence of neutralising antibodies or isotypes was used the negative control.

2.8.4 ILC2 chemotaxis to moDC supernatants

Migration of $0.15x10^6$ ILC2 in 100µl moDC medium in the upper chamber was assessed to supernatants from moDC treated with ILC2 supernatants, diluted in moDC medium, in the presence of anti-CCL22 (10 µg/ml), anti-CCL17 (10 µg/ml) or isotype controls (10 µg/ml) in the lower chamber. MoDC medium in the presence of neutralising antibodies or isotypes was used the negative control.

2.9 Co-culture of ILC2-induced moDC and CD1a-reactive T cell clones

$0.15x10^6$ ILC2-induced moDC or control moDC were co-cultured with $0.1x10^6$ CD1a-reactive T cell clones in 96-well flat-bottom plates for 24h in the presence of IL-12 (1 ng/ml), IL-18 (1 ng/ml) and IL-2 (25 IU/ml). Prior to co-culture, moDC were treated for 1h with anti-HLA-ABC (10 µg/ml, clone W6/32, Biolegend 311402), HLA-DR (10 µg/ml, clone L243, Biolegend 307602) blocking antibodies and/or anti-CD1a blocking antibody (10 µg/ml, clone HI149, Biolegend 300102). Following 24h co-culture at 37°C, 5% CO2, cell suspensions were centrifuged at 1500rpm for 5mins, cells stained for flow cytometry and supernatants stored at -80°C for IFN-γ ELISA.

2.10 Bioinformatic analysis

Bioinformatics analysis was performed by Dr Jeongmin Woo. SOMAscan RFU values were log2 transformed and Luminex concentration values were pre-processed by log2(concentration+1) prior to downstream analysis (Fig. A.3). Principal component analysis (PCA) was performed using R's prcomp() function and PCA plots were generated using R's plotly package (version 4.9.2.1). Differential protein expression analysis of the SOMAscan and Luminex ILC2 supernatant datasets was performed using R's linear models for microarray data (limma) package (version.3.42.2) followed by Benjamini-Hochberg (BH)-multiple testing correction (216). For the Luminex ILC2 supernatant dataset, batch correction was performed using the removeBatchEffect() function of R's limma package. For Luminex serum and blister fluid datasets, which didn`t require consideration of batch effects, differential protein expression analysis was performed by Student's *t*-tests followed by BH- multiple testing correction. Heatmaps were generated using R's pheatmap package (version 1.0.12). Univariate and multivariate logistic regression

models of the Luminex serum dataset were generated using R's rstanarm package (version 2.21.1).

2.11 Statistical analysis

One- and two-way ANOVA tests with Tukey's or Sidak's post hoc multiple comparison tests, paired and unpaired Student's *t*-tests or non-parametric Wilcoxon matched-pairs tests were performed using GraphPad Prism version 9.00 (GraphPad Software), as indicated in the figure legends.

2.12 Illustrations

Illustrations were created on BioRender.com

Chapter 3: Investigation of cutaneous and systemic immune responses in AD and the potential contribution of ILC2

3.1 Introduction

3.1.1 Cytokines

Cytokines are key modulators of the immune system, initiating, coordinating, and regulating both innate and adaptive immune responses. Cytokines have context-dependent roles and can act on target cells in an autocrine, paracrine and endocrine manner. Pro-inflammatory cytokines play critical roles in the defence against pathogens by alerting other immune cells to the presence of infectious agents or danger signals. In contrast, anti-inflammatory cytokines, such as IL-10 and TGF-β, act to limit immune responses, prevent immunopathology and promote repair. However, dysregulated, chronic or inappropriate expression of pro-inflammatory cytokines contributes to the development of autoimmune diseases and allergic inflammatory disorders (217, 218). It is increasingly being recognised that some cytokines may have pleiotropic functions, acting in both immunostimulatory and immunosuppressive ways depending on the microenvironment (219).

3.1.2 Chemokines

Selective recruitment of distinct effector immune cells to sites of inflammation, injury or infection is essential for the establishment of effective immune responses. Migration of circulating immune cells from the bloodstream into tissues is mediated in a step-wise manner involving selectin-mediated tethering to endothelial cells of blood vessels, rolling along the blood vessel wall, integrin-dependent firm adhesion and arrest, and finally chemokine-induced extravasation and migration into underlying tissues. The interaction between chemokine ligands and their cognate

G-protein-coupled receptors guides leukocyte trafficking along a chemokine gradient (220, 221). *In vitro* experiments have established that chemokine receptors frequently have more than one ligand (Table 5). This redundancy has been proposed to impart robustness in the chemokine system (222). However, it is believed that there are temporal and spatial control mechanisms within the chemokine system *in vivo* that confer a higher degree of specificity than observed *in vitro*. Factors including sequential chemokine activity in specific tissue sites, differences in binding affinities, differential induction of receptor internalisation and desensitisation might determine the biological response and outcome (221, 223).

Table 5 Chemokine receptors and their cognate ligands and target cells.

CXCL, C-X-C chemokine ligand; CXCR, C-X-C chemokine receptor. Adapted from (224, 225).

Receptor	Ligand	Target cell
CCR1	CCL3, CCL5, CCL7, CCL14, CCL23	T cells, monocytes, eosinophils, basophils
CCR2	CCL2, CCL8, CCL7, CCL13, CCL16	Monocytes, immature DC, memory T cells
CCR3	CCL11, CCL24, CCL26, CCL7, CCL5, CCL8, CCL13	Eosinophils, basophils, mast cells, Th2 cells
CCR4	CCL17, CCL22	Th2 cells, skin-homing T cells, Th17 cells, Tregs, DC, basophils, macrophages
CCR5	CCL3, CCL4, CCL5, CCL11, CCL14, CCL16, CCL23	Naïve CD8+ T cells, Th1 cells, cytotoxic CD8+ T cells, monocytes
CCR6	CCL20	Th17 cells, memory T cells, B cells, DC
CCR7	CCL19, CCL21	Naïve T cells, memory T cells, mature DC
CCR8	CCL1, CCL8	Th2 cells, Tregs, skin-homing γδ T cells, monocytes, DC
CCR9	CCL25	Gut-homing T cells

CCR10	CCL27	Skin-homing T cells
CXCR1	CXCL8, CXCL6	Neutrophils, monocytes, cytotoxic CD8+ T cells
CXCR2	CXCL8, CXCL1, CXCL2, CXCL3, CXCL5, CXCL6	Neutrophils, monocytes
CXCR3	CXCL9, CXCL10, CXCL11	Th1 cells, cytotoxic CD8+ T cells, Th17 cells, NKT cells, mast cells
CXCR4	CXCL12	Memory T cells, naïve T cells, widely expressed
CXCR5	CXCL13	Follicular helper T cells, B cells
CXCR6	CXCL16	CD8+ T cells, NK cells, NKT cells, memory CD4+ T cells
CX3CR1	CX3CL1	Macrophages
XCR1	XCL1, XCL2	T cells, NK cells

3.1.3 The pathogenesis of AD

AD is a common pruritic inflammatory skin disease that affects approximately 11-20% of children and 5-10% of adults in the UK and is associated with epidermal barrier defects and dysregulated type 2 inflammation (226).

3.1.3.1 Role of dysfunctional skin barrier in AD pathogenesis

There is longstanding evidence that defects in epidermal barrier function contribute to the pathogenesis of AD. Epidermal barrier integrity is maintained by barrier structures, such as the stratum corneum and tight junctions (227, 228). The protein filaggrin is thought to play a critical role in the formation of a functional stratum corneum barrier. Loss-of-function mutations in *FLG*, the gene encoding filaggrin, have been identified as a major predisposing factor for the development of AD (229). Reduced filaggrin expression has been reported in both non-lesional and lesional skin of patients with AD (230) and filaggrin-deficient mice spontaneously develop

AD-like skin lesions (231, 232). However, *FLG* loss-of-function mutations are rare (233), which suggests contribution of other genetic and environmental factors to AD pathogenesis. Tight junctions contribute to epidermal barrier function by sealing intercellular spaces and limiting paracellular leakage of water-soluble molecules. Reduced expression of the key tight junction protein claudin-1 has been detected in the epidermis of patients with AD, which implies an involvement of epidermal tight junction defects in the development of AD (228). Furthermore, changes in the skin lipid content, such as reduction of phospholipids, sterol esters and ceramides, have been suggested to contribute to defective skin barrier function in AD (227). Epidermal barrier dysfunction not only allows penetration of exogenous allergens, but also bacterial, viral and fungal pathogens. Indeed, *Staphylococcus aureus* skin colonisation is a common feature of AD and positively correlates with disease severity (234).

3.1.3.2 Role of dysregulated immune responses in AD pathogenesis

AD is associated with a strong type 2 immune response, characterised by increased production of type 2 cytokines, elevated serum IgE levels, and accumulation and activation of innate and adaptive immune cells, including eosinophils, mast cells, ILC2 and Th2 cells. Epithelial release of alarmins, such as IL-33, IL-25 and TSLP, may form a critical link between dysfunctional skin barrier and type 2 inflammation in AD (235). Skin exposure to allergens, such as HDM, and mechanical skin injury, such as scratching, triggers the release of alarmin cytokines from keratinocytes. Increased levels of IL-33 (93, 236), IL-25 (93, 237) and TSLP (238) have been detected in AD lesional skin. A further increase in the expression of IL-33 and its receptor ST2 in lesional AD skin was observed following exposure to HDM or *S.*

aureus-produced enterotoxin (236). In mice, cutaneous IL-33 overexpression resulted in spontaneous AD-like skin inflammation accompanied by increased type 2 cytokine levels and accumulation of ILC2, eosinophils and mast cells (239). Treatment of moderate-to-severe AD patients with the anti-IL-33 monoclonal antibody etokimab (240) or the anti-TSLP monoclonal antibody tezepelumab improved AD symptoms (241), highlighting the role of alarmins upstream of dysregulated type 2 immunity in AD.

Type 2 cytokines are critical in the development and exacerbation of AD. Lesional AD skin is characterised by increased IL-4, IL-5 and IL-13 expression (242, 243). The contribution of type 2 cytokines to AD pathogenesis is highlighted by the efficacy of a human monoclonal antibody against IL-4Rα, dupilumab, in the treatment of moderate-to-severe AD (244). While the acute phase of AD is dominated by an exacerbated type 2 immune response, evidence exists for a role of type 1 cytokines, such as IFN-γ and IL-1β, and Th17-associated cytokines, including IL-17A, during the chronic phase of the disease (245). Chronic AD lesions are characterised by upregulated expression of type 1 cytokines and IL-17A in addition to persistently high levels of type 2 cytokines (246).

Accumulating evidence exists for an exacerbation loop between barrier defects and dysregulated immune responses. Cytokines associated with type 2 inflammation have been demonstrated to aggravate barrier dysfunction by downregulating the expression of structural proteins. Treatment of keratinocytes with IL-33 (247), IL-25 (237) or IL-4 and IL-13 (248) resulted in downregulated filaggrin expression. Moreover, IL-4 and IL-13 have been shown to suppress the expression of proteins important to epidermal barrier formation and integrity, such as loricrin and involucrin

(249). Improvement of AD symptoms following treatment with dupilumab was associated with increased expression of genes encoding proteins with roles in epidermal barrier formation and integrity, such as filaggrin, loricrin and claudins (250).

While it is unclear whether skin barrier dysfunction predates cutaneous inflammation, known as the “outside-in” hypothesis, or whether dysregulates immune responses mediate barrier breakdown, referred to as the “inside-out” hypothesis (251), it has become evident that AD is a multifactorial disease involving complex interactions between genetic, environmental and immunological factors.

3.1.4 Role of ILC2 in AD inflammation

As potent type 2 cytokine-producers, ILC2 have been implicated in AD immunopathology. Increased frequencies of ILC2 have been reported in lesional biopsies from AD patients (93, 141, 252) as well as non-lesional skin from AD patients with filaggrin mutations (253). ILC2 in AD lesions were found to display an activated phenotype with increased expression of receptors for IL-33, IL-25 and TSLP (93). Increased expression of the ILC2 activatory NKp30 ligand B7-H6 was observed in AD lesional skin and type 2 cytokines induced the upregulation of B7-H6 on keratinocytes (164). Moreover, expression of the ILC2-inhibitory molecule E-cadherin was found to be reduced in AD lesions (93). Thus, increased expression of ILC2 stimulatory signals couples with loss of suppressive signals might result in ILC2 dysregulation in AD skin.

Murine studies have revealed a critical role for ILC2 in promoting the development of cutaneous inflammation independent of adaptive lymphocytes. IL-33-induced spontaneous AD-like inflammation was associated with an accumulation of IL-5- and

IL-13-producing ILC2 in lesional skin (239). In the absence of adaptive lymphocytes, IL-2 treatment induced expansion of activated IL-5-producing dermal ILC2 and the development of spontaneous dermatitis (11). Depletion of ILC2, but not T or B cells, resulted in diminished cutaneous inflammation (93, 254). Mechanistically, ILC2 have been proposed to contribute to AD inflammation through type 2 cytokine production and the subsequent activation of inflammatory immune cells including eosinophils, basophils and mast cells (254, 255). Through type 2 cytokine production, particularly IL-13, ILC2 may contribute to the downregulation of epidermal protein expression, such as filaggrin (248), loricrin and involucrin, and consequently epidermal barrier dysfunction.

3.1.5 Hypothesis and aims

It has become evident that multiple factors contribute to AD pathogenesis, including genetic predisposition, skin barrier dysfunction and dysregulated immune responses. I hypothesised that the cutaneous microenvironment and the local immune response may be significantly altered in individuals with AD. An *in vivo* human skin blister allergen challenge model was used to profile the proteome of healthy and AD skin at steady state and following exposure to common environmental allergens (Fig. 3.1, A). With the aim to characterise systemic immune responses in AD, multi-analyte profiling was performed on sera from individuals with or without AD with a focus on chemokine and cytokine expression (Fig. 3.1, B). While dysregulated ILC2 responses have been implicated in AD pathogenesis through production of type 2 cytokines, less is known about the secretion of other pro-inflammatory cytokines and chemokines by human ILC2. This project aimed to analyse the cytokine and chemokine expression profile of activated human ILC2 and

investigate the potential contribution of ILC2 in cutaneous inflammation. The gene expression profile of skin ILC2 in response to allergen challenge was analysed by bulk RNA-sequencing on ILC2 from skin suction blister fluids following intradermal HDM challenge (Fig. 3.1, A). Moreover, ILC2 cytokine and chemokine production in response to alarmin stimulation was assessed by Luminex multi-analyte profiling (Fig. 3.1, B).

The objectives of this project included:

a. Perform large-scale proteomics on healthy and AD skin during steady state and following intradermal challenge with common environmental allergens
b. Determine specific concentrations of cytokines and chemokines in healthy and AD skin
c. Compare cytokine and chemokine concentrations in sera from individuals with AD and healthy controls
d. Assess cytokine and chemokine expression by human ILC2 at both the gene and protein level
e. Identify mechanisms by which ILC2 may contribute to allergic inflammation

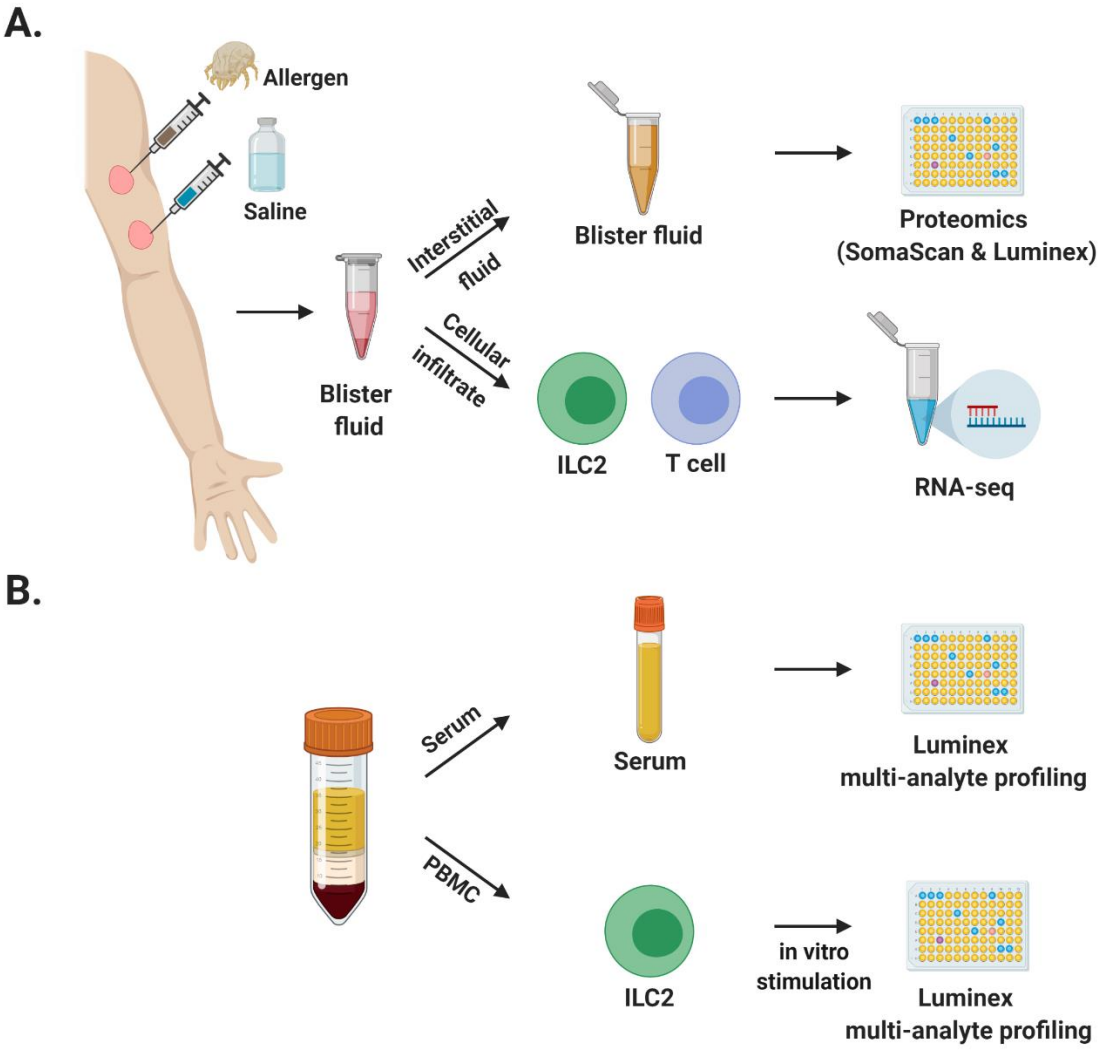


Figure 3.1 Study design.

(**A**) Skin suction blisters were formed on the upper arms of individuals with AD and healthy volunteers following intradermal injection of allergens or saline. After 24h, skin suction blister fluids were collected and protein content in the interstitial fluid analysed by SOMAscan assay and Luminex multi-analyte profiling. ILC2 and T cells were isolated from skin suction blister fluids by FACS and gene expressed analysed by bulk RNA-sequencing. (**B**) Peripheral blood was taken from individuals with AD and healthy controls and separated by density gradient centrifugation. Protein expression in sera was analysed by Luminex multi-analyte profiling. ILC2 were isolated by FACS, expanded *in vitro* and protein production following stimulation assessed by Luminex multi-analyte profiling.

3.2 Results

3.2.1 Comparison of the protein signature of healthy and AD skin

3.2.1.1 SOMAscan analysis of the skin proteome of individuals with AD and healthy volunteers

To profile the cutaneous microenvironment during steady state and allergic inflammation, large scale proteomics was performed on skin suction blister fluids following intradermal injection of saline or common environmental allergens including HDM and ALT.

3.2.1.1.1 Study design and participants

In collaboration with SomaLogic, an aptamer-based proteomic technology, called SOMAscan assay, was used to perform proteomics on skin suction blister fluids. The SOMAscan platform enables detection of 1305 human protein analytes simultaneously by using so called slow off-rate modified DNA aptamers (SOMAmers), single-stranded oligonucleotides that capture proteins with high affinity and specificity. Protein expression is measured as a proportional quantity of a specific SOMAmer by hybridisation to a DNA microarray (215).

Table 6 Study participants

Participants (Disease status)	Intradermal Challenge	Number of Participants
Healthy control (HC)	Saline (Nil)	5
	House dust mite (HDM)	5
Atopic asymptomatic (AA)	Saline (Nil)	2
	House dust mite (HDM)	4
Atopic dermatitis (AD)	Saline (Nil)	4
	House dust mite (HDM)	7
	Alternaria alternata (ALT)	4
	Lesional skin (Eczema)	5

A total of five healthy controls (HC), seven individuals with AD and four atopic asymptomatics (AA), patients with diagnosed allergies who did not suffer from AD, were enrolled in this study (Table 6). All participants were challenged intradermally with the allergen HDM. Data for one HC HDM blister fluid was identified as an outlier and excluded from analysis (Fig. 3.2). To analyse the proteome of AD lesional skin, skin suction blisters were formed over AD lesions. As the formation of skin suction blisters and collection of blister fluids was not always successful, the number of samples analysed may vary between challenge conditions. For example, AA blister fluids following saline injection were only successfully collected from two donors (Table 6). Therefore, analysis of the proteomic data focused on the results from HC and AD patients following saline or HDM challenge. The bioinformatic data presented in the chapter were analysed with the help of Dr Jeongmin Woo.

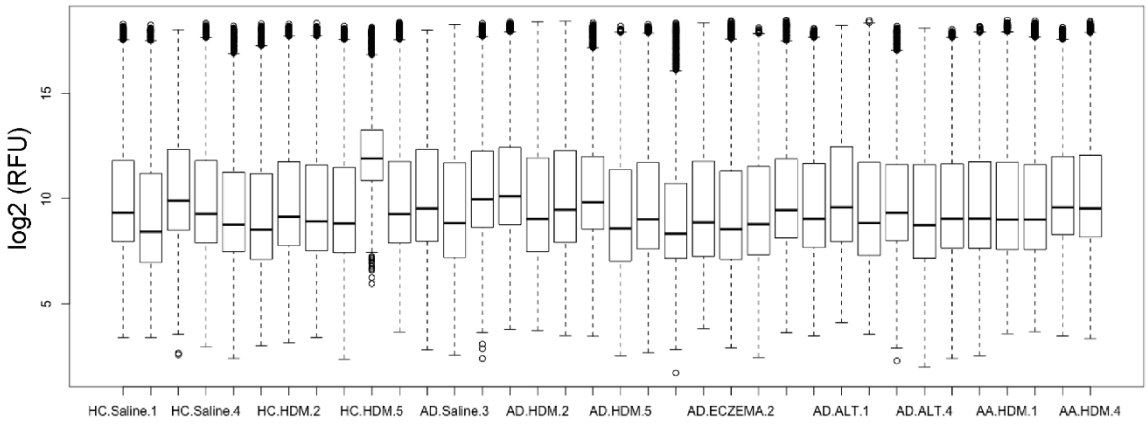


Figure 3.2 Distribution of skin blister fluid SOMAscan data.

Data distribution of log2 transformed SOMAscan skin suction blister fluid results. The readout of the SOMAscan assay is relative fluorescent units (RFU). Outlier HC.HDM.5 was removed from further analysis.

3.2.1.1.2 Comparison of healthy, atopic asymptomatic and AD cutaneous protein expression profiles

Unbiased dimensionality reduction analysis of the SOMAscan dataset with principal component analysis (PCA) revealed separation of HC and AD samples with AA samples interspersed between HC and AD samples. AD samples clustered into two distinct groups, labelled AD_1 and AD_2, based on the cutaneous protein profile (Fig. 3.3, A). To identify confounding factors splitting the AD samples into 2 clusters, samples were labelled according to the type of intradermal challenge administered. AD_2 group contained three HDM samples and one sample of each saline, ALT and lesional skin (Fig. 3.3, B).

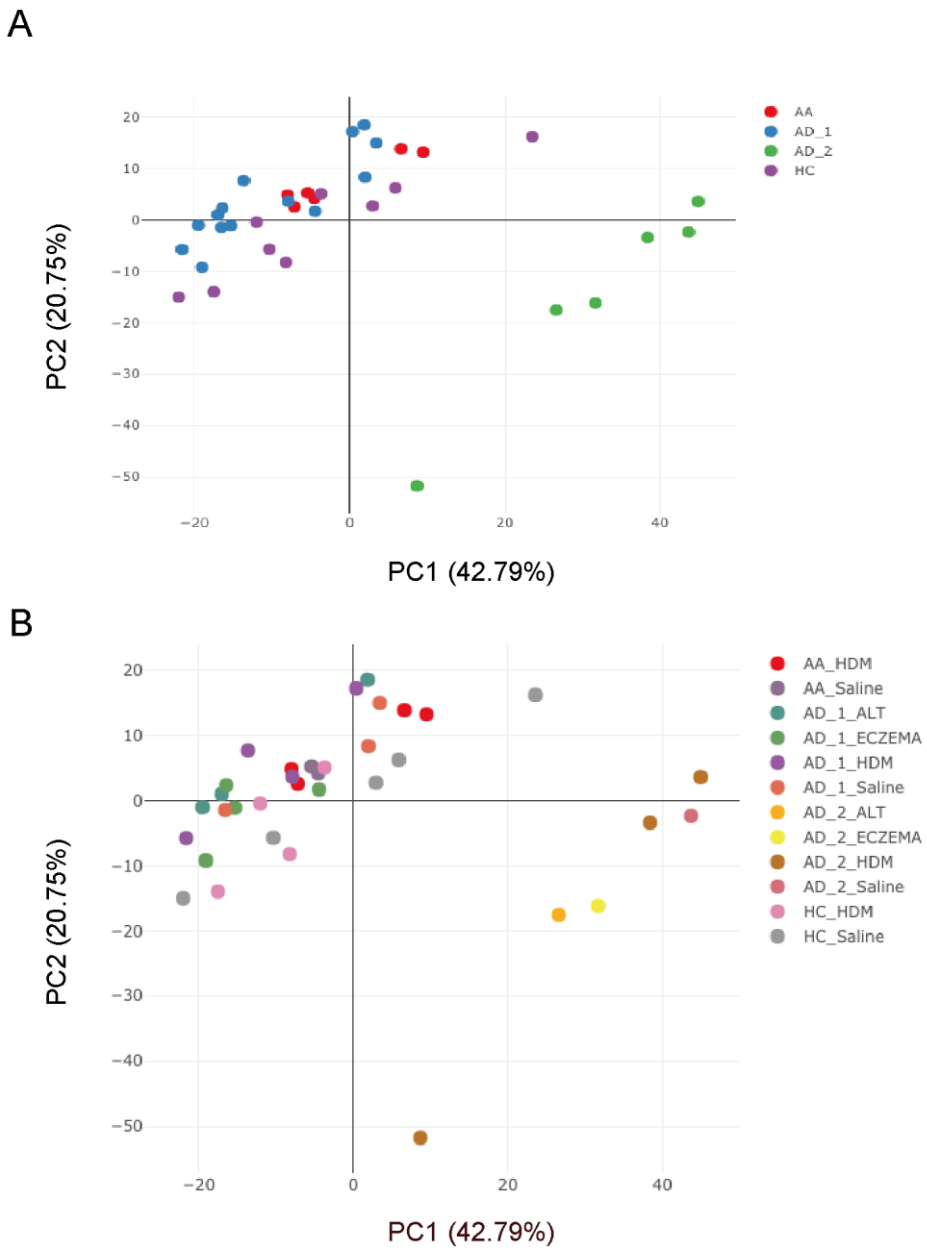


Figure 3.3 Two-dimensional PCA of SOMAscan skin proteomic data.
(**A and B**) PCA was performed on log2 normalised RFU data of 1305 proteins, generated by SOMAscan assay. Two-dimensional PCA plot showing sample disease status (HC, AD and AA) (**A**) and type of intradermal challenge administered (**B**). Each dot represents a challenge condition. (n=16; data representative of 1 independent experiment).

Given that HC and AD samples appeared to cluster separately in the dimensionality reduction analysis, differences in the cutaneous protein expression profile were investigated in more detail. Increased total protein expression was found in blister

fluids from AA individuals compared to HC, as visualised in volcano plots and heatmaps (Fig. 3.4, A). Nine differentially expressed proteins (DEP) were identified between AA and HC blister fluids, including epidermal growth factor (EGF) and eight intracellular proteins (BH-adj. p-value < 0.05; log2FC > 1). The chemokines CXCL10, CXCL11 and CCL7 and the cytokine IL-6 were found to be upregulated and the cytokine IL-36A downregulated in AA compared to HC samples (log2FC > 1), however did not pass BH correction for multiple comparisons (Fig. 3.4, A). 35 proteins were found to be differentially expressed in AD_1 compared to HC blister fluids, including IgE, IL-22 and CCL23 upregulated in AD_1, and IL-20, which was found to be significantly downregulated in AD_1 compared to HC samples; and IL-20 has previously been implicated in psoriasis (256). However, the majority of DEPs were identified as intracellular proteins (Fig. 3.4, B). Distinct protein profiles were observed in AD_2 compared to HC blister fluids, as evident by the identification of 414 DEPs and distinct hierarchical clustering (Fig. 3.4, C). Significant upregulation of intracellular proteins and secreted proteins associated with type 2 inflammation (IL-4, IL-5, IL-9, CCL2, CCL7, CCL13, CCL24), type 1 responses (IFN-γ), Th17 cells (IL-22, IL-17D), neutrophil recruitment (CXCL8), complement activation (C5), tissue remodelling (TGF-β, matrix metalloproteinases) and allergy (IgE) was observed in AD_2 compared to HC blister fluids (Fig. 3.4, C).

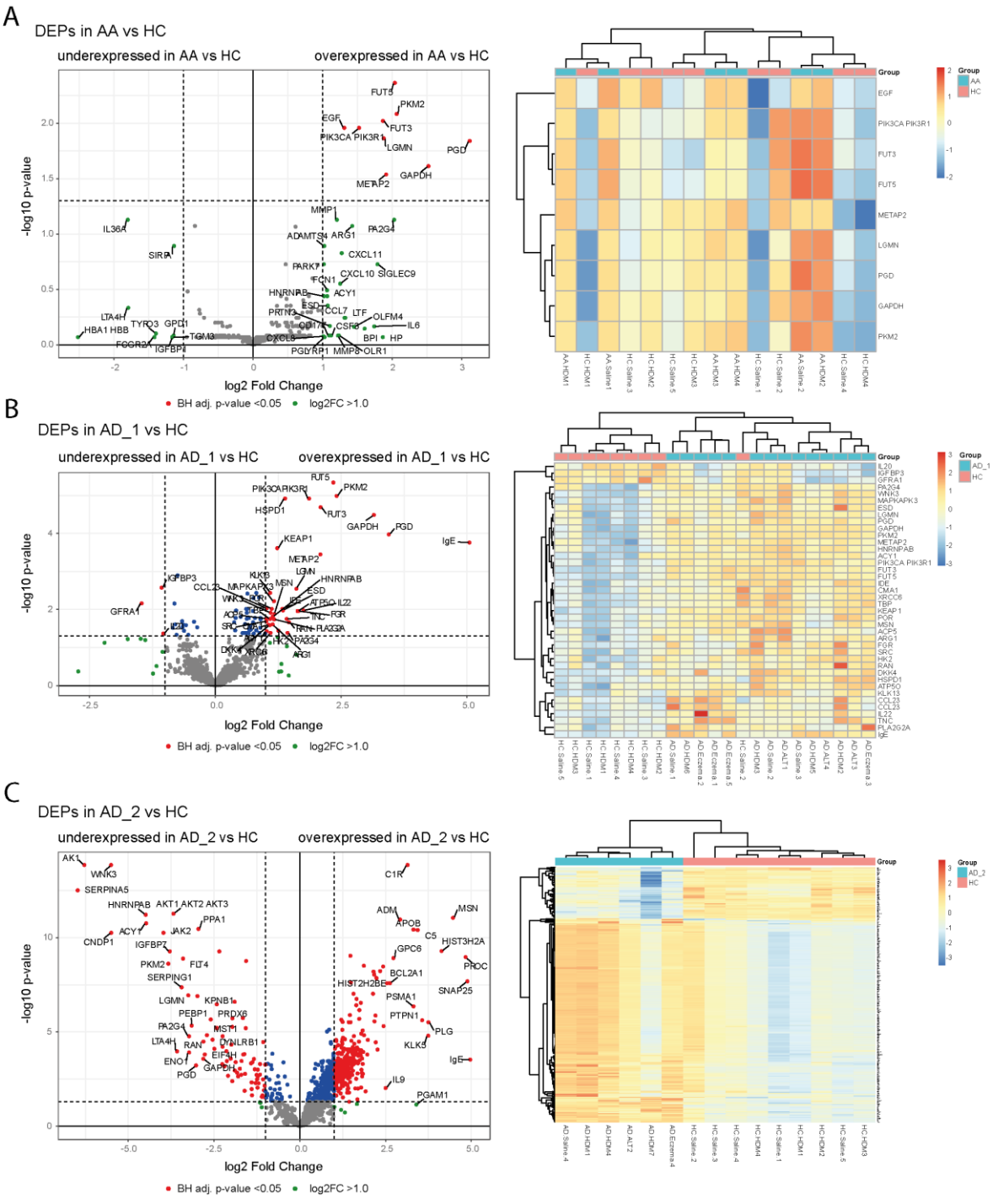


Figure 3.4 Comparison of proteomic data of HC, AA and AD skin.

(**A-C**) Volcano plots and heatmaps visualising differences in the cutaneous protein expression profile of AA vs HC samples (**A**), AD_1 vs HC (**B**) and AD_2 vs HC (**C**). DEPs were identified by limma followed by BH-multiple testing correction (BH-adjusted p-value < 0.05; log2FC > 1.0). (n=4-7 in each challenge condition; data representative of 1 independent experiment).

3.2.1.1.3 Investigation of factors responsible for separate clustering of AD_1 and AD_2 blister fluid SOMAscan data

To further investigate the factors responsible for the observed separation of the AD sample data, fold change differences in protein expression of AD_1 and AD_2 relative to HC samples were compared and visualised in a four-way plot. 476 proteins were found to be differentially expressed between AD_1 and AD_2 samples (BH-adj. p-value < 0.05; log2FC > 1). Immune-related proteins were found to be primarily upregulated in AD_2 samples. However, DEPs in AD_1 or AD_2 samples included intracellular proteins. For example, the serine/threonine kinase WNK3 and the adenylate kinase enzyme AK1 were differentially upregulated in the AD_1 cluster. Similarly, the intracellular proteins SNAP25, involved in synaptic vesicle membrane docking, and PSMA1, a component of the 20S core proteasome complex involved in intracellular proteolytic degradation, were found to be differentially upregulated in AD_2 samples. (Fig. 3.5, A). Due to similarities of SOMAscan with gene expression microarray, functional enrichment analysis was performed on DEPs between AD_1 and AD_2 by gene ontology (GO) enrichment analysis. We observed enrichment of terms related to T cell activation and other immune processes such cell adhesion, lymphocyte activation and leukocyte migration. Consistent with the identification of intracellular proteins as DEPs, functional enrichment analysis revealed enrichment of terms related to intracellular signalling pathways such as peptidyl-tyrosine modification, regulation of peptidase activity and ERK1/ERK2 cascade (Fig., 3.5, B). Shared differentially upregulated proteins in AD samples included immune-related proteins such as IgE, IL-9 and IL-22. There were no obvious clinical differences in term of disease phenotype or severity.

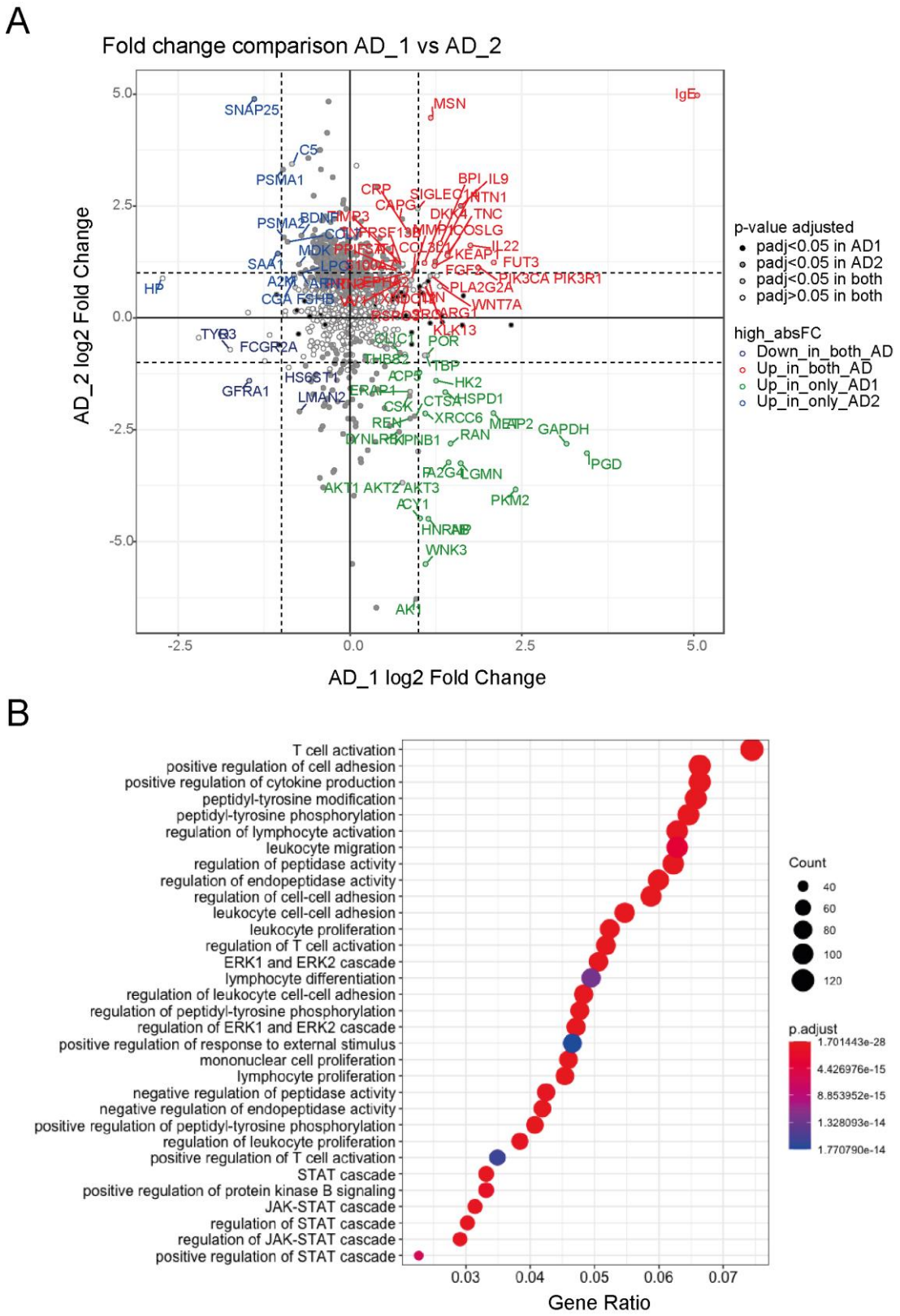


Figure 3.5 Comparison of AD_1 vs AD_2 clusters.

(**A**) Four-way plot visualising log2 fold change differences between AD_2 and AD_1 clusters relative to HC samples. (BH-adjusted p-value < 0.05; log2FC > 1.0. (**B**) Gene ontology (GO)

enrichment analysis of differentially expressed proteins between AD_1 and AD_2 clusters using entire human gene list. x-axis refers to ratio of differentially expressed proteins enriched in GO terms, count refers to number of proteins enriched in GO terms. (n=5-7 in each challenge condition; data representative of 1 independent experiment).

3.2.1.1.4 Effect of intradermal allergen challenge on cutaneous protein expression

Cutaneous exposure to common environmental allergens, such as HDM, has been associated with AD pathogenesis and exacerbation. No significant differences in the protein expression following HDM or ALT intradermal challenge compared to control saline injection were observed in HC or AD_1 blister fluids (Fig. A.4). No comparison could be performed between allergen and saline challenge for AA and AD_2 blister fluids due to low donor numbers. There were no differentially expressed proteins detected between AA and HC following HDM challenge, after BH-correction for multiple comparisons (Fig. 3.6, A). The differentially expressed protein profile of AD_1 or AD_2 compared to HC blister fluid samples following HDM challenge (Fig. 3.6, B and C) resembled results of the overall comparison analysis (Fig. 3.4, B and C). Blister fluids formed over AD lesional skin showed slight, but not significant, differences in protein content compared to non-lesional saline-treated AD skin, such as slight IL-22 overexpression and IL-20 downregulation (Fig. 3.6, D).

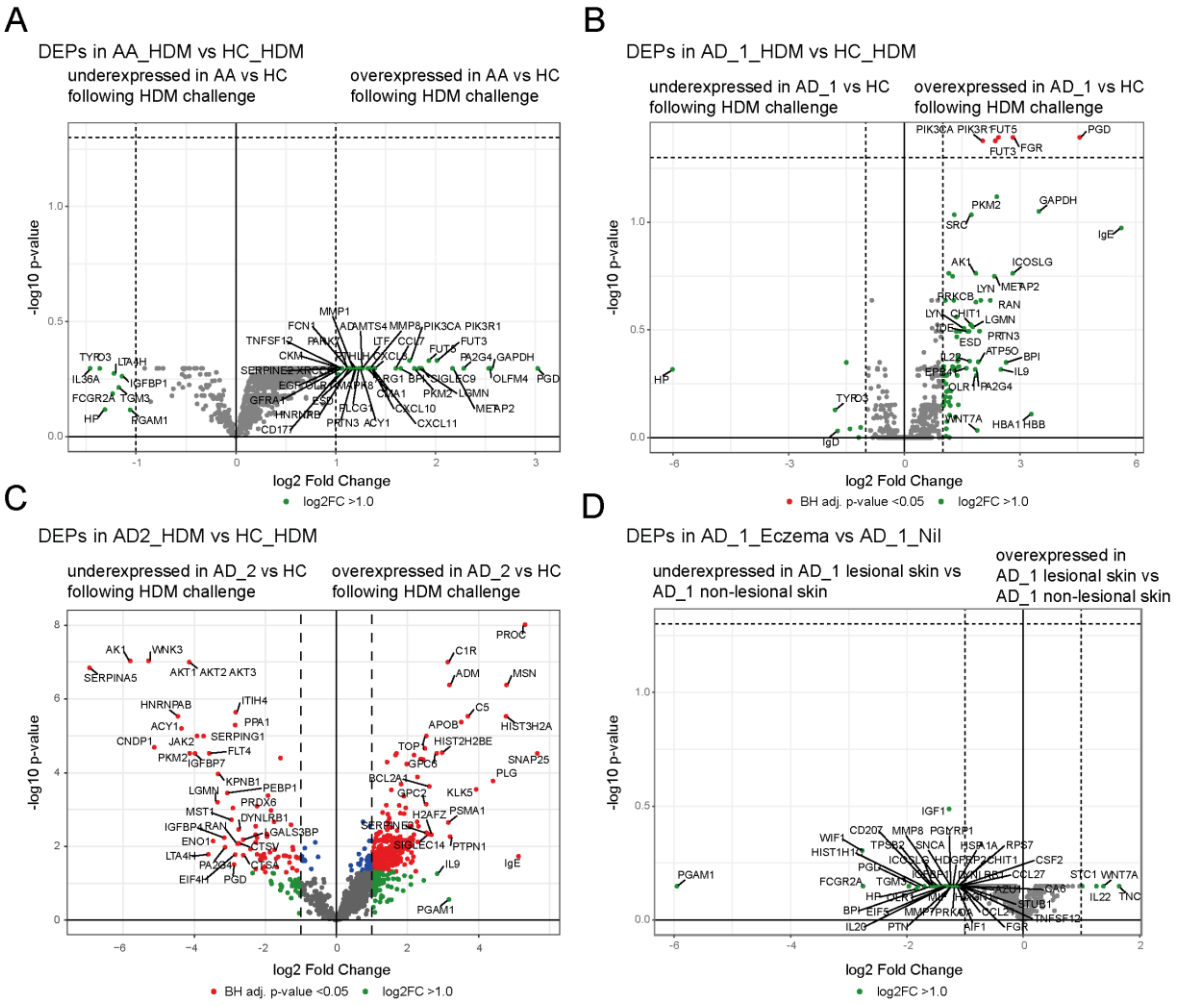


Figure 3.6 Comparison of protein expression profiles of HC, AA and AD skin following intradermal allergen challenge.

(**A-D**) Volcano plots visualising blister fluid protein expression differences following intradermal HDM challenge between AA and HC (**A**) AD_1 and HC (**B**), AD_2 and HC (**C**) and differences between lesional skin and non-lesional saline-treated skin from AD patients (**D**). BH-adjusted p-value < 0.05; log2FC > 1.0. (n=4-7 in each challenge condition; data representative of 1 independent experiment).

3.2.1.1.5 Comparison of cytokine and chemokine expression in healthy and AD skin

The detection of intracellular proteins, potentially due to factors discussed in 3.3.1, resulted in the occurrence of noise in the SOMAscan blister fluid dataset. As dysregulated immune responses have been implicated in AD, further analysis was

performed with a focus on cytokines and chemokines. 98 cytokines and chemokines were included in the SOMAscan assay. Dimensionality reduction analysis by PCA of the blister fluid cytokine/chemokine expression revealed some separation of AD, AA and HC samples, and AD and AA samples located at opposition sides of the PCA plot. Although there appeared to be some clustering of AD samples into separate groups (Fig. 3.7, A), it was less pronounced than was observed for the 1305 protein dataset. Correlation matrix PCA indicated that expression of CCL23, CCL17, IL-22, IL-9 and CX3CL1 was positively correlated and was driving the separation of AD blister fluid data from HC and AA samples. In contrast, IL-6 appeared to contribute to separation of AA blister fluid samples (Fig. 3.7, B). Enrichment analysis of chemokine and cytokine expression in skin suction blister fluids using the AUCell algorithm indicated enrichment of chemokines in AD and AA samples and of cytokines in AD blister fluid, particularly in AD_2 samples (Fig. 3.7, C and D).

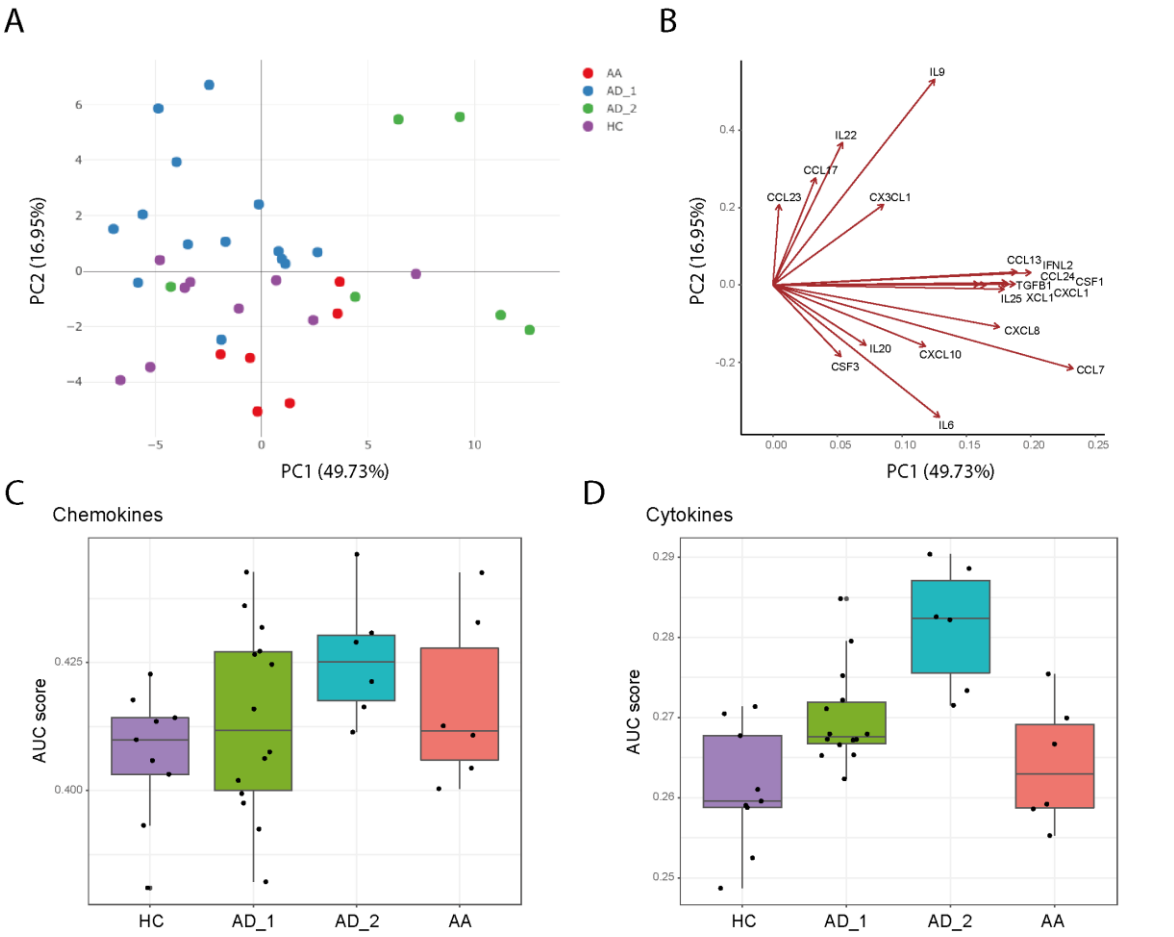


Figure 3.7 Comparison of chemokine and cytokine expression profiles in HC, AD and AA skin.

(**A**) PCA plot of 98 cytokines and chemokines expressed in AD, AA and HC skin suction blister fluids as measured by SOMAscan assay. Each dot represents a challenge condition. (**B**) Correlation biplot of the PCA plot of skin suction blister fluid cytokine/chemokine expression. The direction of each variable arrow indicates the direction of its influence. The angle between the arrows indicates the correlation between the variables. (**C and D**) AUCell analysis of enrichment of 47 chemokines (**C**) and 51 cytokines (**D**) within the SOMAscan blister fluid protein expression dataset. AUC = Area Under the Curve. AUC score indicates the proportion of proteins in the blister fluid dataset that are highly expressed in each group. (n=16; data representative of 1 independent experiment).

3.2.1.2 Luminex multianalyte profiling of chemokine and cytokine levels in healthy and AD skin

While the expression of cytokines/chemokines in human healthy and inflamed skin biopsies has been studied by means of immunohistochemistry and at the mRNA level by real-time PCR, little is known about skin-specific protein concentrations. Our *in vivo* human skin suction blister allergen challenge model provided the opportunity to measure skin-specific protein levels during acute sterile cutaneous inflammation. To validate the results of the SOMAscan analysis and measure cutaneous cytokine and chemokine levels, Luminex multianalyte profiling was performed on skin suction blister fluid samples available after SOMAscan analysis (Table A.1). In contrast to SOMAscan assays, that assess relative protein expression, Luminex assays enable accurate measurements of multiple cytokines/chemokines simultaneously (257). This allowed me to measure concentrations of 26 cytokines/chemokines in blister fluids and compare overall cytokine/chemokine profiles of AD and healthy skin.

3.2.1.2.1 Analysis of overall cutaneous cytokine/chemokine profiles

Dimensionality reduction of the Luminex blister fluid data with PCA indicated a degree of separation of AD samples from HC and AA samples, with three AD samples appearing interspersed between HC and AA samples (Fig. 3.8, A). Correlation matrix analysis implied a role for IL-5 and CCL17 as variables driving separation of most AD samples (Fig. 3.8, B). CCL27 was identified as a DEP that was significantly downregulated in AD compared to HC blister fluids. Distinct clustering of AD and HC samples was observed based on the cytokine/chemokine expression profile (Fig. 3.8 C). Comparison of chemokine/cytokine concentrations between AA and HC or AD blister fluids did not identify any DEP following statistical

correction for multiple comparison. While IL-6 appeared to be slightly upregulated in AA compared to HC and AD samples, several chemokines and cytokines, including CCL17, CX3CL1 and M-CSF, seemed to be downregulated in AA samples (Fig. 3.8, D and E).

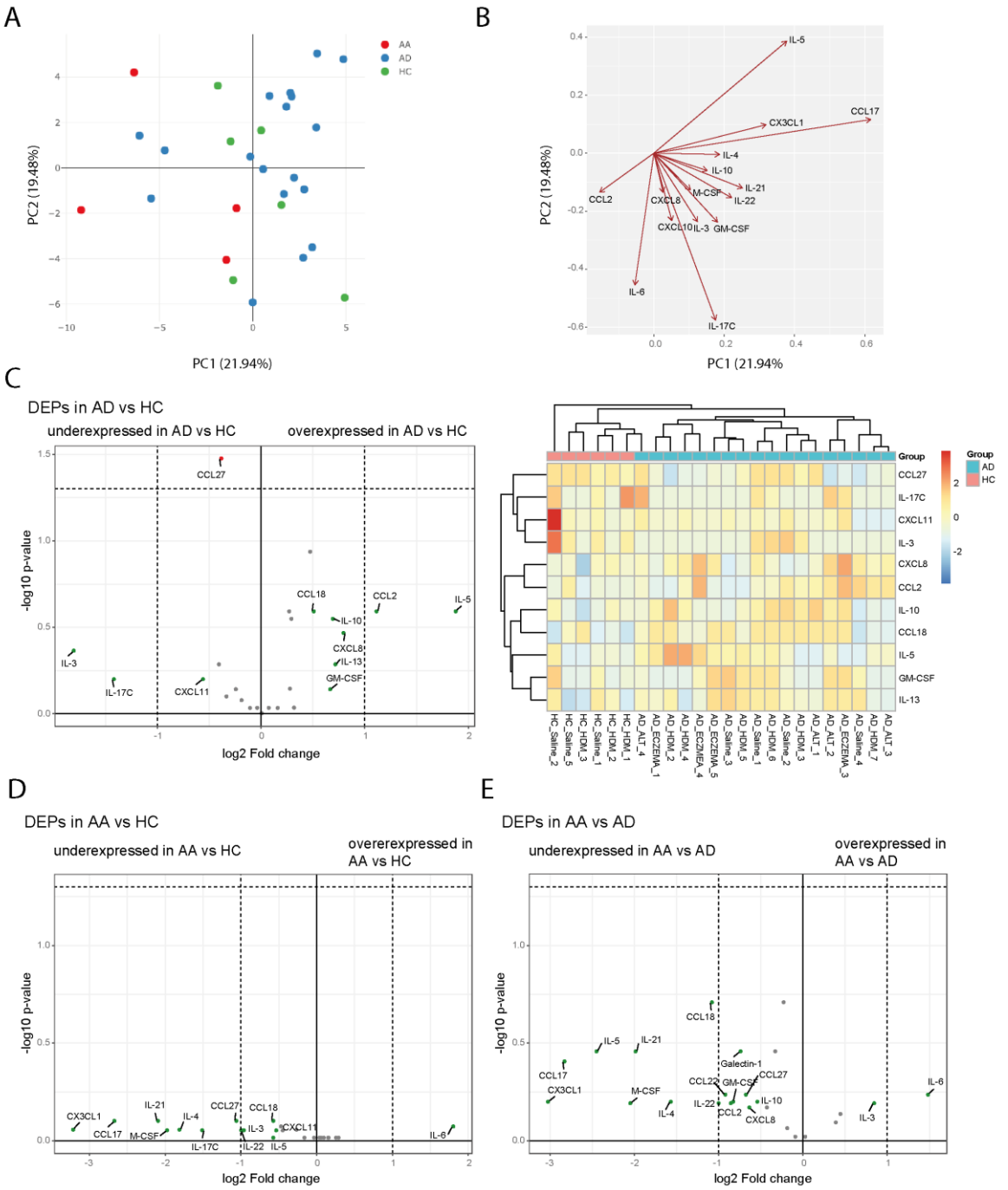


Figure 3.8 Overall comparison of Luminex cytokine/chemokine expression data of HC, AA and AD skin blister fluids.

(**A-E**) Protein concentrations, as measured by Luminex assay, were log2(concentration+1)-transformed prior to downstream analysis. (**A**) PCA plot of 26 cytokine/chemokine concentrations detected in AD, AA and HC skin suction blister fluids. Each dot represents a challenge condition. (n=12). (**B**) Correlation biplot of the PCA of Luminex skin blister fluid results showing structural relationships between cytokine/chemokine variables and their

direction of influence. (**C**) Volcano plot and heatmap visualising DEPs between AD and HC blister fluids. (**D and E**) Volcano plots showing DEPs between AA and HC (**D**) and AA and AD (**E**) samples. DEPs were identified by Student's *t*-test followed by BH-multiple comparison correction. (BH-adj. p-value < 0.05; log2FC > 1.0). (n=1-6 in each challenge condition; data representative of 1 independent experiment).

3.2.1.2.2 Analysis of skin-specific cytokine levels during sterile allergic skin inflammation

To characterise the local cytokine/chemokine response to cutaneous HDM exposure, cytokine/chemokine levels in skin suction blister fluids following intradermal HDM challenge were compared between healthy and AD participants. Luminex assays utilise microspheres conjugated to a specific capture antibody for a particular cytokine of interest. As each microsphere serves as an individual test, concentrations of measured proteins can be analysed individually (257). Likely because of low donor numbers and high donor variability, no statistically significant differences could be observed between cytokine levels detected in healthy and AD blister fluids (Fig. 3.9). The type 2 cytokines IL-4 and IL-5 were detected at relatively low levels in both healthy and AD skin with a slight increase noticed in IL-5 levels in AD blister fluids (Fig. 3.9, A and B). High cutaneous IL-13 levels were measured and appeared to be increased in HDM-challenge AD blister fluids (Fig. 3.9, C). A trend towards increased levels of the pro-inflammatory cytokine IL-22 and the anti-inflammatory cytokine IL-10 in AD compared to HC blister fluids was observed (Fig. 3.9, D and E).

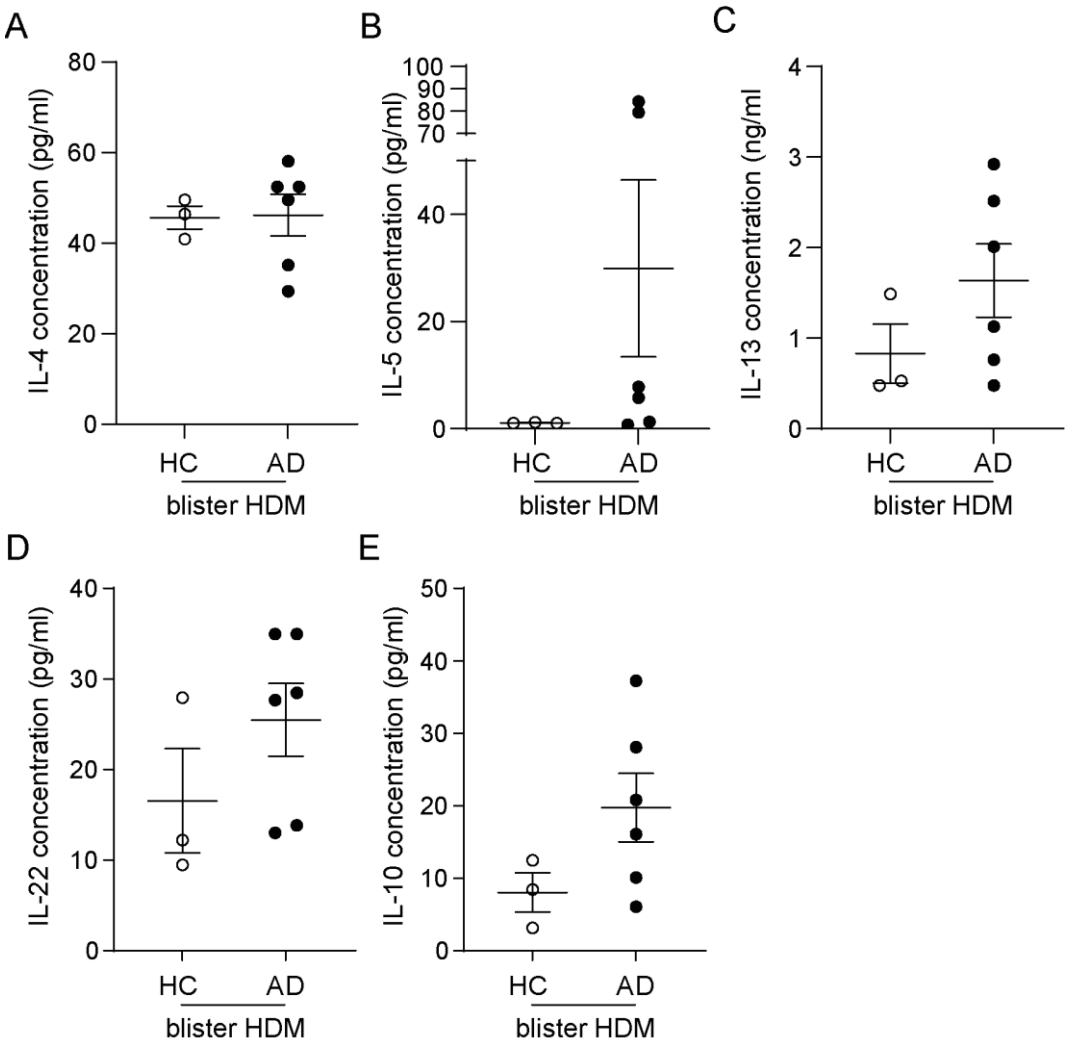


Figure 3.9 Cytokine levels in HC and AD skin blister fluids following intradermal allergen challenge.

(**A-E**) Levels of IL-4 (**A**), IL-5 (**B**), IL-13 (**C**), IL-22 (**D**) and IL-10 (**E**) were measured by Luminex assay in skin suction blister fluids from HC (n=3) and individuals with AD (n=6) following HDM challenge. AD data includes both AD_1 and AD_2 group blister fluids. (n=3-6; data representative of 1 independent experiment). ns with unpaired Student's *t*-test.

3.2.1.2.3 Analysis of skin-specific chemokines levels during sterile allergic skin inflammation

Significantly increased levels of CCL22 were detected in HDM-exposed skin suction blister fluids from individuals with AD compared to HC with average concentration of 13.41 ng/ml and 9.416 ng/ml, respectively (Fig. 3.10, A). CCL17, which binds the

same receptor as CCL22, was also expressed at slightly increased levels in AD compared to HC samples at mean concentration of 5.727 ng/ml and 1.495 ng/ml, respectively (Fig. 3.10, B). Following HDM challenge, there was a trend towards increased concentrations of CCL2 and CXCL8 (Fig. 3.10, C and D) and decreased CXCL10 and CXCL11 (Fig. 3.10, E and F) in AD compared to HC blister fluids. The chemokine CCL27 was found to be highly expressed in skin suction blister fluids following HDM challenge, at concentrations above the upper detection limit of the assay (Fig. 3.10, G), which might have skewed the DEP analysis (Fig. 3.8, C).

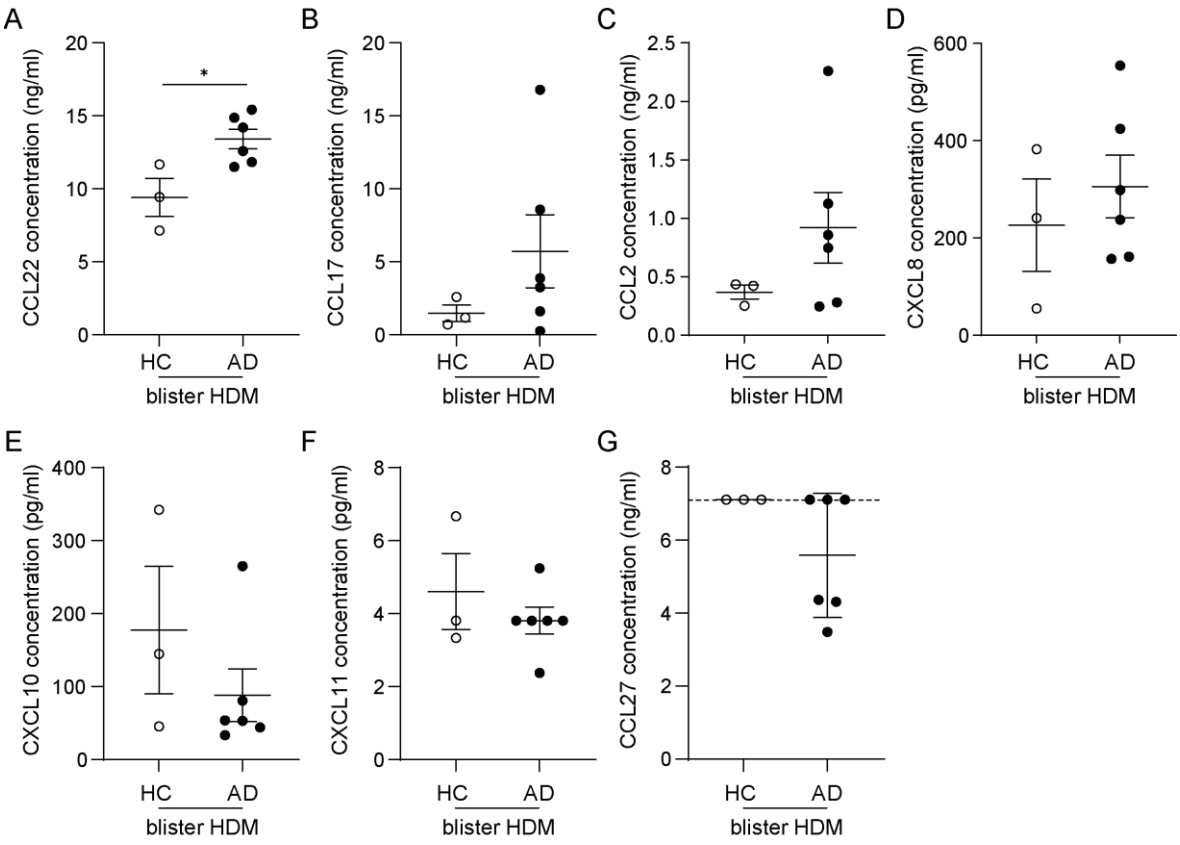


Figure 3.10 Chemokine levels in HC and AD skin blister fluids following intradermal allergen challenge.

(**A-G**) Levels of CCL22 (**A**), CCL17 (**B**), CCL2 (**C**), CXCL8 (**D**), CXCL10 (**E**), CXCL11 (**F**) and CCL27 (**G**) were measured by Luminex multiplex assay in skin suction blister fluids from HC (n=3) and AD patients (n=6) following HDM challenge. AD data includes both AD_1

and AD_2 group blister fluids. (n=3-6; data representative of 1 experiment). *P < 0.05; unpaired Student's *t*-test.

3.2.2 Analysis of serum cytokine and chemokine profiles of individuals with AD and healthy volunteers

Following investigation of cutaneous immune responses in AD, systemic immune responses were assessed by Luminex multianalyte profiling of chemokine and cytokine levels in sera from individuals with AD and healthy volunteers.

3.2.2.1 Differences in the overall serum cytokine/chemokine expression patterns

Dimensionality reduction analysis of the serum Luminex data by PCA did not show clear separation of AD and HC samples based on the cytokine/chemokine profile (Fig. 3.11, A). However, AD disease severity appeared to correspond to increasing total serum cytokine/chemokine concentrations. In the two-dimensional PCA plots, mild AD patients were found interspersed between HC samples, while individuals with severe AD appeared to cluster separately due to increased average serum protein concentrations (Fig. 3.11, B and C). Comparison of log fold change differences in the cytokine/chemokine levels in AD and HC sera identified six DEPs (BH-adj. p-value <0.05; log2FC >1), including the chemokines CCL26, CCL17, CCL27, CCL22, CCL23 and the cytokine IL-2 (Fig. 3.11, D).

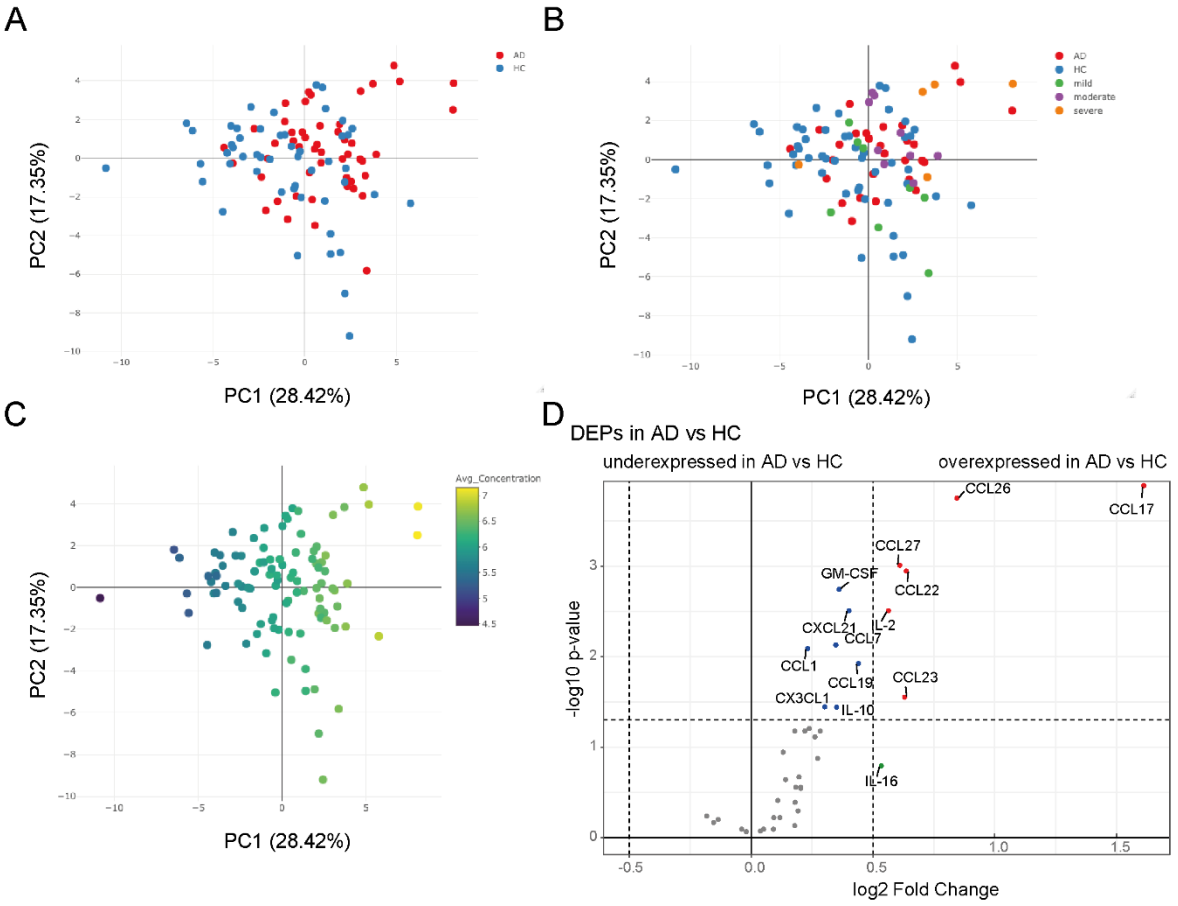


Figure 3.11 Comparison of cytokine/chemokine expression profiles of HC and AD sera.

(**A-D**) Concentrations of 30 chemokines and 10 cytokines were measured in sera from individuals with AD (n=50) and HC (n=50) by Luminex assays. Concentrations were log2(concentration+1)-transformed prior to downstream analysis. (**A-C**) PCA plot of serum Luminex data visualising AD vs HC (**A**), HC vs mild, moderate and severe AD (**B**) and average log2(concentration+1) range (**C**). AD donors with unknown disease severity scores were coloured red. Each dot represents a donor. (**D**) Volcano plot showing comparison of cytokine/chemokine levels in sera from HC vs AD. DEPs were identified by Student`s *t*-test followed by BH multiple comparison correction. (adj. p-value < 0.05; log2FC > 1.0). (n=100; data representative of 2 independent experiments).

3.2.2.2 Analysis of pro-inflammatory serum cytokine levels

Increased levels of a range of pro-inflammatory cytokines were detected in sera from AD compared to HC participants. Serum levels of IL-2, a lymphocyte survival

factor, and the type 2 cytokine IL-4 (Fig. 3.12, A and B) were found to be significantly higher in individuals with AD. There was no difference in IL-6 levels between AD and HC sera (Fig., 3.12, C). IFN-γ, IL-1β and in particular GM-CSF were detected at increased levels in sera from individuals with AD compared to HC (Fig. 3.12, D, E and F).

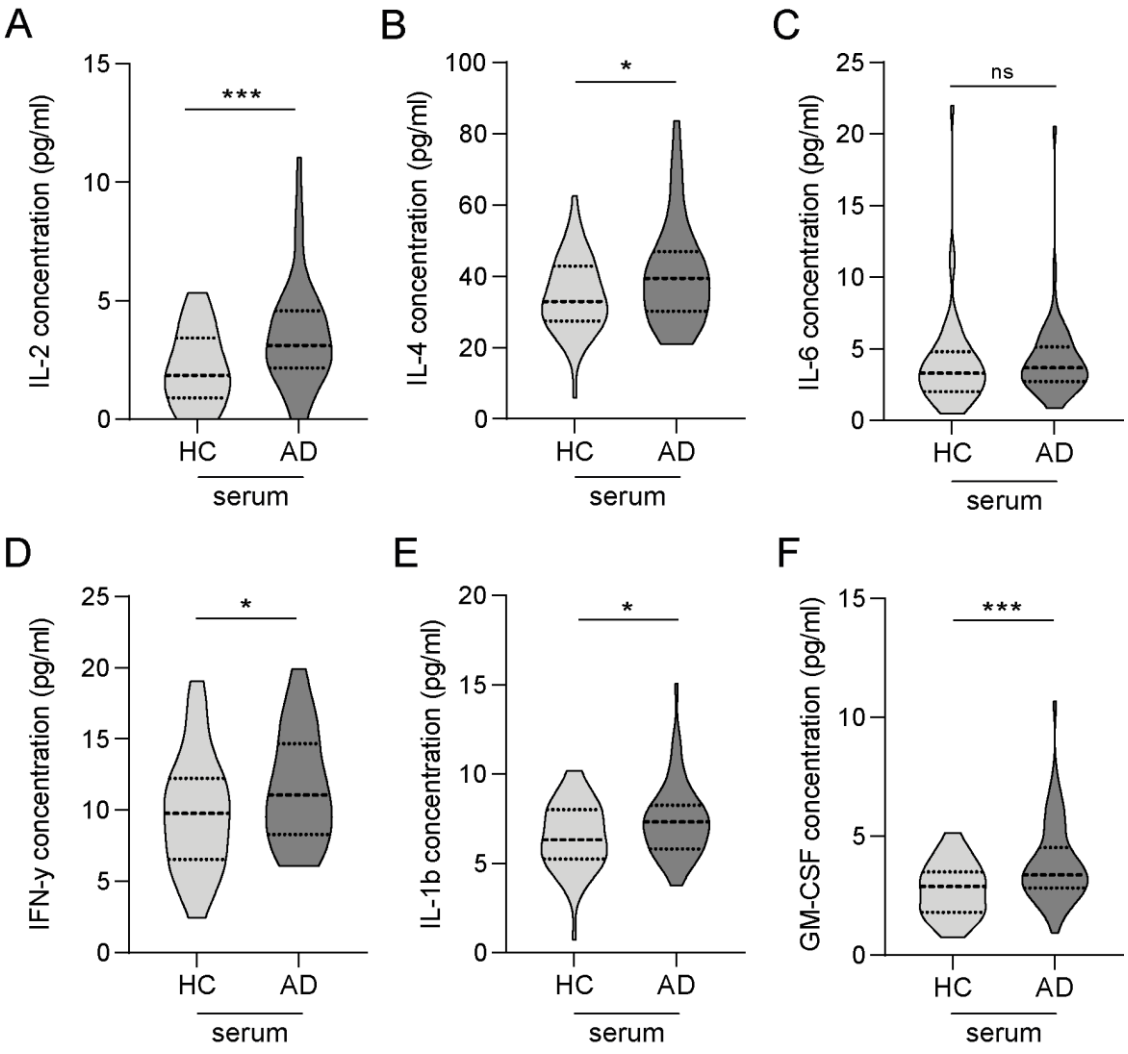


Figure 3.12 Levels of pro-inflammatory cytokines in HC and AD sera.

(**A-F**) Concentrations of IL-2 (**A**), IL-4 (**B**), IL-6 (**C**), IFN-γ (**D**), IL-1β (**E**) and GM-CSF (**F**) were measured in sera from individuals with AD (n=50) and HC (n=50) by Luminex assay. Violin plots with median and quartile lines show the distribution of serum cytokine levels. (n=100; data representative of 2 independent experiments). *P < 0.05; **P < 0.01; ***P < 0.001; unpaired Student's *t*-test.

3.2.2.3 Analysis of serum chemokine levels

Chemokines associated with Th2 cells recruitment, such as CCL7, CCL17 and CCL22, were detected at increased levels in sera from individuals with AD compared to HC (Fig. 3.13, A). In contrast, there was no difference in levels of Th1-recruiting chemokines, including CXCL9, CXCL10 and CXCL11 between AD and HC sera (Fig. 3.13, B). AD sera contained increased levels of CCL23 and CCL26, mediating recruitment of granulocytes, and the skin-homing chemokine CCL27 (Fig. 3.13, C-E).

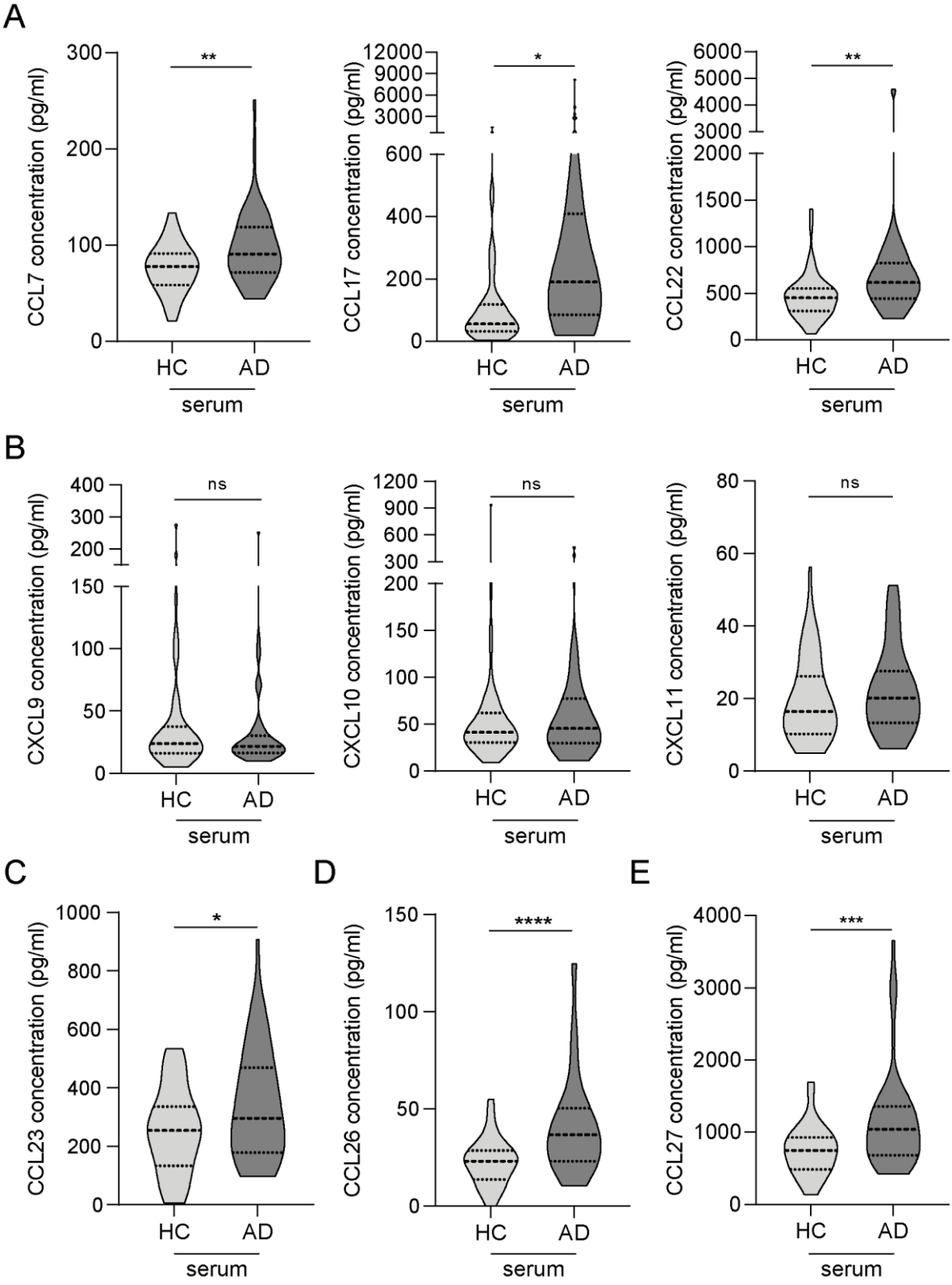


Figure 3.13 Levels of chemokines in HC and AD sera.

(**A-E**) Concentrations of chemokines with Th2 cell chemotactic activities (**A**), Th1 cell-recruiting functions (**B**) as well as of CCL23 (**C**), CCL26 (**D**) and CCL27 (**E**) were measured

in sera from individuals with AD (n=50) and HC (n=50) by Luminex assay. Violin plots with median and quartile lines show the distribution of serum chemokine levels. (n=100; data representative of 2 independent experiments). *P < 0.05; **P < 0.01; ***P < 0.001; ****P < 0.001; unpaired Student's *t*-test.

3.2.2.4 Serum chemokine levels as predictors of AD

Given the finding that serum CCL17, CCL22, CCL26 and CCL27 levels were differentially upregulated in AD patients, the disease predictive values of those chemokines were assessed in logistic regression models. Univariate logistic regression modelling of each of the selected chemokines identified serum CCL17, CCL22, CCL26 and CCL27 concentrations as factors strongly associated with AD (Fig. 3.14, A-D). In a multivariate logistic regression model, serum levels of CCL17 and CCL22 were found to predict AD with an accuracy score (AUC) of 0.769 (Fig, 3.14, E). This can be interpreted as a 76.9% probability that subjects expressing high serum levels of CCL17 and CCL22 would be identified as individuals with AD. Similarly, serum levels of CCL17, CCL26 and CCL27 or CCL17, CCL22 and CCL27 were identified as predictors of AD using multivariate logistic regression modelling with AUC scores of 0.779 and 0.785, respectively (Fig. 3.14, F and G). Posterior distribution analysis showed that the prediction models have high discriminative power with low uncertainty (Fig. A.5). CCL17, CCL22 and CCL26 serum concentrations were found to be significantly higher in individuals with severe compared to mild AD (Fig., 3.14, H-J). In contrast, there was no significant difference between CCL27 levels in mild, moderate or severe AD sera (Fig. 3.14, K). This suggests that serum CCL17, CCL22 and CCL26 levels positively correlate with AD disease severity.

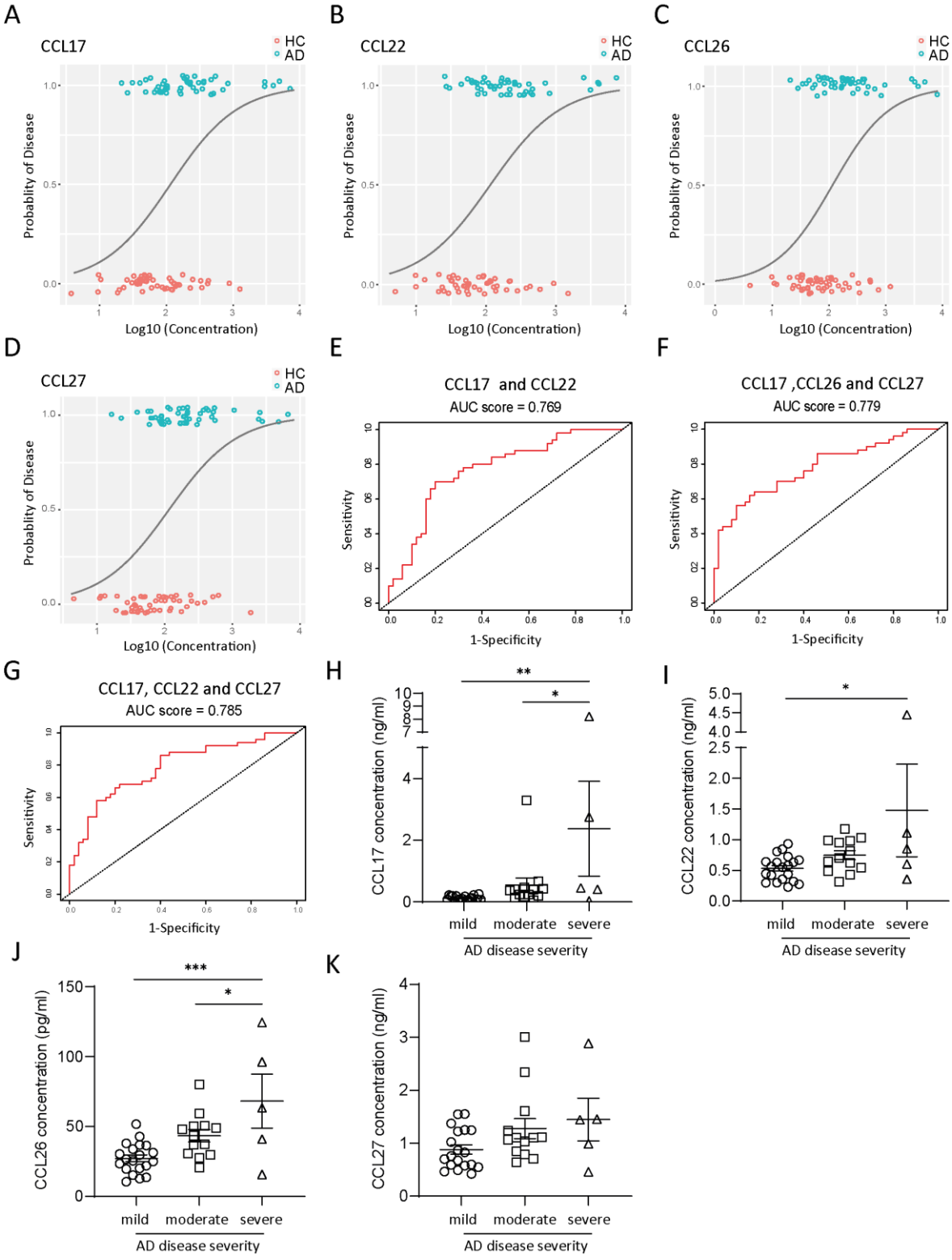


Figure 3.14 Analysis of serum chemokine levels as predictors of AD.

(**A-D**) Univariate logistic regression curves that model the probability of AD based on serum levels of CCL17 (**A**), CCL22 (**B**), CCL26 (**C**) and CCL27 (**D**). (**E-G**) Receiver operating characteristic (ROC) curve of multivariate logistic regression model for CCL22 and CCL17

(**E**), CCL17, CCL26 and CCL27 (**F**) and CCL17, CCL22, CCL27 (**G**) to predict AD. (n=100; data representative of 2 independent experiments). The area under the curve (AUC) is a measure of prediction accuracy. (**H-K**) Concentrations of CCL17 (**H**), CCL22 (**I**), CCL26 (**J**) and CCL27 (**K**) measured in sera from AD patients with diagnosed mild (n=19), moderate (n=13) and severe (n=5) by Luminex assay. (n=37; data representative of 2 independent experiments). *P < 0.05; **P < 0.01; ***P < 0.001; repeated-measures (RM) one-way ANOVA with Tukey`s post hoc multiple comparisons test (mean ± SEM).

3.2.3 Tissue-specific chemokine and cytokine profiles

To investigate whether chemokine/cytokine profiles were tissue-specific, PCA was performed on protein levels in sera and skin suction blister fluids as measured by Luminex multianalyte profiling. Distinct clustering of serum and skin suction blister fluid data was observed (Fig. 3.15. A). Clustering appeared to be based on average log2-transformed concentrations detected, with samples of lower protein concentrations clustering within the serum data and samples expressing higher protein levels within the skin suction blister fluid data (Fig. 3.15, B). This suggested that cutaneous and systemic chemokine/cytokine profiles are distinct, with overall chemokine and cytokine levels being increased within the skin microenvironment.

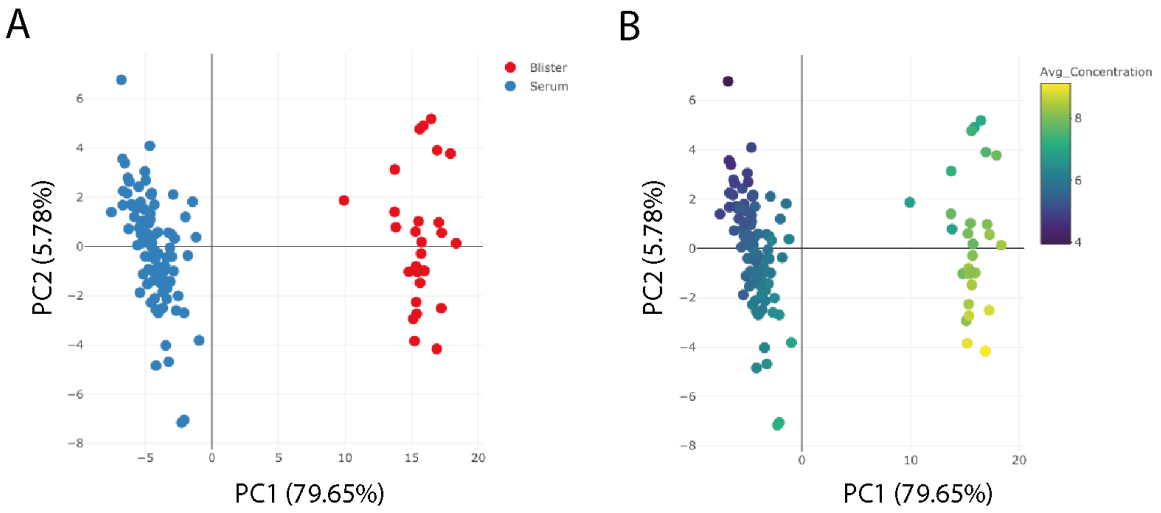


Figure 3.15 Analysis of cutaneous and serum cytokine/chemokine profiles.
(**A and B**) PCA of serum and skin suction blister fluid cytokine/chemokine profiles as measured by Luminex assay. (**A**) PCA plot showing blister fluid (red) and serum (blue). (**B**) PCA plot visualising average log2(concentration+1) range (blue = low; yellow = high). Each dot represents a separate donor and/or challenge condition. (n=16-100; data representative of 1-2 independent experiments).

3.2.4 Potential contribution of ILC2 in cutaneous inflammation

Dysregulated ILC2 responses have been implicated in allergic inflammatory disorders. This project aimed to investigate potential functions of human ILC2 in allergic inflammation with a particular focus on their role in cutaneous inflammation.

3.2.4.1 RNA-sequencing analysis of cutaneous human ILC2 upon *in vivo* allergen challenge

To assess the potential contribution of ILC2 to the altered cutaneous cytokine/chemokine profile observed in AD, we analysed a previously generated RNA-sequencing data set for expression of a broad range of cytokines and chemokines. Previously, skin suction blisters were formed on the arm of one healthy HDM-sensitive volunteer following intradermal HDM challenge and ILC2 gene expression analysed by RNA-sequencing, performed by Dr Maryam Salimi. While

labour intensive and technically challenging, the skin suction blister model enables analysis of cutaneous cells without the need for enzymatic processing, that is required for cell isolation from conventional skin biopsies and comes with a risk of modulating gene expression. To enable comparison of skin ILC2 gene expression, blood-derived ILC2 and blood- and skin-derived T cells from the same donor were analysed in parallel. ILC2 were identified as Lin^- $CD45^+$ $CD3^-$ IL-7Rα^+ $CRTH2^+$ lymphocytes (Fig. 3.16, A). Skin and blood ILC2 were found to express a range of cytokine- and chemokine-encoding genes. Expression of *IL13* and *AREG*, the gene encoding amphiregulin, were specifically upregulated in skin blister-derived ILC2 compared to blood-derived ILC2 or T cells (Fig. 3.16, B), which implies a role for ILC2-derived IL-13 and amphiregulin in cutaneous inflammation. ILC2-derived amphiregulin has been found to promote wound healing and the maintenance of tissue homeostasis (88). In addition to expressing genes encoding anti-inflammatory cytokines such as TGF-β, blood and skin ILC2 were found to express genes encoding pro-inflammatory cytokines including IL-1β (Fig. 3.16, B). A range of chemokine-encoding genes were detected in both blood and skin ILC2. ILC2 were not only found to transcriptionally express chemokines associated with Th2 cell homing, such as CCL7, CCL17, CCL22, but also chemokines that predominantly mediate recruitment of DC, neutrophils and Th1 cells (Fig. 3.16, C). *CCL22* and *CCL17* were highly and specifically upregulated in skin blister- and/or blood-derived ILC2 compared to T cells (Fig. 3.16, C). These results suggest an unrecognised role for ILC2 in the chemotactic recruitment of innate and adaptive immune cells. Although our RNA-sequencing data were obtained from a single healthy individual only, it gives an insight into the transcriptomic phenotype of cutaneous and circulating ILC2 and provides the basis of generating new hypotheses. Based on

the RNA-sequencing results indicating the expression of a broad range of cytokines and chemotactic factors by human ILC2, and alignment of these with skin and serum cytokine levels, I hypothesised that the function of ILC2 extends beyond their recognised role as type 2 cytokine producers.

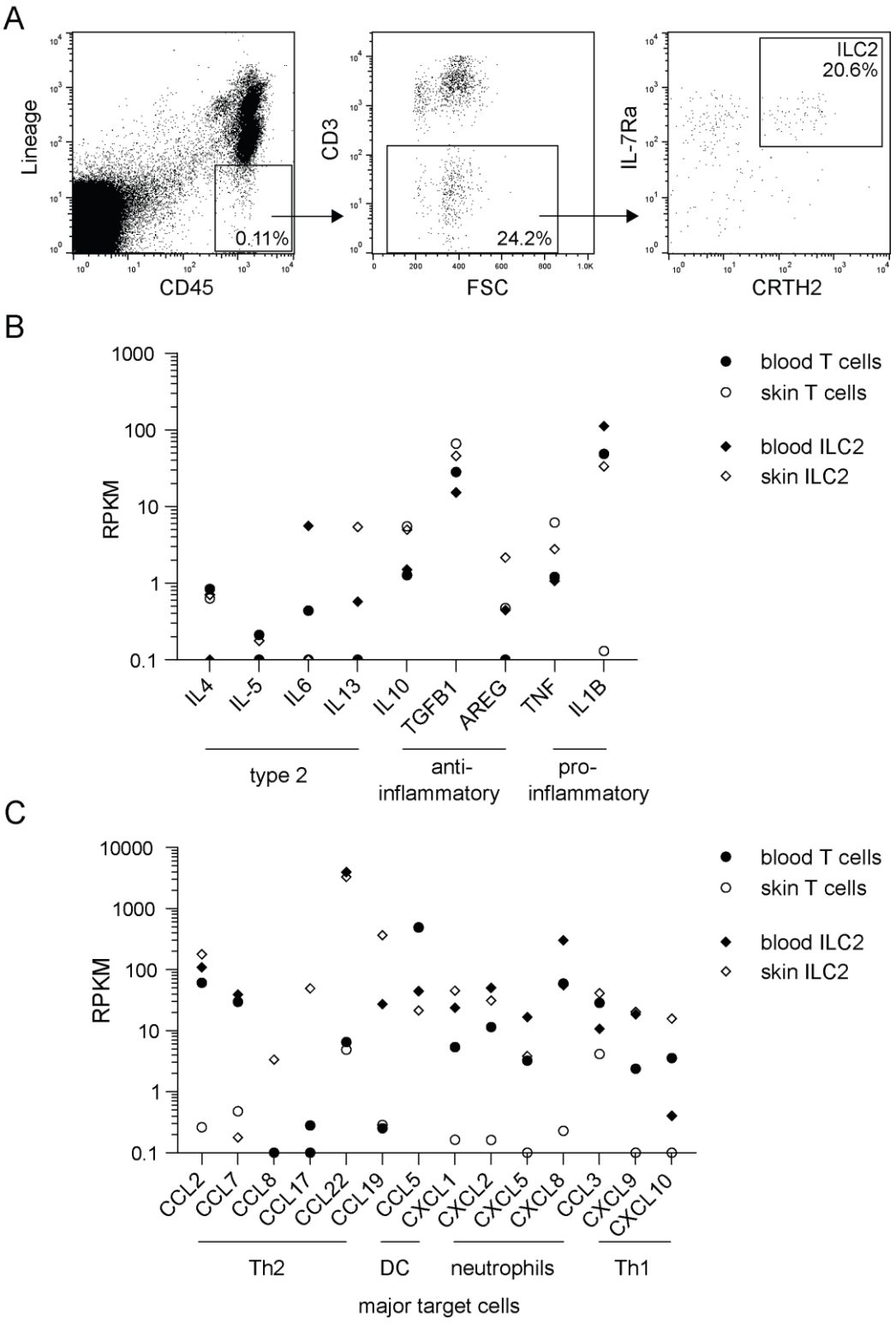


Figure 3.16 RNA-sequencing analysis of human ILC2 and T cells.

(**A**) Flow cytometry gating strategy used to FACS isolate ILC2 from skin blister fluids following 24h intradermal HDM challenge. ILC2 are defined as Lineage$^-$ CD45$^+$ CD3$^-$ IL-7Rα$^+$ CRTH2$^+$. Numbers indicate percentages of cells within the indicated gates, gated on

the parent population. (**B and C**) Cytokine (**B**) and chemokine (**C**) gene expression of skin blister- and blood-derived ILC2 and T cells from the same donor determined by RNA-sequencing and measured in Reads Per Kilobase of transcript per Million mapped reads (RPKM). (n=1).

3.2.4.2 Isolation and expansion of human ILC2

ILC2 represent a rare lymphoid cell population, which have been reported to make up 2.94% and up to 0.18% of lymphocytes in human skin and blood, respectively (93). Consist with these reports, we detected higher frequencies of ILC2 in the skin compared to peripheral blood from healthy volunteers (Fig 3.17, A and B). To obtain sufficient ILC2 numbers for *in vitro* experiments, human ILC2 were isolated and expanded *in vitro* in the presence of IL-2 (Fig. 3.17, C). Following *in vitro* expansion, the purity of the expanded ILC2 cell lines was assessed by flow cytometry and lines with a purity of over 90% were used for *in vitro* functional experiments (Fig. 3.17, D).

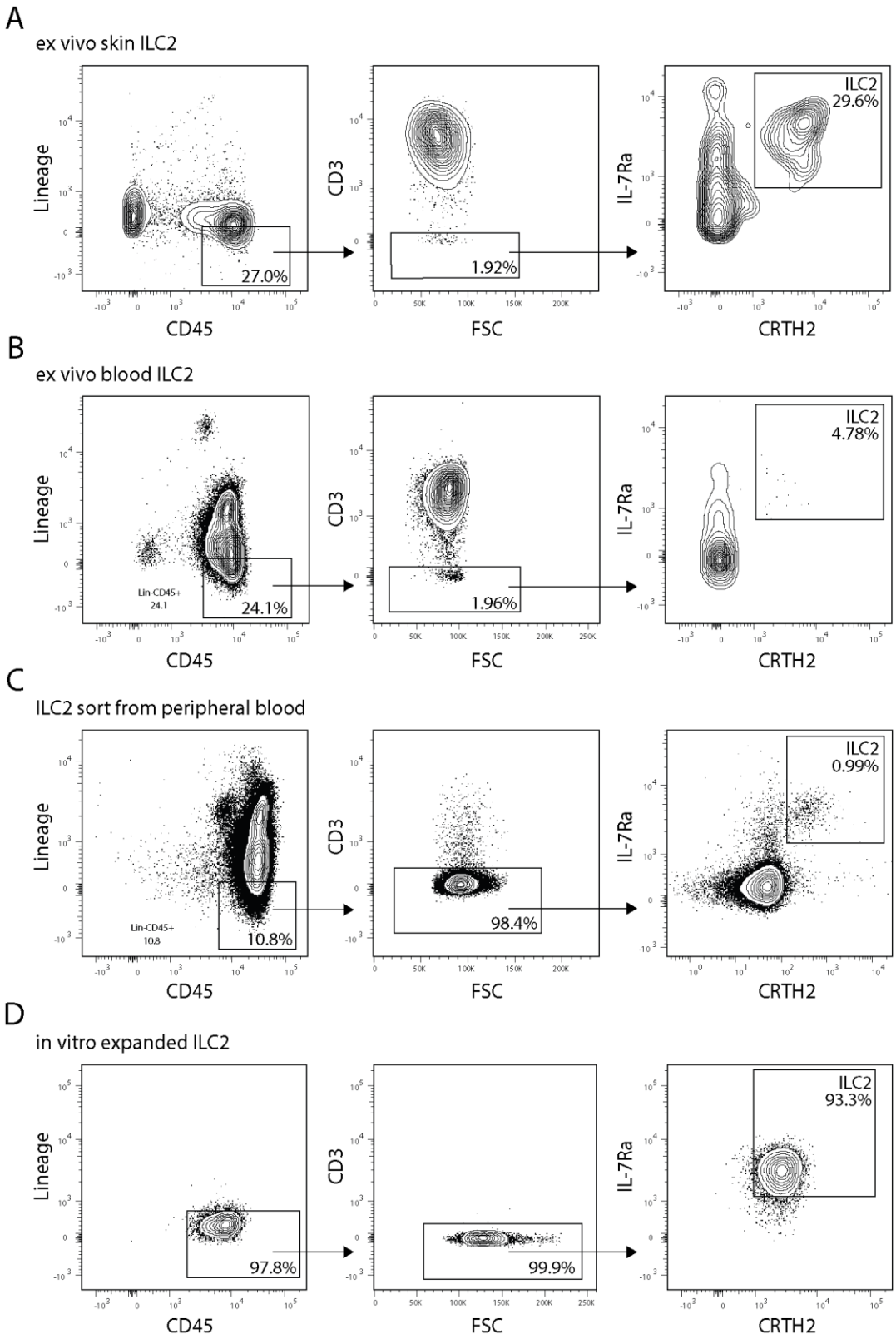


Figure 3.17 Human ILC2 isolation and *in vitro* expansion.

(**A and B**) Flow cytometry gating strategy for identifying human *ex vivo* ILC2 in skin biopsies (**A**) and peripheral blood (**B**). (**C**) Representative plots of ILC2 isolation by FACS for *in vitro*

expansion. (**D**) Following expansion in the presence of IL-2 (200 IU/ml), the purity of ILC2 was confirmed by flow cytometry. Numbers indicate percentages of cells within the indicated gates, gated on the parent population.

3.2.4.3 Investigation of cytokine and chemokine production by activated human ILC2

To validate the RNA-sequencing results and to assess cytokine and chemokine production by human ILC2, blood-derived ILC2 were stimulated with alarmins IL-33, IL-25 and TSLP and levels of 40 different cytokines/chemokines in ILC2 supernatants were measured by Luminex assay. Unbiased dimensionality reduction by PCA showed a noticeable batch effect in the Luminex data (Fig. 3.18, A). Following batch effect correction (Fig. 3.18, B), ILC2 supernatants were clustered by PCA based on cytokine/chemokine profiles. A clear separation was observed between unstimulated or TSLP-stimulated ILC2 and ILC2 that were stimulated with IL-33 or a combination of IL-33, IL-25 and TSLP. IL-25-treated ILC2 appeared interspersed between the two clusters (Fig. 3.18, C). The separation was found to correlate with average protein concentration, with unstimulated or TSLP-stimulated ILC2 supernatants being associated with lower and IL-33- or IL-33, IL-25 and IL-33-treated ILC2 supernatants correlating with higher average cytokine/chemokine concentrations (Fig. 3.18, D).

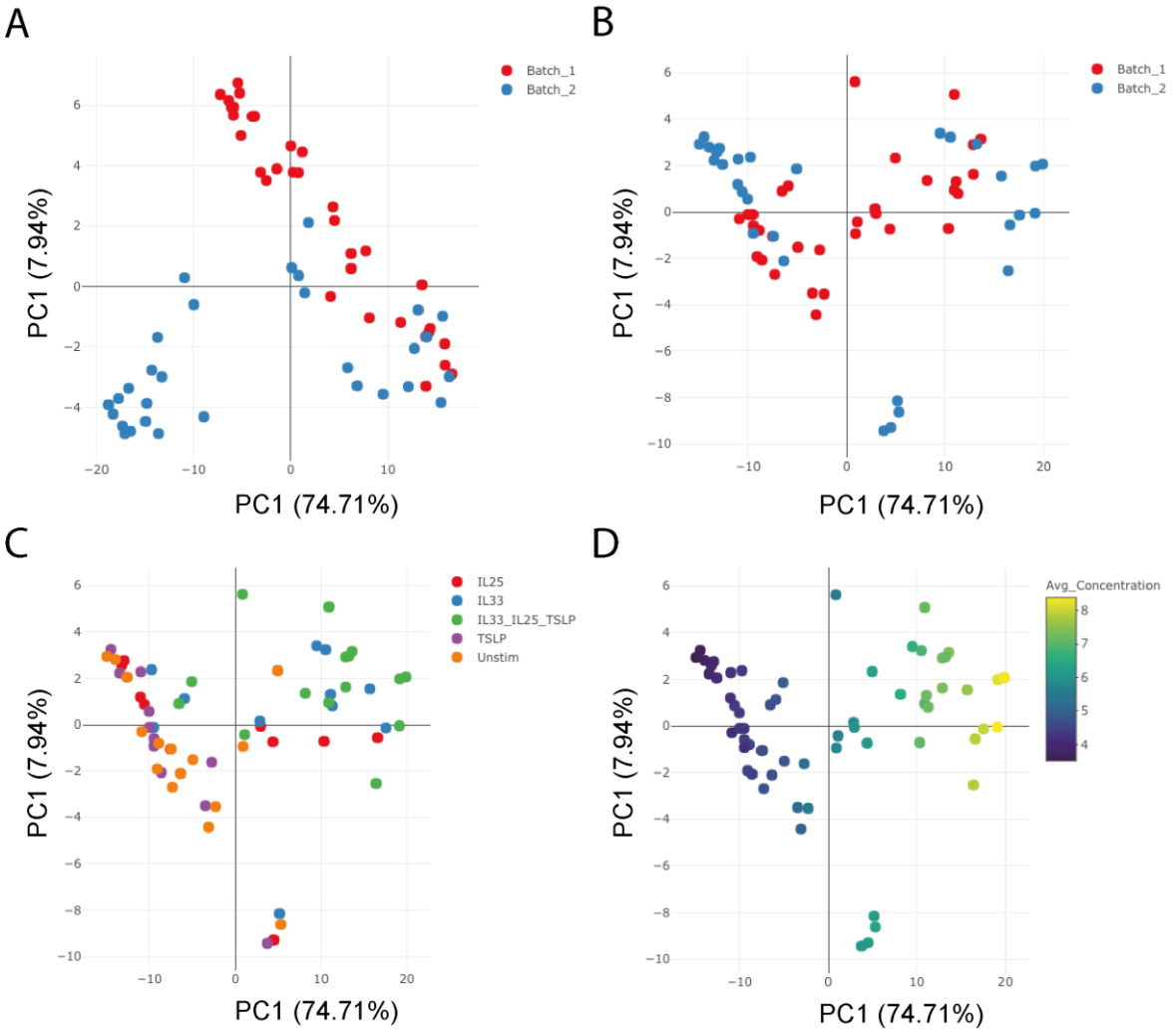


Figure 3.18 Two-dimensional PCA of cytokine/chemokine expression profiles of human ILC2.

(**A-D**) ILC2 isolated from blood of HC (n=12) and individuals with AD (n=3) were cultured in medium alone (unstim) or stimulated for 72h with IL-33 (50 ng/ml), IL-25 (50 ng/ml), TSLP (50 ng/ml) individually or in combination and supernatants analysed by 40-plex Luminex assay. Concentrations were log2(concentration+1)-transformed prior to further analysis. (**A**) PCA plot showing batch effect (red = batch 1; blue = batch 2). (**B**) PCA plot after batch correction. (**C**) PCA plot showing ILC2 stimulation conditions. (**D**) PCA plot visualising average log2(concentration+1) range (blue = low; yellow = high). Each dot represents a separate ILC2 stimulation condition. (n=15; data representative of 2 independent experiments).

The secreted protein profile of unstimulated and stimulated ILC2 was compared by limma analysis correcting for batch and donor effects followed by BH-multiple testing

correction. 17 differentially upregulated proteins were identified in IL-33, IL-25, TSLP-stimulated compared to unstimulated ILC2 supernatants, including cytokines IL-6, IL-10 and GM-CSF and chemokines CCL1, CXCL8 and CCL3 (BH-adj. $p < 0.05$; log2FC > 1.0). Surprisingly, the pro-inflammatory cytokines IL-1β, TNF-α and IFN-γ were found to be upregulated in IL-33, IL-25 and TSLP-stimulated ILC2 supernatants (Fig. 3.19, A). Hierarchical clustering of ILC2 supernatants based on DEP expression revealed separation into IL-33, IL-25, TSLP-stimulated vs unstimulated ILC2 groups (Fig. 3.19, B). Comparison of IL-33- and unstimulated ILC2 supernatants revealed upregulated cytokines/chemokine production by IL-33-treated ILC2, resembling IL-33, IL-25, TSLP-stimulated ILC2, with IL-6, GM-CSF, CXCL8, CCL3, and CCL1 being identified as DEPs (Fig. 3.19, C and D). In contrast, treatment of ILC2 with IL-25 or TSLP did not appear to induce significant upregulation of cytokine/chemokine production (Fig. 3.19, E and F). It is noteworthy that IL-13 was not included in this Luminex assay.

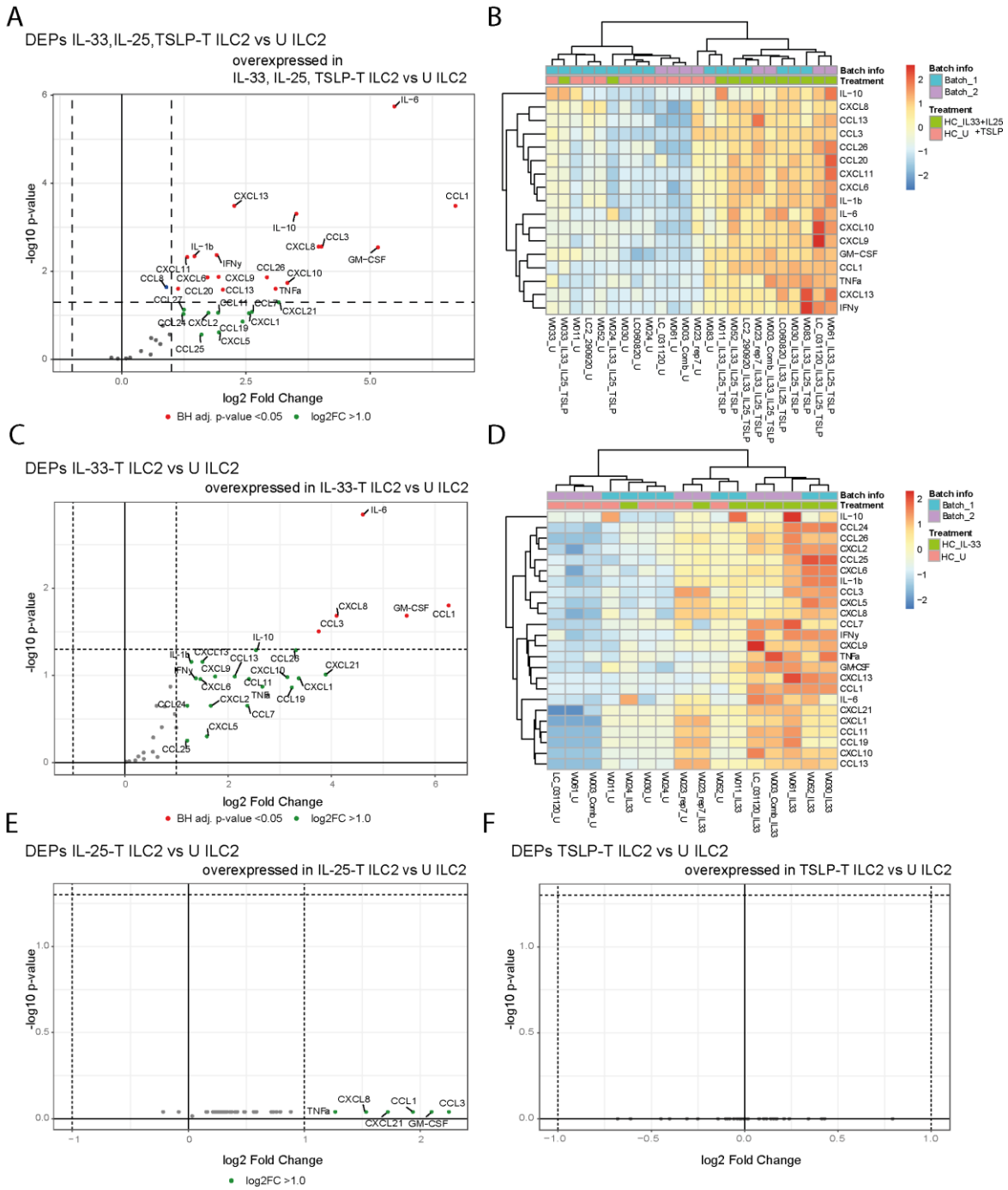


Figure 3.19 Cytokine/chemokine expression profile of human ILC2 following stimulation.

(**A-F**) Luminex supernatant data for blood-derived ILC2 from HC treated with various stimulants was compared to unstimulated ILC2 supernatants. DEPs were identified by limma followed by BH multiple testing correction (adj. p-value < 0.05; log2FC > 1.0). (**A and B**) Volcano plot (**A**) and heatmap (**B**) visualising DEPs between IL-33, IL-25, TSLP-stimulated and unstimulated ILC2 supernatants. (n=12). (**C and D**) Volcano plot (**C**) and

heatmap (**D**) showing DEPs between IL-33-treated and unstimulated ILC2 supernatants. (n=8). (**E and F**) Volcano plots visualising comparison of ILC2 supernatants from IL-25-treated (**E**) or TSLP-treated (**F**) ILC2 with unstimulated ILC2 supernatants. (n=8; data representative of 2 independent experiments).

To assess whether ILC2 in individuals with AD show an altered cytokine/chemokine profile in response to alarmin stimulation, blood-derived ILC2 were isolated from individuals with AD and stimulation-induced protein production measured by Luminex multianalyte profiling. No DEPs were identified in the comparison of Luminex supernatant data from stimulated and unstimulated AD ILC2. However, data were obtained from only three AD donors and the response of stimulated ILC2 appeared to be driven by one donor (Fig. 3.20, A and B). Therefore, we were unable to perform comparison analysis of HC and AD ILC2 responses. Upregulated cytokines and chemokines in stimulated AD ILC2 supernatants, that passed the fold change increase threshold but did not pass BH-multiple testing correction, included CCL1, GM-CSF, CXCL8 and CCL3 (Fig. 3.20, A and B). This resembled the response to stimulation observed for HC ILC2, suggesting that after expansion *in vitro* ILC2 derived from individuals with AD share many characteristics of ILC2 derived from HC.

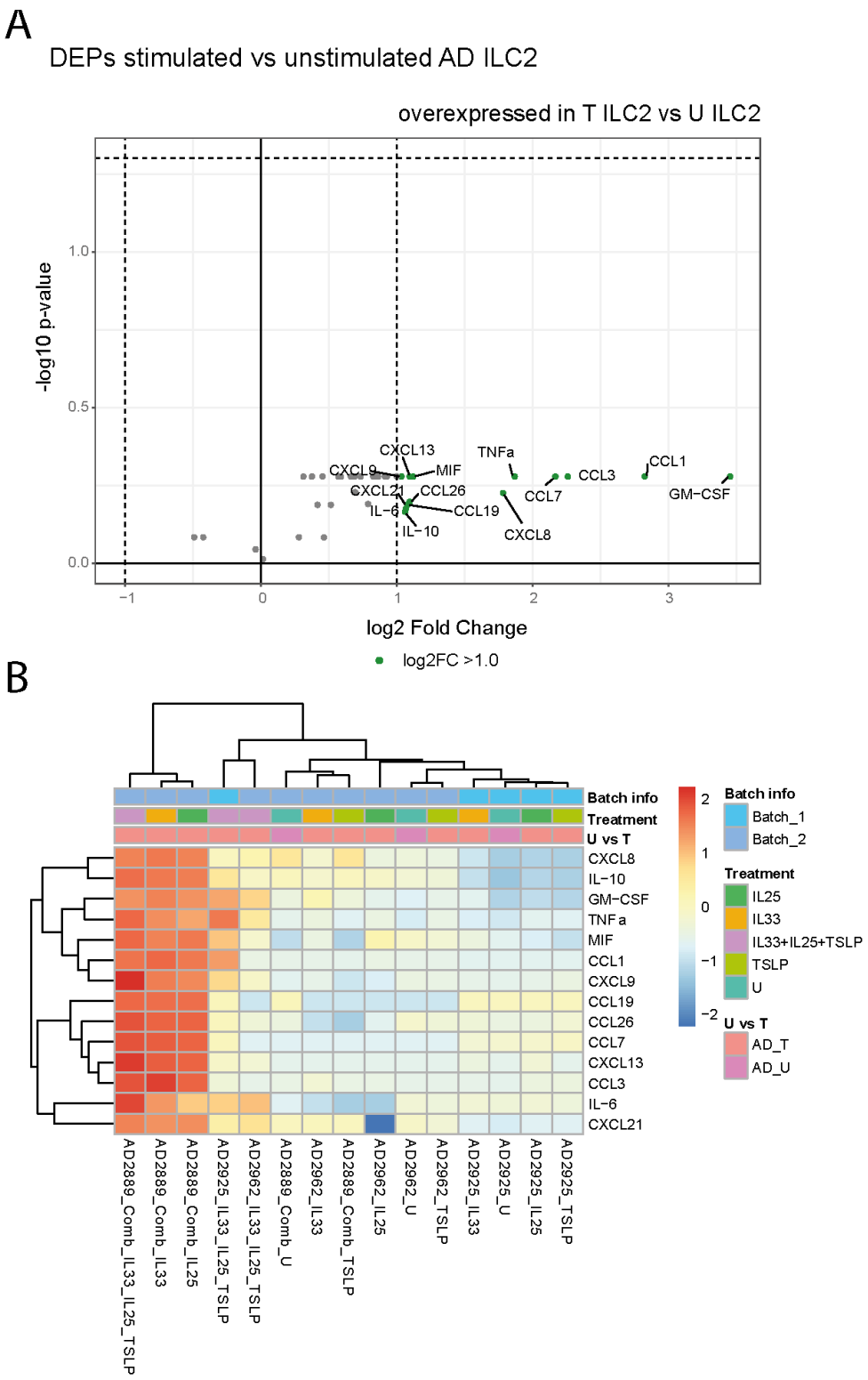


Figure 3.20 Cytokine/chemokine expression profile of human AD ILC2.

(**A and B**) ILC2 were isolated from peripheral blood from individuals with AD, cultured in medium alone (U) or stimulated (T) for 72h with various stimulants and supernatants analysed by 40-plex Luminex assay. DEPs were identified by limma followed by BH-multiple testing correction (adj. p-value < 0.05; log2FC > 1.0). Volcano plot (**A**) and heatmap (**B**)

visualising comparison of protein profiles of stimulated and unstimulated AD ILC2 supernatants. (n=3; data representative of 2 independent experiments).

3.2.4.4 Analysis of cytokine and chemokine levels secreted by stimulated human ILC2

Following analysis of stimulation-induced ILC2 cytokine/chemokine patterns, levels of specific cytokines and chemokines secreted *in vitro* by human ILC2 were assessed by ELISA and Luminex assay. Firstly, we analysed the concentrations of proteins that were found to be differentially upregulated in stimulated ILC2 supernatants. IL-33, IL-25, TSLP stimulation of ILC2 was found to significantly induce the secretion of high levels of GM-CSF, CXCL8 and CCL3 (Fig. 3.21, A, B and C). While CXCL13 was significantly upregulated in IL-33, IL-25, TSLP-stimulated ILC2 supernatants, levels detected were low and just above the bottom detection limit of the assay (Fig. 3.21, D). High donor variability was observed for IL-6 and IL-10 production, with only a small subset of ILC2 lines secreting high IL-6 and IL-10 levels in response to combined alarmin stimulation (Fig. 3.21, E and F). While IL-33 appeared to be the main factor driving the combined IL-33, IL-25, TSLP-induced upregulation of cytokine/chemokine production in ILC2, a contribution of IL-25 was observed. ILC2 treatment with IL-33 alone significantly upregulated the secretion of GM-CSF, but not of CXCL8, CCL3 or CXCL13. IL-25 or TSLP did not induce significant ILC2 cytokine/chemokine production when present in isolation. However, incubation with IL-25 resulted in slightly increased production of GM-CSF, CXCL8, CCL3 and CXCL13, while TSLP had no effect on ILC2 cytokine/chemokine production. The finding that combined IL-33, IL-25 and TSLP treatment induced the

strongest cytokine/chemokine response in ILC2 implies a synergistic effect of alarmin cytokines (Fig. 3.21, A-D).

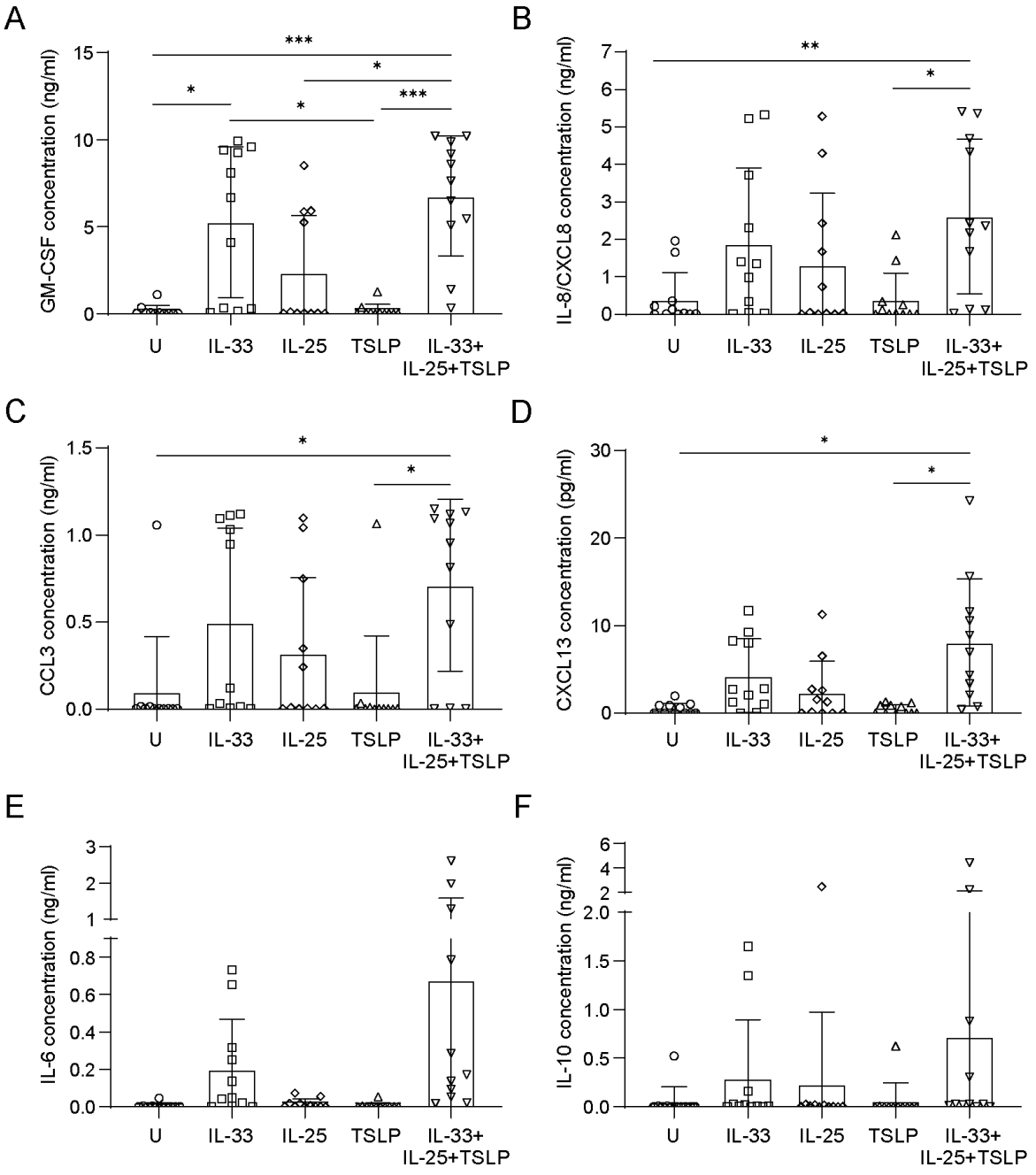


Figure 3.21 ILC2 cytokine and chemokine production in response to alarmin stimulants.

(**A-F**) Blood-derived ILC2 were left untreated (U) or cultured for 72h in IL-33 (50 ng/ml), IL-25 (50 ng/ml), TSLP (50 ng/ml) individually or combined and levels of GM-CSF (**A**), CXCL8 (**B**), CCL3 (**C**), CXCL13 (**D**), IL-6 (**E**) and IL-10 (**F**) in culture supernatants measured by

Luminex assay. (n=11; data representative of 2 independent experiments). *P < 0.05; **P < 0.01; RM one-way ANOVA with Tukey`s post hoc multiple comparisons test (mean ± SD).

Investigation of alarmin-induced cytokine production by ILC2 confirmed secretion of high levels of IL-13 in response to IL-33, IL-25 and TSLP stimulation, reaching average concentrations of 95.38 ng/ml (Fig. 3.22, A). In addition to IL-13, activated ILC2 were found to secrete significantly increased levels of pro-inflammatory cytokines including TNF-α and IL-1β (Fig. 3.22, B and C). Surprisingly, alarmin stimulation of ILC2 also induced the production of IL-22 and low levels of IFN-γ, generally associated with ILC3 and ILC1 responses, respectively (Fig. 3.22, D and E). In contrast, ILC2 stimulation did not upregulate the production of the cytokine IL-16 (Fig. 3.22, F). ILC2 lines producing more than 500 pg/ml of the anti-inflammatory cytokine IL-10 were found to simultaneously produce pro-inflammatory cytokines including TNF-α, GM-CSF and IL-8/CXCL8 (Fig. 3.22, G).

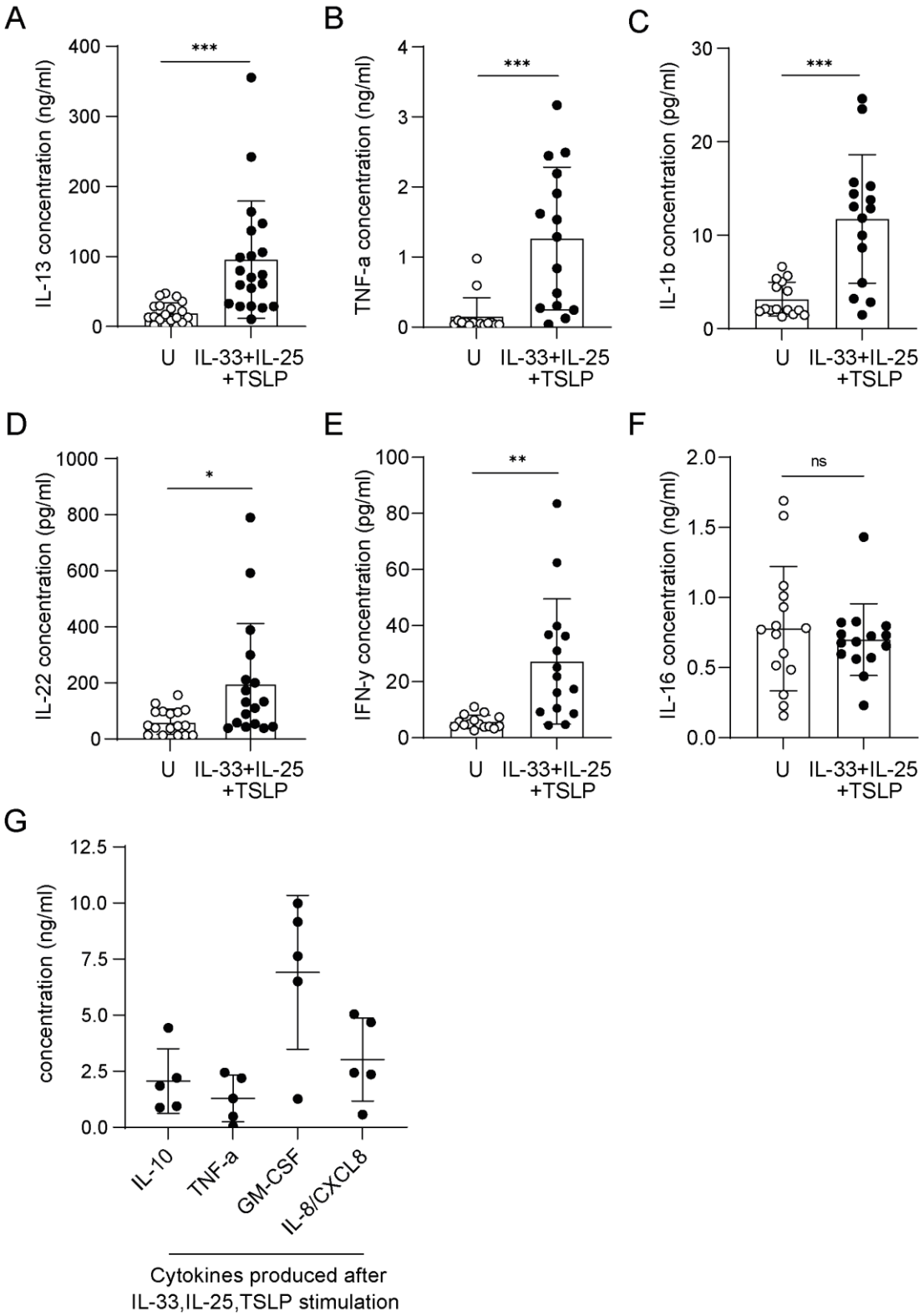


Figure 3.22 ILC2 cytokine production in response to stimulation with IL-33, IL-25 and TSLP.

(**A-G**) Blood-derived ILC2 were left untreated (U) or stimulated for 72h with a combination of IL-33, IL-25 and TSLP (50 ng/ml each) and cytokine levels measured by ELISA and

Luminex. (**A**) IL-13 levels in ILC2 supernatants measured by ELISA (n=20; data representative of ≥ 3 independent experiments). (**B-F**) Levels of TNF-α (B), IL-1β (C), IL-22 (**D**), IFN-y (**E**) and IL-16 (**F**) in ILC2 supernatants measured by Luminex (n=15; data representative of 2 independent experiments). *P < 0.05; **P < 0.01; ***P < 0.001; paired Student's *t* test (mean ±SD). (**G**) ILC2 lines producing > 500 pg/ml IL-10 were analysed for their secretion of TNF-α, GM-CSF and IL-8/CXCL8 following 72h stimulation with IL-33, IL-25 and TSLP (50 ng/ml), as measured by Luminex assay. (n=5; data representative of 2 independent experiments). (mean ±SD).

Little is known about the role of ILC2 in the chemotactic recruitment of immune cells to inflammatory sites. ILC2 production of the chemokines CCL22 and CCL17 and its functional implications will be discussed in chapter 4. Following *in vitro* ILC2 activation with IL-33, IL-25 and TSLP, ILC2 were found to produce significantly higher levels of a broad range of chemokines including the Th2 cell-recruiting chemokines CCL7 and CCL13 (Fig. 3.23, A), the gut-homing factor CCL25 (Fig. 3.23, B), the skin-homing factor CCL27 (Fig. 3.23, C), CXCL9 and CXCL11 mediating Th1 cell recruitment (Fig. 3.23, D), the neutrophil-recruiting chemokines CCL1 and CXCL5 (Fig. 3.23, E), and the eosinophil- and basophil-recruiting chemokines CCL11 (eotaxin) and CCL26 (Fig. 3.23, F). These results imply an involvement of ILC2 in coordinating innate and adaptive immune cell homing.

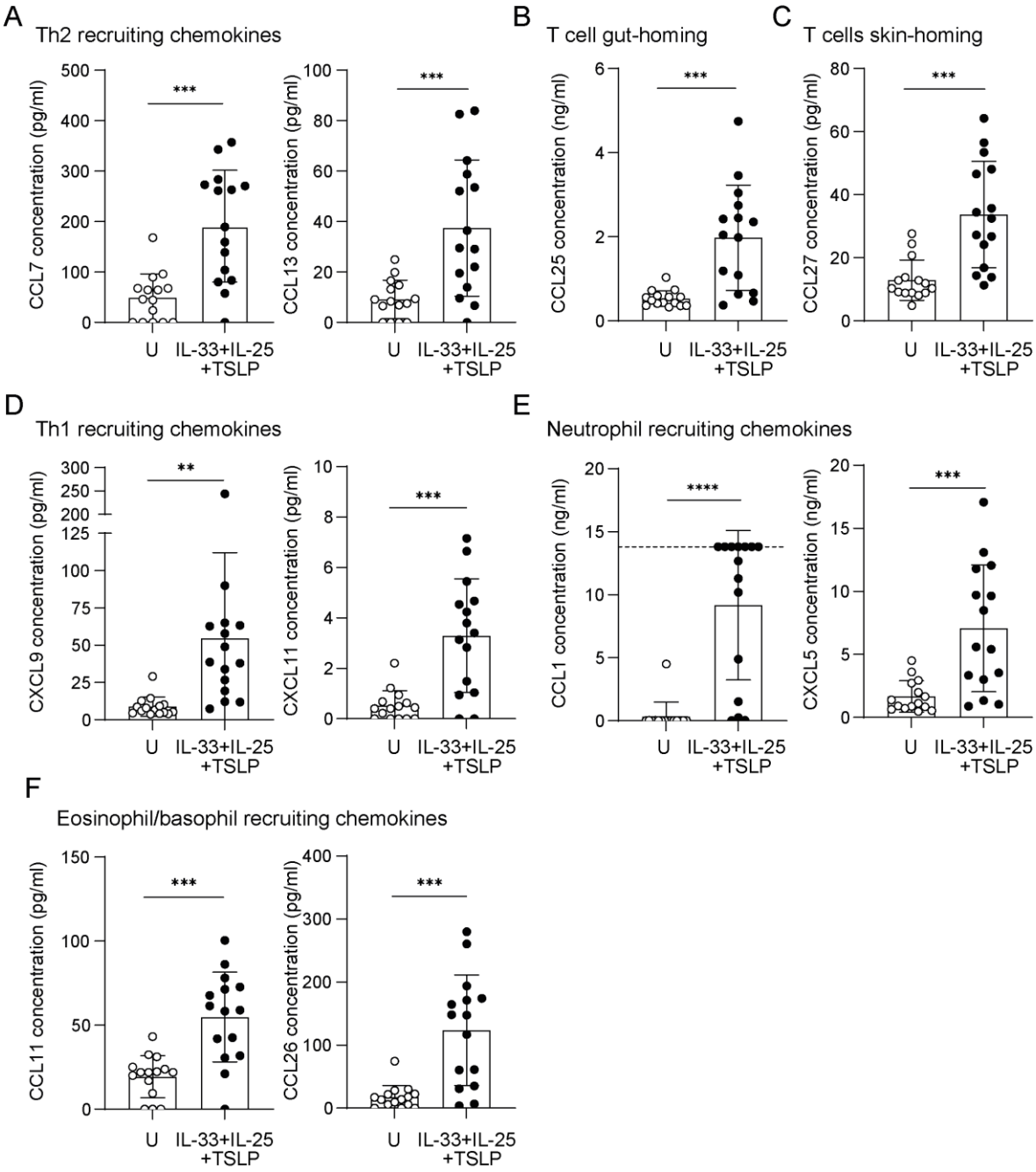


Figure 3.23 ILC2 chemokine production in response to stimulation with IL-33, IL-25 and TSLP.

(**A-F**) Blood-derived ILC2 were left untreated (U) or cultured for 72h in the presence of IL-33, IL-25 and TSLP (50 ng/ml each) and chemokine levels in ILC2 supernatants measured by Luminex assay. (**A**) Levels of CCL7 and CCL13, associated with Th2 cell homing. (**B**) Levels of CCL25, a gut homing factor. (**C**) Levels of CCL27, a skin homing factor. (**D**) Levels of CXCL9 and CXCL11, associated with Th1 cell homing. (**E**) Levels of CCL1 and CXCL5, mediating neutrophil recruitment. (**F**) Levels of CCL11 and CCL26, mediating eosinophil

and basophil recruitment. (n=15; data representative of 2 independent experiments). *P < 0.05; **P < 0.01; ***P < 0.001; paired Student's *t* test. (mean ±SD).

3.3 Discussion

3.3.1 AD skin shows an altered proteome signature in an *in vivo* human skin blister model

Skin transcriptome studies have revealed broad dysregulation in the gene signature of AD skin, characterised by disturbed epidermal differentiation, itch signalling and immune modulation (258, 259). However, relatively little is known about the proteome profile of AD skin especially during allergen challenge. Here, an *in vivo* human skin blister allergen model was used to study the cutaneous microenvironment in individuals with AD. Protein analysis of skin suction blister fluids revealed an altered cutaneous proteome signature in individuals with AD when compared to healthy or atopic asymptomatic skin. Overall, there seemed to be enrichment for chemokines and cytokines in AD blister fluids. Significantly increased levels of the type 2 chemokine CCL22 were detected in AD compared to HC blister fluids following HDM challenge. CCL22 is believed to be critically involved in AD pathogenesis, supported by the finding that cutaneous CCL22 gene expression was significantly downregulated following effective dupliumab treatment of individuals with AD (259). Cutaneous expression of type 2 cytokines, such as IL-4, IL-5, IL-9, and chemokines, including CCL2, CCL7, CCL13, CCL24 and CXCL8 was found to be significantly increased in a subset of AD samples analysed by SOMAscan assay. Similarly, a trend towards increased levels of IL-5, CCL2, and CXCL8 in AD blister fluids following HDM challenge was observed by Luminex multianalyte profiling. These results are indicative of an exacerbated type 2 immune response and

increased leukocyte recruitment in AD skin. Indeed, intradermal HDM challenge has been shown to induce infiltration of various immune cells, including granulocytes, ILC2 and T cells (93, 240). AD treatment with dupliumab or the immunosuppressant cyclosporine has been associated with downregulated cutaneous *CXCL8* expression, and etokimab, an anti-IL-33 monoclonal antibody, inhibited CXCL8-mediated neutrophil recruitment into AD skin (240, 258), suggesting a role of neutrophils in AD pathogenesis. Tissue eosinophilia is a prominent feature of acute and, to a greater extent, chronic AD (260). Intradermal injection of CCL24 has been demonstrated to induce local accumulation of eosinophils and basophils (261), suggesting that elevated CCL24 and/or IL-5 levels in AD blister fluids may contribute to increased eosinophil and basophil infiltration. While acute AD is dominated by a potent type 2 immune response, chronic AD is associated with increased cutaneous expression of type 1 cytokines including IFN-γ (262). Consistent with this, significantly increased IFN-γ expression was detected in a subset of AD blister fluid samples. Moreover, IL-22 expression was significantly increased in AD blister fluids compared to HC samples. IL-22 may contribute to AD pathogenesis by promoting keratinocyte hyperplasia and production of pro-inflammatory S100 calcium-binding proteins such as S100A7 (263), which was detected at significantly increased expression levels in some AD blister fluids. Chronic AD is associated with excessive skin remodelling and dermal fibrosis, which contributes to formation of pruritic eczematous lesions (264). Increased expression of TGF-β1 and matrix metalloproteinases, involved in tissue remodelling and skin fibrosis, was detected in a subset of AD compared to HC blister fluids. Increased cutaneous IgE levels were measured in all AD blister fluid samples, consistent with the majority of individuals with AD showing allergic sensitisation to common environmental allergens (265).

IgE binding to FcƐRI on mast cells results in release of a diverse range of pro-inflammatory mediators, including the lipid mediator PGD2. Therefore, cutaneous IgE likely exacerbates type 2 immune responses in AD skin by promoting ILC2 and Th2 cell activation and type 2 cytokine production in part through mast cell-derived PGD2 (136, 266).

While our *in vivo* human skin suction blister model enabled the investigation of local immune responses at steady state and following allergen exposure, the analysis of proteome profiles of saline- or allergen-challenged skin was complicated by several factors. The skin suction blister technique is labour intensive, technically challenging and requires considerable participant involvement. Therefore, participant numbers were limited, which made comparison of treatment groups difficult. Small volumes of skin suction blister fluids meant that not all samples could be analysed by both SOMAscan and Luminex assays. Analysis of the SOMAscan data was complicated further by the finding of significant differences within the AD group and the detection of intracellular proteins, perhaps explained by cell death. 6 AD samples were found to cluster separately in dimensional reduction analysis of SOMAscan proteomics data. This separate AD group, labelled AD_2, was enriched for blister fluids collected following intradermal injection of allergens, especially HDM. AD_2 samples showed enrichment for immune-related pathways, such as T cell activation, and comparison of protein expression in AD_2 with the remaining AD samples or HC blister fluids revealed significant upregulation of pro-inflammatory cytokines and chemokines in AD_2 samples. While this may be indicative of increased immune activation in response to allergen challenge, experimental factors cannot be excluded. Detection of high expression of intracellular proteins, such as signalling

molecules, was surprising as cells were removed from blister fluids by centrifugation prior to downstream analysis. It is noteworthy that blister fluids were frozen prior to proteome analysis. Detection of intracellular proteins may be explained by incomplete cell removal and cell lysis during the freezing process. Moreover, skin suction blisters represent a form of physical trauma to the skin and can be associated with some bleeding. This is reflected in the detection of haemoglobin subunit alpha one in all samples. It cannot be excluded that the extent of bleeding and presence of erythrocytes and platelets was variable across blister fluid samples thereby affecting protein levels. While we could observe overall differences in the proteome signature of AD and HC blister fluids, we did not detect significant differences in protein expression between saline-treated and allergen-challenged skin or blister fluids formed over AD lesions. However, this was not particularly surprising given the low sample size in each treatment group. Further analysis of additional skin suction blister fluid samples will help to decipher the cutaneous proteome profile at homeostasis and during allergic inflammation.

3.3.2 AD patients are characterised by an altered systemic cytokine and chemokine signature with CCL17, CCL22 and CCL27 positively correlating with disease severity

To characterise the systemic inflammatory signature in AD, expression of 40 cytokines and chemokines was measured in sera from individuals with or without AD by Luminex multianalyte profiling. Overall, individuals with AD were characterised by an elevated systemic cytokine/chemokine profile, with highest concentrations detected in individuals with severe AD. Levels of Th2 cell-recruiting chemokines, especially CCL17 and CCL22, were significantly increased in AD sera

with highest levels detected in sera from individuals with severe AD, confirming previous reports (267, 268). In contrast, serum levels of Th1 cell-homing factors, such as CXCL9, CXCL10 and CXCL11, were unchanged in individuals with AD. Other chemokines significantly upregulated in AD sera included the CCR1 ligand CCL23 and the CCR3 ligand CCL26. CCL23-expressing cells, such as monocytes, have been detected at increased frequencies in the epidermis of AD patients, and IL-4 and IL-13 have been shown to induce CCL23 secretion by monocytes (269). The CCR3 ligands CCL11, CCL24 and CCL26 are chemotactic factors for eosinophils and basophils, but CCR3 has also been implicated in the recruitment of Th2 cells during allergic airway inflammation (270). Previously, CCL26, but not CCL24, has been detected at increased levels in AD serum (271). The data of this study extend these findings showing elevated levels of CCL26, but not CCL11 or CCL24, in AD serum with CCL24 expression instead being increased in the skin of individuals with AD. Significantly higher levels of the skin-homing factor CCL27 were detected in AD compared to HC sera. CCL27 levels were highest in sera from individuals with severe AD, consistent with reported positive correlation of serum CCL27 levels with AD severity (272).

We identified serum levels of CCL17, CCL22, CCL26 and CCL27 as markers of AD, reliably distinguishing between HC and AD samples. In children with AD, serum levels of CCL17, CCL22 and CCL27 have been found to significantly correlate with AD severity (273) and effective dupliumab AD treatment was associated with reduced serum CCL17 concentrations (250). It has been proposed that elevated serum protein levels in individuals with AD are a result of proteins overexpressed in the skin leaking into blood (274). This would explain the detection of CCL27,

exclusively produced in the skin (275), at elevated levels in AD serum. Consistent with a predominantly cutaneous expression of CCL27, high levels of CCL27 were measured in skin suction blister fluids from both HC and AD participants. Overall comparison of cutaneous and systemic cytokine/chemokine profiles revealed higher average levels in the skin compared to blood, supporting the hypothesis of the inflamed skin being the source of upregulated chemokine and cytokine levels in serum from individuals with AD.

3.3.3 Human ILC2 may perform functions beyond their role as potent type 2 cytokine producers with implications for allergic inflammation

ILC2 perform crucial functions as type 2 cytokine producers in the defence against parasitic infections and the induction of type 2 inflammation. Evidence is emerging for ILC2 effector functions beyond the production of type 2 cytokines. The data presented herein supports this notion and indicates that human ILC2 are capable of producing a broad range of pro- and anti-inflammatory cytokines and chemokines.

ILC lack antigen-specific receptors and instead respond to environmental cues. Alarmins, cytokines predominantly released by the epithelium in response to parasite- or allergen-induced damage, have been identified as potent ILC2 stimulants (90, 93, 94, 98, 100, 140–142). Comparison of *in vitro* human ILC2 cytokine/chemokine production in response to stimulation with IL-33, IL-25 or TSLP identified IL-33 as the predominant ILC2-inducing alarmin. This is consistent with previous analysis of *in vivo* mouse (90, 140, 142) and *in vitro* human ILC2 (93, 144). *In vivo,* ILC2 tissue-residency has been proposed to determine ILC2 responsiveness to specific alarmins (124). *In vitro,* TSLP treatment of human blood-derived ILC2 was found to have no effect on ILC2 cytokine/chemokine secretion,

while IL-25 induced stimulation of some *in vitro* ILC2 lines. Previously, an IL-25-responsive ILC2 population was described that appeared in response to *N. brasiliensis* infection or IL-25 treatment (143). Instead of activating ILC2 cytokine/chemokine production, TSLP might predominantly act as an ILC2 survival factor (144). Human ILC2 cytokine/chemokine production was found to be most potently induced *in vitro* with a combination of IL-33, IL-25 and TSLP suggesting a synergistic effect of alarmins on ILC2 activation. This might be due to reciprocal alarmin-induced receptor upregulation (93, 144).

Following *in vitro* stimulation with a combination of alarmins, human ILC2 were found to secrete increased levels of a broad range of cytokines and chemokines. In addition to secreting high levels of the type 2 cytokine IL-13, activated ILC2 were demonstrated to produce high levels of pro-inflammatory cytokines, such as TNF-α and GM-CSF, and chemokines, including CCL1, CXCL5, CXCL8, CCL3 and CCL25. While ILC2 production of GM-CSF has previously been reported (134, 136), little is known about its functional involvement in the regulation of myeloid cell survival and differentiation, which will be explored in chapter 5. The detection of neutrophil-recruiting chemokines, including CCL1, CXCL5 and CXCL8, in activated ILC2 supernatants implies a role for ILC2 in neutrophil chemotaxis to sites of inflammation. Indeed, increased neutrophil tissue infiltration has been observed in human allergic lung and skin inflammation (240, 276). In addition, detection of increased levels of chemotactic factors for eosinophils and basophils, such as CCL11 and CCL26, in stimulated ILC2 supernatants implies a role for ILC2 in tissue accumulation of eosinophils and basophils. ILC2 have previously been implicated in eosinophil recruitment during influenza virus infection (190) and allergic airway

inflammation (145, 208, 277) by producing IL-5. Moreover, activated ILC2 were found to produce a range of chemokines that regulate T cell trafficking, such as CCL25 and CCL27 that mediate gut- and skin-homing, respectively. Previously, mouse intestinal $CCR9^{+}$ ILC were shown to migrate to CCL25 (128), while human ILC2 have been shown to express the CCL27 receptor CCR10 (93). The findings of this study suggest that ILC2 may be involved in ILC and T cell gut and skin homing through production of CCL25 and CCL17, respectively. The functional implications of ILC2-derived T cell homing factors in tissue homeostasis and inflammation will be explored in chapter 4.

Analysis of stimulation-induced fold change increases in ILC2 cytokine/chemokine production revealed differential upregulation of cytokines including IL-6, IL-10 and surprisingly IFN-γ and IL-22, generally associated with ILC1 and ILC3 responses, respectively. ILC2 heterogeneity and plasticity in regard to phenotype and effector cytokine production is increasingly being recognised (124, 131, 132, 142, 148). Following stimulation, upregulated IL-6 and IL-10 production was observed in a small proportion of ILC2 lines. Several studies have reported the production of the non-classical type 2 cytokine IL-6 by activated ILC2 (93, 134, 148). IL-6 has pleiotropic functions demonstrated by abnormalities of IL-6-deficient mice in the defence against viral and bacterial pathogens, in the induction of effective immune responses to tissue damage and in wound healing responses (278, 279). Recently, our lab has identified a pathway by which ILC2-derived IL-6 might contribute to the defence against bacterial pathogens. *In vitro* exposure of ILC2 to heat-killed skin-resident bacteria, such as *S. aureus* and *S. epidermidis*, resulted in the induction of IL-6 production by human ILC2 involving the intracellular PRR NOD2 (135).

Through secretion of both IL-6 and TNF-α, ILC2 may be involved in the generation of the acute phase response following tissue damage or infection. IL-10-producing ILC2 have been reported by a number of studies, such as during pulmonary and intestinal inflammation in mice (110, 111) and in human peripheral blood and gut at homeostasis (111, 112). Following *in vitro* stimulation with IL-2, IL-7, IL-33 and retinoic acid, IL-10-producing ILC2 were found to simultaneously produce IL-13 (111, 112). Together with the data presented herein, showing simultaneous production of anti-inflammatory IL-10 and pro-inflammatory cytokines, such as TNF-α, GM-CSF and IL-8/CXCL8, this implies that IL-10-producing ILC2 might not represent a distinct ILC2 subset but instead might represent an activation state. *In vivo,* the balance between production of pro-inflammatory and anti-inflammatory cytokines might determine the effect of ILC2 on local inflammation. Indeed, allergic individuals were found to have a lower proportion of ILC2 capable of producing IL-10 *in vitro* (112). Moreover, the effect of negative ILC2 regulators, such as IFN-γ and IL-27, on IL-10 production has not yet been explored. Detection of IFN-γ and IL-22 in activated ILC2 supernatants was surprising given their predominant expression by ILC1 and ILC3, respectively. However, it is becoming evident that ILC2 display a degree of phenotypic and functional plasticity, such as conversion into IFN-γ-producing ILC1/ILC2 (131, 132, 280) and IL-22-producing ILC2/ILC3 (280) while retaining type 2 cytokine producing capacities. Interestingly, similar to the results of alarmin-stimulated ILC2 cytokine production presented in this study, a small percentage of human blood ILC2 were reported to produce IFN-γ and IL-22 upon *in vitro* PMA plus ionomycin stimulation (280). While this suggests that ILC2 have the capacity to produce cytokines associated with type 1 and type 17 responses, it cannot be excluded that it is an artefact of *in vitro* ILC2 culture.

Although *in vitro* ILC2 expansion is required to obtain sufficient ILC2 numbers for functional experiments and offer the unique opportunity to study the activity and function of human ILC2, *in vitro* culture may nevertheless result in changes to some aspects of ILC2 biology. *In vivo*, ILC2 activity is tightly regulated by control mechanisms, while *in vitro* culture conditions are highly stimulatory potentially giving rise to mildly activated ILC2. Moreover, *in vitro,* ILC2 responses are assessed in response to stimulants in isolation. However, *in vivo*, ILC2 phenotype and function appears to be dictated by a plethora of tissue-specific environmental cues (124, 142, 148). Further studies on *ex vivo* human and *in vivo* mouse ILC2 will aid in the characterisation of tissue- and context-specific ILC2 cytokine and chemokine profiles.

Overall, the data presented herein suggest functions of human ILC2 beyond their established role as type 2 cytokine producers with implications for allergic inflammation, which will be discussed in chapter 6 with a particular focus on AD. Enriched at barrier and mucosal tissue sites, ILC2 are likely involved in immunosurveillance and the maintenance of tissue homeostasis. Following sensing of invading viral (281) and bacterial (10) pathogens, ILC2 production of cytokines, such as IL-6, TNF-α, and chemokines, such as neutrophil-homing factors CXCL8, CCL1 and CXCL5, may contribute to defence during viral and bacterial infection. Moreover, ILC2-derived IL-10 might be involved in limiting tissue inflammation. However, through excessive and dysregulated pro-inflammatory cytokine and chemokine production, ILC2 may directly promote accumulation and activation of inflammatory immune cells resulting in chronic inflammation (Fig. 3.24). The next chapters address such ILC2 functionality.

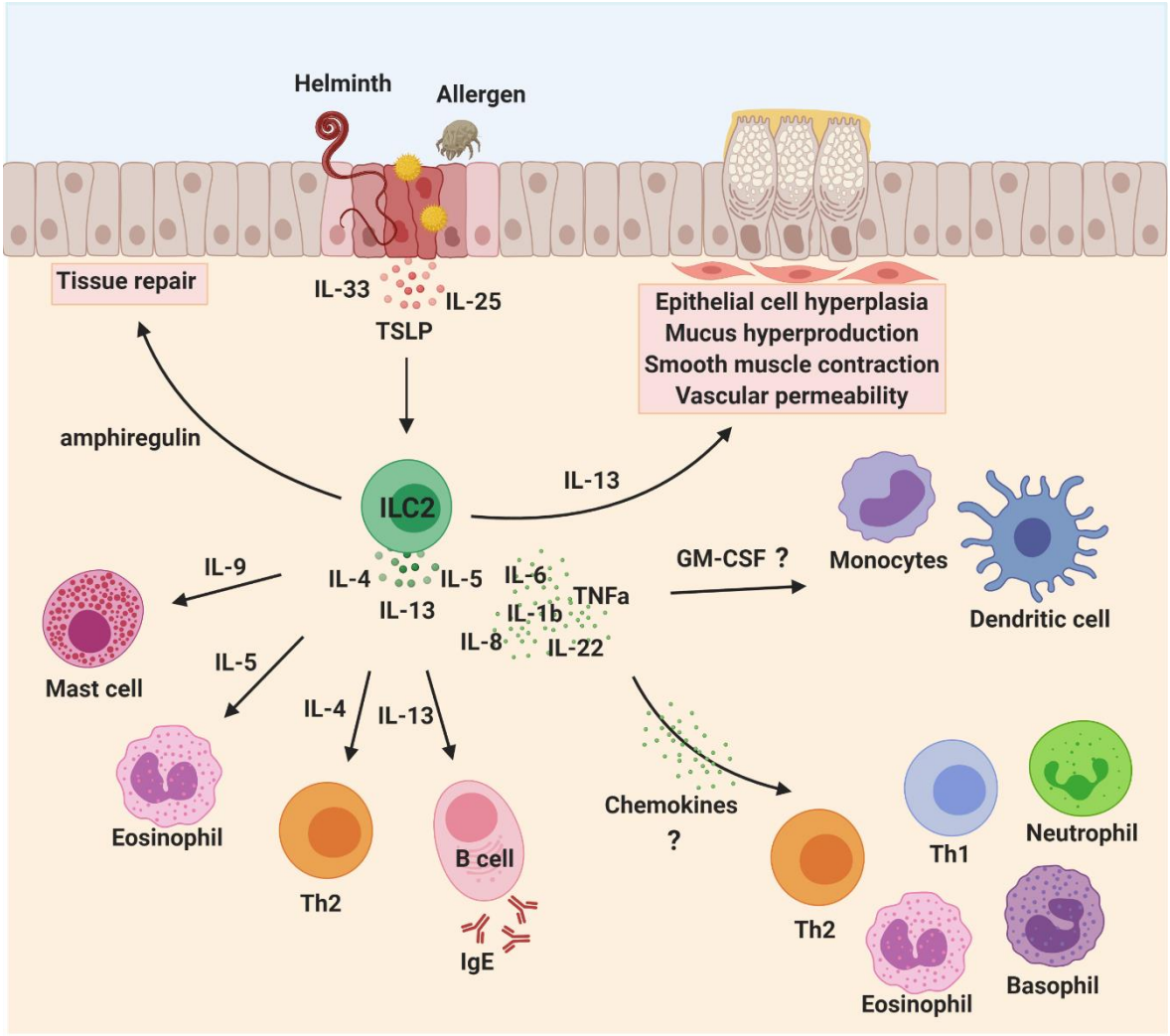


Figure 3.24 Potential contribution of ILC2 to protective immunity and allergic inflammation through cytokine- and chemokine-mediated mechanisms.

Through production of type 2 cytokines, ILC2 are critically involved in the induction of type 2 immune responses in the context of parasitic infection and allergic inflammation. By producing amphiregulin, ILC2 contribute to wound healing and the maintenance of tissue integrity. ILC2 may be able to produce cytokines not classically associated with type 2 immune responses, such as IL-6, IL-8, IL-22, TNF-α and GM-CSF. ILC2-derived GM-CSF might contribute to the survival and differentiation of monocytes/monocyte-derived cells. Moreover, ILC2 may be able to regulate tissue homing of both innate and adaptive immune cells through the secretion of chemokines.

Chapter 4: ILC2 amplify type 2 immune responses by promoting the recruitment of CCR4$^+$ ILC2 and T cells

4.1 Introduction

4.1.1 Regulation of T cell homing

T cell trafficking through lymphoid and non-lymphoid tissues is essential for immune homeostasis and the induction of adaptive immune responses, and is coordinated by chemotactic factors and their cognate receptors as well as adhesion molecules (225) (Fig 4.1). Adhesion molecules, including selectins, cadherins and integrins, mediate tethering, rolling and firm arrest on endothelial cells before extravasation into tissues (220, 225). While the essential involvement of adhesion molecules in leukocyte homing should be acknowledged, this chapter will focus on the role of chemokines and chemokine receptors in T cell trafficking. T cell activation and differentiation is accompanied by the acquisition of activation state-, subset- and tissue-specific chemokine receptor expression profiles that result in differential homing patterns. Following activation, both naïve CD4$^+$ and CD8$^+$ T cells upregulate the expression of the inflammatory chemokine receptor CXCR3 (282). Differentiated Th1 cells are characterised by the expression of CCR5, CXCR3 and CXCR6, while Th2 cells preferentially express CCR4, CCR8 and the homing PGD2 receptor CRTH2 (225, 283, 284). Cytokines polarising the differentiation of T helper cell subsets have been identified as regulators of differential chemokine expression. Upregulation of CXCR3 on Th1 cells is dependent on IL-12/STAT4/T-bet-signalling (285, 286), while induction of CCR4 expression on Th2 cells has been found to depend on IL-4 and the TFs STAT6 and GATA3 (286, 287). Consistently, induction of CCR6 on Th17 cells appears to be dependent on TGF-β and TFs RORα and

RORγt (288, 289). Moreover, chemokines and their receptors guide T cell trafficking into specific tissues, such as CCR9 directing gut tropism (290) and CCR4 and CCR10 primarily being associated with skin-homing T cells (291). Circulating Foxp3$^+$ Tregs express a wide range of chemokine receptors, such as CCR5 and CXCR3, CCR4 and CCR8, and CCR6, that mediate homing to non-lymphoid tissues such as the lung, gut and skin and are normally associated with Th1, Th2 and Th17 cells, respectively. Heterogeneous expression of chemokine receptors by activated Tregs has been postulated to enable homing into a wide range of tissues, which is essential for the regulation of immune responses and the maintenance of tissue homeostasis (225, 292).

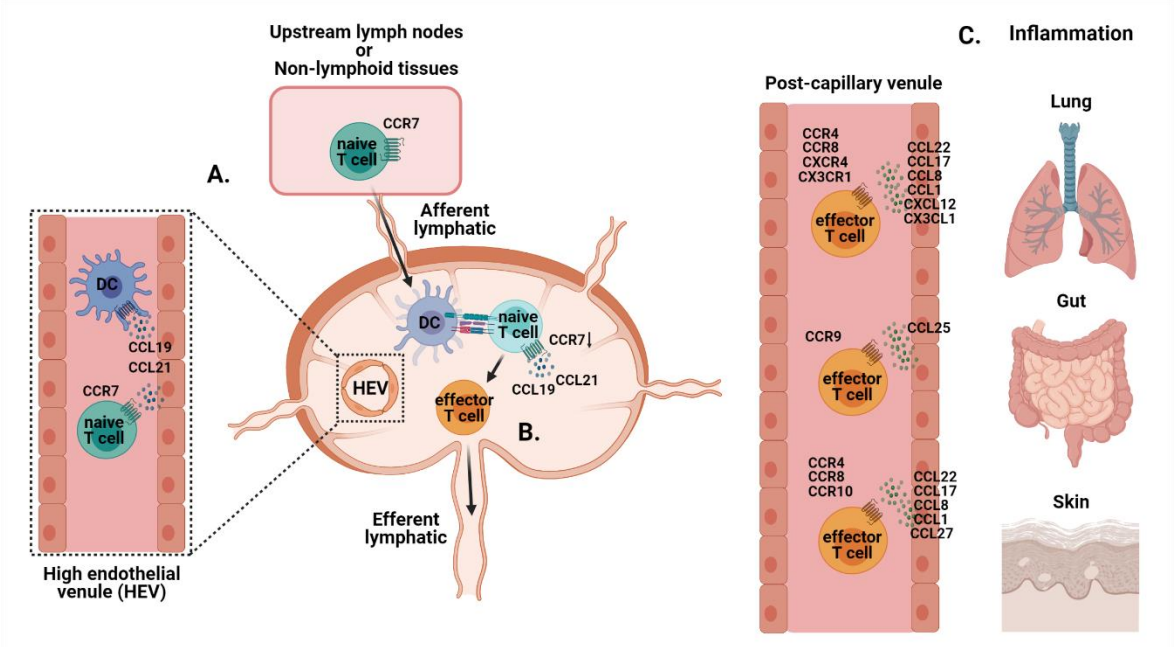


Figure 4.1 T cell homing is regulated by chemokine receptors and their ligands.
(**A**) CCR7$^+$ naïve T cells and APC enter lymph nodes from the blood via high endothelial venules (HEVs) or via the lymphatics from upstream lymph nodes or non-lymphoid tissues in a CCL19/CCL21-dependent manner. Chemotaxis into the T cell zone is dependent on CCR7. (**B**) Following T cell activation and differentiation, which is associated with CCR7 downregulation, effector T cells, expressing subset and tissue-specific homing receptors, leave lymph nodes via efferent lymphatics to the thoracic duct before entering the

circulation. (**C**) During inflammation, increased chemokine expression in inflamed tissues induces tissue infiltration of specific chemokine receptor-expressing effector T cells. The role of adhesion molecules in T cell homing is not depicted here. Adapted from (293, 294).

4.1.2 Role of CCL22 and CCL17 in the recruitment of CCR4$^+$ T cells

Initially, CCR4 was thought to be predominantly expressed by Th2 cells (295, 296). It has become evident that CCR4 is also expressed by other effector and memory T cell subsets including skin-homing T cells expressing the adhesion molecule cutaneous lymphocyte antigen (CLA) (297, 298), Tregs (299) and Th17 cells (300). CCR4 facilitates chemotaxis to its chemokine ligands CCL22 and CCL17 (295) that have been shown to be produced by vascular endothelial cells (297), activated epidermal keratinocytes (301, 302), airway epithelial cells (303) and APC such as monocytes, macrophages and DC (295, 304–306). Although both CCL22 and CCL17 are high-affinity ligands for CCR4, the two CCR4 ligands have been proposed to play non-redundant functions in T cell recruitment. CCL22 has been identified as the higher affinity CCR4 ligand and *in vitro* triggered integrin-dependent T cell adhesion more efficiently than CCL17, which suggests that CCL17 may selectively recruit cells expressing high levels of CCR4 (307). CCL22 potently induced the internalisation of CCR4 on human Th2 cells in a manner involving lipid raft and clathrin-coated pits, while CCL17 only weakly did so. CCL22-induced CCR4 internalisation was found to result in transient loss of chemotactic responsiveness to both CCL22 and CCL17. In contrast, CCL17 caused transient loss of Th2 cell responsiveness to CCL17 but not CCL22. Functional responsiveness of CCR4 is restored upon removal of exogenous chemokines involving receptor recycling (308). Differential expression patterns and non-reductant functional activities suggest that CCL22 and CCL17 may mediate recruitment of CCR4$^+$ cells in a sequential manner.

CCL17 might promote vascular recognition and cell arrest while preserving CCR4 responsiveness to CCL22. Subsequently, CCL22 may mediate cell homing within the tissue microenvironment (307, 308).

CCR4 is involved in T cell homing to the skin, especially during cutaneous inflammation, as discussed below, as well as to asthmatic lungs. Increased mRNA expression and levels of CCL22 and CCL17 have been detected in bronchial biopsies and BAL fluid from individuals with asthma (309). Following allergen challenge, analysis of bronchial biopsies of atopic asthmatics indicated increased infiltration of $CCR4^+$ Th2 cells (303). In a model of allergic airway inflammation, repeated allergen exposure resulted in increased infiltration of $CCR4^+$ Th2 cells, implicating CCR4 in long-term recruitment of adaptive Th2 cells in chronic lung inflammation (270). Consistently, blockade of CCR4 in a humanised mouse model of allergic lung inflammation resulted in reduced infiltration of Th2 cells and abrogated airway eosinophilia, goblet cell hyperplasia and bronchial hyperresponsiveness (310).

4.1.3 Role of CCR4 and its chemokine ligands in the maintenance of skin homeostasis

CCR4 has been demonstrated to be highly expressed on skin-infiltrating lymphocytes (298, 311). The less potent CCR4 ligand CCL17 has been detected in human non-inflamed skin, which implies a role for CCL17-mediated selective cell homing in cutaneous immune surveillance (312). In mice, loss of CCR4 expression on Tregs resulted in the development of severe skin inflammation (313). In humans, clinical trials of anti-CCR4 monoclonal antibody, mogamulizumab, in the treatment of adult T cell leukaemia/lymphoma reported cases of severe skin inflammation as

adverse events. Severe skin inflammation was associated with a complete loss of Foxp3$^+$ Tregs in the affected skin (314). These results highlight the important role of CCR4-mediated cell recruitment, especially of Tregs, in the maintenance of skin homeostasis.

4.1.4 Role of CCR4 and its chemokine ligands in AD pathogenesis

CCL22 and CCL17 have been implicated in the pathogenesis of AD by contributing to the accumulation of pathogenic Th2 cells in inflamed skin. We and others have reported significantly increased levels of both CCL22 and CCL17 in sera from individuals with AD, which positively correlate with disease severity (267, 315). In AD lesional skin, *CCL17* and *CCR4* mRNA expression were significantly higher than in healthy skin or chronic AD lesions highlighting a role of CCR4 and its ligands in acute skin inflammation (316). Consistent with this, the majority of CD4$^+$ T cells in AD lesions were found to express CCR4 (317). Immunohistochemical analysis of inflamed human skin from individuals with AD and psoriasis revealed differential expression patterns of CCL22 and CCL17, with CCL17 being expressed by vascular endothelial cells and tissue-infiltrating DC while CCL22 could only be detected within skin-infiltrating cells of the cutaneous tissue microenvironment (307). In mice, overexpression of CCL17 in keratinocytes resulted in increased recruitment of CCR4$^+$ Th2 cells and the development of allergic skin inflammation following chronic antigen exposure (318). Stimulation of human primary keratinocytes with IL-13 upregulated the production of CCL22 and induced preferential recruitment of CCR4$^+$ T cells. This implies an amplification loop between CCL22-secreting keratinocytes and IL-13-producing CCR4+ T cells, which might contribute to AD exacerbation (302). Moreover, increased production of TSLP by keratinocytes in AD skin has

been suggested to contribute to DC stimulation and induction of CCL22 and CCL17 production (238). Colonisation of lesional skin with the gram-positive bacterium *S. aureus* is a common feature of AD and positively correlates with disease severity (319). *In vitro*, monocyte-derived Langerhans cells and moDC from individuals from AD produced increased levels of both CCL22 and CCL17 at steady state compared to cells isolated from healthy individuals and responded to peptidoglycan from gram-positive bacteria by further upregulation of CCL22 and CCL17 secretion (320). This suggests a mechanism of AD exacerbation driven by an *S. aureus*-induced increase in CCR4 ligand production by skin-resident and -infiltrating APC. In murine AD-like skin inflammation, cutaneous administration of a CCR4 antagonist significantly improved AD-like skin lesions (321, 322). Together, these reports highlight the role of CCR4 and its ligands CCL22 and CCL17 in AD pathogenesis and disease exacerbation, making CCR4 a potential therapeutic target.

4.1.5 ILC2 homing

ILC2 tissue homing is increasingly being recognised. In mice, ILC2 were found to constitutively express the gut-homing receptor CCR9 (323). During *N. brasiliensis* infection, IL-25-induced iILC2 chemotactically migrated from the intestine to the lymphatics, blood circulation and eventually to the lung, involving S1P receptors, which was crucial for worm clearance, tissue repair and host survival (127). *In vitro,* lipid mediators PGD2 and LTE4 have been identified as potent chemoattractants for human ILC2 (136, 155). PGD2-mediated recruitment contributed significantly to the accumulation of ILC2 in the lung in a murine model of helminth-induced pulmonary inflammation (151). Following allergen challenge of individuals with asthma, ILC2 numbers in BAL fluid were found to be increased while peripheral blood ILC2

frequency decreased, which implies recruitment of blood ILC2 to inflamed lungs (197). In a mouse model of IL-33-induced lung inflammation, increased ILC2 numbers were detected in the lung (324) and IL-33 has been implicated in the egress of ILC2 progenitors from the bone marrow and infiltration into the lung following tissue disruption (325). Consistently, IL-33 has been demonstrated to induce human ILC2 migration *in vitro* (93). IL-33 treatment of mice resulted in increased expression of CCR8 and CCR1 on lung ILC2 and CCR8-mediated ILC2 chemotaxis appeared to play a role in ILC2 accumulation in the peribronchial space (324). In the skin, murine dermal ILC2 were characterised by migratory bursts followed by interactions with skin-resident mast cells (11). Human skin-derived ILC2 were shown to express the skin-homing receptors CLA, CCR4 and CCR10 (93) and intradermal allergen challenge of individuals with AD was associated with ILC2 infiltration to the skin (240). Collectively, this suggests that ILC2 migrate between tissues and that chemotactic homing is important for the function of ILC2 in the maintenance of tissue homeostasis and in allergic inflammation. However, much remains to be understood regarding the expression of homing receptors and the migratory patterns of ILC2.

4.1.6 Hypothesis and aims

Analysis of human ILC2 in skin suction blister RNA sequencing data, generated previously in our lab, revealed upregulated expression of *CCL22* and *CCL17* in ILC2 compared to T cells following *in vivo* HDM intradermal challenge (chapter 3). Additionally, the gene encoding CCR4, the shared receptor for CCL22 and CCL17, was found to be highly expressed in blood- and skin-derived ILC2 (Fig. 4.2). This, together with our findings of increased levels of CCL22 and CCL17 in skin blister

fluids from individuals with AD compared to healthy volunteers (chapter 3), suggests a potential involvement of ILC2 in the CCR4-mediated accumulation of ILC2 and Th2 cell in inflamed skin. Previously, a mouse model of allergic lung inflammation has demonstrated a role for ILC2-derived IL-13 in the induction of CCL17 production by pulmonary DC and the recruitment of $CCR4^+$ memory Th2 cells into the lung (212). Therefore, I hypothesised that ILC2 may be involved in the direct and/or indirect recruitment of $CCR4^+$ ILC2 and T cells.

To test this hypothesis, the following aims were addressed:

a. Investigate the production of CCL22 and CCL17 by human ILC2
b. Compare CCL22 and CCL17 secretion by blood- and skin-derived ILC2 from healthy volunteers and individuals with AD
c. Determine the effect of human ILC2 on the production of CCL22 and CCL17 by moDC
d. Analyse the expression of CCR4 on ILC2 from healthy volunteers and individuals with AD
e. Study the mechanisms regulating the expression and responsiveness of CCR4 on ILC2
f. Assess chemotaxis of ILC2 and T cells to skin tissue levels of CCL22 and CCL17
g. Evaluate the ability of human ILC2 to recruit both ILC2 and T cells
h. Determine the contribution of ILC2-derived CCL22 and CCL17 to the recruitment of CCR4-expressing ILC2 and T cells

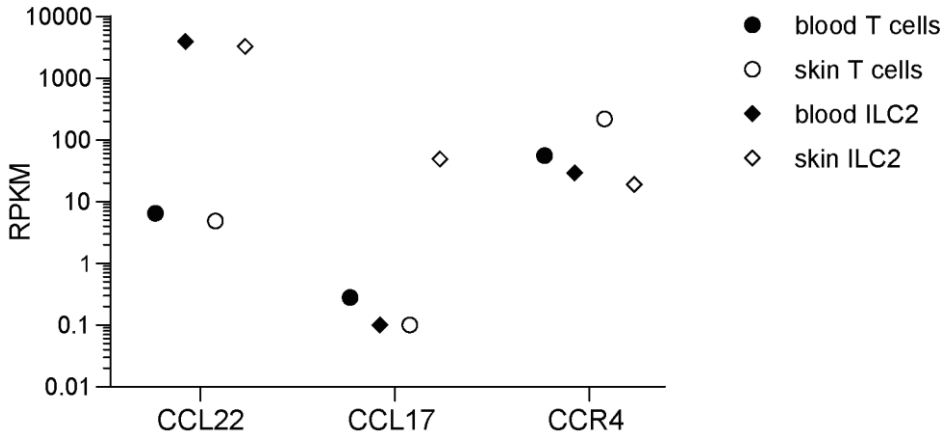


Figure 4.2 *CCL22*, *CCL17* and *CCR4* expression in ILC2 and T cells upon *in vivo* allergen challenge.
ILC2 and T cells were isolated from peripheral blood or skin suction blister fluids following 24h intradermal HDM challenge. Gene expression of *CCL22*, *CCL17* and *CCR4* in blood- and skin blister fluid-derived ILC2 and T cells was determined by RNA sequencing and measured in RPKM (n=1).

4.2 Results

4.2.1 CCL22 and CCL17 expression by human ILC2

4.2.1.1 Transcriptional expression of *CCL22* and *CCL17* in human ILC2

To assess transcriptional expression of *CCL22* and *CCL17* in human ILC2, human blood ILC2 were isolated and expanded, stimulated with alarmins IL-33, IL-25 and TSLP, and *CCL22* and *CCL17* expression analysed by real-time PCR. ILC2 activation induced a significant upregulation of *CCL22* and *CCL17* expression (Fig. 4.3, A and B). There was no significant difference in the activation-induced fold increase in *CCL22* compared to *CCL17* expression (Fig. 4.3, C). These data confirm our *ex vivo* RNA sequencing results showing *CCL22* and *CCL17* expression by human ILC2.

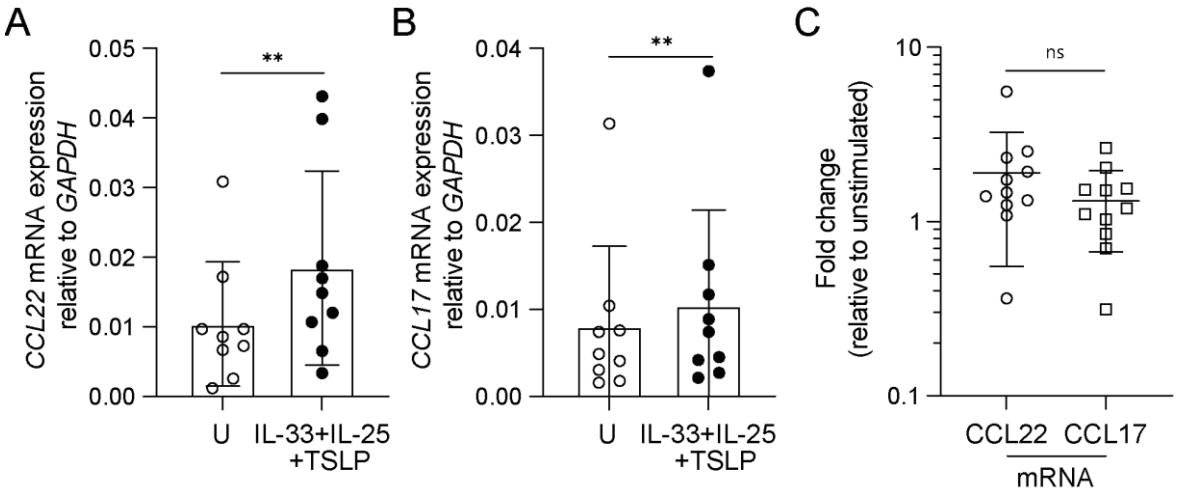


Figure 4.3 *CCL22* and *CCL17* mRNA expression in human ILC2.

(**A-C**) Blood-derived ILC2 from healthy donors were cultured in medium alone (U) or with IL-33, IL-25 and TSLP (50ng/ml each) for 6h. (**A and B**) *CCL22* (**A**) and *CCL17* (**B**) mRNA expression levels relative to *GAPDH* were measured by qRT-PCR. (**C**) Fold change of *CCL22* and *CCL17* expression in stimulated ILC2 relative to unstimulated ILC2. (n=9; representative of ≥ 3 independent experiments). *P < 0.05, **P < 0.01, Wilcoxon matched-pairs test (mean ± SD).

4.2.1.2 CCL22 and CCL17 secretion by human ILC2

To investigate whether activation-induced *CCL22* and *CCL17* mRNA expression was accompanied by increased CCL22 and CCL17 protein secretion, blood-derived ILC2 from healthy donors were stimulated with IL-33, IL-25 and TSLP for 72h and chemokine levels in culture supernatants measured by ELISA. ILC2 were found to secrete tonic low level CCL22 and CCL17, at average concentrations of 79.74pg/ml and 47.14pg/ml respectively. ILC2 activation significantly upregulated the secretion of both CCL22 and CCL17 (Fig. 4.4, A and B). The activation-induced fold increase in CCL17 production was significantly higher than that of CCL22 (Fig. 4.4, C). ILC2 production of CCL22 and CCL17 appeared to be donor dependent as some donors were found to produce noticeably higher CCL22 and CCL17 levels at baseline and following activation than others. Overall, these results show that human ILC2

constitutively secrete low levels of CCL22 and CCL17 with further upregulation observed following activation with alarmin cytokines. The effects of culture on ILC2 phenotype is tested later in the chapter.

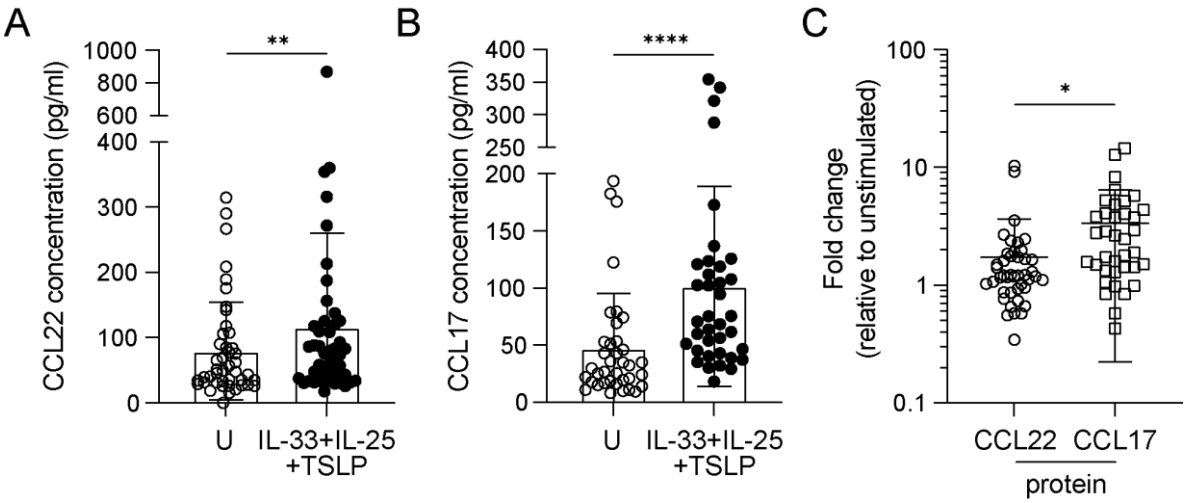


Figure 4.4 CCL22 and CCL17 secretion by human ILC2.

(**A-C**) Blood-derived ILC2 from healthy donors were cultured in medium alone (U) or stimulated with IL-33, IL-25 and TSLP (50ng/ml each) for 72h. (**A and B**) Concentrations of CCL22 (**A**) and CCL17 (**B**) in ILC2 culture supernatants were measured by ELISA. (**C**) Fold change of CCL22 and CCL17 levels in culture supernatants from stimulated relative to unstimulated ILC2 (n=37-44; representative of ≥3 independent experiments). *P < 0.05; **P < 0.01; ***P < 0.001; ****P < 0.0001, Wilcoxon matched-pairs test (mean ± SD).

4.2.1.3 CCL22 and CCL17 secretion by skin ILC2

The chemokines CCL22 and CCL17 are believed to play an important role in cutaneous recruitment of CCR4^{+} cells. This, together with the fact that ILC2 are enriched in the skin, raises the possibility of tissue-dependent differential expression of CCL22 and CCL17 by skin ILC2. To address this question, CCL22 and CCL17 secretion by skin-derived ILC2 was assessed. There was no significant difference in the levels of CCL22 and CCL17 secreted by unstimulated and activated skin-derived compared to blood-derived ILC2 (Fig. 4.5, A and B). Similar to blood-derived

ILC2, skin-derived ILC2 were found to constitutively secrete low level CCL22 and CCL17 (Fig. 4.5, A and B). Activation of skin-derived ILC2 appeared to slightly, but not significantly, upregulate CCL22 and CCL17 production. However, stimulation of skin-derived ILC2 was found to induce an approximate 1.756- and 4.016-fold increase in CCL22 and CCL17 levels, respectively, which was comparable to blood-derived ILC2 (Fig. 4.5, C and D). Analysis of the proportion of ILC2 lines analysed that secreted CCL22 and CCL17 levels of at least 100 pg/ml, suggested an increased frequency of $CCL22^{high}$- and $CCL17^{high}$-producing steady state skin-derived compared to blood-derived ILC2 (Fig. 4.5, E and F).

These results suggest that, *in vitro*, ILC2 derived from healthy skin secrete CCL22 and CCL17 at levels similar to blood-derived ILC2. However, proportional analysis implied an increased frequency of ILC2 producing substantial levels of CCL22 and CCL17 in the skin-derived population at steady state.

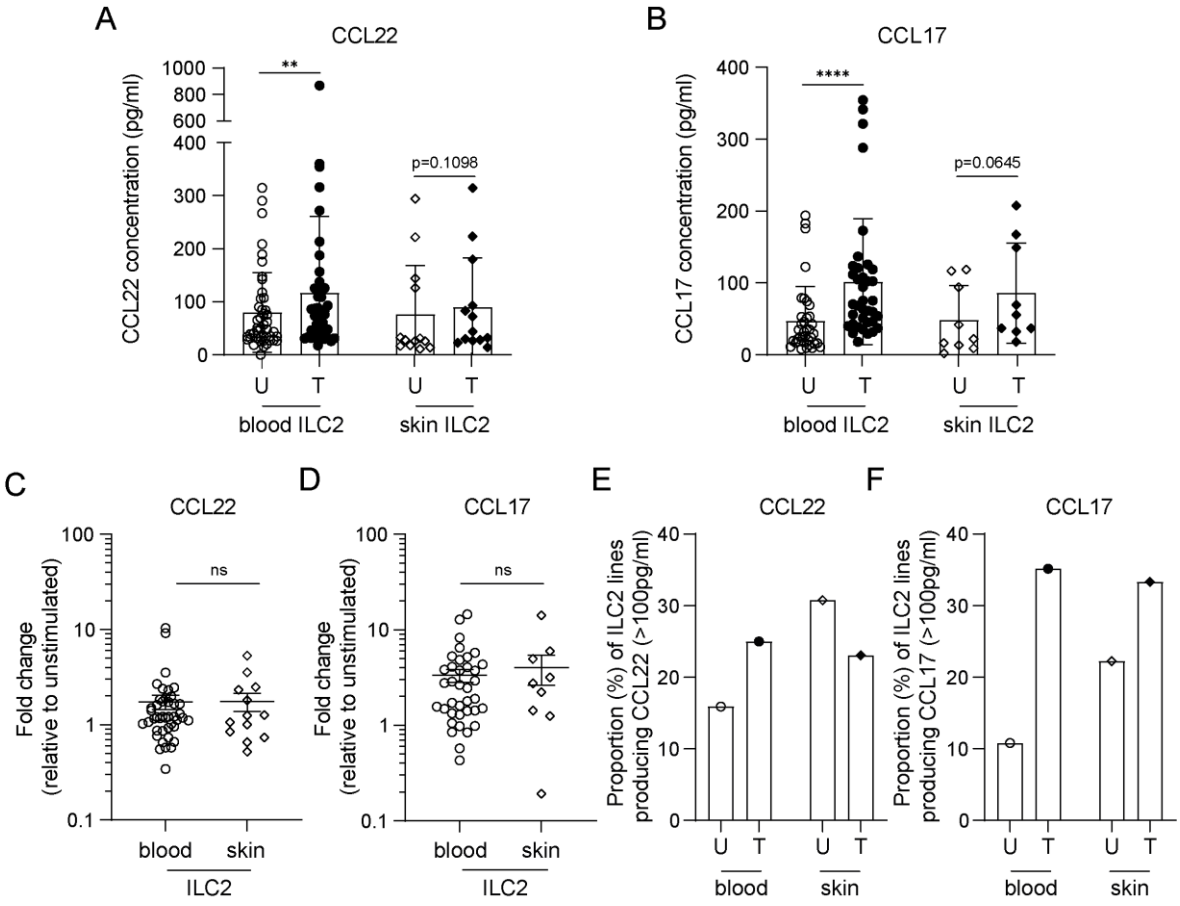


Figure 4.5 Comparison of CCL22 and CCL17 secretion by skin- and blood-derived ILC2.

(**A-F**) ILC2 derived from HC blood and skin were cultured in medium alone (U) or stimulated with IL-33, IL-25 and TSLP (T) (50 ng/ml each) for 72h. Blood ILC2 data is same as in Fig. 4.4. (**A and B**) Concentrations of CCL22 (**A**) and CCL17 (**B**) in blood- and skin-derived ILC2 culture supernatants were measured by ELISA (n=9-44; representative of ≥ 3 independent experiments). *P < 0.05; **P < 0.01; ***P < 0.001, ****P < 0.0001. Two-way ANOVA with Sidak's post hoc multiple comparisons test (mean ± SD). (**C and D**) Fold change of CCL22 (**C**) and CCL17 (**D**) levels in culture supernatants from stimulated relative to unstimulated blood- and skin-derived ILC2 (n=9-44; representative of ≥ 3 independent experiments). unpaired Student`s *t* test (mean ± SEM). (**E and F**) Proportion (%) of blood- and skin-derived ILC2 lines analysed that secrete ≥ 100 pg/ml CCL22 (**E**) and CCL17 (**F**). (n=9-44; representative of ≥ 3 independent experiments).

4.2.1.4 CCL22 and CCL17 secretion by ILC2 from individuals with AD

Given the increased CCL22 and CCL17 levels detected in the blood and skin of individuals with AD and the positively correlation with AD severity, production of CCL22 and CCL17 by ILC2 from individuals with AD was analysed. Following stimulation, ILC2 from individuals with AD significantly upregulated the secretion of both CCL22 and CCL17, reaching average levels of 110 pg/ml and 125 pg/ml, respectively (Fig. 4.6, A and B). ILC2 from individuals with AD appeared to produce slightly higher average levels of CCL17 compared to HC ILC2, however, differences were not statistically significant (Fig. 4.6, B). There was no significant difference in the activation-induced fold increase in CCL22 and CCL17 secretion by AD ILC2 compared to HC ILC2 (Fig. 4.6, C and D). The AD ILC2 lines analysed appeared to contain an increased frequency of $CCL22^{high}$- and $CCL17^{high}$-producing cells at both steady state and following activation compared to the HC ILC2 population (Fig. 4.6, E and F).

While no significant difference was detected between the levels of CCL22 and CCL17 produced *in vitro* by ILC2 isolated from individuals with AD compared to HC, individuals with AD may display a higher proportion of ILC2 that produce substantial levels of CCR4 ligands. I go on to investigate changes of ILC2 phenotype during culture later in the chapter.

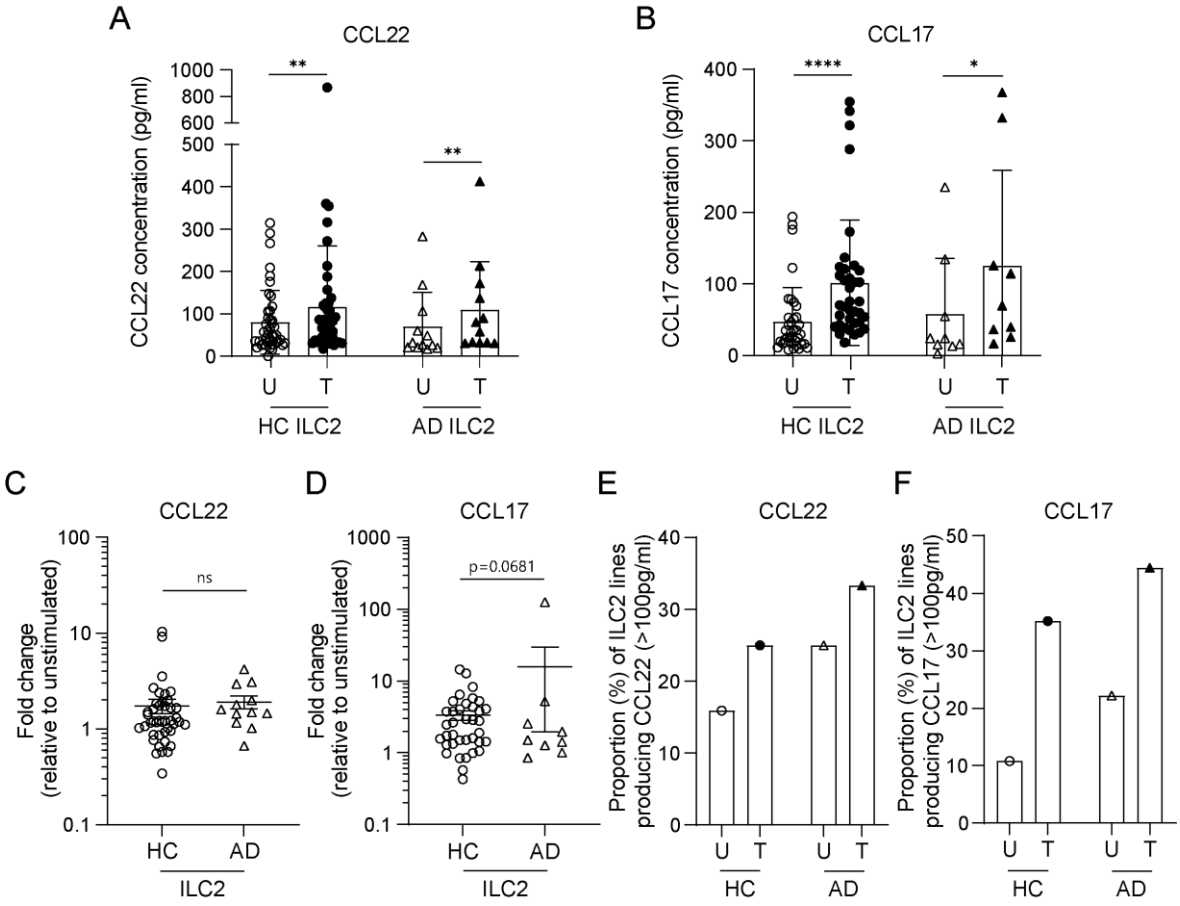


Figure 4.6 Comparison of CCL22 and CCL17 secretion by HC- and AD-derived ILC2. (**A-F**) Blood-derived ILC2 from individuals with AD and healthy donors were left unstimulated (U) or stimulated with IL-33, IL-25 and TSLP (T) (50 ng/ml each) for 72h. HC blood ILC2 data is same as in Fig. 4.4. (**A and B**) Concentrations of CCL22 (**A**) and CCL17 (**B**) in HC and AD ILC2 culture supernatants were measured by ELISA (n=9-44; representative of ≥ 3 independent experiments). *P < 0.05; **P < 0.01; ***P < 0.001, ****P < 0.0001. Two-way ANOVA with Sidak's post hoc multiple comparisons test (mean ± SD). (**C and D**) Fold change of CCL22 (**C**) and CCL17 (**D**) levels in culture supernatants from stimulated relative to unstimulated HC and AD ILC2 (n=9-44; representative of ≥ 3 independent experiments). unpaired Student's *t* test (mean ± SEM). (**E and F**) Proportion (%) of HC and AD ILC2 lines analysed that secrete ≥ 100 pg/ml CCL22 (**E**) and CCL17 (**F**). (n=9-44; representative of ≥ 3 independent experiments).

4.2.2 ILC2 promote moDC CCL22 and CCL17 production

Pulmonary DC have been identified as major producers of CCL22 and CCL17 during allergic airway inflammation (310, 326). IL-13 has been suggested to play an

important role in the induction of CCL22 and CCL17 production by pulmonary DC (326). Indeed, in a murine model of allergic lung inflammation, ILC2-derived IL-13 was found to stimulate the secretion of CCL17 by lung DC in response to allergen re-challenge (212). This suggests that ILC2 may amplify type 2 immune responses by promoting the production of CCL22 and CCL17 by DC. To investigate whether human ILC2 induce the secretion of CCR4 ligands by DC, moDC were generated *in vitro* and cultured for 24h in supernatants from unstimulated and IL-33, IL-25, TSLP-activated ILC2. *In vitro* differentiated immature moDC were characterised by lack of surface CD14 and CD80, high expression of CD1a and DC-SIGN and moderate expression of MHCI (HLA-ABC), MHCII (HLA-DR) and CD86 (Fig. 4.7, A). Culture of moDC in ILC2 supernatants resulted in the production of high levels of CCL22 and CCL17 (Fig. 4.7, B and C). Supernatants from stimulated ILC2 significantly upregulated the secretion of CCL22 by moDC compared to the negative control (Fig. 4.7, B). To account for the presence of ILC2 stimulants, medium plus IL-33, IL-25, TSLP was used as a negative control. While negative control moDC supernatants contained average CCL17 levels of 0.466 ng/ml, culture of moDC in unstimulated and stimulated ILC2 supernatants resulted in average CCL17 levels of 1.04 ng/ml and 2.495 ng/ml in moDC supernatants, respectively. However, ILC2-induced upregulation of CCL17 secretion by moDC did not reach statistical significance, likely due to high variability (Fig. 4.7, C). Blocking of IL-4Rα, the receptor subunit for both IL-4 and IL-13, and IL-13Rα2 signalling resulted in a slight, but not statistically significant, reduction in CCL22 and CCL17 production by moDC following culture in ILC2 supernatants (Fig. 4.7, B and C).

These results suggest that activated ILC2 induce moDC to secrete high levels of CCL22 and potentially CCL17, in a manner that might partially involve ILC2-derived IL-4 and/or IL-13.

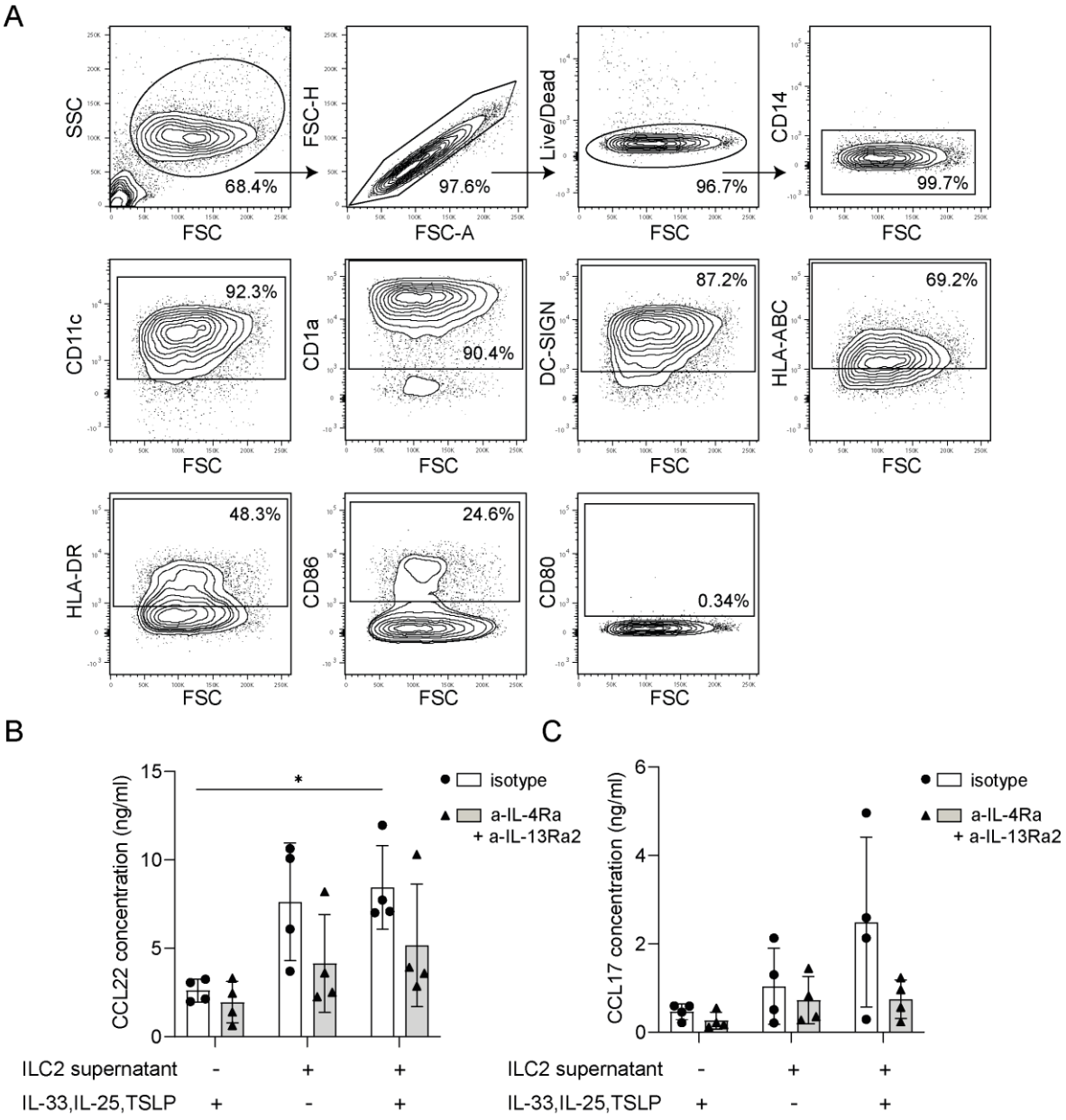


Figure 4.7 ILC2-induced secretion of CCL22 and CCL17 by moDC.

(**A**) Monocytes were isolated by CD14 MACS separation and differentiated to moDC by 5d culture in IL-4 (10 ng/ml) and GM-CSF (100 ng/ml). moDC differentiation was confirmed by FACS analysis. Plots representative of n=4. (**B and C**) ILC2 were stimulated with IL-33, IL-25, TSLP (50 ng/ml each) or control medium for 48h and ILC2 supernatants added to d5

moDC for 24h in the presence or absence of anti-IL-4Rα (a-IL-4Ra, 10 µg/ml) and anti-IL-13Rα2 (a-IL-13Ra2, 10 µg/ml) antibodies. Levels of CCL22 (**B**) and CCL17 (**C**) in moDC supernatants were measured by ELISA (n=4; representative of ≥ 3 independent experiments). *P < 0.05. RM two-way ANOVA with Tukey's post hoc multiple comparisons test (mean ± SD).

4.2.3 CCR4 expression on human ILC2

Our previously generated RNA sequencing data revealed expression of *CCR4*, the common receptor for CCL22 and CCL17, by both blood and skin ILC2 and T cells. CCR4 contributes to recruitment of T cells to the skin (327) and has been implicated in AD pathogenesis. A significantly higher proportion of $CD4^+$ T cells from individuals with AD have been found to express CCR4 (317). Our lab has previously reported expression of CCR4 on human skin-derived ILC2 (93). However, CCR4 expression on ILC2 and its functional relevance have not yet been studied in detail.

4.2.3.1 Comparison of CCR4 expression on *ex vivo* blood and skin ILC2 and T cells from healthy donors and individuals with AD

To study the expression of CCR4 on *ex vivo* human ILC2 and compare it with T cell CCR4 expression, ILC2 and T cells were isolated from blood and skin of healthy donors and individuals with AD and CCR4 expression analysed by flow cytometry (Fig. 4.8, A). Consistent with published data, the frequency of $CCR4^+$ T cells was significantly enriched in HC skin (Fig. 4.8, A and B). However, circulating T cells from individuals with AD expressed significantly higher levels of surface CCR4 compared to HC T cells (Fig. 4.8, C). The frequency of circulating CCR4-expressing ILC2 in healthy individuals varied substantially between donors, clustering into $CCR4^{high}$ and $CCR4^{low}$ groups (Fig. 4.8, D). On average, blood ILC2 were found to contain a higher proportion of $CCR4^+$ cells compared to blood T cells (Fig. 4.8, A, B

and D). In contrast to T cells, there was no noticeable enrichment of $CCR4^+$ ILC2 in the skin compared to blood. However, the average frequency of $CCR4^+$ T cells and ILC2 in the skin was approximately 40%. Differences in the pattern of CCR4 expression between ILC2 and T cells could be due to comparison of ILC2 with all $CD3^+$ cells and not with Th2 cells. There was no significant difference in the frequency of $CCR4^+$ ILC2 between HC blood and skin, and AD blood (Fig. 4.8, D). Similar to AD T cells, blood ILC2 from individuals with AD were found to express significantly higher surface CCR4 levels compared to HC blood ILC2 (Fig. 4.8, E).

These results demonstrate that human ILC2 are characterised by surface CCR4 expression and indicate that CCR4 expression on both circulating ILC2 and T cells is upregulated in individuals with AD.

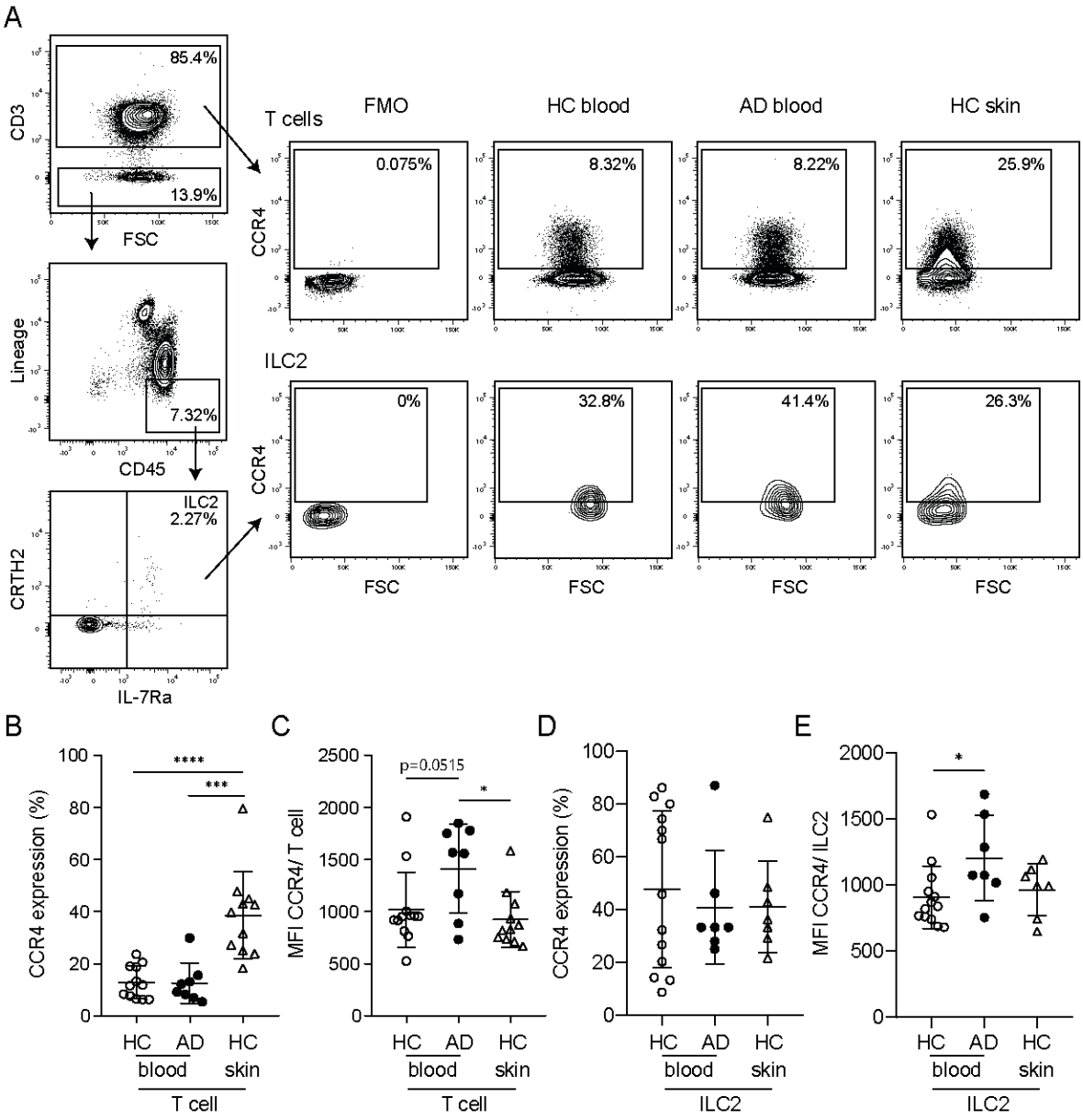


Figure 4.8 CCR4 surface expression on *ex vivo* human ILC2 and T cells.

(**A**) PBMC were isolated from HC blood and skin, and AD blood and CCR4 expression on $CD3^+$ T cells and $CD3^-$ Lin^- $CD45^+$ $IL\text{-}7R\alpha^+$ $CRTH2^+$ ILC2 analysed by flow cytometry. Numbers indicate percentages of cells within the indicated gates, gated on the parent population. Plots representative of n=7-13. (**B**) Percentage of $CCR4^+$ T cells. (**C**) CCR4 expression levels per $CD3^+$ T cell. (**D**) Percentage of $CCR4^+$ ILC2. (**E**) CCR4 protein expression levels per ILC2. MFI, mean fluorescence intensity. FMO, fluorescence minus one control. (n=7-13; data representative of ≥ 3 independent experiments). *P < 0.05; **P < 0.01; ***P < 0.001, ****P < 0.0001; One-way ANOVA with Tukey`s post hoc multiple comparisons test (mean ± SD).

4.2.3.2 CCR4 expression on *in vitro* cultured ILC2

To investigate whether CCR4 may define a distinct ILC2 subpopulation and to assess the effect of the *in vitro* expansion and culturing process on the expression of CCR4 on ILC2, ILC2 were isolated from HC blood and CCR4 expression on *in vitro* cultured ILC2 analysed by flow cytometry. Following *in vitro* expansion, a range of CCR4 expression on ILC2 was observed. While some cultured ILC2 lacked surface CCR4, other expanded ILC2 lines were characterised by a high frequency of $CCR4^+$ cells (Fig. 4.9, A). CCR4 expression did not appear to be donor dependent. Next, $CCR4^-$ and $CCR4^+$ ILC2 were sorted and CCR4 expression assessed following *in vitro* expansion. Surface CCR4 did not seem to be stably expressed on ILC2, as CCR4 down- and upregulation was observed on $CCR4^+$- and $CCR4^-$-sorted ILC2, respectively, following *in vitro* expansion (Fig. 4.9, B and C).

These results indicate that CCR4 does not define a distinct ILC2 subpopulation and suggest that CCR4 is dynamically expressed on ILC2, changing extensively during the expansion and culturing process. I next proceeded to test relevant pathways underlying CCR4 regulation.

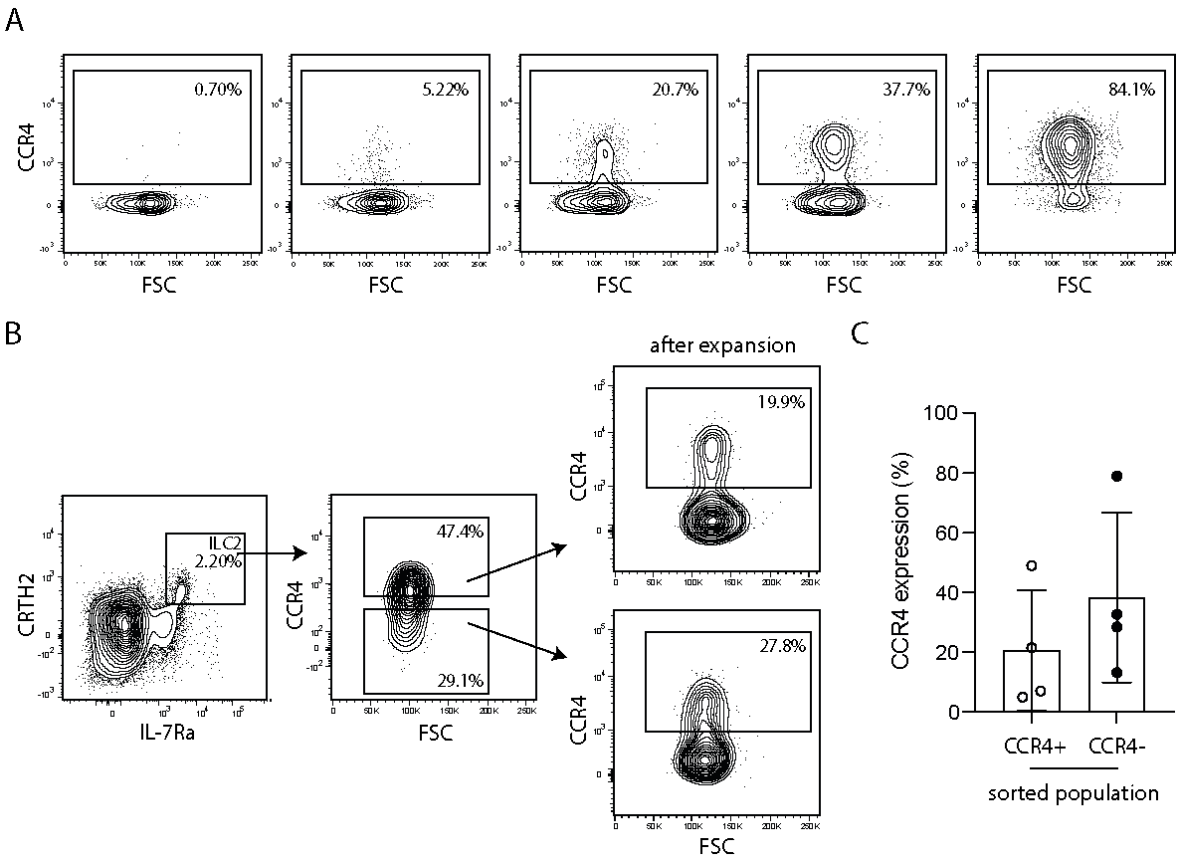


Figure 4.9 CCR4 expression on *in vitro* cultured ILC2.

(**A**) HC blood ILC2 were isolated and expanded *in vitro*. CCR4 expression on *in vitro* cultured ILC2 was analysed by flow cytometry. Numbers indicate percentages of cells within the indicated gates, gated on live ILC2. (**B**) $CCR4^+$ and $CCR4^-$ ILC2 were sorted from healthy donors and expanded *in vitro*. (**C**) CCR4 expression on $CCR4^-$ and $CCR4^+$ sorted ILC2 following *in vitro* expansion was analysed by flow cytometry. Numbers indicate percentages of cells within the indicated gates, gated on the parent population. (n=4; representative of ≥ 3 independent experiments). ns with paired Student's *t* test (mean ± SD).

4.2.3.3 CCR4 downregulation by CCL22 and CCL17

One mechanism of limiting responsiveness of cells to chemokine gradients is chemokine-induced receptor internalisation and desensitisation. The CCR4 ligand, CCL22 has previously been identified as a strong inducer of CCR4 internalisation on human Th2 cells (308). To investigate whether CCR4 expression on human ILC2

is regulated by a similar mechanism, ILC2 and T cells were incubated with increasing concentrations of recombinant human CCL22 or CCL17 and surface CCR4 expression assessed by flow cytometry. Consistent with its reported role as an inducer of CCR4 internalisation, CCL22 triggered a noticeable dose-dependent reduction in the percentage of CCR4 expression on both T cells and ILC2 (Fig. 4.10, A and B). CCL22-mediated CCR4 downregulation was found to be rapid. Within 30 minutes, 10 ng/ml of CCL22 induced the downregulation of surface CCR4 on both T cells and ILC2 by approximately 30%. Incubation with increasing concentrations of CCL22 resulted in further surface CCR4 downregulation, by an average of 53% and 56% at 100 ng/ml for T cells and ILC2, respectively (Fig. 4.10, C and D). In contrast, CCL17 was found to induce CCR4 downregulation to a lesser extent than CCL22. While CCL17 at concentrations over 50 ng/ml triggered CCR4 downregulation by about 25% on T cells, culture of ILC2 in the presence of CCL17 resulted in a slight reduction in the percentage expression of surface CCR4 (Fig. 4.10, E and F). Differences in the extent of chemokine-induced CCR4 downregulation between T cells and ILC2 might be due to the analysis of all $CD3^+$ T cells and not Th2 cells.

Overall, these data indicate differential potency of CCL22 and CCL17 to induce the downregulation of surface CCR4 on human ILC2, in a similar manner to T cell CCR4. While CCL22 was demonstrated to efficiently mediate CCR4 downregulation on ILC2 in a dose-dependent manner, CCL17 only weakly did so.

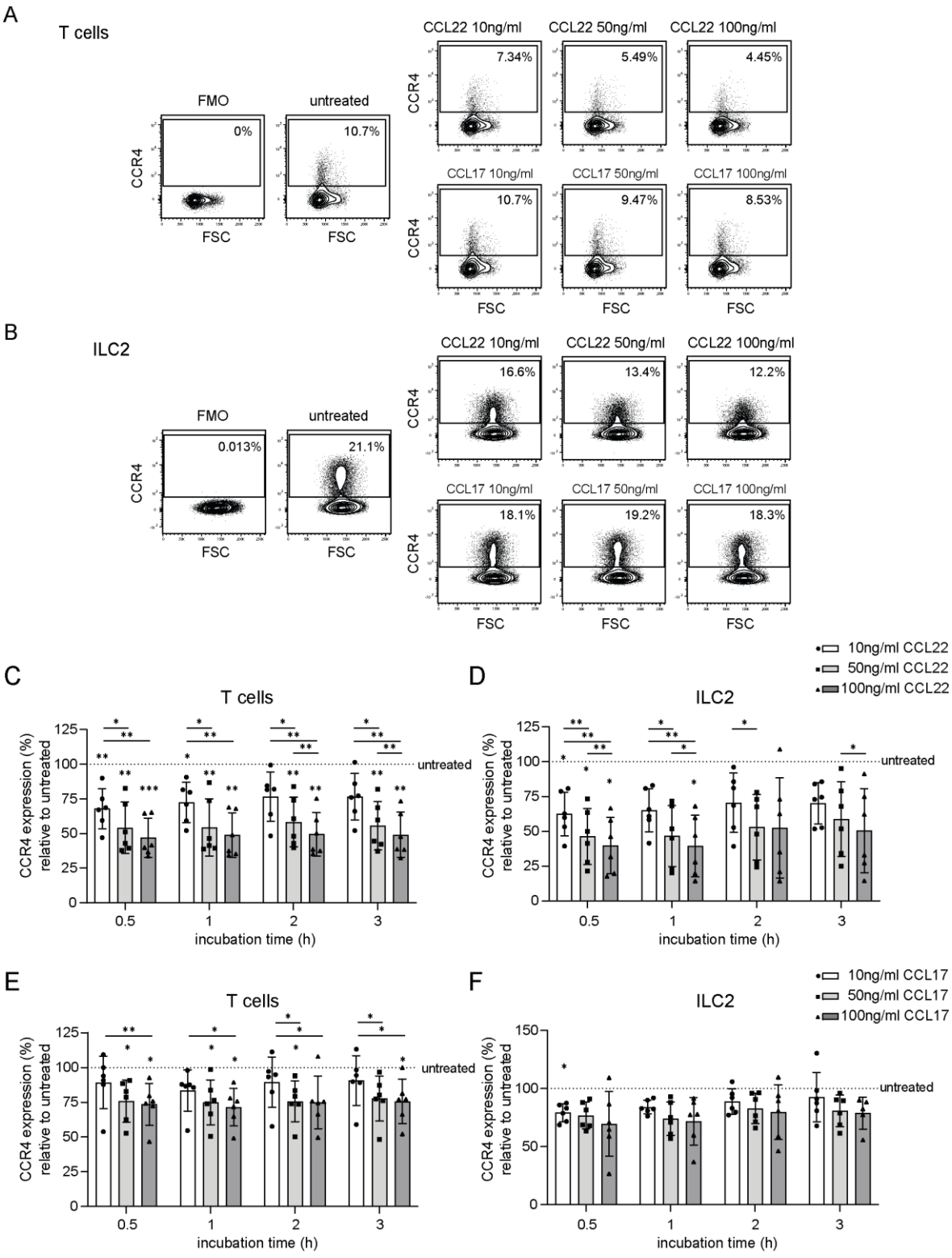


Figure 4.10 Analysis of CCL22- and CCL17-mediated downregulation of surface CCR4 on ILC2 and T cells.

(**A and B**) *Ex vivo* blood-derived T cells (**A**) and cultured blood-derived ILC2 (**B**) were incubated with increasing concentrations (10 ng/ml, 50 ng/ml, 100 ng/ml) of CCL22 or

CCL17 for 30mins and surface CCR4 expression analysed by flow cytometry. Numbers indicate percentages of cells within the indicated gates. Plots representative of n=4-6. (**C and D**) Percentage CCR4 expression on T cells (**C**) and ILC2 (**D**) relative to untreated control (100%) following incubation with increasing concentrations (10 ng/ml, 50 ng/ml, 100ng/ml) of CCL22 for 30mins, 1h, 2h or 3h. (**E and F**) Percentage of CCR4 expression on T cells (**E**) and ILC2 (**F**) relative to untreated control (100%) following incubation with increasing concentrations (10 ng/ml, 50 ng/ml, 100 ng/ml) of CCL17 for 30mins, 1h, 2h or 3h. (n=4-6; data representative of ≥ 3 experiments). *P < 0.05; **P < 0.01; RM two-way ANOVA with Tukey's post hoc multiple comparisons test (mean ± SD).

4.2.3.4 Activation-induced upregulation of surface CCR4 on human ILC2

Following activation, human naïve $CD4^+$ T cells have been demonstrated to upregulate expression of CCR4, which is increased further during differentiation into Th2 cells (283). To study the modulation of CCR4 expression in human ILC2 in response to activation, blood-derived ILC2 were stimulated with IL-33, IL-25 and TSLP individually or in combination, and CCR4 expression assessed at both the protein and mRNA level. Flow cytometry analysis revealed a progressive and significant upregulation of surface CCR4 expression over a 24-hour period following stimulation with IL-33 or a combination of IL-33, IL-25 and TSLP (Fig. 4.11, A and B). Following 24-hour culture in IL-33 or in the combination of IL-33, IL-25 and TSLP, a significant increase in the frequency of $CCR4^+$ ILC2 was detected, by an average factor of 5.01 and 7.17 compared to the unstimulated control, respectively. There was no significant difference in the percentage of CCR4 expression following stimulation with IL-33 alone compared to IL-33, IL-25 and TSLP in combination, which suggests that IL-33 is the major factor inducing CCR4 upregulation. However, 12 hours after activation with IL-33, IL-25 and TSLP combined, but not with IL-33 alone, the frequency of $CCR4^+$ ILC2 was found to be significantly increased compared to the unstimulated control. Moreover, at 24 hours, the average

percentage expression of CCR4 was slightly higher on ILC2 cultured in IL-33, IL-25 and TSLP compared to IL-33 alone. At 24 hours, there was also a 2.5-fold increase in the frequency of $CCR4^+$ ILC2 following culture in IL-25 compared to medium alone. This indicates that while IL-33 appears to be the main inducer of CCR4 upregulation on ILC2, IL-25 may also contribute (Fig. 4.11, B). Analysis of mRNA by real-time PCR showed a slight transcriptional upregulation of *CCR4* in response to IL-33, IL-25 and TSLP-mediated ILC2 activation (Fig. 4.11, C).

These results indicate that ILC2 activation by IL-33, IL-25 and TSLP is accompanied by an upregulation of CCR4 transcriptional and protein expression. This suggests that activated ILC2 may display increased chemotactic responsiveness to CCL22 and CCL17.

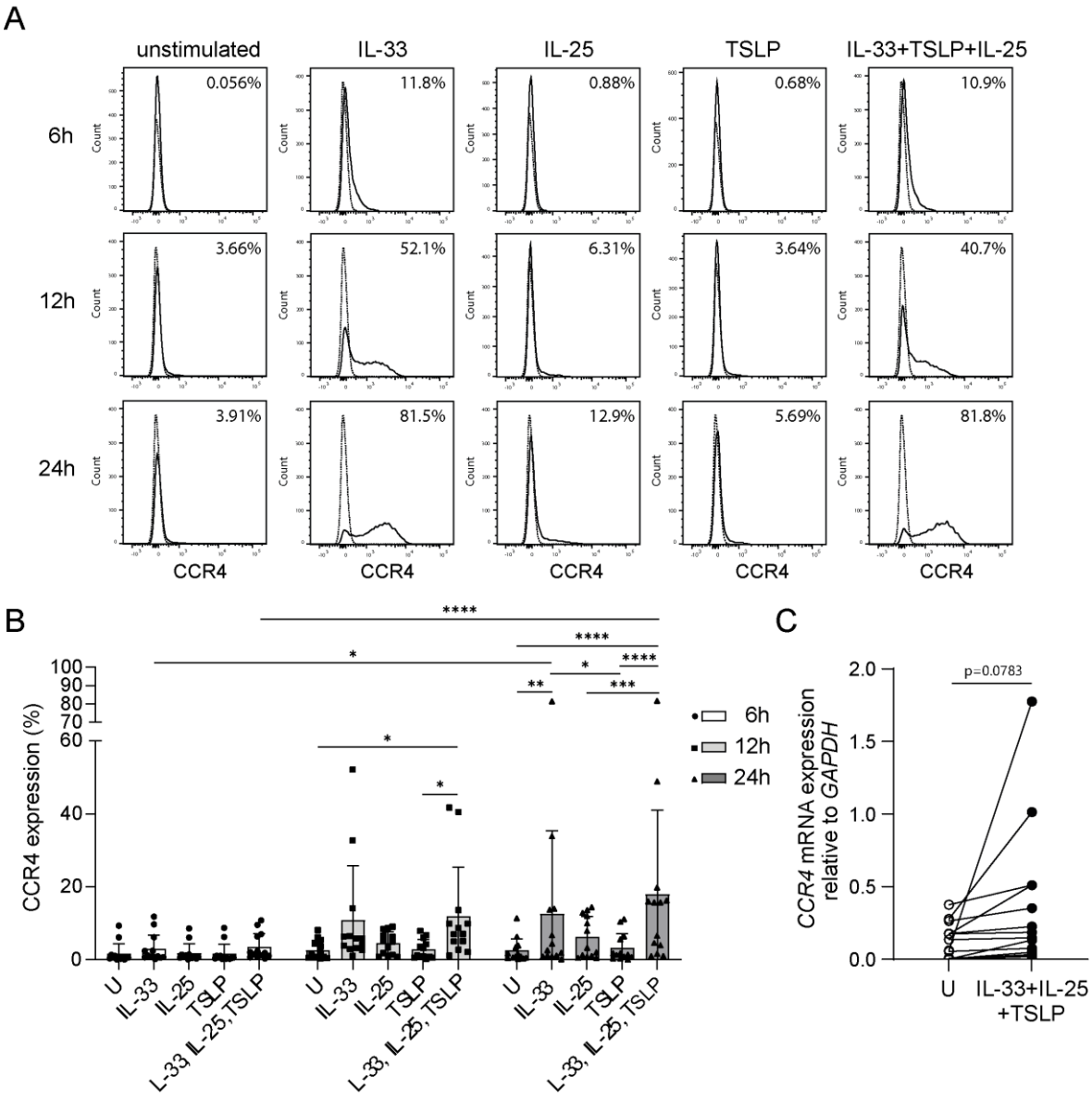


Figure 4.11 Regulation of CCR4 surface expression on ILC2 by alarmins.

(**A**) ILC2 were left untreated (U) or stimulated with IL-33 (50 ng/ml), IL-25 (50 ng/ml), TSLP (50 ng/ml) or a combination of IL-33, IL-25 and TSLP (50 ng/ml each) for 6h, 12h or 24h and cell surface CCR4 expression analysed by flow cytometry. Numbers indicate percentages of $CCR4^+$ cells, gated on live ILC2. Plots representative of n=13. (**B**) Percentage of $CCR4^+$ ILC2 following 6h, 12h or 24h culture in the presence of alarmins. (n=13, representative of ≥ 3 independent experiments). *P < 0.05; **P < 0.01; ***P < 0.001, ****P < 0.0001; RM two-way ANOVA with Tukey's post hoc multiple comparisons test (mean ± SD). (**C**) ILC2 were left untreated (U) or stimulated with a combination of IL-33, IL-25 and TSLP (50 ng/ml) for 6h and *CCR4* mRNA expression relative to *GAPDH* measured by qRT-

PCR. (n=14; representative of >3 independent experiments). Paired Student's *t*-test (mean ± SD).

4.2.4 Chemotactic responsiveness of CCR4$^+$ ILC2 and ILC2-mediated recruitment of ILC2 and T cells

The expression of surface CCR4 by a significant proportion of *ex vivo* and *in vitro* cultured ILC2 indicates that ILC2 may be chemotactically responsive to CCR4 ligands CCL22 and CCL17. Moreover, the finding that ILC2 not only promote the production of CCL22 and CCL17 by moDC but also secrete CCL22 and CCL17, suggests that ILC2 might be able to recruit CCR4-expressing cells both indirectly, via moDC, and directly. To evaluate the chemotactic responsiveness of CCR4$^+$ ILC2 and assess ILC2-mediated recruitment of ILC2 and T cells, *in vitro* chemotaxis assays were performed.

4.2.4.1 Optimisation of *in vitro* chemotaxis assay

As chemotaxis of CCR4$^+$ T cells toward CCL22 and CCL17 has been well studied, CCR4$^+$ T cells were sorted, expanded and used for the optimisation of *in vitro* migration assays (Fig. 4.12, A). Firstly, migration of CCR4$^+$ T cells to dose titrations of recombinant human CCL22 and CCL17 was assessed. The degree of migration, referred to as migration index, was determined by the number of migrated cells relative to the number of cells migrated to the medium alone control, known as random migration. Both CCL22 and CCL17 were found to induce CCR4$^+$ T cell chemotaxis in a dose-dependent manner, peaking at approximately 1000 ng/ml for CCL22 and 500 ng/ml for CCL17 (Fig. 4.12, B and C). CCR4$^+$ T cell chemotaxis to CCL22 and CCL17 in combination peaked at approximately 300 ng/ml of both chemokines (Fig., 4.12, D). Reduced migration was observed at very high

concentrations of CCL22 and CCL17, such as 1500 ng/ml, due to maximum receptor occupancy and loss of chemotactic gradient (Fig. 4.12, B, C and D). In response to intradermal HDM challenge, skin suction blister fluids from healthy controls were found to contain CCL22 and CCL17 concentrations between 2.39-11.68 ng/ml and 0.26-2.6 ng/ml, respectively, with increased levels detected in blister fluids from individuals with AD (chapter 3). Based on these results, we considered 10 ng/ml as physiologically relevant skin-tissue levels of CCL22 and CCL17. Recruitment of $CCR4^+$ T cells to skin-tissue levels of CCL22 and CCL17 was confirmed *in vitro*. Migration of $CCR4^+$ T cells was significantly higher than that of $CCR4^-$ T cells, which showed minimal migration to CCL22 and CCL17 (Fig. 4.12, E). This confirmed receptor specificity of the *in vitro* CCL22- and CCL17-mediated chemotaxis assay and showed that receptor responsiveness was retained on sorted $CCR4^+$ T cells.

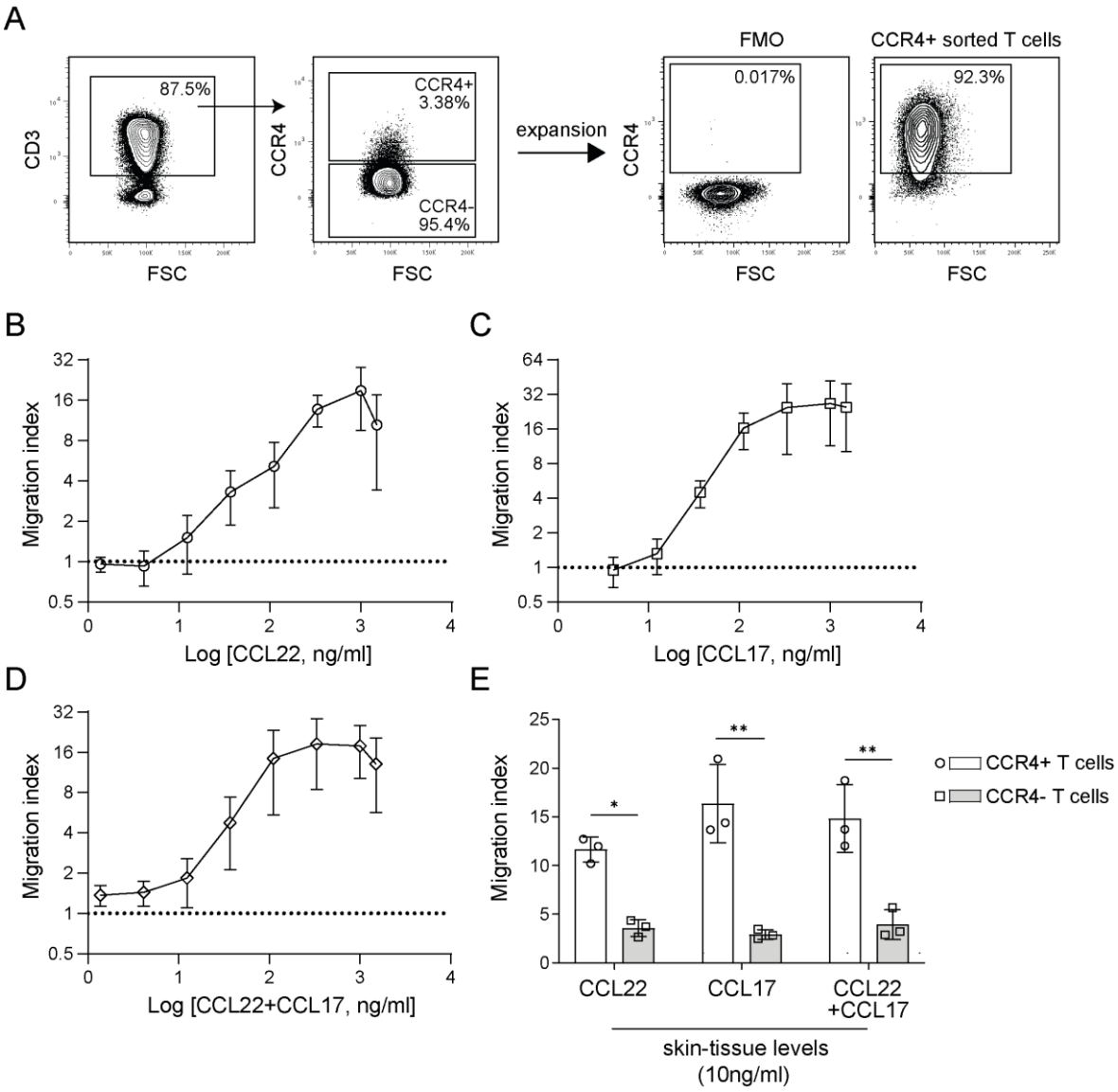


Figure 4.12 Migration of CCR4⁺ T cells to recombinant CCL22 and CCL17.

(**A**) CCR4⁺ and CCR4⁻ CD3⁺ T cells were sorted by FACS, expanded *in vitro* and CCR4 expression confirmed on CCR4+ sorted T cells by flow cytometry. Numbers indicate percentages of cells within the indicated gates. (**B-D**) Migration of CCR4⁺ T cells to increasing concentrations (1.372 ng/ml – 1500 ng/ml) of CCL22 (**B**), CCL17 (**C**) and CCL22 plus CCL17 (**D**) was assessed using *in vitro* transwell chemotaxis assays. Migration was determined by means of IncuCyte live imaging microscopy. Migration index was plotted on a log2 axis (mean ± SEM). (n=3-4; representative of 3 independent experiments). (**E**) Migration of CCR4⁺ and CCR4⁻ T cells to 10 ng/ml of CCL22, CCL17 or CCL22 plus CCL17. (n=3; representative of 2 independent experiments). *P < 0.05, **P < 0.01; RM two-way ANOVA with Tukey`s post hoc multiple comparisons test (mean ± SD).

Next, inhibition of CCL22- and CCL17-mediated chemotaxis was optimised using sorted $CCR4^+$ T cells and neutralising antibodies against CCL22 and CCL17 as no anti-CCR4 blocking antibody was commercially available. Both anti-CCL22 and anti-CCL17 antibodies were demonstrated to reduce $CCR4^+$ T cell migration in response to skin-tissue levels of recombinant human CCL22 and CCL17, respectively, in a dose-dependent manner (Fig. 4.13, A, B and C). Antibody concentrations of 10 µg/ml were found to fully inhibit chemotaxis to the combination of CCL22 and CCL17, reducing migration to the level of baseline random migration (Fig. 4.13, C). Therefore, 10 µg/ml was determined as the optimum antibody concentration to ensure inhibition of CCL22- and CCL17-induced chemotaxis.

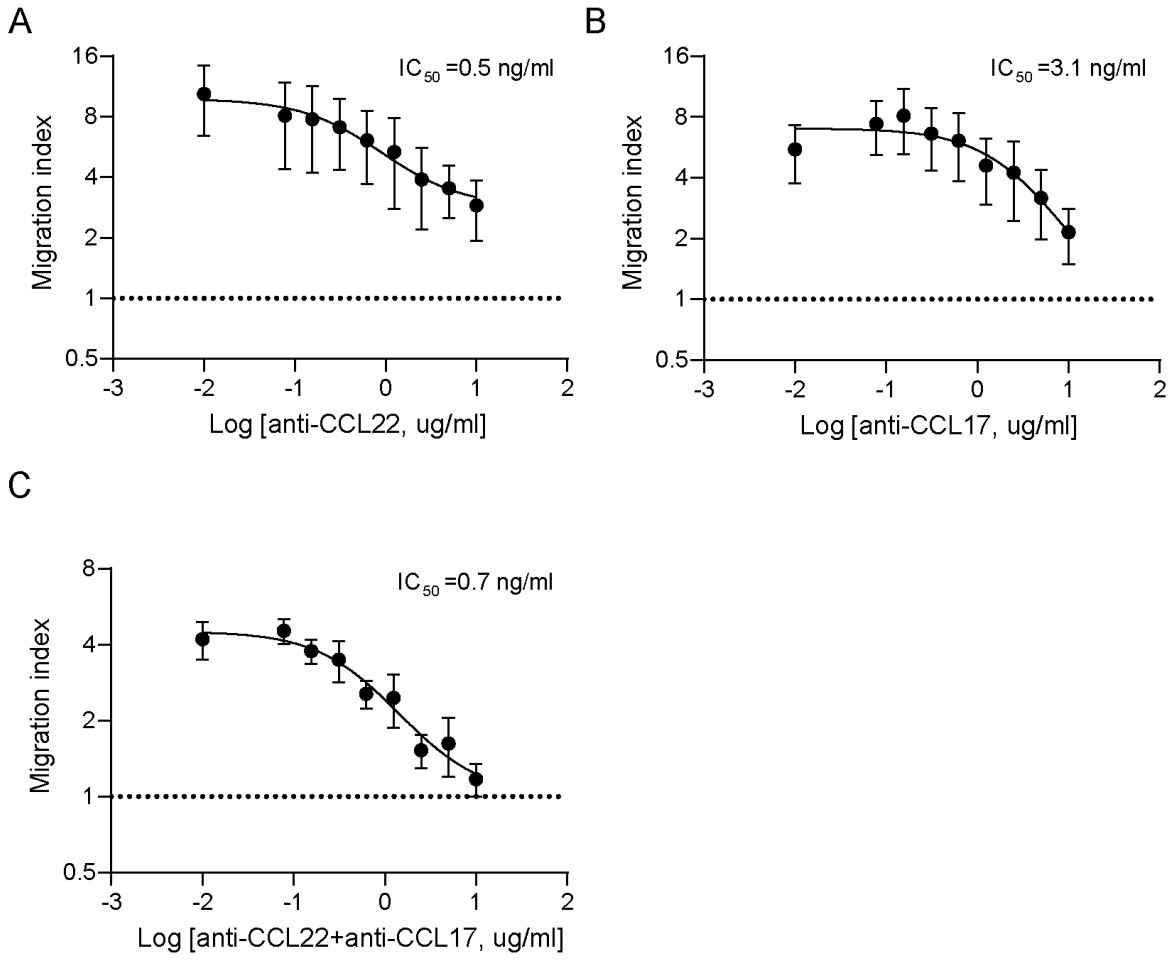


Figure 4.13 Inhibition of CCR4-mediated T cell chemotaxis.

(**A-C**) Migration of CCR4$^+$ T cells to CCL22 (**A**), CCL17 (**B**) and CCL22 plus CCL17 (**C**) in the presence of increasing concentrations (0.001 µg/ml – 10 µg/ml) of neutralising anti-CCL22 and/or anti-CCL17 antibodies. Migration index was plotted on a log2 axis (mean ± SEM). (n=4-8; representative of ≥ 3 independent experiments).

4.2.4.2 Chemotactic recruitment of *ex vivo* T cells to skin-tissue levels of CCL22 and CCL17

Due to the artificial nature of sorting and expanding CCR4$^+$ T cells, migration of *ex vivo* T cells, of which approximately 15% were determined to express surface CCR4, to CCL22 and CCL17 was assessed by *in vitro* chemotaxis assays. A substantial proportion of *ex vivo* T cells were found to migrate to recombinant human CCL22 and CCL17, at levels measured in skin blister fluids, compared to random migration.

There was no significant difference between the degree of T cell migration induced by CCL22 compared to CCL17, highlighting the chemotactic potential of both molecules. No additive effect was detected when chemokines were combined (Fig. 4.14, A). T cell migration to CCL22 and CCL17 in combination was significantly reduced by the addition of neutralising anti-CCL22 and anti-CCL17 antibodies, confirming antibody functionality and chemotactic specificity. Addition of isotype controls had no significant effect on CCL22- and CCL17-induced T cell chemotaxis (Fig. 4.14, B). These results demonstrate that skin-tissue levels of CCL22 and CCL17 efficiently induce *in vitro* migration of *ex vivo* T cells.

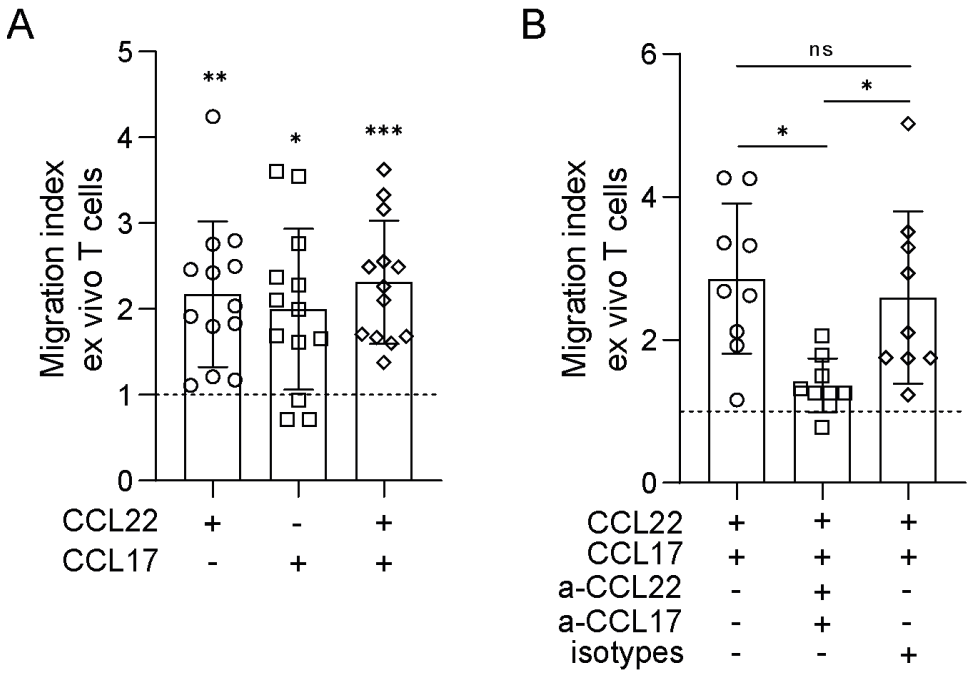


Figure 4.14 Migration of T cells to skin-tissue levels of CCL22 and CCL17.

(**A**) T cells were isolated from HC blood by CD3 MACS separation and migration to 10 ng/ml of CCL22, CCL17 or CCL22 plus CCL17 assessed by transwell chemotaxis assays, measured by IncuCyte live-cell imaging and compared to random migration (n=13; representative of ≥ 3 independent experiments). *P < 0.05; **P < 0.01; ***P < 0.001; RM one-way ANOVA with Tukey`s post hoc multiple comparisons test (mean ± SD). (**B**) Migration of *ex vivo* $CD3^+$ T cells to CCL22 and CCL17 combined in the absence or presence of anti-CCL22 (10 µg/ml) and anti-CCL17 (10 µg/ml) antibodies or isotype controls

(10 µg/ml). (n=9; data representative of ≥ 3 independent experiments). *P < 0.05; **P < 0.01; ***P < 0.001; RM one-way ANOVA with Tukey`s post hoc multiple comparisons test (mean ± SD).

4.2.4.3 Recruitment of T cells by ILC2-derived CCL22 and CCL17

The finding that human ILC2 produce CCL22 and CCL17 suggests that ILC2 may be able to recruit CCR4-expressing T cells. Human blood-derived ILC2 were stimulated with alarmins and the T cell chemotactic effect of ILC2 supernatants tested in *in vitro* transwell chemotaxis assays. Prior to chemotaxis assays, CCL22 and CCL17 levels in ILC2 supernatants were measured by ELISA, and supernatants containing at least 100 pg/ml of either CCL22 or CCL17 following ILC2 stimulation were selected for use in migration assays. This was done to account for the donor effect previously observed and to ensure testing of CCL22- and CCL17-producers only. Supernatants from both unstimulated and stimulated ILC2 induced the migration of *ex vivo* T cells. The addition of neutralising anti-CCL22 and anti-CCL17 antibodies significantly reduced T cell chemotaxis to stimulated ILC2 supernatants but did not significantly alter the degree of T cell migration to unstimulated supernatants (Fig. 4.15, A). The presence of ILC2 stimulants IL-33, IL-25 and TSLP did not appear to contribute to the T cell chemotactic effect of stimulated ILC2 supernatants as medium containing IL-33, IL-25 and TSLP did not induce T cell migration (Fig. 4.15, B).

These data show that both unstimulated and activated ILC2 secrete chemotactic factors that induce the migration of T cells. ILC2-derived CCL22 and CCL17 were found to significantly contribute to ILC2-mediated recruitment of T cells.

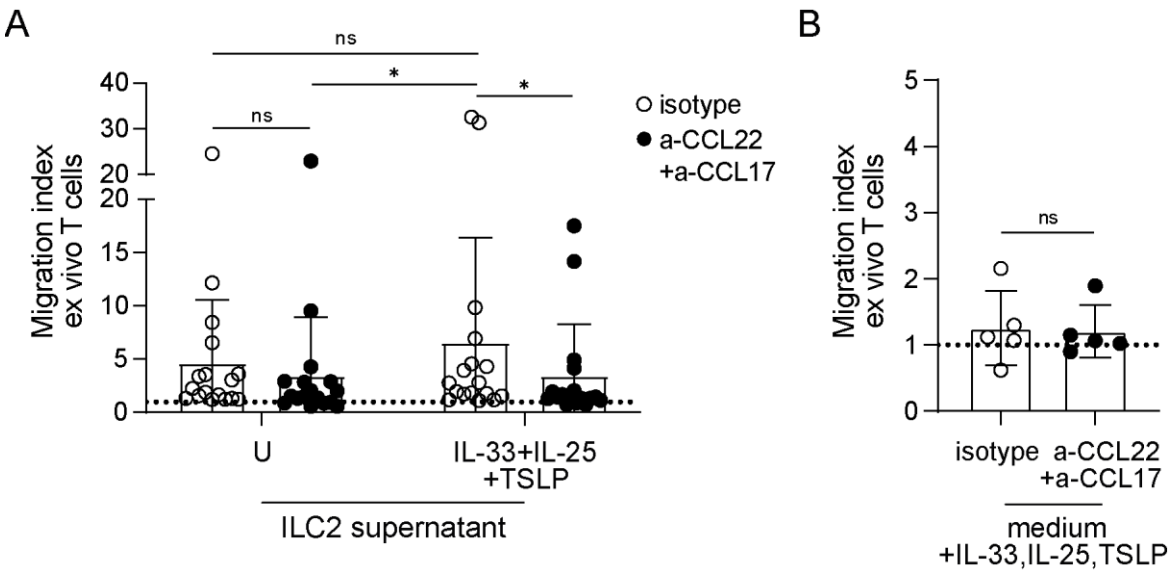


Figure 4.15 Migration of T cells to ILC2 supernatants.

(**A**) ILC2 were cultured in medium alone (U) or stimulated with IL-33, IL-25, TSLP (50 ng/ml each) for 72h when supernatants were collected. T cells were isolated from HC blood by CD3 MACS separation and migration to ILC2 supernatants in the presence of anti-CCL22 (10 µg/ml) and anti-CCL17 (10 µg/ml) antibodies or isotype controls (10 µg/ml) was measured by IncuCyte live-cell imaging (n=17; data representative of ≥ 3 independent experiments). *P < 0.05; RM two-way ANOVA with Tukey's post hoc multiple comparisons test (mean ± SD). (**B**) Medium containing ILC2 stimulants IL-33, IL-25, TSLP (50ng/ml each) was incubated for 72h and used in T cell chemotaxis assays in the presence of anti-CCL22 (10 µg/ml) and anti-CCL17 (10 µg/ml) antibodies or isotype controls (10 µg/ml). (n=5; data representative of ≥ 3 independent experiments). ns with paired Student's *t*-test (mean ± SD).

4.2.4.4 ILC2 chemotaxis to CCL22 and CCL17

Recently, human ILC2 were demonstrated to migrate to high levels of recombinant CCL17 and CCL22 *in vitro* (197). However, the detection of approximately 10 ng/ml in skin suction blister fluids suggests that CCL22 and CCL17 levels are much lower *in vivo*. Therefore, we assessed the ability of CCR4-expressing ILC2 to migrate towards skin-tissue levels of CCL22 and CCL17. Prior to *in vitro* chemotaxis assays, CCR4 expression on ILC2 was confirmed by flow cytometry and ILC2 with at least

20% CCR4 surface expression were selected. Skin-tissue levels of CCL22 and CCL17 were found to significantly induce ILC2 migration compared to the medium alone control (Fig. 4.16, A). CCL22- and CCL17-mediated ILC2 chemotaxis could be inhibited by the addition of neutralising antibodies, demonstrating specificity (Fig. 4.16, B). Based on the finding that ILC2 produce the CCR4 ligands CCL22 and CCL17, we tested the ability of ILC2 supernatants to recruit ILC2. Both unstimulated and, to a greater extent, stimulated ILC2 supernatants strongly induced ILC2 migration. Antibody-mediated neutralisation of ILC2-derived CCL22 and CCL17 resulted in significantly lower levels of ILC2 migration to ILC2 supernatants. This suggests that ILC2-derived CCL22 and CCL17 contribute significantly to the ILC2-induced recruitment of ILC2. Increased ILC2 chemotaxis to supernatants from activated ILC2 compared to resting ILC2 indicates that activation of ILC2 induces increased secretion of chemotactic factors. Higher levels of ILC2 migration to stimulated ILC2 supernatants was not due to the presence of recombinant IL-33, IL-25 and TSLP as cultured medium containing ILC2 stimulants did not significantly induce migration when compared to random migration (Fig. 4.16, C).

These results are indicative of CCL22- and CCL17-dependent ILC2 tissue homing. The finding that ILC2 supernatants induced ILC2 chemotaxis *in vitro* suggests that ILC2 may be able to directly recruit ILC2 into tissues, in part by producing CCR4 ligands.

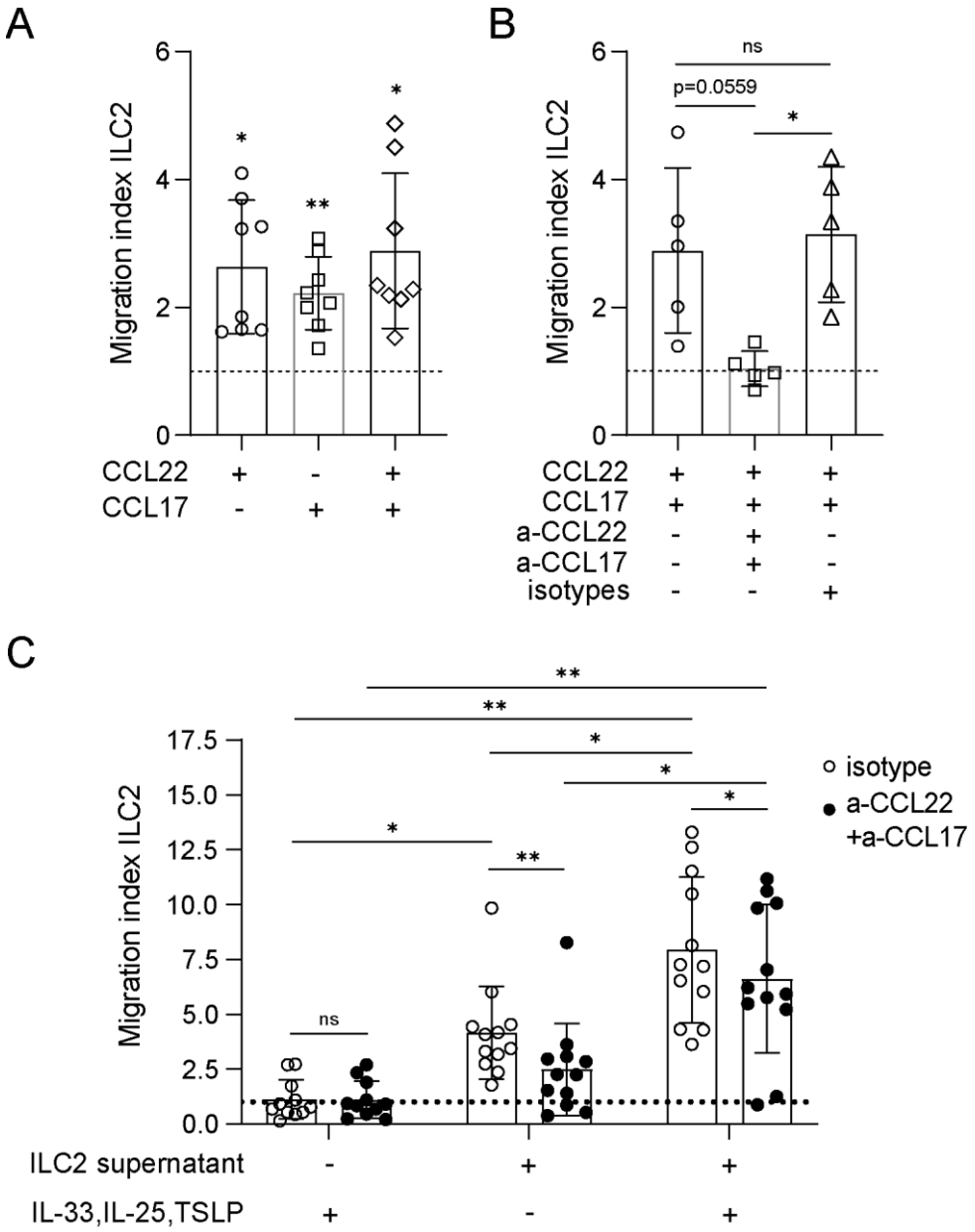


Figure 4.16 ILC2 migration to skin-tissue levels of CCL22 and CCL17 and to ILC2 supernatants.

(**A**) Migration of ILC2, expressing ≥ 20% surface CCR4, to 10 ng/ml of CCL22, CCL17 or CCL22 plus CCL17 was assessed in *in vitro* transwell chemotaxis assays, measured by IncuCyte live-cell imaging and compared to random migration. (n=7; data representative of ≥ 3 independent experiments). *P < 0.05; **P < 0.01; RM one-way ANOVA with Tukey`s post hoc multiple comparisons test (mean ± SD). (**B**) Migration of CCR4-expressing ILC2 to CCL22 plus CCL17 (10 ng/ml) in the presence of neutralising anti-CCL22 (10 µg/ml) and anti-CCL17 (10 µg/ml) antibodies or isotype controls (10 µg/ml). (n=5; data representative of ≥ 3 independent experiments). *P < 0.05; **P < 0.01; RM one-way ANOVA with Tukey`s post hoc multiple comparisons test (mean ± SD). (**C**) ILC2 were cultured in medium alone

or stimulated with IL-33, IL-25 and TSLP (50 ng/ml each) for 72h when supernatants were collected. Supernatants containing ≥ 100 pg/ml CCL22 and/or CCL17, assessed by ELISA, were used in *in vitro* transwell chemotaxis assays. ILC2 migration to ILC2 supernatants in the presence of anti-CCL22 (10 µg/ml) and anti-CCL17 (10 µg/ml) antibodies or isotype controls (10 µg/ml) was measured by IncuCyte live-cell imaging. (n=14-15; data representative of ≥ 3 independent experiments). *P < 0.05; **P < 0.01; RM two-way ANOVA with Tukey's multiple comparisons test (mean ± SD).

4.2.4.5 ILC2 can induce ILC2 recruitment indirectly through induction of chemokine production by moDC

The finding that ILC2 increase the production of CCL22 and potentially CCL17 by moDC suggests that human ILC2 may be able to promote the recruitment of ILC2 indirectly through induction of chemokine production by DC. To test this hypothesis, moDC were incubated with ILC2 supernatants for 24 hours and transwell chemotaxis assays performed to assess migration of ILC2 to moDC supernatants, diluted to avoid saturation of the chemotactic response. MoDC supernatants were found to strongly induce ILC2 chemotaxis. Supernatants from moDC treated with activated ILC2 supernatants had a significantly higher chemotactic effect on ILC2 than supernatants from moDC cultured in unstimulated ILC2 supernatants or medium alone. Unstimulated ILC2-treated moDC supernatants induced ILC2 migration to levels comparable to control moDC supernatants. ILC2 chemotaxis to moDC supernatants was significantly reduced by the addition of anti-CCL22 and anti-CCL17 neutralising antibodies. However, the presence of anti-CCL22 and anti-CCL17 antibodies also resulted in significantly reduced ILC2 migration to control moDC supernatants (Fig. 4.17, A). Having demonstrated chemotactic activity of ILC2 supernatants, chemotactic contribution of ILC2 supernatants used for the treatment of moDC was assessed. Levels of ILC2 migration to diluted ILC2

supernatants were noticeable lower than to moDC supernatants, which indicates that ILC2 chemotaxis to ILC2-treated moDC supernatants was most likely not due to the presence of ILC2 supernatants (Fig. 4.17, B).

These data demonstrate recruitment of ILC2 by moDC and suggest that activated ILC2 promote the production of increased levels of ILC2 chemotactic factors by moDC. MoDC-derived CCL22 and CCL17 appear to play an important role in the recruitment of ILC2.

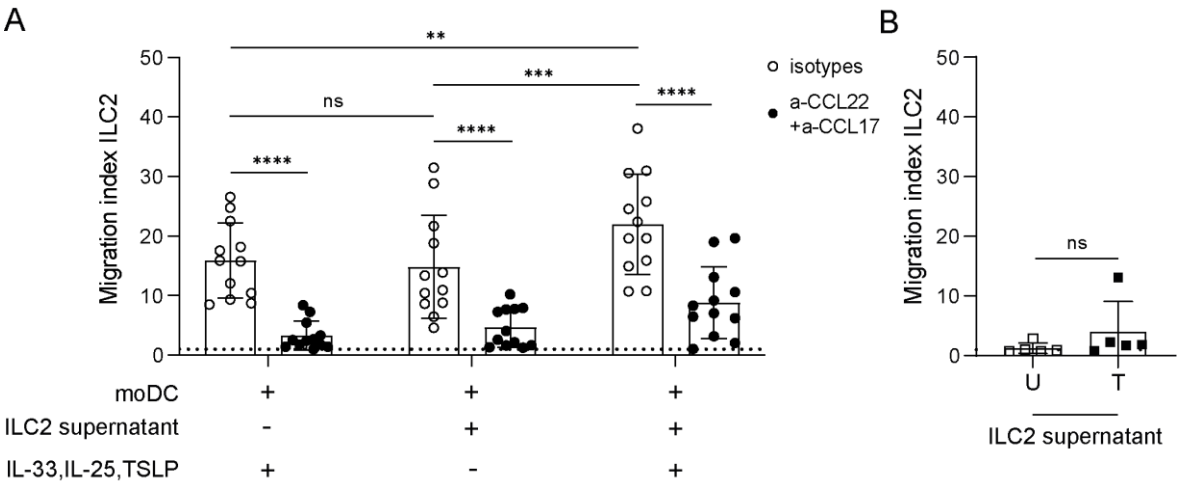


Figure 4.17 Migration of ILC2 to ILC2-treated moDC supernatants.

(**A**) moDC were cultured in supernatants from unstimulated and IL-33, IL-25, TSLP-stimulated ILC2 or in medium containing IL-33, IL-25 and TSLP for 24h. Migration of ILC2, expressing ≥ 20% CCR4, to supernatants from ILC2 supernatant-treated moDC (DF=2) in the presence of neutralising anti-CCL22 (10µg/ml) and anti-CCL17 (10µg/ml) antibodies or isotype controls was assessed in *in vitro* transwell migration assays. (n=12; data representative of ≥ 3 independent experiments). **P < 0.01; ***P < 0.001; ****P < 0.0001; RM two-way ANOVA with Tukey`s post hoc multiple comparisons test (mean ± SD). (**B**) Migration of ILC2 to unstimulated (U) and IL-33, IL-25, TSLP-stimulated (T) ILC2 supernatants (DF=2) used for moDC treatment. (n=5; data representative of ≥ 3 independent experiments). ns with paired Student's *t*-test (mean ± SD).

4.3 Discussion

A central feature of inflammation is the accumulation of immune cells in affected tissue sites, which is regulated by chemotactic factors and their corresponding receptors. ILC2 play an important role in type 2 immune responses by potent secretion of type 2 cytokines and coordinating functions of surrounding immune cells. Allergic inflammatory disorders, including AD and asthma, have been associated with increased ILC2 frequencies within affected tissues (93, 141, 195–198, 328). While increased expression of chemokines in inflamed tissues has been linked to recruitment of specific T cell subsets (293), such as Th2 cells in type 2 inflammation, little is known about the relative contribution of local proliferation and tissue infiltration to ILC2 accumulation at sites of inflammation. It is increasingly being recognised that ILC2 tissue accumulation in response to helminth infection (127) or allergen challenge (151, 197, 324, 325) may at least be in part due to chemotactic recruitment of circulating ILC2. However, in contrast to T cells, ILC2 homing is not well understood. Moreover, ILC2 accumulation in inflamed tissues is accompanied by increased infiltration of immune cells such as eosinophils, mast cells and Th2 cells. While IL-5-producing ILC2 have been implicated in eosinophil recruitment (145, 190, 208, 277), the contribution of ILC2 to chemotactic leukocyte recruitment is not well understood. This study investigated the production of chemokines by human ILC2, with findings that suggest a previously unrecognised mechanism of ILC2-mediated amplification of type 2 immune responses.

4.3.1 Human ILC2 produce the chemokines CCL22 and CCL17

The data presented herein demonstrate for the first time the production of the chemokines CCL22 and CCL17 by human ILC2. Human blood- and skin-derived

ILC2 were found to constitutively secrete low levels of CCL22 and CCL17 *in vitro*. Activation of ILC2 by the alarmins IL-33, IL-25 and TSLP induced increased production of both chemokines. Analysis of mRNA expression confirmed activation-induced upregulation of *CCL22* and *CCL17* in ILC2. IL-33, IL-25 and TSLP have all been shown to individually stimulate the production of CCL22 and/or CCL17 by both mouse and human DC (238, 329, 330). Our findings demonstrate a similar effect of alarmins on ILC2. CCL22 and CCL17 play an important role in skin homeostasis and inflammation. Comparison of *in vitro* cultured blood- and skin-derived ILC2 from healthy volunteers did not reveal a significant difference in the production of CCL22 or CCL17. However, the data implied that the proportion of ILC2 producing substantial levels (>100pg/ml) of CCL22 and CCL17 may be increased in the skin at steady state. Previously performed RNA-sequencing analysis of ILC2 from *in vivo* allergen-challenged skin or blood indicated increased *CCL17* expression by skin ILC2 compared to blood ILC2. Given the lengthy *in vitro* expansion process required to obtain sufficient ILC2 numbers for functional analyses, it is possible that inherent differences between skin and blood ILC2 were lost as a result of *in vitro* culture. Indeed, surface CCR4 expression on ILC2 changed substantially during *in vitro* culture, which implies that *in* vitro expansion may affect ILC2 phenotype. *In vivo*, the phenotype and function of ILC2 has been proposed to be shaped by the local tissue microenvironment (124). Increased expression of CCL22 and CCL17 in the skin and blood of individuals with AD highlights the involvement of both CCR4 ligands in allergic skin inflammation (267, 307, 316). There was no significant difference in the secretion of CCL22 or CCL17 by cultured blood ILC2 from individuals with AD compared to healthy controls. However, the proportion of ILC2 producing substantial levels (≥100 pg/ml) of CCL22 and CCL17 at steady state and following activation

appeared to be increased in ILC2 lines derived from individuals with AD compared to healthy volunteers. Taking into consideration potential effects of the *in vitro* expansion process as well as increased ILC2 frequency and activity in AD lesions (93), it is plausible that *in vivo* ILC2 accumulate in AD lesional skin and produce increased levels of CCL22 and CCL17. Due to the unavailability of antibodies appropriate for intracellular CCL22 and CCL17 staining, chemokine production by *ex vivo* blood and skin ILC2 from individuals with AD and HC could not be assessed. In addition to secreting CCR4 ligands themselves, activated human ILC2 were found to promote the production of high levels of CCL22 and potentially CCL17 by *in vitro* generated moDC, which supports earlier reports of ILC2-induced CCR4 ligand secretion by pulmonary and cutaneous DC in a mouse model of allergic inflammation (212). Noticeable, however not significant, reduction of ILC2-induced CCL22 and CCL17 production by moDC following blocking of IL-4Rα/IL-13Rα2 signalling is consistent with the identification of ILC2-derived IL-13 as a critical factor in the ILC2-induced CCL17 secretion by conventional DC (212).

Collectively, these results identify a role for human ILC2 in the production of type 2-associated chemokines through activation-induced secretion of CCL22 and CCL17 by ILC2 as well as through ILC2-promoted CCL22 production by moDC.

4.3.2 ILC2 express functional CCR4 that enables ILC2 homing to CCL22 and CCL17

A significant proportion of human *ex vivo* blood and skin ILC2 were found to express surface CCR4, the shared receptor for CCL22 and CCL17, which is consistent with previous reports (93). An average of approximately 50% of circulating ILC2 expressed surface CCR4, which resembles the CCR4 expression pattern reported

for Th2 cells (295, 296). We noted that for half of the donors analysed, the frequency of $CCR4^+$ ILC2 was below 40%, while the remaining half displayed a $CCR4^+$ ILC2 frequency of above 60%, indicating varying degrees of CCL22- and CCL17-homing capacity. $CCR4^+$ ILC2 were not found to be enriched in the skin compared to peripheral blood of healthy volunteers, however the frequency of $CCR4^+$ ILC2 in healthy skin was comparable to that of cutaneous $CCR4^+$ T cells, which supports a role of both cell types in cutaneous immunosurveillance (11, 331). Given the expression of CCR4 on both ILC2 and T cells, including Th2 cells (295), CLA^+ skin-homing T cells (297), Tregs (299) and Th17 cells (300), it is likely that ILC2 and T cells show overlapping homing patterns. Similar to T cells, circulating ILC2 from individuals with AD expressed significantly higher CCR4 expression levels per cell than ILC2 from healthy donors, which suggests increased chemotactic responsiveness of ILC2 in the context of allergic skin inflammation.

The capacity of immune cells to respond to continuously changing chemotactic gradients *in vivo* is believed to be regulated by ligand-induced chemokine receptor desensitisation and internalisation. Such a mechanism has been demonstrated for human Th2 cells, identifying CCL22 as a potent inducer of CCR4 internalisation, involving lipid rafts and clathrin-coated pits (307, 308). Here, I demonstrate rapid and dose-dependent downregulation of CCR4 on human ILC2 in response to treatment with exogenous CCL22, but not CCL17. This suggests that chemotactic responsiveness of ILC2 to CCR4 ligands is regulated in a manner similar to that of human Th2 cells. Activation of ILC2 by alarmins IL-33, IL-25, TSLP was accompanied by upregulation of surface CCR4. This effect was mediated predominantly by the activity of IL-33. IL-33, an IL-1 family member, has been

identified as a strong inducer of type 2 cytokine production by ILC2 following binding to T1/ST2 and activation of NF-κB and mitogen-activated protein kinase (MAPK) pathways (90, 93, 94, 98, 100, 140–142). Differentiation-accompanied CCR4 upregulation on Th2 cells has been reported to depend on the STAT6 signalling pathway (287) and a GATA3 site was identified as a major regulatory element in the CCR4 promoter (327). One might speculate that the observed activation-induced increase in CCR4 expression in ILC2 could be attributed to IL-33 stimulating the production of high levels of IL-13 and/or IL-4 by ILC2, which in turn signal through STAT6, upregulating GATA3 expression and subsequently inducing transcriptional and surface expression of CCR4.

Whereas CCR4 remained stably expressed on the surface of *in vitro* cultured blood-derived T cells following fluorescence guided cell sorting, CCR4 expression on blood-derived ILC2 appeared to be less stable and changed dynamically during the *in vitro* expansion process. This may indicate a higher degree of adaptability in the homing potential of ILC2 compared to differentiated T cells. Antigen-specific differentiation of naïve T cells gives rise to effector and memory T cells that can be categorised into subpopulations based on the expression of particular combinations of chemokines and adhesion molecules (225). In contrast, ILC2 are epigenetically poised prior to stimulation, responding rapidly to microenvironmental signals (332). Dynamic expression of homing receptors on ILC2 might allow adaptation of migratory patterns to specific immunological challenges.

Functionality of CCR4 on ILC2 was confirmed by *in vitro* chemotaxis to recombinant CCL22 and CCL17. Previously, *in vitro* chemotaxis assays have shown migration of human ILC2 to high levels of CCL22 and CCL17, at 500 ng/ml and 2000 ng/ml

respectively (197). Here, we demonstrate for the first time ILC2 homing to CCL22 and CCL17 at concentrations of 10 ng/ml, as detected in skin suction blisters from individuals with AD following intradermal allergen challenge. This implies *in vivo* functional relevance of CCL22- and CCL17-mediated ILC2 recruitment. Collectively, these data demonstrate expression of functional CCR4 on human ILC2 and support a role of CCL22- and CCL17-mediated skin homing of $CCR4^+$ ILC2 and T cells in the context of allergic skin inflammation.

4.3.3 ILC2 promote recruitment of ILC2 and T cells

Here, I show for the first time that human ILC2 are capable of promoting chemotactic recruitment of both ILC2 and T cells. Supernatants from activated ILC2 induced *in vitro* migration of cultured ILC2 and *ex vivo* T cells. ILC2-derived CCL22 and CCL17 were found to contribute significantly to ILC2 and T cell recruitment. However, blockade of ILC2-derived CCL22 and CCL17 did not completely inhibit migration, which indicates secretion of other chemotactic factors by ILC2. The combination of alarmins IL-33, IL-25 and TSLP used in the stimulation of ILC2 prior to *in vitro* chemotaxis assays was not found to contribute to chemotactic activity of stimulated ILC2 supernatants. Loss of the previously described ILC2 chemotactic activity of IL-33 (136) might be due to protein degradation during 72 hour culture of control medium containing ILC2 stimulants. Moreover, ILC2 and T cell homing was also induced by supernatants from unstimulated ILC2, albeit to a lesser degree. Low level CCL22 and CCL17 secretion by unstimulated ILC2 did not appear to contribute significantly to T cell recruitment, however, did seem to be involved in the induction of ILC2 migration. ILC2 might exhibit increased chemotactic responsiveness to CCR4 ligands, potentially due to higher CCR4 surface expression. However, it is

important to note that the *in vitro* ILC2 expansion process is highly stimulatory giving rise to ILC2 that might be mildly activated at steady state. Whether T cells are capable of recruiting ILC2 is currently unknown, however, bidirectional interaction between ILC2 and T cells has previously been reported in the context of helminth infection (183).

In addition to directly recruiting ILC2, human ILC2 were found to promote ILC2 homing indirectly through induction of moDC chemokine production. Following treatment with activated ILC2 supernatants, moDC were found to potently induce the migration of ILC2. Chemotactic activity of untreated moDC supernatants indicated high baseline activity and chemokine production by moDC, which might be explained by the stimulatory nature of the *in vitro* moDC differentiation process. Blocking of CCL22 and CCL17 resulted in reduced ILC2 recruitment by activated ILC2 supernatant-treated moDC, supporting previous reports of ILC2-induced CCL17 secretion by conventional DC (212). However, addition of neutralising anti-CCL22 and anti-CCL17 antibodies also significantly reduced ILC2 homing to supernatants from untreated moDC and to a similar extent from moDC cultured in unstimulated ILC2 supernatant. This might be due to *in vitro* generated moDC baseline production of mean CCL22 and CCL17 levels of 2.6 ng/ml and 0.47pg/ml, respectively. ILC2 have been implicated in the recruitment of memory Th2 cells following allergen re-challenge by eliciting secretion of CCL17 from pulmonary and cutaneous conventional DC (212). The results presented herein add to this, suggesting a role for ILC2 in the chemotactic recruitment of both ILC2 and T cells.

4.3.4 Functional implications of ILC2-mediated chemotaxis in homeostasis and inflammation

ILC2, enriched in barrier and mucosal tissues, are involved in immunosurveillance and the maintenance of tissue homeostasis. In the lung, ILC2-derived amphiregulin was identified as a crucial factor in the restoration of airway epithelial integrity and pulmonary tissue homeostasis following experimental influenza virus infection (88). In healthy skin, murine dermal ILC2 constitutively produced IL-13, which was proposed to negatively regulate mast cell activity (11). The results of this study, showing tonic low-level production of the chemokines CCL22 and CCL17 by human unstimulated ILC2, suggest an involvement of ILC2 in the regulation of $CCR4^+$ immune cell homing during steady state (Fig. 4.18, A). Basal expression of CCL17 and adhesion molecules, such as E-selectin and ICAM-1, by dermal blood vessels has previously been proposed to mediate T cell extravasation into non-inflamed skin (312). During homeostasis, CCL17 production by blood vessel endothelial cells might facilitate constitutive tissue infiltration of $CCR4^+$ ILC2 in addition to $CCR4^+$ memory T cells and $CCR4^+$ Tregs. In the absence of inflammation, recruited ILC2 and memory T cells may perform tissue immunosurveillance, while Tregs may regulate the activity of tissue-resident immune cells. A significant proportion of cutaneous ILC2 and T cells (331) were found to express CCR4 in healthy skin (331). Tonic low-level production of CCL22 and CCL17 by tissue-resident ILC2 may regulate homing of tissue-resident $CCR4^+$ cells within the tissue microenvironment. Constitutive immune cell homing to and within barrier tissues, such as the skin and lung, might be reflective of the requirement for continuous immunosurveillance at sites that form the primary interface with the environment.

In the context of allergic inflammation or helminth infection, production of chemotactic factors by activated ILC2 may contribute to the initiation and amplification of local type 2 inflammatory responses (Fig. 4.18, B). Following barrier compromise and/or allergen entry, tissue-resident ILC2 are activated by alarmins released from damaged epithelial cells and respond with rapid type 2 cytokine and chemokine production. Through direct secretion of CCR4 ligands and simultaneously acting upstream of tissue-resident DC, such as Langerhans cells in the skin, to induce CCL22 and CCL17 production, activated ILC2 may be involved in increased recruitment of $CCR4^+$ ILC2 and effector and/or memory Th2 cells. Allergic inflammatory disorders, such as asthma and AD, have been associated with elevated levels of CCL22 and CCL17 and increased infiltration of $CCR4^+$ Th2 cells into the inflamed tissue (303, 309, 316, 317). Although accumulation of ILC2 at sites of inflammation is at least in part due to activation-induced local proliferation (93, 141), simultaneous reduction in the frequency of peripheral blood ILC2 suggests tissue-infiltration of circulating ILC2 (197). PGD2, derived from activated mast cells, has previously been identified as a potent inducer of ILC2 chemotaxis (136). By demonstrating the expression of functional CCR4 on human blood and skin ILC2, the findings of this study describe an additional pathway of ILC2 recruitment. An amplification loop between ILC2-induced chemokine production by tissue-resident DC and epithelial cells, such as keratinocytes (302), and further recruitment of pathogenic $CCR4^+$ Th2 cells and ILC2 might contribute to the exacerbation of allergic inflammation.

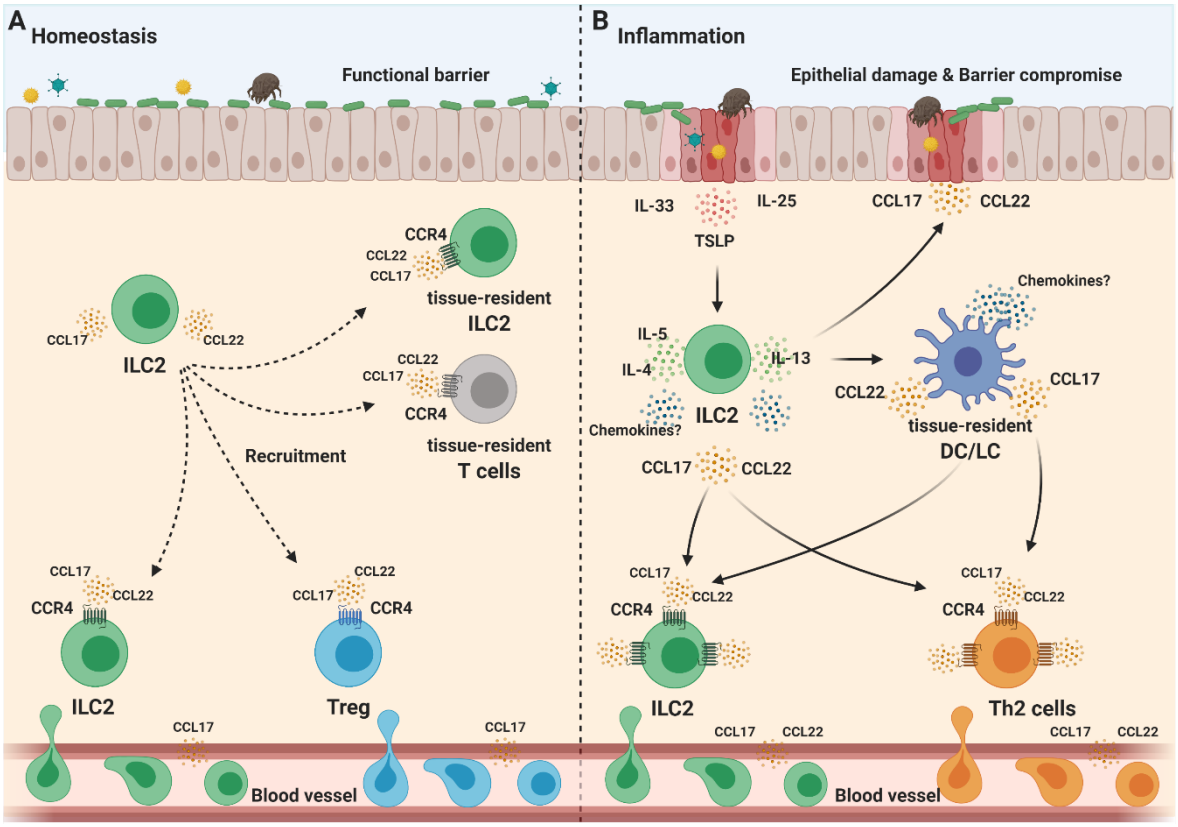


Figure 4.18 Potential role of ILC2 in the recruitment of ILC2 and T cells during homeostasis and inflammation.

(**A**) At steady state, tissue-resident ILC2 may constitutively produce low levels of CCL22 and CCL17 that may guide migration of CCR4^{+} ILC2, tissue-resident T cells and Tregs within the tissue microenvironment. (**B**) Following epithelial damage and barrier breach, alarmin cytokines activate tissue-resident ILC2 that respond rapidly by producing type 2 cytokines. Activation-induced upregulated production of chemokines, including CCL22 and CCL17, by ILC2 may contribute to increased tissue infiltration of CCR4^{+} ILC2 and effector and/or memory Th2 cells. Simultaneously, ILC2-derived IL-13 might promote CCL22 and CCL17 production by epithelial cells and tissue-resident DC, amplifying the recruitment of CCR4^{+} cells.

Chapter 5: ILC2 orchestrate innate and adaptive immune responses

5.1 Introduction

ILC2 play an important role in the coordination of both innate and adaptive immune responses during homeostasis and inflammation.

5.1.1 Role of ILC2 in the induction of adaptive immune responses

ILC2 play a critical role in the transition from innate to adaptive immune responses. One mechanism by which ILC2 bridge innate and adaptive immune responses is by influencing DC responses, such as through promoting DC migration to draining lymph nodes (211) and inducing DC-mediated recruitment of memory Th2 cells (212). In addition to influencing the activity of APC, it has become evident that ILC2 are capable of directly activating T cell responses by forming cell contact-dependent interactions with T cells. Both mouse and human ILC2 are capable of processing and presenting protein antigens, such as the HDM allergen *Der p 1*, to $CD4^+$ T cells in an MHCII-dependent manner, favouring Th2 differentiation (183). Human ILC2 have also been found to present endogenous lipid antigens to CD1a-reactive T cells, implying a role for ILC2 in lipid surveillance (10). Furthermore, besides antigen presentation, ILC2 have been reported to engage in cell-contact-dependent OX40L-OX40 interaction with $CD4^+$ T cells. This dialogue has been shown to enhance Th2 effector functions and IL-4 production by ILC2, synergistically promoting type 2 immune responses in the context of allergic airway inflammation and helminth infection (333, 334).

5.1.2 Monocyte-derived dendritic cells

5.1.2.1 *In vitro* differentiated monocyte-derived dendritic cells

In vitro, immature moDC can be generated by culturing peripheral blood-derived monocytes in GM-CSF and IL-4 and are characterised by moderate expression of antigen-presenting molecules such as MHCI/II and CD1 molecules as well as lack of CD14 expression (335). Low concentrations of IL-4 are required to ensure monocyte differentiation into moDC instead of monocyte-derived macrophages by stabilising the surface expression of the GM-CSF receptor (336, 337). Removal of GM-CSF and IL-4 has been reported to result in reversal to monocyte form or conversion to monocyte-derived macrophages, highlighting the phenotypic instability of immature moDC (338, 339). Pro-inflammatory mediators, such as TNF-α, IFN-γ, CD40L and lipopolysaccharide (LPS), induce the maturation of moDC, which is accompanied by upregulation of surface MHCII, co-stimulatory molecules and CCR7. As a result, mature moDC display reduced antigen processing activity and instead show an increased ability to present antigens to T cells (339).

5.1.2.2 *In vivo* monocyte-derived dendritic cells

In vivo, moDC have been identified at steady state within epithelial and mucosal tissues, such as the skin, lung and intestine. Inflammation is associated with increased frequencies of infiltrating monocytes as well as tissue moDC, referred to as “inflammatory moDC” (21). It is believed that under inflammatory conditions, infiltrating monocytes, recruited in a CCR2-dependent manner, rapidly differentiate into moDC that drive the local inflammatory response (340, 341). In a murine model of allergic airway inflammation, moDC were identified as the principal DC subset inducing type 2 inflammation in the lung following local allergen challenge (342).

Human AD lesions were reported to contain increased frequencies of "inflammatory" $CD1a^+$ moDC compared to healthy skin (343), supporting the notion that moDC differentiation plays a role in the context of allergic inflammation. To what extent these *in vivo* inflammatory moDC contribute to the induction of T cell responses remains to be addressed.

5.1.3 CD1a and the activation of CD1a-restricted T cells

CD1 glycoproteins, including group 1 CD1a, CD1b and CD1c and group 2 CD1d in humans, are MHC class I-like antigen presentation molecules that specialise in the presentation of lipid antigens to CD1-reactive T cells. CD1 molecules are made up of a heavy chain with three extracellular domains non-covalently associated with β2-microglobulin, resembling the structure of MHCI (344). CD1-restricted T cells have been identified as $CD4^+$, $CD8^+$ or $CD4^-CD8^-$ T cells expressing either αβ or γδ TCR and exhibiting adaptive-like effector functions similar to conventional MHC-restricted T cells (345).

CD1a presents both endogenous lipid antigens, such as squalene and fatty acids, and foreign lipid antigens derived from exogenous sources, such as pollen and mycobacteria, to CD1a-restricted T cells (346). Antigen loading onto CD1a involves insertion of the alkyl chains of lipid antigens into two hydrophobic A′ and F′ pockets of the CD1a binding groove (347) and is believed to take place at the cell surface and in early endosomes (348). The mode of the TCR recognition of CD1a-lipid complexes varies. The activation of CD1a-autoreactive T cells, a common subset of the human αβ T cell repertoire that recognises endogenous lipids, appears to be less dependent on the recognition of specific lipid antigens and instead lipid binding enables direct interaction of the TCR with CD1a itself. In response to binding to

endogenous lipid-bound CD1a *in vitro*, human CD1a-autoreactive T cells were found to upregulate the production of IL-22 as well as IFN-γ (349). Evidence has emerged suggesting that activation of CD1a-autoreactive T cells is dependent on whether CD1a loaded lipids allow or interfere with direct TCR binding to CD1a. Accordingly, “permissive” ligands, small hydrophobic lipids, sequester inside the CD1a protein and enable interaction of the autoreactive TCR with CD1a, while “non-permissive” ligands, lipids with polar head groups, sterically hinder direct TCR-CD1a binding and thereby inhibit T cell activation (350–352). Conversely, some CD1a-restricted T cells recognise specific lipid ligands presented by CD1a, such as the mycobacterial lipopeptide didehydroxymycobactin. The peptide moiety of didehydroxymycobactin protrudes the F` pocket and is directly recognised by the TCR (353, 354).

CD1a is believed to play an important role in skin homeostasis, supported by constitutively high expression on skin-resident Langerhans cells. Langerhans cells, ideally positioned to detect changes in the skin microenvironment, have been found to efficiently present microbial lipid antigens to CD1-restricted T cells (355). In the context of skin inflammation, other cutaneous CD1a-expressing cells include dermal myeloid DC (77, 356), BDCA2^{+}CD123^{int} DC, a recently identified DC subset that was observed infiltrating the skin upon acute sterile inflammation (357), and ILC2, that have been found to upregulate CD1a in response to TSLP (10). Enrichment of CD1a-expressing cells in skin inflammatory conditions, such as AD and psoriasis, suggests a contribution of CD1a-dependent T cell activation. In AD skin, the common allergen HDM was found to generate neolipid antigens that could be presented to CD1a-reactive T cells. Individuals with AD were shown to have increased frequencies of HDM-responsive CD1a-reactive T cells in the blood and

skin, that positively correlate with disease severity, supporting the notion that CD1a-reactive T cells play a pathogenic role in skin inflammation (214).

5.1.4 Hypothesis and aims

Inflammatory responses are associated with the recruitment and expansion of a wide variety of innate immune cells, including ILC2, monocytes and myeloid DC. During inflammation, circulating monocytes infiltrate inflamed tissues and differentiate into macrophages or DC in response to local signals (358). While ILC2 have been shown to influence migration and chemokine production of DC (211, 212), little is known about the effect of ILC2 on the survival, phenotype and activity of myeloid cells. Given that ILC2 largely function as tissue-resident cytokine and chemokine producers, I hypothesised that ILC2 may directly affect myeloid cell function.

To address this hypothesis, the aims of this project included:

a. Determine the effect of ILC2 on the survival and phenotype of *in vitro* fully differentiated moDC
b. Determine the effect of ILC2 on the *in vitro* differentiation process of moDC
c. Investigate the effect of ILC2 on the survival and phenotype of *ex vivo* monocytes
d. Identify ILC2-secretory factors contributing to the observed effects on myeloid cells
e. Determine the effect of ILC2 on moDC antigen-presenting capacity

5.2 Results

5.2.1 Effect of ILC2 on fully differentiated moDC

To study the impact of ILC2-derived soluble factors on survival and phenotype of immature moDC, *in vitro* differentiated moDC were cultured in ILC2 culture supernatants for 48 hours and the effect assessed by flow cytometry analysis (Fig. 5.1).

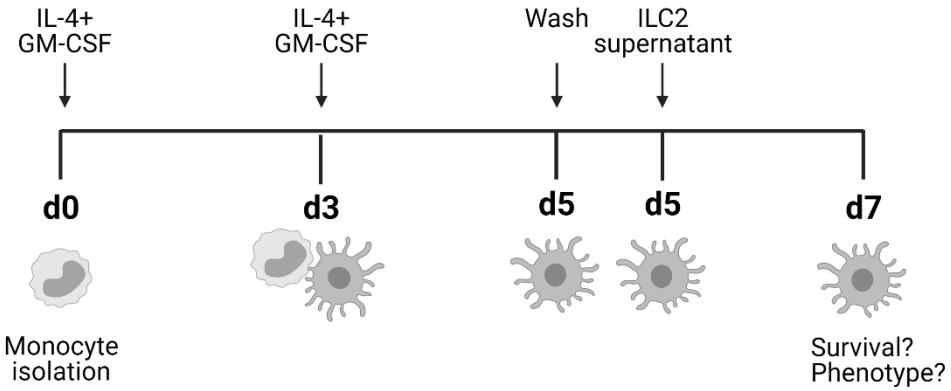


Figure 5.1 Experimental design – effect of ILC2 supernatants on fully differentiated moDC.

Peripheral blood monocytes were isolated by CD14 MACS separation and cultured with IL-4 and GM-CSF in FCS-containing medium for five days to induce differentiation into immature moDC, termed $DC_{IL\text{-}4/GM\text{-}CSF}$. On d5, ILC2 supernatants were added to moDC for 48h and the effect on moDC survival and phenotype assessed by flow cytometry.

5.2.1.1 Effect of ILC2 on the survival and phenotype of fully differentiated moDC

Expression of CD1a, CD1b and CD1c is inhibited by lipids present in human serum (359). Therefore, blood-derived ILC2 were stimulated in FCS-containing medium before addition to *in vitro* differentiated immature moDC, termed $moDC_{IL\text{-}4/GM\text{-}CSF}$. Culture in ILC2 culture supernatants did not significantly affect moDC survival, represented by event percentage in the monocyte-derived cell gate (Fig. 5.2, A and

B). CD14 expression remained low in all treatment conditions, indicative of a stable moDC phenotype (Fig. 5.2, C). Consistent with an immature phenotype (335, 360), moDC across all conditions expressed moderate levels of the co-stimulatory molecule CD86 (Fig. 5.2, D) as well as high levels of both MHCI (HLA-ABC) and MHCII (HLA-DR) (Fig. 5.2, E and F). Alarmins presents in stimulated ILC2 supernatants had no effect on moDC phenotype (Fig. A.6). There appeared to be a slight drop in the viability of moDC cultured in medium alone, termed $moDC_{Nil}$, (54.97% ± 14.2) compared to moDC culture in ILC2 supernatants (U = 61.37% ± 9.504; T = 64.87% ± 7.722) or control $moDC_{IL\text{-}4/GM\text{-}CSF}$ (67.03% ± 9.662) (Fig. 5.2, A and B). This implies that ILC2 may support the survival of immature moDC.

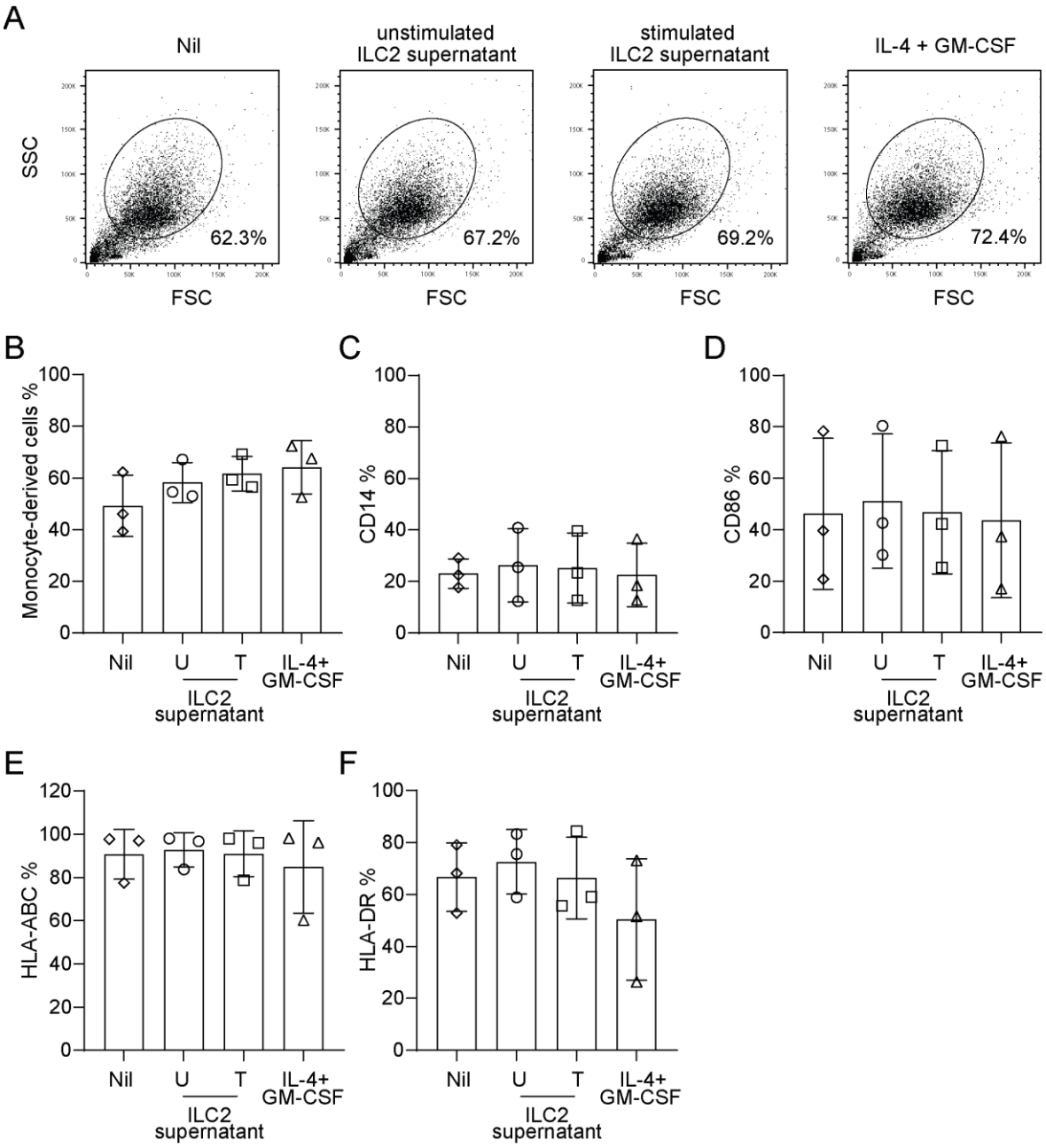


Figure 5.2 Effect of ILC2 supernatants on the survival and phenotype of moDC

(**A-F**) Circulating monocytes were isolated by CD14 MACS separation and differentiated into immature moDC by incubation with IL-4 (10 ng/ml) and GM-CSF (100 ng/ml). On d5, moDC were cultured in medium alone (Nil), culture supernatants from unstimulated (U) or IL-33, IL-25, TSLP (50ng/ml each)-stimulated (T) ILC2 or with IL-4 (10ng/ml) + GM-CSF (100ng/ml) for 48h. (**A**) Flow cytometry analysis of the moDC population. Numbers indicate percentages of cells within the indicated gates. Plots representative of n=3. (**B**) Percentage of viable moDC following 48h treatment. (**C-F**) Summary of flow cytometry analysis of CD14 (**C**), CD86 (**D**) HLA-ABC (**E**) and HLA-DR (**F**) expression on moDC, as percentage of live

moDC. (n=3; data representative of ≥ 3 independent experiments). ns with RM one-way ANOVA with Tukey`s post hoc multiple comparisons test (mean ± SD).

5.2.1.2 Effect of ILC2 on the surface expression of CD1a on fully differentiated moDC

MoDC differentiation is accompanied by the upregulation of surface CD1a expression (335). To examine the effect of ILC2 secretory molecules on the phenotype of immature moDC, the expression of CD1a on moDC was analysed following treatment with ILC2 supernatants. ILC2 supernatants did not appear to affect CD1a expression on moDC, compared with $moDC_{IL\text{-}4/GM\text{-}CSF}$ or $moDC_{Nil}$ (Fig. 5.3, A-C).

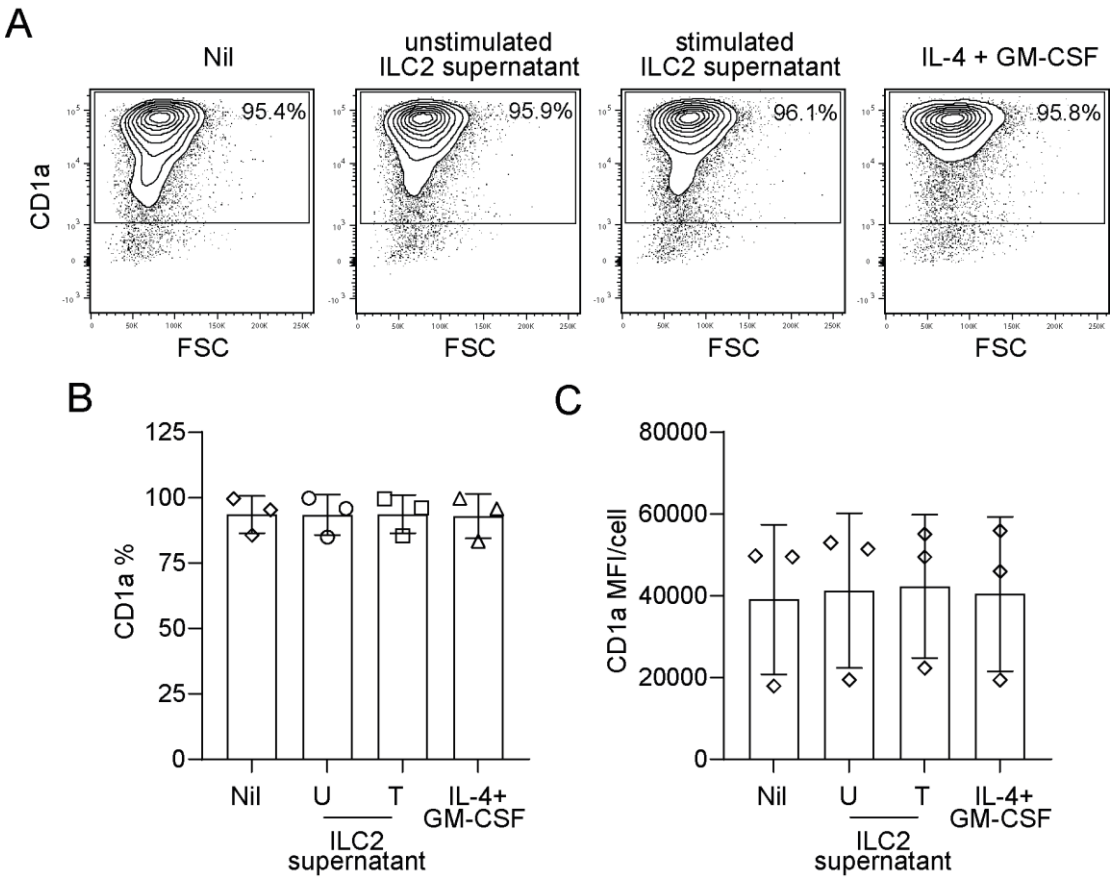


Figure 5.3 Effect of ILC2 supernatants on the expression of CD1a on moDC.
(**A**) CD1a expression on moDC following 48h treatment in medium alone (Nil), supernatants from unstimulated (U) or IL-33, IL-25, TSLP-stimulated (T) ILC2 or IL-4 (10 ng/ml) + GM-

CSF (100 ng/ml), analysed by flow cytometry. Numbers indicate percentages of cells within the indicated gates, gated on live cells. Plots representative of n=3. (**B**) Summary of CD1a expression on moDC, as percentage of live moDC. (**C**) Summary of flow cytometry analysis of CD1a expression (MFI) per live moDC. (n=3; data representative of ≥ 3 independent experiments). ns with RM one-way ANOVA with Tukey`s post hoc multiple comparisons test (mean ± SD).

5.2.1.3 Effect of ILC2 on the surface expression of DC-SIGN on fully differentiated moDC

Expression of the DC-specific C-type lectin, DC-SIGN, has been shown to be upregulated during *in vitro* moDC differentiation. Through binding to ICAM-3, DC-SIGN enables initial transient adhesion of DC to T cells, which facilitates antigen presentation (360). Following 48-hour culture in medium alone, ILC2 supernatants or IL-4 and GM-CSF, the percentage of DC-SIGN$^+$ moDC remained high (Fig. 5.4, A and B). Culture in medium alone resulted in a significant fold change decrease in DC-SIGN expression levels per moDC compared to the positive control condition. In contrast, a high level of DC-SIGN per moDC was observed on moDC cultured in ILC2 supernatants (Fig. 5.4, C and D), but was not statistically significant. Nevertheless, the data may suggest a stabilising effect of ILC2 on the expression of DC-SIGN on the surface of immature moDC.

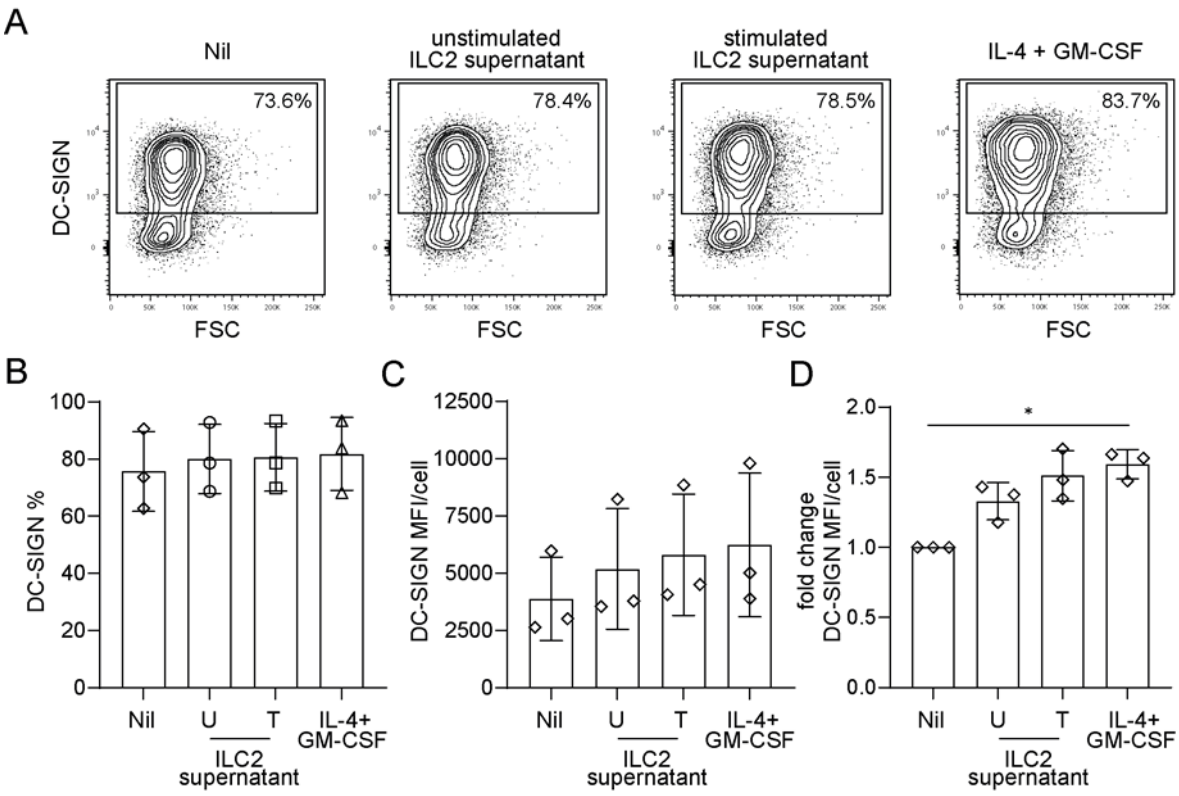


Figure 5.4 Effect of ILC2 supernatants on the expression of DC-SIGN on moDC.

(**A**) DC-SIGN expression on moDC following 48h treatment in medium alone (Nil), supernatants from unstimulated (U) or IL-33, IL-25, TSLP-stimulated (T) ILC2 or IL-4 (10ng/ml) + GM-CSF (100 ng/ml), analysed by flow cytometry. Numbers indicate percentages of cells within the indicated gates, gated on live cells. Plots representative of n=3. (**B**) Summary of DC-SIGN expression on moDC, as percentage of live moDC. (**C**) Summary of flow cytometry analysis of DC-SIGN expression (MFI) per live moDC. (**D**) Fold change DC-SIGN expression (MFI) per live moDC relative to medium alone control. (n=3; data representative of ≥ 3 independent experiments). *P < 0.05; RM one-way ANOVA with Tukey`s post hoc multiple comparisons test (mean ± SD).

5.2.2 Effect of ILC2 on the differentiation process of moDC

Widely used protocols for the *in* vitro generation of human immature moDC require approximately five to seven days of monocyte culture in the presence of recombinant IL-4 and GM-CSF (335, 339). It has been suggested that monocytes display signs of moDC differentiation, such as CD14 downregulation, as early as 48 hours into culture with IL-4 and GM-CSF (361). To assess the effect of ILC2-derived molecules on the differentiation process of moDC, moDC differentiation was induced by 3 day culture of monocytes in IL-4 and GM-CSF before replacement of the medium with supernatants from unstimulated or IL-33, IL-25, IL-33-activated ILC2 for a further 48 hours (Fig. 5.5).

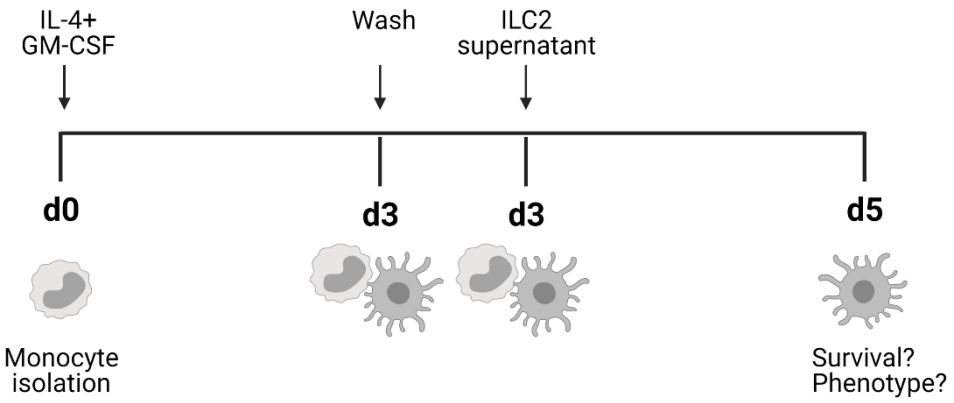


Figure 5.5 Experimental design – effect of ILC2 supernatants on the differentiation process of moDC.

Peripheral blood monocytes were isolated by CD14 MACS separation and cultured with IL-4 and GM-CSF in FCS-containing medium for 72h to induce moDC differentiation. On d3, ILC2 supernatants were added to differentiating moDC for 48h and the effect moDC survival and phenotype assessed by flow cytometry.

5.2.2.1 Effect of ILC2 on the survival of differentiating moDC

Survival of monocyte-derived cells was significantly lower following 48-hour culture of early immature moDC in medium alone compared to maintained IL-4/GM-CSF

treatment. This drop in cell survival upon IL-4/GM-CSF withdrawal was significantly smaller when d3 moDC were cultured in supernatants from activated ILC2 (Fig. 5.6, A and B). There was no significant difference in the percentage of $CD14^{-}CD11c^{+}$ cells across the different culture conditions (Fig. 5.6, C and D). ILC2 stimulants IL-33, IL-25 and TSLP had no effect on the phenotype of differentiating moDC (Fig A.7). Collectively, these results suggest that a large proportion of cells had downregulated CD14 by day 3 of moDC differentiation, indicative of a relatively stable phenotype.

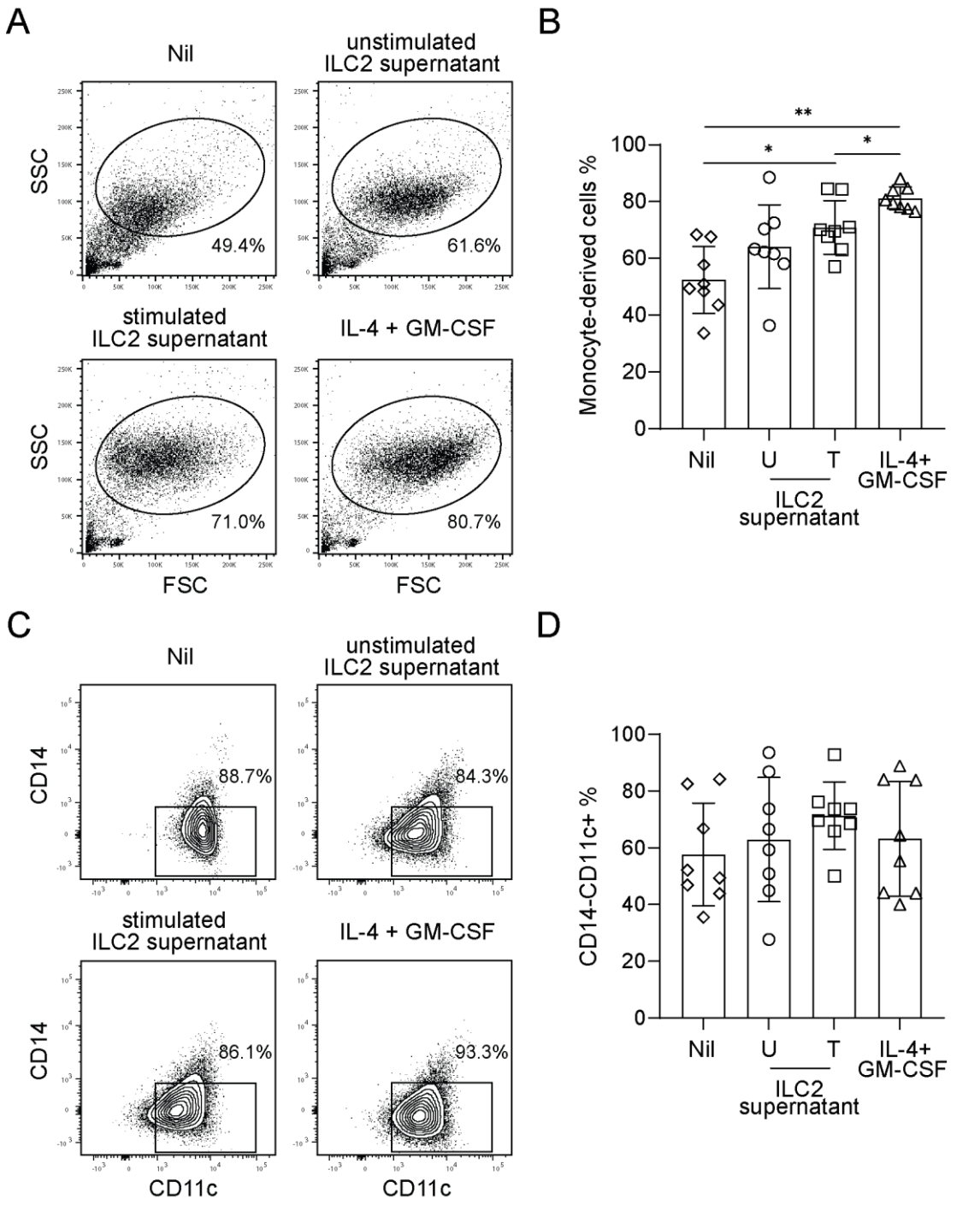


Figure 5.6 Survival of moDC following treatment with ILC2 supernatants during differentiation.

(**A-D**) MoDC differentiation was induced by culturing monocytes in IL-4 (10 ng/ml) and GM-CSF (100 ng/ml) for 3 days. On d3, differentiating moDC were washed and cultured for 48h in medium alone (Nil), unstimulated (U) or IL-33, IL-25, TSLP-stimulated (T) ILC2 supernatants or IL-4 (10 ng/ml) + GM-CSF (100 ng/ml). (**A**) Gating on monocyte-derived cells to assess survival of moDC on d5. Numbers indicate percentages of cells within the indicated gates. Plots representative of n=8. (**B**) Percentage of viable monocyte-derived

cells on d5. (**C**) Flow cytometry analysis of cells expressing CD11c and lacking surface CD14. Numbers indicate percentages of cells within the indicated gates, gated on live cells. Plots representative of n=8. (**D**) Summary of percentage of $CD14^{-}$ $CD11c^{+}$ cells, gated on live monocyte-derived cells. (n=8; data representative of ≥ 3 independent experiments). *P < 0.05; **P < 0.01; RM one-way ANOVA with Tukey`s post hoc multiple comparisons test (mean ± SD).

5.2.2.2 Effect of ILC2 on the expression of CD1a on differentiating moDC

On d5 of differentiation, over 80% of monocyte-derived cells across all conditions stained positively for surface CD1a, implying CD1a upregulation during the first 3 days of moDC differentiation (Fig. 5.7, A and B). Culture of differentiating moDC in medium alone appeared to result in reduced surface CD1a expression levels compared to control $moDC_{IL\text{-}4/GM\text{-}CSF}$. However, moDC cultured in activated ILC2 supernatants during the differentiation process expressed CD1a at levels comparable to $moDC_{IL\text{-}4/GM\text{-}CSF}$ (Fig. 5.7, C). These results suggest that supernatants from activated ILC2 stabilise the expression of CD1a on early immature moDC.

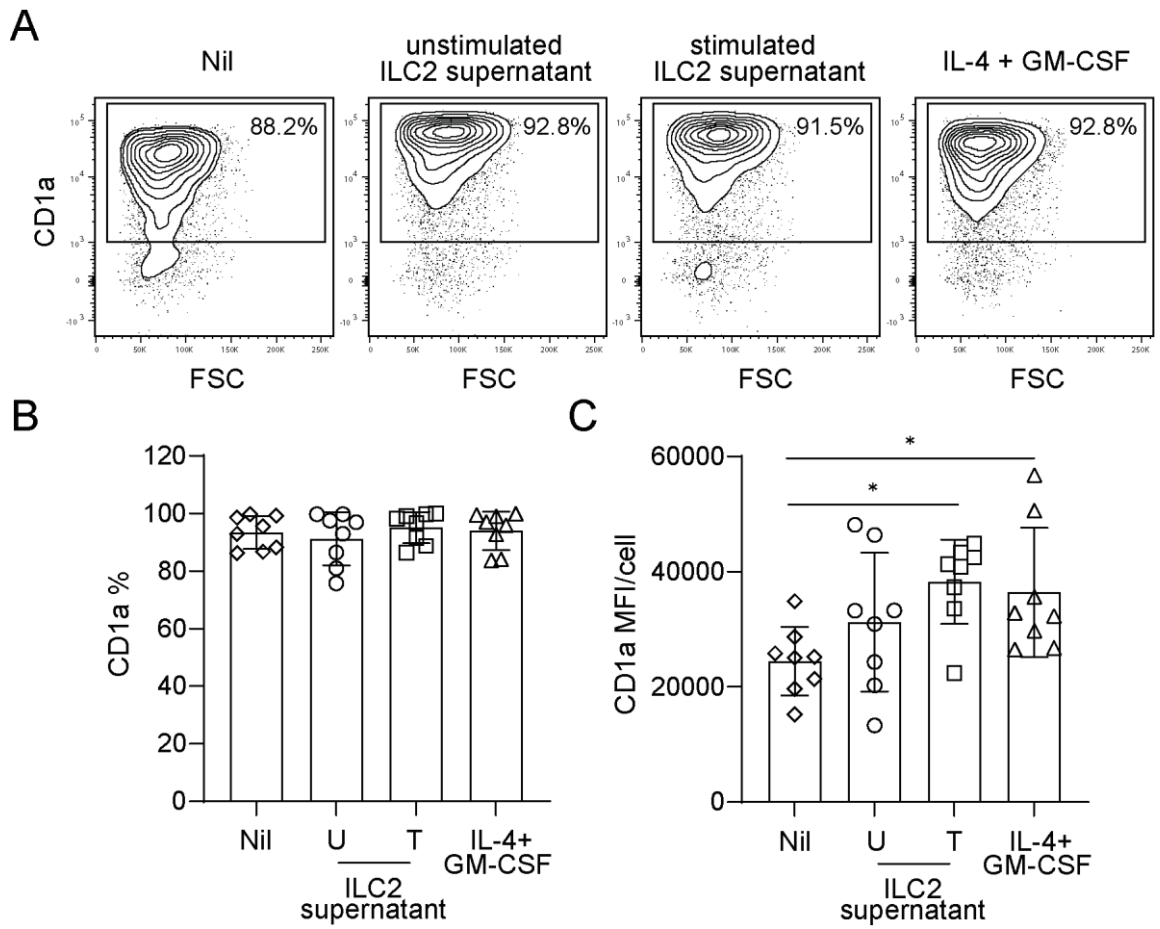


Figure 5.7 Expression of CD1a on moDC following treatment with ILC2 supernatants during differentiation.

(**A**) Flow cytometry analysis of CD1a expression on d5 following 48h culture in medium alone (Nil), unstimulated (U) or IL-33, IL-25, TSLP-stimulated (T) ILC2 supernatants or IL-4 (10 ng/ml) + GM-CSF (100 ng/ml), gated on live monocyte-derived cells. Numbers indicate percentages of cells within the indicated gates, gated on live cells. Plots representative of n=8. (**B**) Summary of CD1a expression, as percentage of live monocyte-derived cells. (**C**) Summary of CD1a expression levels (MFI) per live monocyte-derived cell. (n=8; data representative of ≥ 3 independent experiments). *P < 0.05; RM one-way ANOVA with Tukey`s post hoc multiple comparisons test (mean ± SD).

5.2.2.3 Effect of ILC2 on the expression of DC-SIGN on differentiating moDC

The effect of culturing differentiating moDC in ILC2 supernatants on the expression of the DC receptor DC-SIGN was assessed by flow cytometry. On d5 of differentiation, a significantly higher percentage of moDC cultured in activated ILC2

supernatants (80.28% ± 17.44) were found to express DC-SIGN compared to $moDC_{Nil}$ (65.8% ± 17.98) (Fig. 5.8, A and B). Additionally, moDC cultured in both unstimulated and stimulated ILC2 supernatants during differentiation displayed high surface levels of DC-SIGN per cell that were comparable to levels found on $moDC_{IL-4/GM-CSF}$ and significantly higher than on $moDC_{Nil}$ (Fig. 5.8, C). These data indicate that ILC2 produce factors that stabilise the expression of DC-SIGN on differentiating moDC.

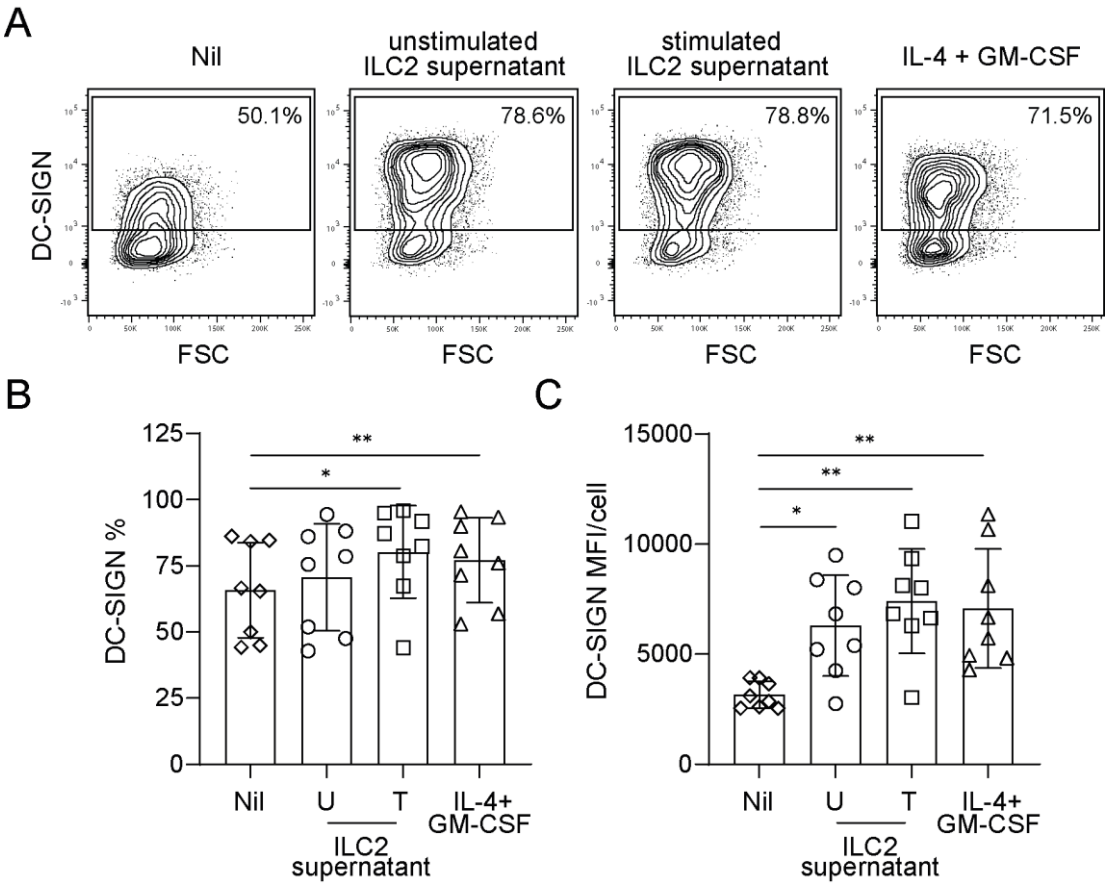


Figure 5.8 Expression of DC-SIGN on moDC following culture in ILC2 supernatants during differentiation.

(**A**) DC-SIGN expression on monocyte-derived cells was assessed by flow cytometry on d5 of differentiation following 48h incubation in medium alone (Nil), unstimulated (U) or IL-33, IL-25, TSLP-stimulated (T) ILC2 supernatants or IL-4 (10 ng/ml) + GM-CSF (100 ng/ml). Plots representative of n=8. Numbers indicate percentages of cells within the indicated gates, gated on live cells. (**B**) Summary of DC-SIGN expression, as percentage of live

monocyte-derived cells. (**C**) Summary of DC-SIGN expression levels (MFI) per live monocyte-derived cell. (n=8; data representative of ≥ 3 independent experiments). *P < 0.05; **P < 0.01; RM one-way ANOVA with Tukey`s post hoc multiple comparisons test (mean ± SD).

5.2.2.4 Effect of ILC2 on the expression of MHC and co-stimulatory molecules on differentiating moDC

DC play an important role as APC by processing and presenting antigens to T cells. While immature moDC are specialised in the update and processing of antigens, moDC maturation, induced by exposure to pro-inflammatory molecules, is associated with an increased antigen presentation capacity (339). ILC2 supernatants did not seem to significantly affect the percentage of moDC expressing MHCI (HLA-ABC), MHCII (HLA-DR), CD80 or CD86 (Fig. 5.9, A-F). MoDC differentiation in exogenous IL-4 and GM-CSF appeared to be associated with a reduction in the percentage of cells expressing MHCI or MHCII (Fig. 5.9 A, B and C). CD80 and CD86 were found to be expressed at low or moderate levels, respectively, on moDC across all conditions (Fig., 5.9, D, E and F). The expression pattern of MHC and co-stimulatory molecules on moDC, cultured in medium alone, ILC2 supernatants or exogenous IL-4 and GM-CSF during the last 48 hours of differentiation, was consistent with an immature moDC phenotype characterised by intermediate expression of MHCI, MHCII and CD86 and low or lack of CD80 expression (362, 363).

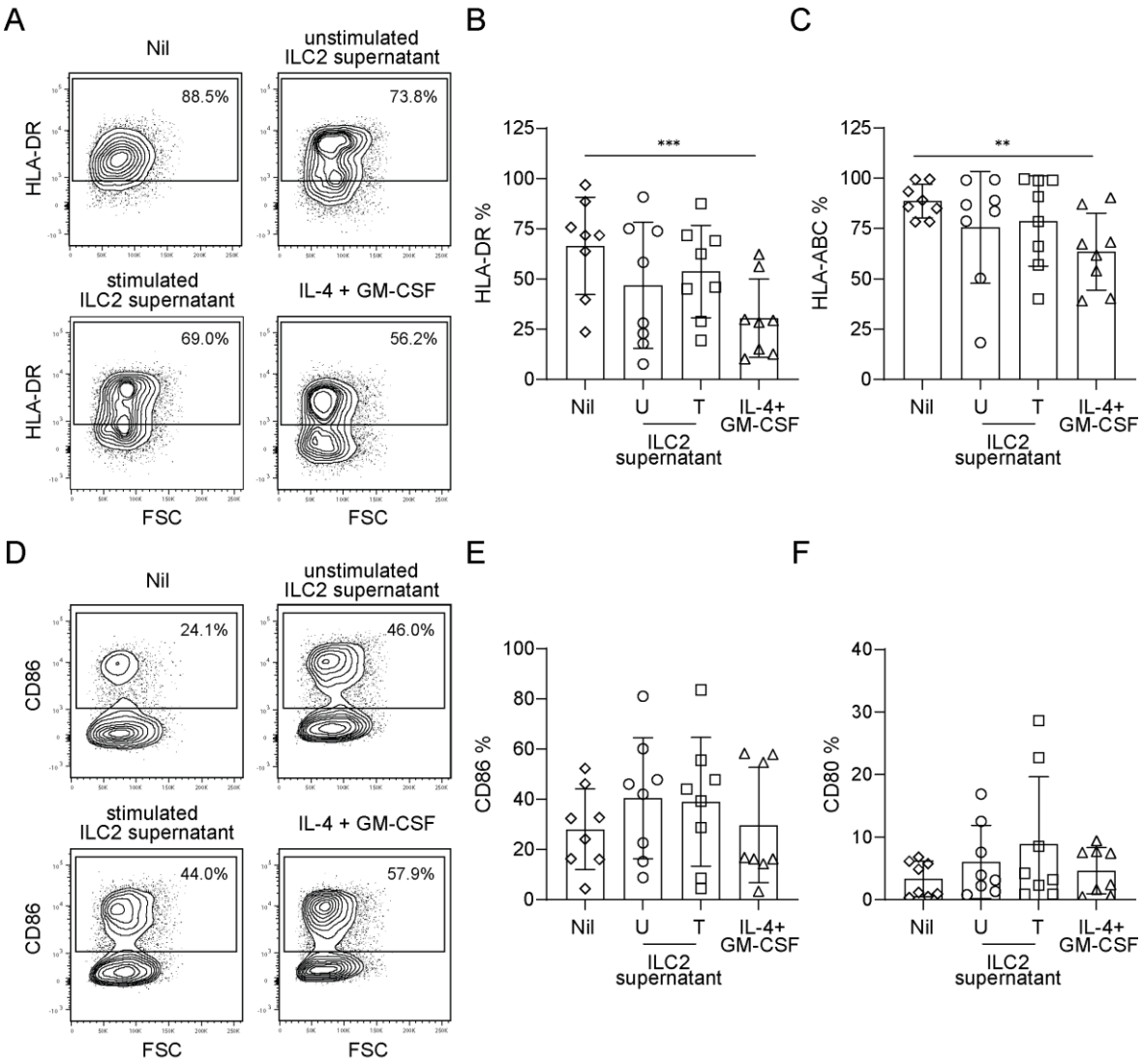


Figure 5.9 Expression of MHC and co-stimulatory molecules on moDC following culture in ILC2 supernatants during differentiation.

(**A**) Flow cytometry analysis of MHCII gated on live monocyte-derived cells on d5 of differentiation following 48h culture in medium alone (Nil), unstimulated (U) or IL-33, IL-25, TSLP-stimulated (T) ILC2 or IL-4 (10 ng/ml) + GM-CSF (100 ng/ml). Numbers indicate percentages of cells within the indicated gates, gated on live cells. Plots representative of n=8. (**B-C**) Percentage of live monocyte-derived cells expressing MHCII (**B**) or MHCI (**C**). (**D**) Surface expression of CD86 on monocyte-derived cells on d5 of differentiation, assessed by flow cytometry. Numbers indicate percentages of cells within the indicated gates, gated on live cells. Plots representative of n=8. (**E-F**) Summary of CD86 (**E**) and CD80 (**F**) expression, as percentage of live monocyte-derived cells. (n=8; data representative of ≥ 3 independent experiments). **P < 0.01; ***P < 0.001; RM one-way ANOVA with Tukey`s post hoc multiple comparisons test (mean ± SD).

5.2.3 Effect of ILC2 on the survival and phenotype of ex vivo monocytes

In humans, the majority of circulating monocytes are characterised by CD14 expression and lack of CD16 expression, referred to as classical monocytes. Classical monocytes have a very short lifespan of about one day in the circulation before either migrating into tissues or undergoing apoptosis (364). The finding that ILC2 supernatants support the survival of differentiating moDC prompted me to investigate the effect of ILC2 supernatants on *ex vivo* monocytes (Fig. 5.10).

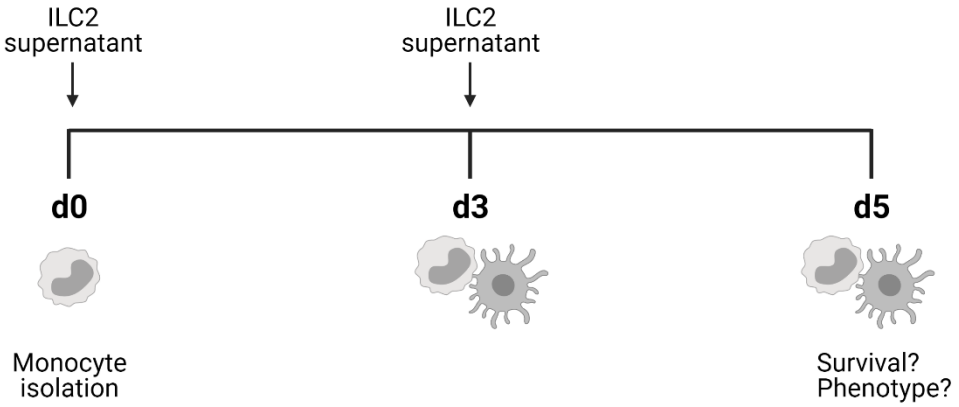


Figure 5.10 Experimental design – effect of ILC2 supernatants on monocytes.
Peripheral blood monocytes were isolated by CD14 MACS separation and cultured in ILC2 supernatants for 5 days without exogenous IL-4 or GM-CSF. The effect on cell survival and phenotype was assessed on d5 by flow cytometry.

5.2.3.1 Effect of ILC2 on the survival of monocytes/monocyte-derived cells

Circulating $CD14^+$ monocytes were isolated and cultured for 5 days in medium alone ($monocytes_{Nil}$), supernatants from unstimulated or IL-33, IL-25, TSLP-stimulated ILC2 or the positive control combination of recombinant IL-4 and GM-CSF ($moDC_{IL\text{-}4/GM\text{-}CSF}$). While $monocytes_{Nil}$ were characterised by a spherical shape, monocyte-derived cells cultured in ILC2 supernatants exhibited a morphology similar to control $moDC_{IL\text{-}4/GM\text{-}CSF}$ characterised by loosely adherent or detached clusters of cells with

cytoplasmic protrusions indicative of dendrites (Fig. 5.11, A). Flow cytometry analysis of scatter parameters was used to assess the survival and purity of the monocyte/monocyte-derived cell population. By d5 of culture, there were few surviving $monocytes_{Nil}$. In contrast, culture in ILC2 supernatants, especially in supernatants from stimulated ILC2, supported monocyte-derived cell survival (Fig. 5.11, B and C). Forward and side scatter signals show that monocytes cultured in supernatants from activated ILC2 were characterised by increased cell size and granularity on d5 of culture compared to monocytes cultured in unstimulated ILC2 supernatants (Fig. 5.11, B). This might be indicative of a higher degree of differentiation of monocytes cultured in activated ILC2 supernatants. Percentages of viable monocyte-derived cells cultured in ILC2 supernatants (U = 48.64% ± 12.92; T = 56.84% ± 12.69) were significantly higher than those cultured in medium alone (33.12% ± 10.79) and comparable to $moDC_{IL\text{-}4/GM\text{-}CSF}$ (62.96% ± 10.26) (Fig. 5.11, C). Cell viability in cultures on d5 was evaluated by trypan blue exclusion. The number of viable cells was significantly higher in the ILC2 supernatant cultures compared to $monocytes_{Nil}$, approximately equalling that of $moDC_{IL\text{-}4/GM\text{-}CSF}$ (Fig. 5.11, D). moDC are characterised by high expression of CD11c and lack of surface CD14. While $monocytes_{Nil}$ contained few $CD14^{-}CD11c^{+}$ cells, the majority of cells cultured in ILC2 supernatants were identified as $CD14^{-}CD11c^{+}$ cells. The percentage of $CD14^{-}CD11c^{+}$ cells cultured in activated ILC2 supernatants (80.93 ± 10.29) was similar to $moDC_{IL\text{-}4/GM\text{-}CSF}$ (84.57% ± 8.719) (Fig. 5.11, E) suggesting that ILC2 supernatants induce the differentiation of monocytes into moDC. Alarmins present in stimulated ILC2 supernatants had no effect on the survival or phenotype of *ex vivo* monocytes (Fig. A.8).

Collectively, these results show that supernatants from both resting and activated ILC2 support the survival and differentiation of $CD14^{-}CD11c^{+}$ moDC. Here, ILC2-induced moDC will be referred to as $moDC_{ILC2}$. To distinguish between moDC differentiated in supernatants from unstimulated and stimulated ILC2, the terms $moDC_{ILC2(U)}$ and $moDC_{ILC2(T)}$ will be used.

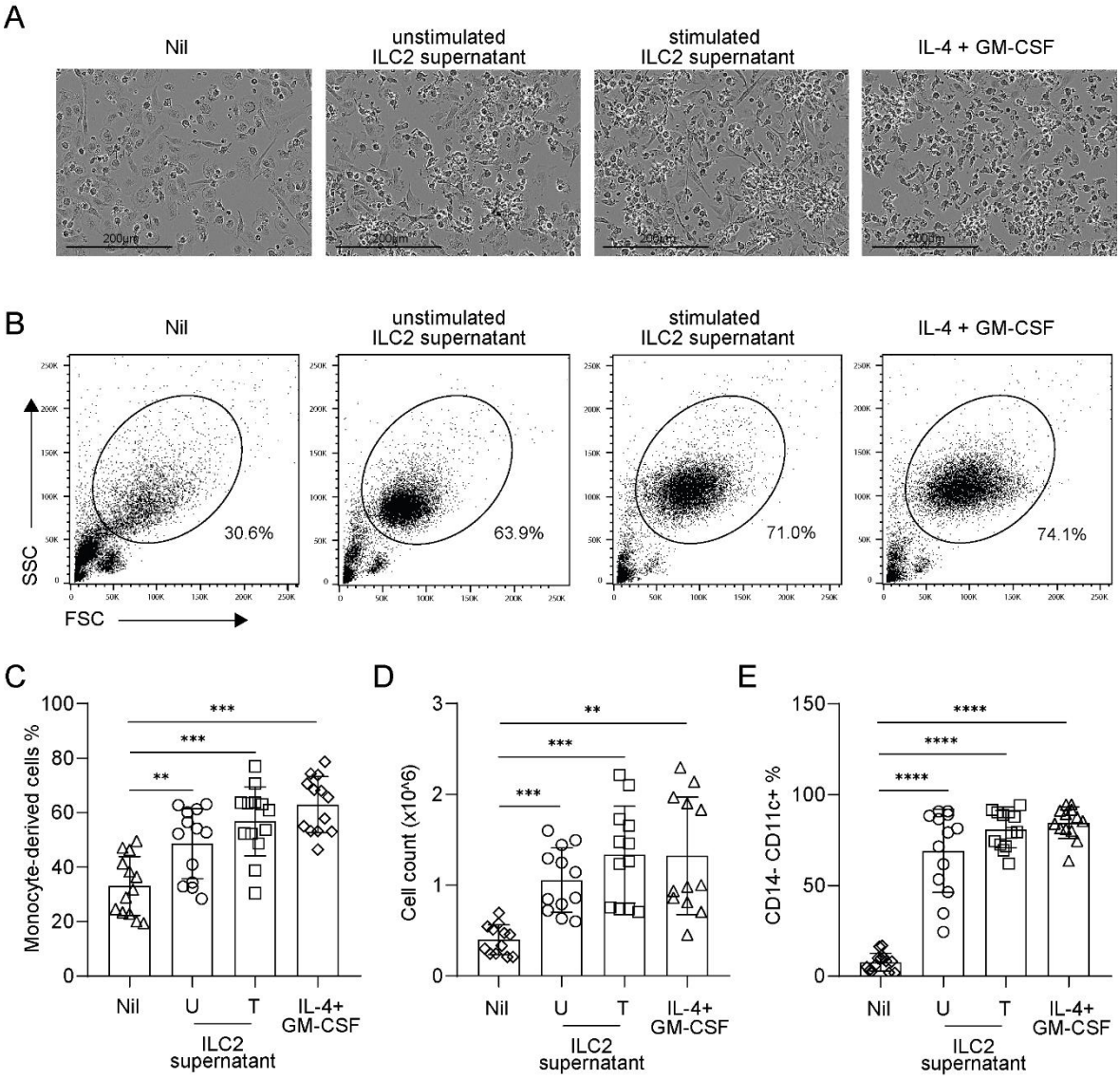


Figure 5.11 ILC2 supernatants induce differentiation of monocytes into moDC.

(**A-E**) Monocytes were cultured for 5 days in medium alone (Nil), supernatants from unstimulated (U) and IL-33,IL-25,TSLP-stimulated (T) ILC2 or IL-4 (10ng/ml) + GM-CSF (100ng/ml). (**A**) Cell morphology was assessed on d5 by IncuCyte live-cell imaging (20x objective), representative of n=13. (**B**) Flow cytometry analysis of scatter parameters to

assess survival of the monocyte/monocyte-derived cell population following 5d treatment. Numbers indicate percentages of cells within the indicated gates. Plots representative of n=13. (**C**) Percentage of viable monocyte-derived cells following 5d treatment as assessed by flow cytometry. (**D**) Number of viable cells following treatment of $1.5x10^6$ monocytes for 5d. (**E**) Percentage of $CD14^-$ $CD11c^+$ cells, gated on live monocyte-derived cell population. (n=13; data representative of ≥ 3 independent experiments). *P < 0.05; **P < 0.01; ***P < 0.001, ****P < 0.0001; RM one-way ANOVA with Tukey`s post hoc multiple comparisons test (mean ± SD)

5.2.3.2 Expression of CD1 molecules on ILC2-induced moDC

While monocytes do not express CD1 molecules, moDC differentiation is accompanied by upregulation of CD1a, CD1b and CD1c expression (335). A high percentage of $moDC_{ILC2}$ were found to express substantial levels of surface CD1a, while surviving $monocytes_{Nil}$ lacked surface CD1a (Fig. 5.12, A-C). CD1a expression was highest on $moDC_{IL\text{-}4/GM\text{-}CSF}$ (Fig. 5.12, C). In addition to CD1a, the majority of $moDC_{ILC2}$ also expressed CD1b and CD1c (Fig. 5.12, D-F). The percentage of $CD1b^+$ cells was significantly increased following culture in supernatants from activated compared to unstimulated ILC2 (Fig. 5.12, E).

Overall, these findings demonstrate that ILC2 supernatants induce the upregulation of CD1a, CD1b and CD1c on the surface of monocyte-derived cells.

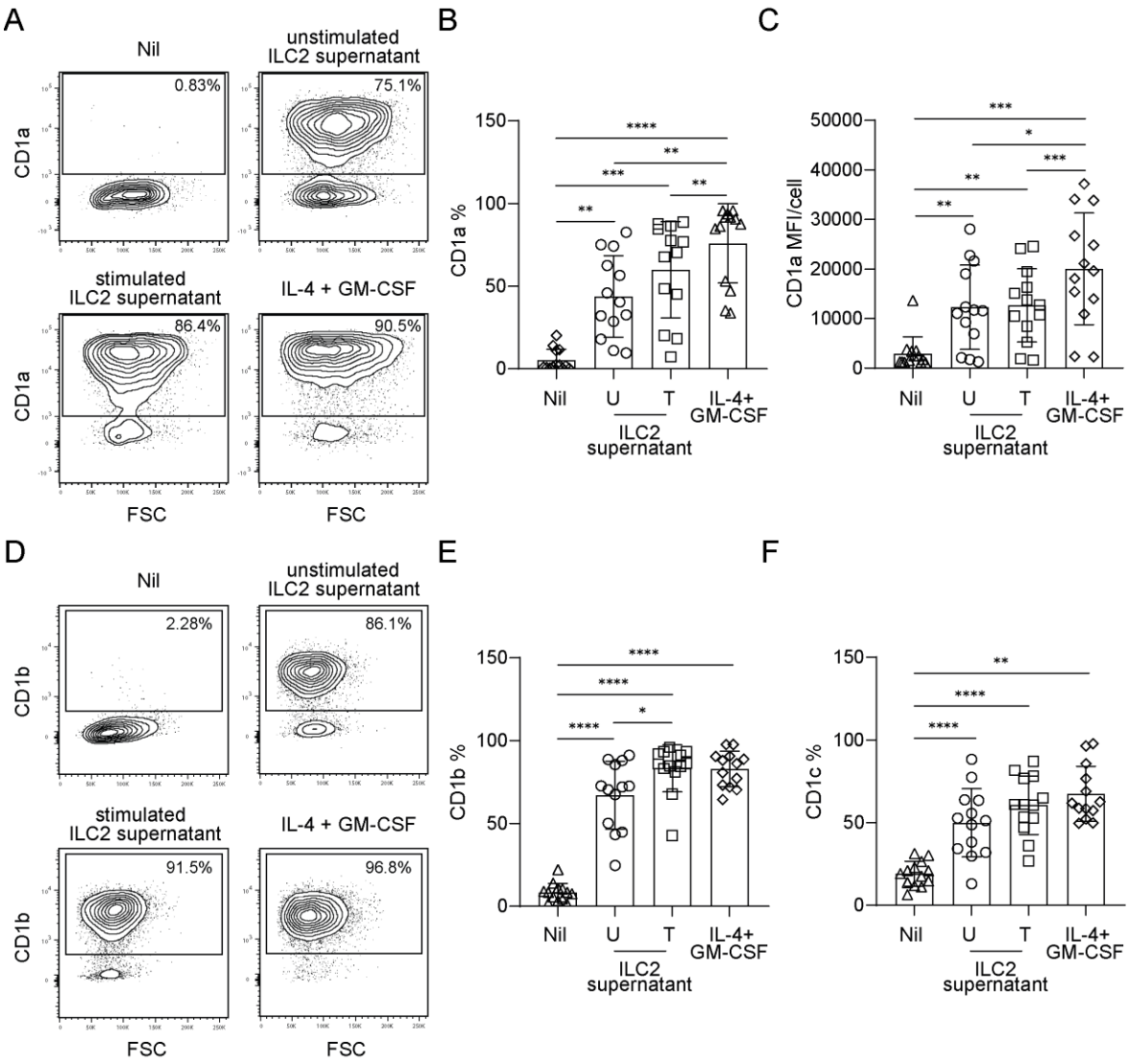


Figure 5.12 Expression of CD1 molecules on ILC2-induced moDC.

(**A**) CD1a expression on monocyte-derived cells was analysed by flow cytometry following 5 day culture in medium alone (Nil), unstimulated (U) or IL-33, IL-25, TSLP-stimulated (T) ILC2 or IL-4 (10 ng/ml) + GM-CSF (100 ng/ml). Numbers indicate percentages of cells within the indicated gates, gated on live cells. Plots representative of n=13. (**B**) Summary of CD1a expression, as percentage of live monocyte-derived cells. (**C**) Summary of CD1a expression (MFI) per live monocyte-derived cell. (**D**) Flow cytometry analysis of CD1b expression on monocyte-derived cells on d5. Numbers indicate percentages of cells within the indicated gates, gated on live cells. Plots representative of n=13. (**E and F**) Summary of CD1b (**E**) and CD1c (**F**) expression, as percentage of live monocyte-derived cells. (n=13; data representative of ≥ 3 independent experiments). *P < 0.05; **P < 0.01; ***P < 0.001, ****P < 0.0001; RM one-way ANOVA with Tukey`s post hoc multiple comparisons test (mean ± SD).

5.2.3.3 Expression of DC-SIGN on ILC2-induced moDC

Over 80% of $moDC_{ILC2}$ and $moDC_{IL\text{-}4/GM\text{-}CSF}$ were found to express high levels of surface DC-SIGN, while only an average of 17.4% of surviving $monocytes_{Nil}$ were DC-SIGN$^+$ (Fig. 5.13, A, B and C). The percentage of DC-SIGN-expressing cells was highest for $moDC_{ILC2(T)}$ (91.59% ± 5.8), while the percentage of DC-SIGN$^+$ $moDC_{ILC2(U)}$ (80.95% ± 10.7) was approximately equivalent to $moDC_{IL\text{-}4/GM\text{-}CSF}$ (83.2% ± 7.718) (Fig. 5.13, B). Similarly, the level of surface DC-SIGN expression was significantly higher on $moDC_{ILC2(T)}$ compared to $moDC_{IL\text{-}4/GM\text{-}CSF}$ (Fig. 5.13, C).

Collectively, these results show that ILC2 supernatants potently induce the expression of DC-SIGN on monocyte-derived cells.

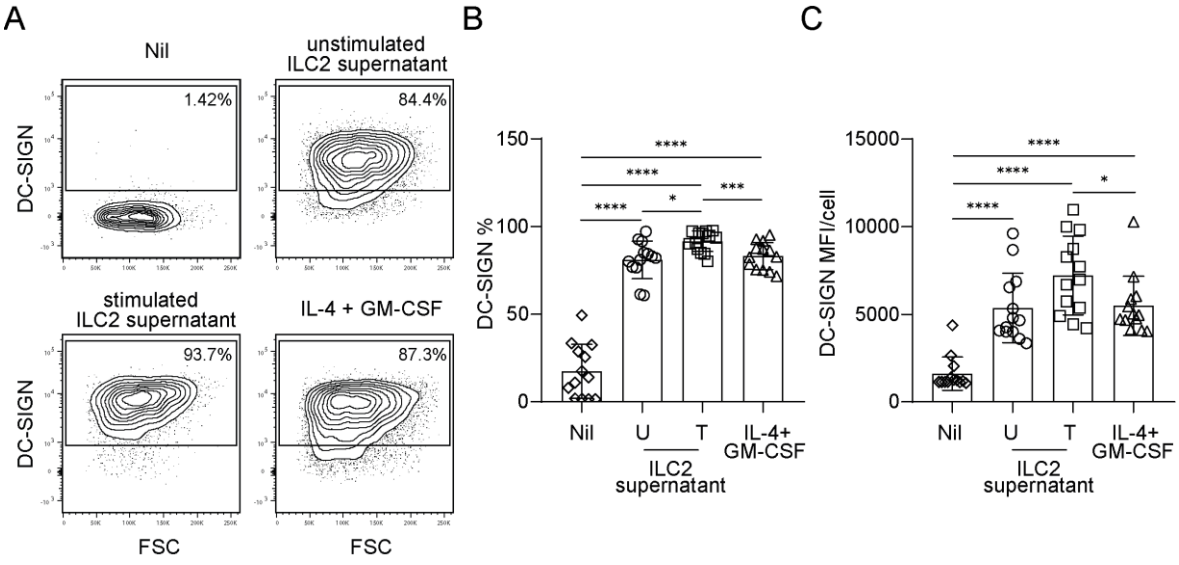


Figure 5.13 DC-SIGN expression on ILC2-induced moDC.

(**A**) Flow cytometry analysis of DC-SIGN expression on monocyte-derived cells following 5 day culture in medium alone (Nil), unstimulated (U) or IL-33, IL-25, TSLP-stimulated (T) ILC2 or IL-4 (10 ng/ml) + GM-CSF (100 ng/ml). Numbers indicate percentages of cells within the indicated gates, gated on live cells. Plots representative of n=13. (**B**) Summary of DC-SIGN expression, as percentage of live monocyte-derived cells. (**C**) Summary of DC-SIGN expression levels (MFI) per live monocyte-derived cells. (n=13; data representative of ≥ 3 independent experiments). *P < 0.05; **P < 0.01; ***P < 0.001, ****P < 0.0001; RM one-way ANOVA with Tukey`s post hoc multiple comparisons test (mean ± SD).

5.2.3.4 Expression of MHC and co-stimulatory molecules on ILC2-induced moDC

Both monocytes and monocyte-derived cells act as APC with the capacity to process and present antigens to T cells via MHC and co-stimulatory molecules. While a large percentage of $monocytes_{Nil}$ were found to express high levels of both MHCI/II and the co-stimulatory molecule CD86, the percentage of cells expressing MHCI, MHCII and CD86 appeared to be lower following 5 day culture in ILC2 supernatants or recombinant IL-4 and GM-CSF (Fig. 5.14, A, B and C). The majority of cells across all conditions were found to be $CD80^{-/low}$ (Fig. A.8). Likewise, $moDC_{ILC2}$ expressed significantly lower levels of surface MHCI and MHCII compared to $monocytes_{Nil}$. MHCI and MHCII levels on $moDC_{ILC2(T)}$ were comparable to levels on control $moDC_{IL\text{-}4/GM\text{-}CSF}$ (Fig. 5.14, D and E). Interestingly, $moDC_{ILC2}$ and $moDC_{IL\text{-}4/GM\text{-}CSF}$ were found to express significantly higher levels of CD86 per cell compared to $monocytes_{Nil}$. Notably, CD86 levels per cell were significantly higher on $moDC_{ILC2(U)}$ compared to $moDC_{ILC2(T)}$ (Fig. 5.14, F).

These data suggest that surviving monocytes retain the expression of molecules involved in antigen presentation, while the lower percentage of $MHCI/II^{+}$ and $CD86^{+}$ cells following culture in ILC2 supernatants or exogenous IL-4 and GM-CSF may be indicative of an immature moDC phenotype.

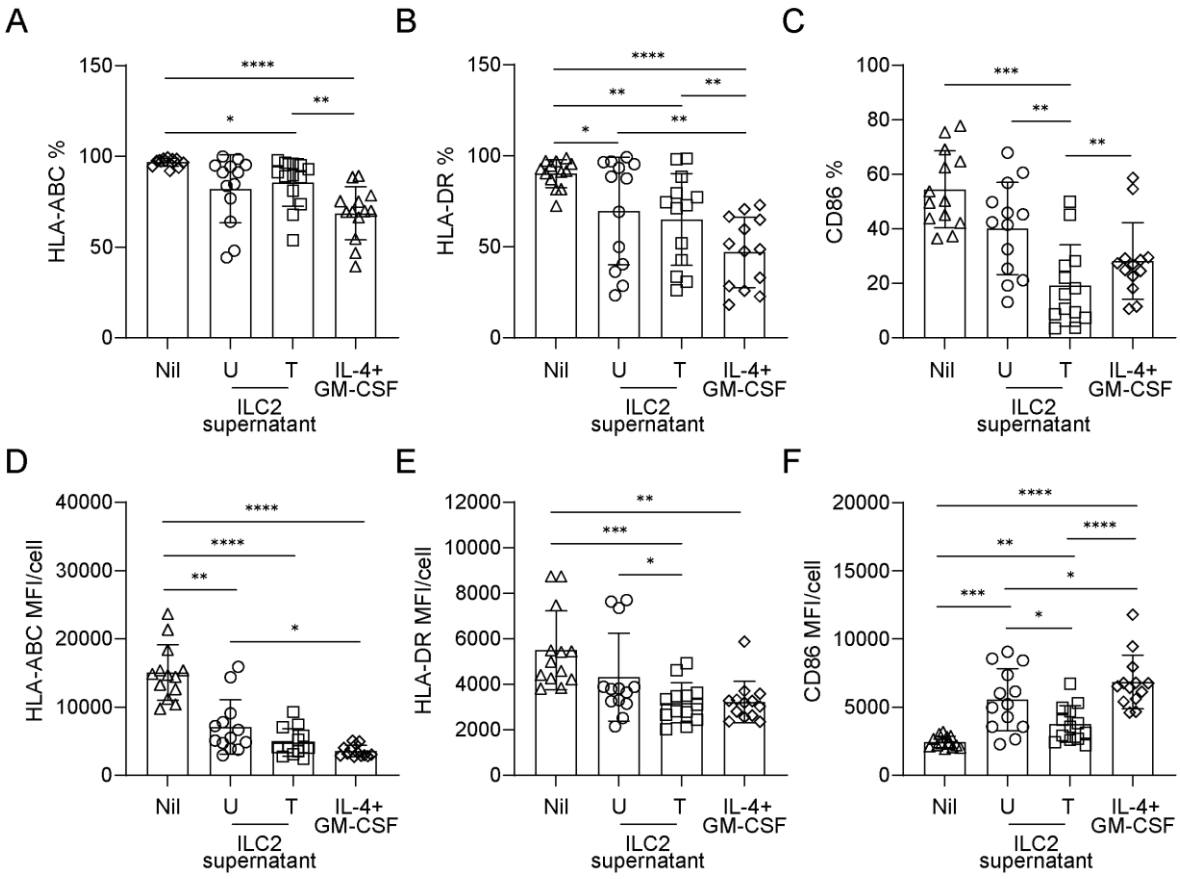


Figure 5.14 Expression of MHC and co-stimulatory molecules on ILC2-induced moDC.

(**A-C**) Flow cytometry analysis of MHCI (**A**), MHCII (**B**) and CD86 (**C**) expression on monocyte-derived cells following 5 day culture in medium alone (Nil), unstimulated (U) or IL-33, IL-25, TSLP-stimulated (T) ILC2 or IL-4 (10 ng/ml) + GM-CSF (100 ng/ml). Plots representative of n=13. (**D-F**) Summary of the expression levels (MFI) per live monocyte-derived cell of MHCI (**D**), MHCII (**E**) and CD86 (**F**). (n=13; data representative of ≥ 3 independent experiments). *P < 0.05; **P < 0.01; ***P < 0.001, ****P < 0.0001; RM one-way ANOVA with Tukey`s post hoc multiple comparisons test (mean ± SD).

5.2.4 Identification of ILC2-secretory factors that contribute to the induction of moDC differentiation

Following on from the finding that ILC2 supernatants induced the differentiation of monocytes into moDC, I aimed to identify the ILC2-secretory factors responsible for this effect.

5.2.4.1 IL-4 and GM-CSF production by ILC2

As IL-4 and GM-CSF are known inducers of *in vitro* moDC differentiation, secretion of IL-4 and GM-CSF by human ILC2 was assessed (as in section 3.2.4.4). Alarmin-induced activation of ILC2 was found to significantly upregulate the secretion of both IL-4 and GM-CSF, an effect that was particularly pronounced for GM-CSF (Fig. 5.15, A and B).

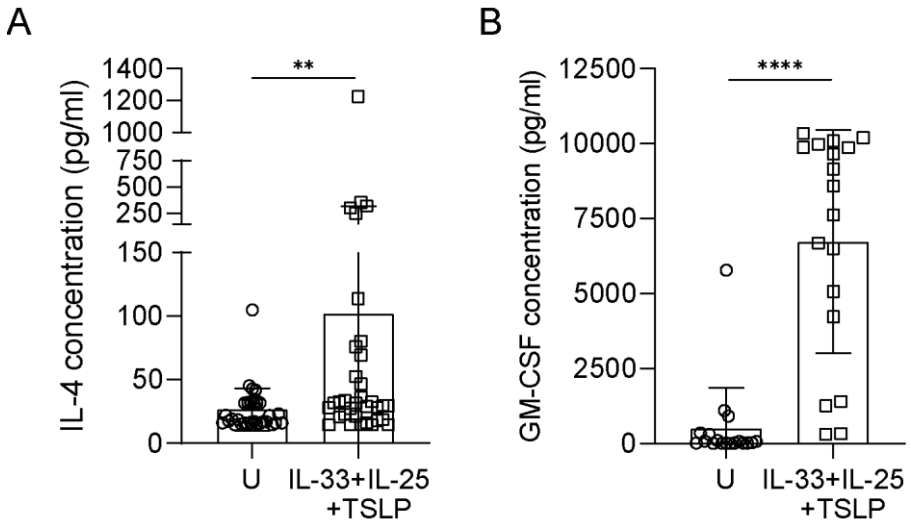


Figure 5.15 ILC2 upregulate IL-4 and GM-CSF secretion following stimulation with alarmin cytokines.

(**A**) IL-4 levels in ILC2 supernatants following 72h culture in medium alone (U) or in the presence of IL-33, IL-25 and TSLP (50 ng/ml each), measured by Luminex assay. (n=35; representative of ≥ 3 independent experiments). (**B**) GM-CSF levels in unstimulated (U) and IL-33, IL-25, TSLP-stimulated ILC2 supernatants measured by Luminex. (n=18;

representative of ≥ 3 independent experiments). *P < 0.05; **P < 0.01; ***P < 0.001, ****P < 0.0001; paired Student`s *t* test (mean ±SD).

As such, ILC2-derived IL-4 and GM-CSF are good candidates to drive the induction of monocyte differentiation to moDC. To test this hypothesis, monocytes were isolated and cultured for 5 days in ILC2 supernatants in the presence or absence of antibodies blocking signalling through the IL-4Rα and/or neutralising GM-CSF (Fig. 5.16).

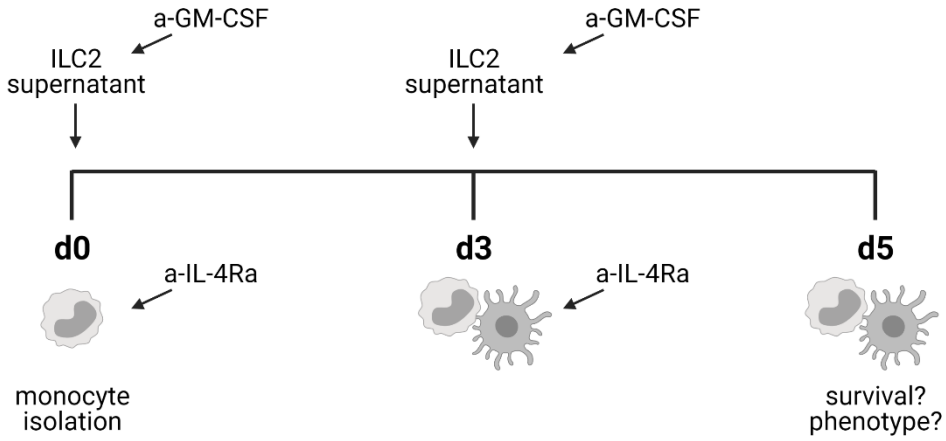


Figure 5.16 Experimental design – testing the contribution of ILC2-secreted IL-4 and GM-CSF on the induction of moDC differentiation.
Peripheral blood monocytes were isolated by CD14 MACS separation and cultured in ILC2 supernatants for 5 days without exogenous IL-4 or GM-CSF in the presence or absence of anti-IL-4Rα (a-IL-4Rα) and anti-GM-CSF (a-GM-CSF) antibodies. The effect on cell survival and phenotype was assessed on d5 of differentiation by flow cytometry.

5.2.4.2 Contribution of ILC2-secreted IL-4 and GM-CSF to the induction of moDC differentiation

The effect of anti-IL-4Rα and anti-GM-CSF antibodies on the survival and differentiation of monocytes$_{Nil}$, moDC$_{ILC2}$ or moDC$_{IL-4/GM-CSF}$ was assessed by flow cytometry. Flow cytometry analysis of scatter parameters demonstrated that the

addition of anti-GM-CSF antibody resulted in a significant drop in the size and survival of the monocyte-derived cell population cultured in stimulated ILC2 supernatants (Fig. 5.17, A and B). Blocking of ILC2-derived IL-4 and GM-CSF signalling significantly reduced the percentage of $CD14^{-}CD11c^{+}$ $moDC_{ILC2(T)}$ (Fig. 5.17, C). However, viability and percentage of $CD14^{-}CD11c^{+}$ expression was higher on $moDC_{ILC2}$ compared to $monocytes_{Nil}$ even in the presence of anti-IL-4Rα and/or anti-GM-CSF antibodies, implying that other factors in ILC2 supernatants may contribute to ILC2-induced moDC differentiation. Blocking IL-4Rα signalling and neutralising GM-CSF had a less pronounced effect on the survival and differentiation of monocytes cultured in exogenous IL-4 and GM-CSF. While a reduction in the percentage of viable $moDC_{IL\text{-}4/GM\text{-}CSF}$ was noticeable (Fig. 5.17, A and B), there was no difference in the percentage of $CD14^{-}CD11c^{+}$ $moDC_{IL\text{-}4/GM\text{-}CSF}$ following culture in the presence of anti-IL-4Rα and/or anti-GM-CSF antibodies (Fig. 5.17, C). This might be due to high concentrations of recombinant GM-CSF used, resulting in antibody saturation. Hence, higher antibody concentrations might be required to see an effect on moDC differentiation in exogenous IL-4 and GM-CSF.

The reduced survival of $moDC_{ILC2}$ as a result of blocking the effect of IL-4Rα signalling and/or GM-CSF suggests that ILC2-derived IL-4 and GM-CSF contribute to the survival and differentiation of monocytes. Due to observed differences in the percentages of $CD14^{-}CD11c^{+}$ cells across conditions, further analysis of cell surface markers was performed on the $CD14^{-}CD11c^{+}$-gated population.

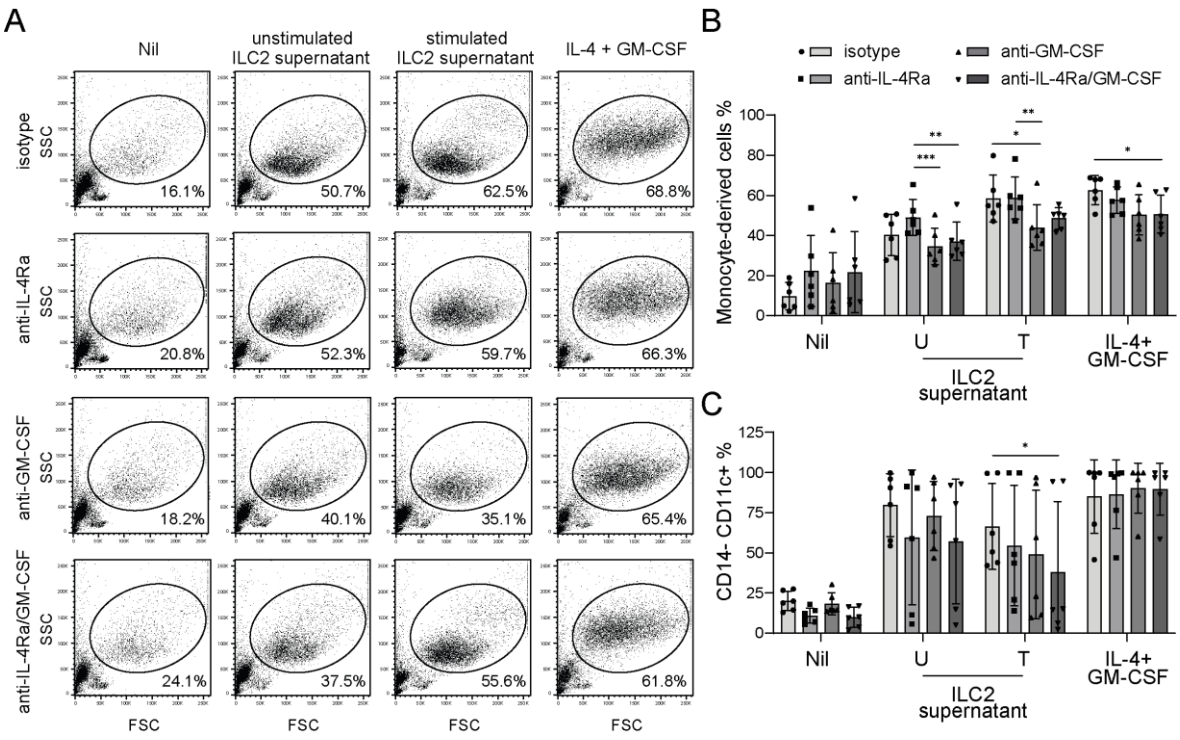


Figure 5.17 ILC2-derived GM-CSF contributes to the induction of moDC differentiation.

(**A-C**) Monocytes were cultured for 5 days in medium alone (Nil), unstimulated (U) or IL-33, IL-25, TSLP-stimulated (T) ILC2 supernatants or IL-4 (10 ng/ml) + GM-CSF (100 ng/ml) in the presence or absence of anti-IL-4Rα blocking antibody (10 µg/ml), anti-GM-CSF neutralising antibody (50 µg/ml) or isotype control (10 µg/ml; 50 µg/ml). (**A**) Flow cytometry analysis of scatter parameters to assess survival of monocyte-derived cell population on d5. Numbers indicate percentages of cells within the indicated gates. Plots representative of n=6. (**B**) Percentage of viable monocyte-derived cells on d5 as assessed by flow cytometry. (**C**) Percentage of $CD14^{-}$ $CD11c^{+}$ cells, gated on the live monocyte-derived cells population. (n=6; data representative of ≥ 3 independent experiments). *P < 0.05; **P < 0.01; ***P < 0.001; RM two-way ANOVA with Tukey`s post hoc multiple comparisons test (mean ± SD).

5.2.4.3 Contribution of ILC2-secreted IL-4 and GM-CSF to the upregulation of CD1a on ILC2-induced moDC

The addition of anti-GM-CSF antibody during moDC differentiation in activated ILC2 supernatants was found to prevent the upregulation of surface CD1a, as demonstrated by flow cytometry analysis (Fig. 5.18, A). The percentage of $CD14^{-}$

$CD11c^+$ $moDC_{ILC2(T)}$ expressing CD1a was significantly reduced by the addition of anti-GM-CSF. Blocking IL-4Rα signalling did not affect CD1a expression on $moDC_{ILC2}$ (Fig. 5.18, B). Expression levels of surface CD1a on $moDC_{ILC2}$ appeared very low in the presence of anti-GM-CSF, however observed differences in the mean fluorescence intensity did not reach statistical significance (Fig. 5.18, C).

Overall, these findings support the hypothesis that ILC2-derived GM-CSF plays an important role in the upregulation of CD1a on ILC2-induced moDC.

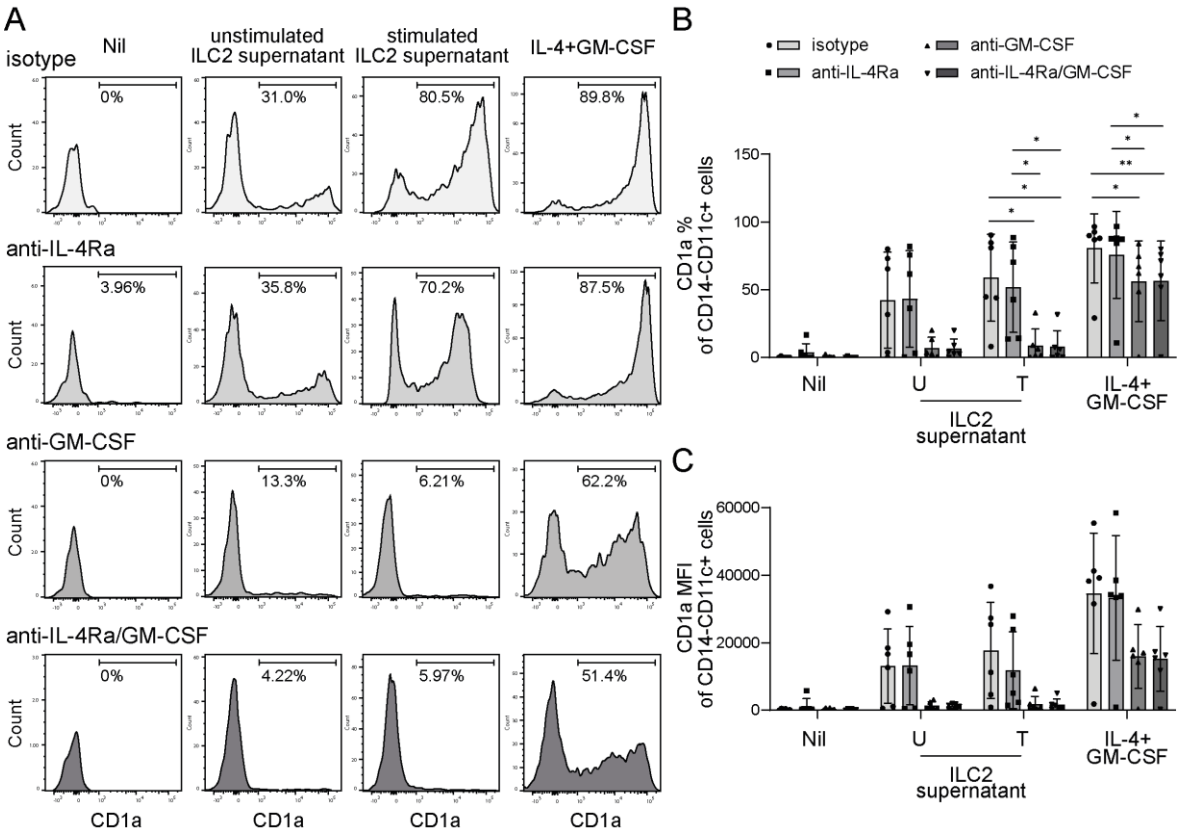


Figure 5.18 ILC2-derived GM-CSF contributes to the upregulation of CD1a on ILC2-induced moDC.

(**A**) Flow cytometry analysis of CD1a expression on $CD14^-CD11c^+$ moDC following 5 day culture in medium alone (Nil), unstimulated (U) or IL-33, IL-25, TSLP-stimulated (T) ILC2 supernatants or IL-4 (10 ng/ml) + GM-CSF (100 ng/ml) in the presence or absence of anti-IL-4Rα blocking antibody (10 µg/ml), anti-GM-CSF neutralising antibody (50 µg/ml) or isotypes (10 µg/ml; 50 µg/ml). Numbers indicate percentages of $CD1a^+$ cells, gated on $CD14^-$ $CD11c^+$ cells. Plots representative of n=6. (**B**) Summary of CD1a expression, as

percentage of $CD14^{-}CD11c^{+}$ cells. (**C**) CD1a expression levels (MFI) on $CD14^{-}CD11c^{+}$ cells. (n=6; data representative of ≥ 3 independent experiments). *P < 0.05; **P < 0.01; RM two-way ANOVA with Tukey`s post hoc multiple comparisons test (mean ± SD).

5.2.4.4 Contribution of ILC2-secreted IL-4 and GM-CSF to the upregulation of DC-SIGN on ILC2-induced moDC

ILC2-derived GM-CSF was found to contribute to the upregulation of DC-SIGN on $moDC_{ILC2}$. No significant change was observed regarding the percentage of DC-SIGN-expressing $CD14^{-}CD11c^{+}$ $moDC_{ILC2}$ following culture in the presence or absence of anti-IL-4Rα and/or anti-GM-CSF antibodies (Fig. 5.19, A and B). However, the level of DC-SIGN expression on $moDC_{ILC2(T)}$ was significantly reduced by the addition of anti-GM-CSF antibody (Fig. 5.19, C). The role of IL-4Rα signalling in the induction of DC-SIGN expression on $moDC_{ILC2}$ was unclear. Blocking IL-4Rα signalling resulted in a slight reduction in the percentage of $DC\text{-}SIGN^{+}$ $moDC_{ILC2}$ as well as in the levels of DC-SIGN expression on $moDC_{ILC2}$, however there was no statistical significance due to relatively large variability (Fig. 5.19, A, B and C). Notably, culture of monocytes in unstimulated and stimulated ILC2 supernatants in the presence of both anti-IL-4Rα and anti-GM-CSF antibodies gave rise to moDC expressing significantly reduced levels of surface DC-SIGN compared to the isotype control (Fig. 5.19, C).

These results indicate that ILC2-derived GM-CSF contributes to the upregulation of DC-SIGN on ILC2-induced moDC, however, it appears that there are other as yet unknown DC-SIGN inducing factors present in ILC2 supernatants.

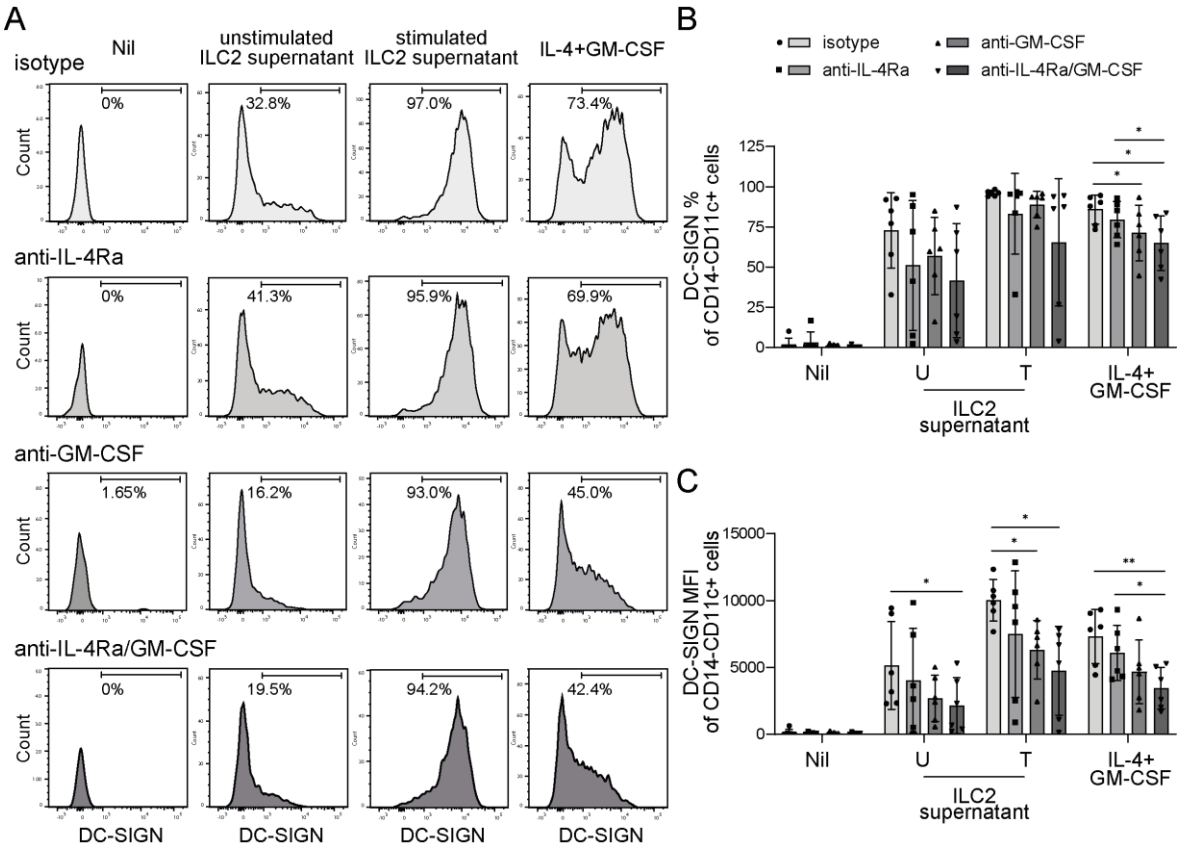


Figure 5.19 ILC2-derived GM-CSF contributes to the upregulation of DC-SIGN on ILC2-induced moDC.

(**A**) Flow cytometry analysis of DC-SIGN expression on $CD14^{-}CD11c^{+}$ moDC following 5 day culture in medium alone (Nil), unstimulated (U) or IL-33, IL-25, TSLP-stimulated ILC2 supernatants or IL-4 (10 ng/ml) + GM-CSF (100 ng/ml) in the presence or absence of anti-IL-4Rα blocking antibody (10 µg/ml), anti-GM-CSF neutralising antibody (50 µg/ml) or isotypes (10 µg/ml; 50 µg/ml). Numbers indicate percentages of $DC\text{-}SIGN^{+}$ cells, gated on the $CD14^{-}CD11c^{+}$ cells. Plots representative of n=6. (**B**) Summary of DC-SIGN expression, as percentage of $CD14^{-}CD11c^{+}$ cells. (**C**) Levels of DC-SIGN expression (MFI) on $CD14^{-}CD11c^{+}$ cells. (n=6; data representative of ≥ 3 independent experiments). *P < 0.05; **P < 0.01; RM two-way ANOVA with Tukey`s post hoc multiple comparisons test (mean ± SD).

5.2.4.5 Contribution of ILC2-secreted IL-4 and GM-CSF to the expression of CD1b and CD1c on ILC2-induced moDC

A significant reduction in the percentage of CD1b- and CD1c-expressing $moDC_{ILC2(T)}$ was observed upon blocking of ILC2-derived GM-CSF, similar to the

effect on CD1a expression (Fig. 5.20, A, B and C). The effect of anti-GM-CSF was found to be particularly pronounced in the case of CD1b expression. In the absence of anti-GM-CSF antibody, an average of 60% of $moDC_{ILC2(U)}$ and 86% of $moDC_{ILC2(T)}$ were found to express cell surface CD1b. In contrast, only approximately 15% of $moDC_{ILC2(U)}$ and 22% of $moDC_{ILC2(T)}$ were $CD1b^+$ when GM-CSF activity was blocked during differentiation (Fig. 5.20, B).

Overall, these results highlight the importance of ILC2-derived GM-CSF in the upregulation of CD1a, CD1b and CD1c on ILC2-induced moDC.

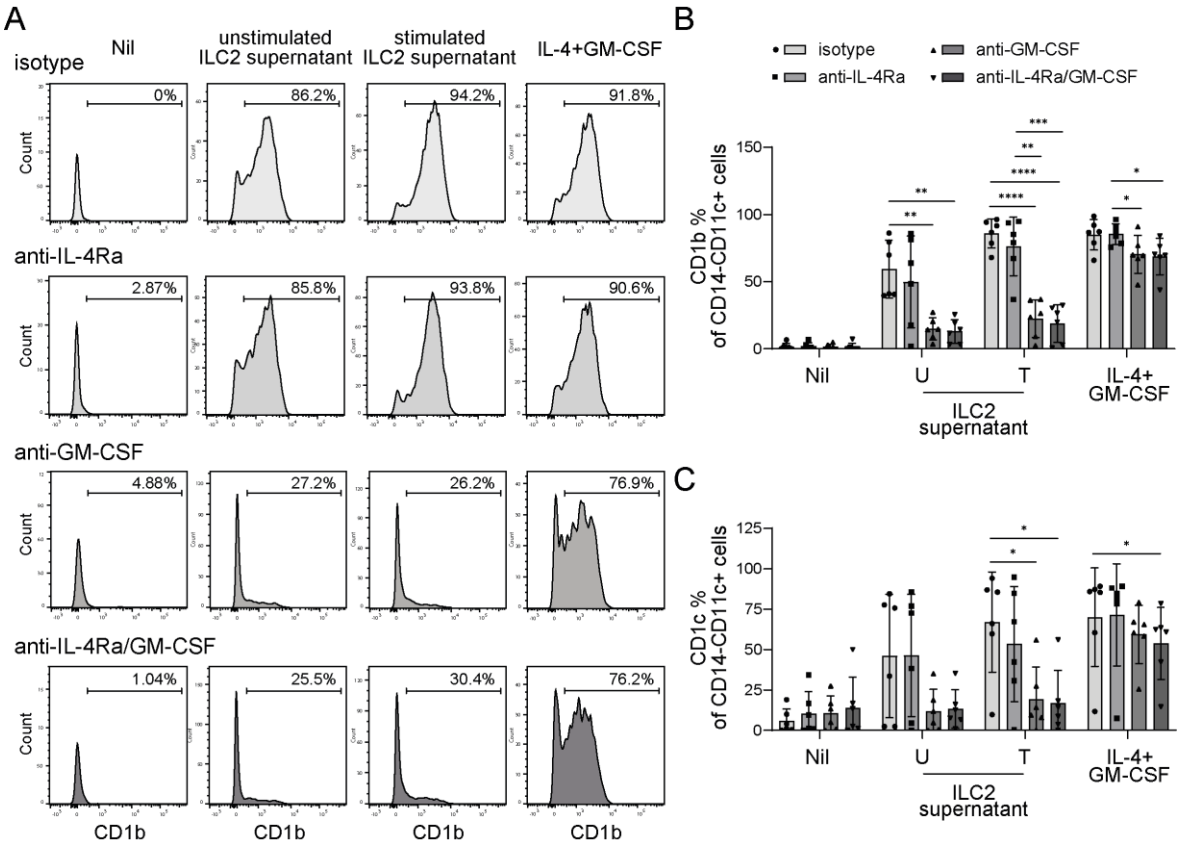


Figure 5.20 ILC2-derived GM-CSF contributes to the induction of CD1b and CD1c on ILC2-induced moDC.

(**A**) Flow cytometry analysis of CD1b expression on $CD14^-CD11c^+$ moDC following 5 day culture in medium alone (Nil), unstimulated (U) or IL-33, IL-25, TSLP-stimulated (T) ILC2 supernatants or IL-4 (10 ng/ml) + GM-CSF (100 ng/ml) in the presence or absence of anti-IL-4Rα blocking antibody (10 µg/ml), anti-GM-CSF neutralising antibody (50 µg/ml) or

isotypes (10 µg/ml; 50 µg/ml). Numbers indicate percentages of $CD1b^+$ cells, gated on $CD14^-$ $CD11c^+$ cells. Plots representative of n=6. (**B and C**) Summary of CD1b (**B**) and CD1c (**C**) expression, as percentage of $CD14^-CD11c^+$ cells. (n=6; data representative of ≥ 3 independent experiments). *P < 0.05; **P < 0.01; ***P < 0.001, ****P < 0.0001; RM two-way ANOVA with Tukey`s post hoc multiple comparisons test (mean ± SD).

5.2.4.6 Contribution of ILC2-secreted IL-4 and GM-CSF to the expression of MHC molecules and CD86 on ILC2-induced moDC

Blocking IL-4Rα signalling or GM-CSF activity during $moDC_{ILC2}$ differentiation did not significantly alter the proportion of $CD14^-CD11c^+$ cells expressing MHCI or MHCII (Fig. 5.21, A and B). The percentage of $CD86^+$ cells was significantly increased on $moDC_{ILC2}$ and control $moDC_{IL\text{-}4/GM\text{-}CSF}$ following differentiation in the presence of anti-GM-CSF antibody (Fig. 5.21, C). Blocking the activity of GM-CSF during $moDC_{ILC2(T)}$ differentiation resulted in increased surface levels of MHCI, MHCII and CD86, an effect that was also observed on $moDC_{IL\text{-}4/GM\text{-}CSF}$ (Fig. 5.21, D, E and F).

These results suggest that GM-CSF contributes to the lower expression of MHC molecules and CD86 observed on moDC that had been differentiated in activated ILC2 supernatants.

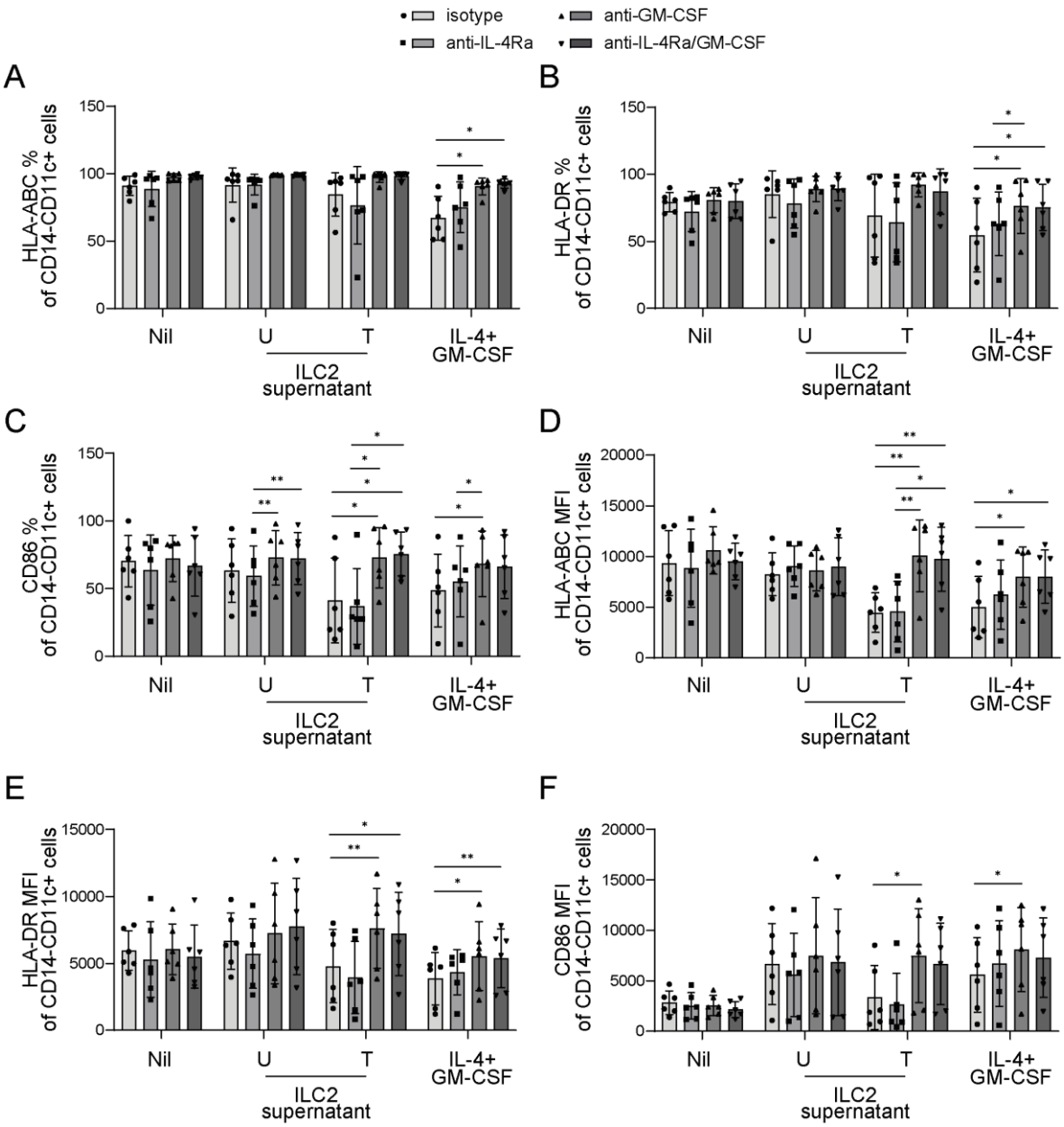


Figure 5.21 Contribution of ILC2-derived IL-4 and GM-CSF to the expression of MHC and CD86 on ILC2-induced moDC.

(**A-F**) Flow cytometry analysis of surface molecules on monocyte-derived cells following 5 day culture in medium alone (Nil), unstimulated (U) or IL-33, IL-25, TSLP-stimulated (T) ILC2 supernatants or IL-4 (10 ng/ml) + GM-CSF (100 ng/ml) in the presence or absence of anti-IL-4Rα blocking (10 µg/ml), anti-GM-CSF neutralising antibody (50 µg/ml) or isotypes (10 µg/ml; 50 µg/ml). (**A-C**) Surface expression of MHCI (**A**), MHCII (**B**) and CD86 (**C**), as percentage of $CD14^{-}CD11c^{+}$ cells. (**D-F**) Expression levels (MFI) of MHCI (**D**), MHCII (**E**) and CD86 (**F**) on $CD14^{-}CD11c^{+}$ cells. (n=6; data representative of ≥ 3 independent experiments). *P < 0.05; **P < 0.01; ***P < 0.001, ****P < 0.0001; RM two-way ANOVA with Tukey`s post hoc multiple comparisons test (mean ± SD).

5.2.5 Lipid antigen presenting capacity of CD1a$^+$ ILC2-induced moDC

To further investigate the finding that ILC2 are capable of inducing differentiation of monocytes into moDC, the functional capacity of $moDC_{ILC2}$ to act as APC was assessed. $moDC_{ILC2}$ were shown to express the lipid antigen presentation molecule CD1a. To determine whether $moDC_{ILC2}$ could generate CD1a-dependent T cell responses, $moDC_{ILC2}$ were co-cultured with CD1a-autoreactive IFN-γ-secreting T cell clones, kindly provided by Dr Yi-Ling Chen. The ability of $moDC_{ILC2}$ to activate CD1a-restricted T cell clones was determined by measuring IFN-γ levels in supernatants following co-culture for 24 hours with or without anti-CD1a blocking antibody. As a precaution, anti-MHCI/II antibodies were included to inhibit MHC-TCR interactions, although activation of T cell clones used here has been confirmed to be CD1a-specific. Monocytes cultured in medium alone did not survive at sufficient numbers (section 5.2.3.1) and were therefore not included in this experiment. Indeed, the finding that viable $monocytes_{Nil}$ on day 5 of culture did not express surface CD1a strongly implies that these monocytes would not be expected to activate T cells in a CD1a-dependent manner. CD1a-reactive T cell clones secreted significantly higher IFN-γ levels following co-culture with $moDC_{ILC(T)}$ compared to $moDC_{ILC(U)}$ or $moDC_{IL\text{-}4/GM\text{-}CSF}$. Blocking CD1a resulted in significantly reduced IFN-γ levels in the supernatant following co-culture of CD1a-restricted T cell clones with $moDC_{ILC2}$ and control $moDC_{IL\text{-}4/GM\text{-}CSF}$. (Fig. 5.22, A). IFN-γ levels were reduced by half by the addition of anti-CD1a to T cell clone co-cultures with $moDC_{ILC2}$ or $moDC_{IL\text{-}4/GM\text{-}CSF}$ (Fig. 5.22, B). IFN-γ measured in co-culture supernatants was confirmed to be derived from T cell clones as supernatants from $moDC_{ILC2}$ or $moDC_{IL\text{-}4/GM\text{-}CSF}$ alone contained low levels of IFN-γ (Fig. A.10). T cell activation was also assessed by flow cytometry analysis of CD69 expression, a

marker for lymphocyte activation. The level of CD69 on CD1a-restricted T cell clones was significantly reduced by the addition of anti-CD1a to co-cultures with $moDC_{ILC2(T)}$, to a similar extent as for co-cultures with $moDC_{IL\text{-}4/GM\text{-}CSF}$ (Fig. 5.22, C and D).

Collectively, these results demonstrate that ILC2-induced moDC are capable of activating CD1a-dependent T cell responses, confirming functionality.

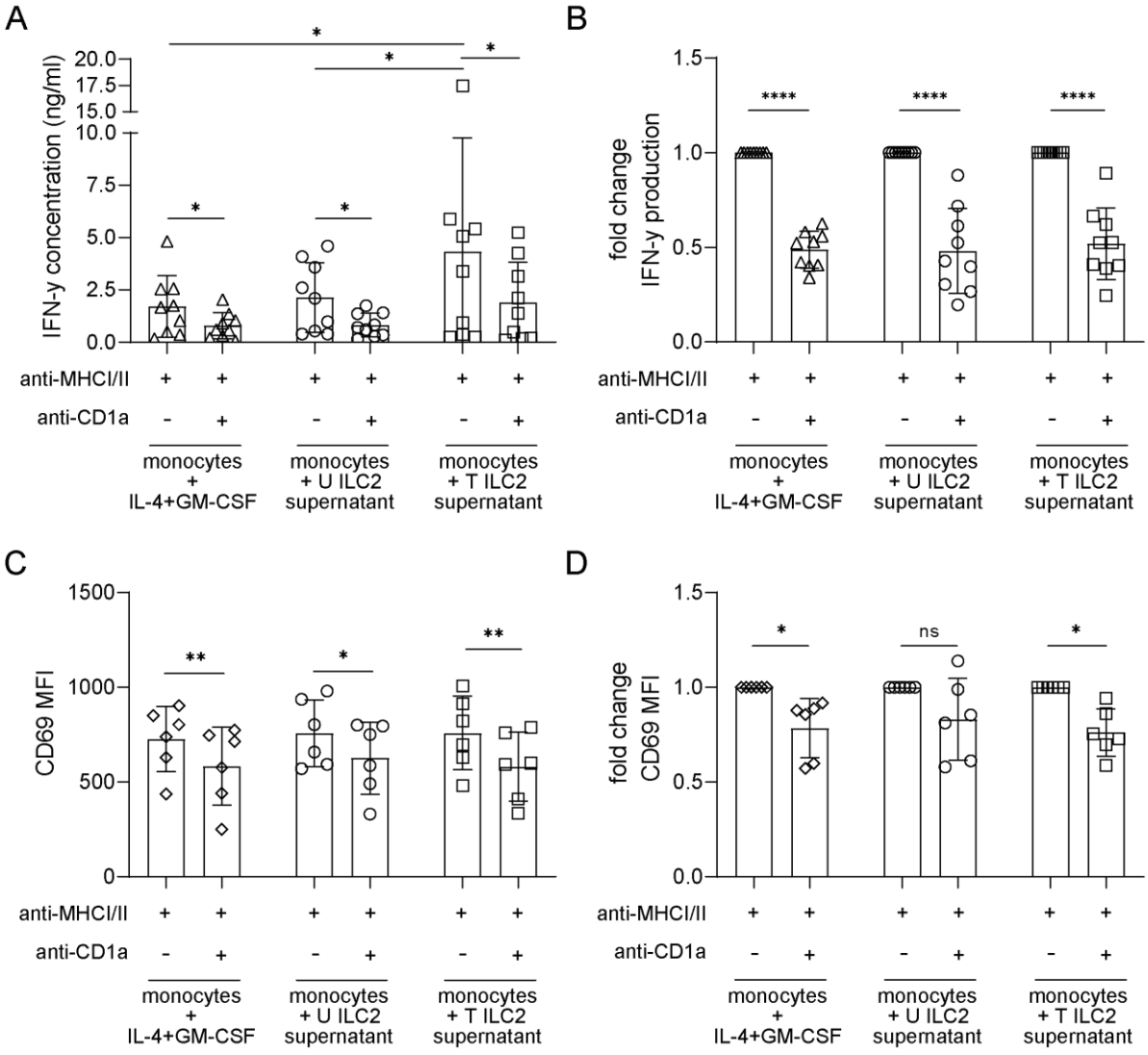


Figure 5.22 Activation of CD1a-restricted T cell clones by ILC2-induced moDC.

(**A-D**) Monocytes were differentiated into moDC by culture in IL-4 (10 ng/ml) + GM-CSF (100 ng/ml) or unstimulated (U) or IL-33, IL-25, TSLP-stimulated (T) ILC2 supernatants. Differentiated moDC were co-cultured with CD1a-restricted IFN-γ T cell clones at a 1.5:1

ratio for 24h in the presence or absence of anti-CD1a blocking antibody (10 µg/ml). Anti-MHCI/II antibodies (10 µg/ml) were present in all conditions. (**A**) IFN-γ concentrations in co-culture supernatants were measured by ELISA. (**B**) Fold change in IFN-γ levels in co-culture supernatants, calculated relative to the anti-MHCI/II antibody baseline response in the absence of anti-CD1a antibody (n=9; data representative of 5 independent experiments). (**C**) Flow cytometry analysis of CD69 expression levels (MFI) on T cell clones following 24h co-culture with moDC. (**D**) Fold change of CD69 levels (MFI) on T cell clones, calculated relative to the anti-MHCI/II antibody baseline response in the absence of anti-CD1a antibody (n=6; data representative of ≥ 3 independent experiments). *P < 0.05; **P < 0.01; ***P < 0.001, ****P < 0.0001; RM two-way ANOVA with Tukey's post hoc multiple comparisons test (mean ± SD).

5.3 Discussion

As predominately tissue-resident type 2 cytokine producers, ILC2 play an important role as inducers of type 2 immune responses. ILC2 have been found to interact with and influence the function of both innate and adaptive immune cells via secretion of soluble factors and cell-to-cell interactions. However, little is known about the interaction of human ILC2 and myeloid cells, specialised sensors of tissue perturbances (365), and its functional implications.

5.3.1 ILC2 support the survival and differentiation of moDC

The data presented herein add to our understanding of the dialogue between ILC2 and moDC and demonstrate that ILC2 can support the survival of both early differentiating and fully differentiated moDC.

While the phenotype of fully differentiated moDC was found to be relatively stable, early differentiating moDC displayed reduced viability and underwent significant phenotypical changes in the absence of IL-4 and GM-CSF during the final stages of differentiation. In contrast to previous reports (338), I did not observe a significant re-expression of CD14 upon removal of IL-4 and GM-CSF on day three of monocyte differentiation, which might be indicative of early commitment to moDC differentiation (337, 339). While the percentage of CD1a-expressing cells remained high upon cytokine removal, there was a significant drop in the CD1a surface protein level per cell, which implies a reduction in the CD1a antigen presentation capacity. We observed a significant drop in the percentage of cells expressing the moDC marker DC-SIGN upon cytokine removal indicating incomplete moDC differentiation or moDC conversion into monocyte-derived macrophages (338, 339). Strikingly, supernatants from IL-33, IL-25, TSLP-activated ILC2 completely rescued

differentiating moDC from the effect of IL-4 and GM-CSF removal. Early differentiating moDC cultured in activated ILC2 supernatants were characterised by high survival rates, lack of CD14 expression and continuous high expression of CD1a and DC-SIGN, resembling positive control moDC. Supernatants from unstimulated ILC2 had a similar effect, however, slightly less pronounced than activated ILC2 supernatants. Moderate expression of MHC molecules and CD86, and low expression of CD80 on moDC cultured in ILC2 supernatants may be representative of an immature state (362).

Overall, these results show that soluble factors secreted by activated ILC2, and to a lesser degree by unstimulated ILC2, support the survival and differentiation as well as stabilise the phenotype of early immature moDC. To what extent *in vitro* moDC, generated in the presence of IL-4 and GM-CSF, resemble *in vivo* DC has been much debated. The use of *in vitro* moDC as a model for *in vivo* human DC function is supported by findings of transcriptional and phenotypic resemblance with *in vivo* inflammatory DC (363, 366).

5.3.2 ILC2 induce the differentiation of monocytes into functional moDC

Remarkably, ILC2 were found to induce the differentiation of *ex vivo* monocytes into functional moDC in the absence of exogenous IL-4 and GM-CSF. During culture in ILC2 supernatants, monocytes lost the expression of the monocyte-specific marker CD14 and upregulated the expression of DC-associated differentiation markers including DC-SIGN and CD1a. Interestingly, supernatants from both unstimulated and IL-33, IL-25, TSLP-activated ILC2 were found to induce moDC differentiation, albeit slightly more efficiently by the latter. However, this might be explained by *in vitro* ILC2 culture conditions being highly stimulatory. In contrast to ILC2-induced

moDC, monocytes cultured in medium alone for five days displayed low viability, retained high CD14 expression, and lacked the expression of moDC markers. Monocytes that survived culture in the absence of differentiation-inducing cytokines retained high expression of MHCI/II and CD86, involved in antigen presentation. In contrast, monocyte differentiation in ILC2 supernatants or recombinant IL-4 and GM-CSF resulted in immature moDC characterised by high antigen uptake and low peptide antigen presentation capacity, reflected in the lower expression of MHC molecules (362). ILC2-induced moDC were characterised by high expression of the lipid antigen-presenting molecule CD1a. Co-culture experiments of ILC2-induced moDC with CD1a-restricted IFN-γ-secreting T cell clones demonstrated that ILC2-induced moDC were capable of functionally engaging CD1a-restricted T cells and inducing IFN-γ production in a CD1a-dependent manner. The efficiency of CD1a-mediated T cell activation by ILC2-induced moDC was similar to activation by control moDC, confirming the functionality of ILC2-induced moDC. Although the study detected T cell activation through measurement of IFN-γ, as this is a robust and established assay system, it will be of interest to examine other cytokine production by responding T cells. Nevertheless, IFN-γ is widely relevant to chronic skin inflammation (367). The finding that alarmin-mediated activation of human ILC2 resulted in upregulated secretion of both IL-4 and GM-CSF is consistent with previous reports (134, 136). GM-CSF levels of up to 10 ng/ml were measured in supernatants from activated ILC2. The fact that control moDC were differentiated in the presence of recombinant GM-CSF at approximately 10-fold higher concentrations than GM-CSF levels measured in stimulated ILC2 supernatants, makes the comparable degree of moDC induction by ILC2 supernatants all the more remarkable. Blocking ILC2-derived GM-CSF with a neutralising antibody resulted in

a reduction in the viability of the monocyte-derived cell population, in the percentage of $CD14^-$ $CD11c^+$ cells as well as in the expression levels of the DC marker DC-SIGN. Blocking IL-4Rα signalling had no significant effects on the survival or differentiation of monocytes cultured in ILC2 supernatants. It is possible that other soluble factors in ILC2 supernatants contribute to the induction of moDC differentiation. Indeed, culture in the presence of anti-IL-4Rα and anti-GM-CSF antibodies did not completely abrogate moDC survival, $CD14^-CD11c^+$ cell percentage and DC-SIGN expression of ILC2-induced moDC. Alternatively, higher antibody concentrations might be required to completely abolish the effect of ILC2-derived IL-4 and GM-CSF on *ex vivo* monocytes. This is supported by the finding that differentiation of control moDC in exogenous IL-4 and GM-CSF is only partially inhibited by the addition of anti-IL-4Rα and anti-GM-CSF antibodies. Upregulation of surface CD1 molecules is a hallmark of moDC differentiation (335). ILC2-derived GM-CSF was found to be an essential factor for the upregulation of CD1 molecules, including CD1a, CD1b and CD1c, on ILC2-induced moDC. Neutralising GM-CSF abrogated the ILC2 supernatant-mediated induction of CD1a, CD1b and CD1c expression on monocytes. These data identified ILC2-derived GM-CSF as the predominant driving factor for the expression of CD1 molecules on ILC2-induced moDC, enabling CD1-mediated lipid antigen presentation to CD1-reactive T cells. While I assessed the effects of ILC2-derived soluble factors on monocytes, cell contact-dependent mechanisms were not investigated. Co-culture experiments of autologous ILC2 and monocytes would enable the study of direct cell-cell interactions as well as the reciprocal effect of monocytes/moDC on ILC2 activity. Moreover, due to the nature of *in vitro* experiments, ILC2-induced moDC differentiation and CD1a-mediated T cell activation were studied in isolation,

independent of the influence of other immune cells and the tissue microenvironment. Hence, it would be of interest to validate our results in an *in vivo* mouse model and study the role of ILC2-induced moDC differentiation during homeostasis and inflammation.

Collectively, these data demonstrate that soluble factors, in particular GM-CSF, secreted by human ILC2 support the survival and induce the differentiation of $CD14^+$ monocytes into moDC capable of activating T cell responses via CD1a.

5.3.3 Functional implications of ILC2-induced moDC differentiation

It is increasingly being recognised that ILC2 act as initiators and modulators of adaptive T cell responses. In addition to instructing DC to induce efficient Th2 cell responses in an IL-13-dependent manner (211, 212), ILC2 have been demonstrated to promote T cell responses directly by presenting both peptide and lipid antigens to T cells via MHCII (183) and CD1a (10), respectively. The identification of ILC2 as inducers of monocyte differentiation into functional moDC suggests a further mechanism by which ILC2 may bridge innate and adaptive immune responses. Based on the findings presented herein, I propose a model in which ILC2-mediated moDC differentiation at barrier sites contributes to lipid surveillance during steady state and inflammation following barrier breach (Fig. 5.23). ILC2 have previously been found to express CD1a and present lipid antigens to CD1a-responsive T cells (10). The findings of the current study, which show activation of CD1a-autoreactive T cells by $CD1a^+$ ILC2-induced moDC, add a further mechanism by which ILC2 may regulate lipid-mediated responses in the skin. The high expression of CD1b and CD1c in addition to CD1a on ILC2-induced moDC suggests that lipid antigen presentation to CD1-restricted T cells might also be relevant to tissues beyond the

skin. High DC-SIGN expression on ILC2-induced moDC may be essential for the formation of initial contacts with T cells (360). The expression of CD1 molecules suggests ILC2-induced moDC presentation of endogenous and exogenous lipid antigens to CD1-reactive T cells (344). Langerhans cells are epidermal-resident professional APC with important functions in skin immunity (368). Given that monocytes have been reported to be capable of acquiring Langerhans cell-like phenotypes (369, 370), it would be of interest to investigate whether ILC2 can induce monocyte differentiation into $CD1a^+$ $langerin^+$ Langerhans cell-like cells.

During homeostasis, circulating monocytes infiltrating barrier sites could be induced to differentiate into moDC by tissue-resident ILC2. ILC2-induced moDC may subsequently contribute to lipid surveillance by presenting endogenous lipid antigens to tissue-resident CD1-reactive T cells. In the skin under homeostatic conditions, presentation of non-permissive/inhibitory CD1a ligands (352) by ILC2-induced moDC may prevent CD1a-dependent T cell activation (Fig. 5.23, A). Whether immature ILC2-induced moDC can act as IL-10- and TGF-β-producing tolerance inducers (371) remains to be addressed.

During acute inflammatory responses, $CD14^+$ monocytes rapidly infiltrate and accumulate at the site of inflammation (372, 373). We suggest that IL-4 and GM-CSF production by ILC2, activated by alarmins released upon barrier disruption, contribute to the induction of monocyte differentiation into $CD1a^+$ inflammatory moDC. ILC2-induced moDC may in turn present lipid antigens to CD1a-reactive T cells, which have been detected at increased frequencies during chronic inflammation and found to rapidly infiltrate the skin in response to allergen challenge (214). Barrier compromise has been suggested to allow entry of natural CD1a autoantigens, such as skin oils squalene and wax esters, normally restricted to the

skin surface, into deeper intraepithelial layers resulting in an altered lipid profile (350). ILC2-induced moDC presentation of permissive/stimulatory lipids, including natural CD1a autoantigens and CD1a neolipid antigens generated by allergen-derived lipid modifying enzymes (214), to CD1a-reactive T cells may result in the activation and secretion of pro-inflammatory cytokines such as IFN-γ, IL-22, IL-17A/F, GM-CSF, TNF-α and IL-13 (214, 374). Activated ILC2-induced moDC may further amplify local ILC2 responses through production of IL-33 (375), forming a positive feedback loop. Furthermore, the pro-inflammatory microenvironment might promote the maturation of ILC2-induced moDC. Mature ILC2-induced moDC might activate tissue-resident memory T cells or prime naïve T cells, following CCR7-mediated homing to draining lymph nodes, through MHCI/II-mediated peptide antigen presentation (339, 376) (Fig. 5.23, B).

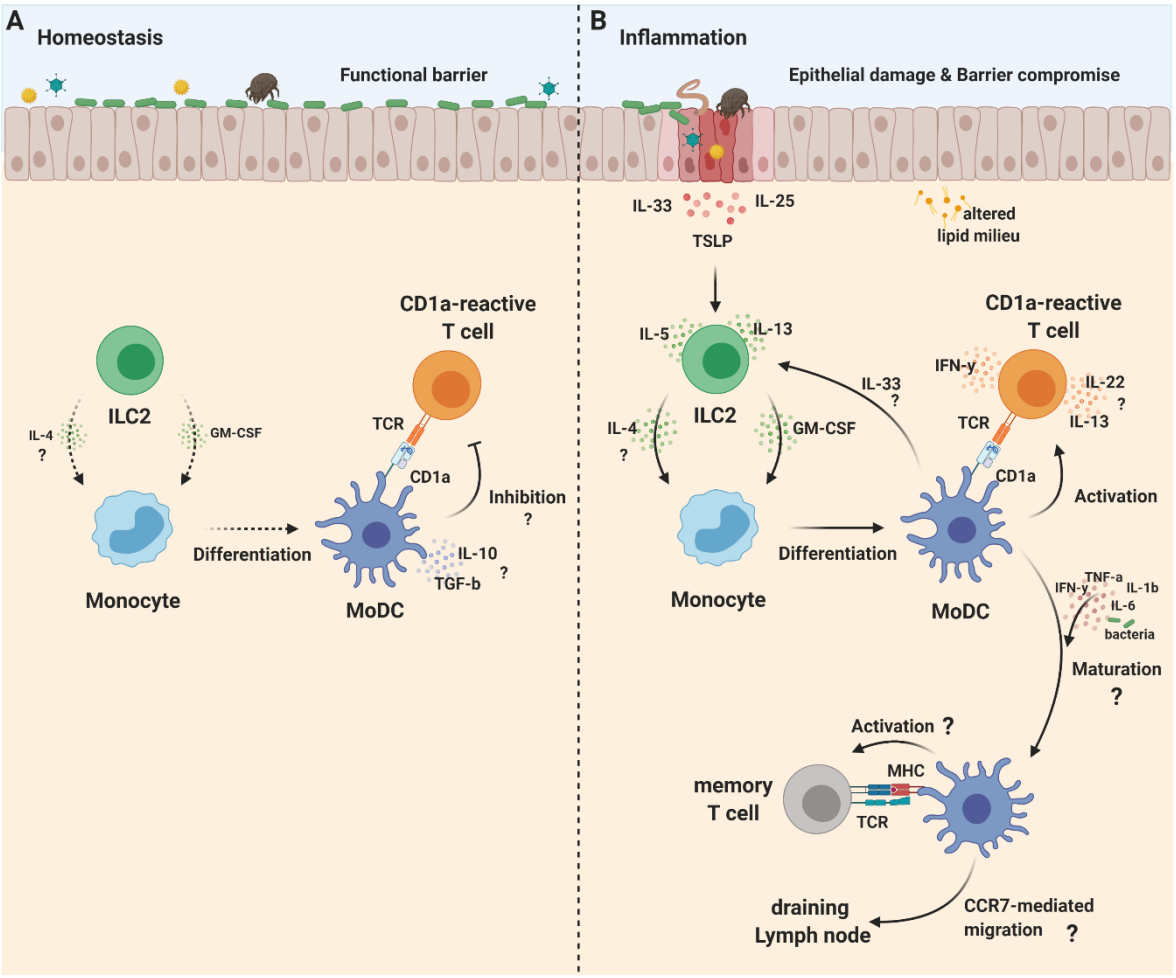


Figure 5.23 Proposed mechanism of ILC2-mediated moDC differentiation at barrier sites and its contribution to homeostasis and inflammation.

(**A**) At steady state, tissue-resident ILC2 may secrete low levels of IL-4 and GM-CSF that induce moDC differentiation. Presentation of non-permissive/inhibitory CD1a ligands by ILC2-induced moDC to CD1a-reactive T cells may prevent T cell activation. ILC2-induced moDC might contribute to tissue homeostasis by producing suppressive cytokines such as IL-10 and TGF-β. (**B**) Barrier breach leads to entry of pathogens and allergens, changes in the lipid milieu and the release of alarmin cytokines. Through secretion of GM-CSF, alarmin-activated ILC2 may induce monocyte differentiation to immature moDC that subsequently present permissive/stimulatory lipid antigens to CD1a-reactive T cells leading to the secretion of proinflammatory cytokines. Pro-inflammatory cytokines and bacterial components may induce maturation of ILC2-induced moDC. Mature inflammatory ILC2-induced moDC might present peptide antigens to tissue-resident memory T cells and migrate to draining lymph nodes for naïve T cell priming.

Chapter 6: Final Discussion and Future Directions

6.1 Main findings and functional implications

ILC are enriched at barrier sites, such as the skin, lung and intestine, and so are well positioned to act in the maintenance of tissue homeostasis and in response to barrier compromise (87, 88, 93). In contrast to T cells, ILC lack rearranged antigen-specific receptors and are epigenetically poised to react to environmental cues (332). In the skin, ILC2 are the predominant ILC population and are increased in abundance within lesions of individuals with AD (93, 141). Through rapid production of type 2 cytokines following activation by primarily damage-associated cytokines, ILC2 play an important role in type 2 immune responses in the context of helminth infection (87, 98–100) and allergic inflammation (93, 205). The data presented herein identify previously unrecognised ILC2 effector functions with implications for their role in type 2 inflammation, such as in AD (Fig. 6.1).

Here, I demonstrate for the first time roles for human ILC2 as inducers of moDC differentiation and in the chemotactic recruitment of ILC2 and T cells. In an *in vivo* human skin allergen challenge model, cutaneous ILC2 were found to express genes encoding a broad range of cytokines and chemokines. Genes encoding the chemokines *CCL22* and *CCL17* were highly and specifically expressed in ILC2 compared to T cells. *In vitro* experiments confirmed secretion of CCL22 and CCL17 by human ILC2 following activation by alarmin cytokines IL-33, IL-25 and TSLP (Fig. 6.1, 1). CCL22 and CCL17 are critically involved in the recruitment of pathogenic $CCR4^+$ T cells into AD skin (316–318). Consistent with this, significantly increased levels of CCL22 were detected in skin suction blister fluids from individuals with AD compared to healthy volunteers following intradermal HDM challenge. Moreover,

consistent with published reports (250, 267, 268, 273), elevated serum CCL22 and CCL17 levels were identified as markers of AD, positively correlating with disease severity. ILC2-derived CCL22 and CCL17 contributed significantly to the recruitment of both ILC2 and T cells *in vitro*. The proportion of ILC2 producing substantial levels of CCL22 and CCL17 was indicated to be increased in individuals with AD. Together with the finding of increased surface CCR4 expression on circulating ILC2 and T cells (317) in individuals with AD, this implies a role for ILC2 in promoting increased homing of $CCR4^+$ ILC2 and T cells, predominately Th2 cells (295, 296), into AD lesional skin. CCL22 and CCL17 expression is not unique to ILC2. In inflamed skin, CCL22- and CCL17-producers include tissue and immune cells such as keratinocytes (301, 302), vascular endothelial cells (297) and Langerhans cells (377) and production might be upregulated by ILC2-derived IL-4 and IL-13 (302, 377) (Fig. 6.1, 2a). Indeed, soluble factors secreted by activated human ILC2 promoted the production of high levels of CCL22 and potentially CCL17 by moDC, akin to previous reports in the context of allergic airway inflammation (212). MoDC-derived CCL22 and CCL17 in turn were found to induce ILC2 chemotaxis. Thus, ILC2 may amplify cutaneous type 2 inflammatory responses through direct and indirect CCR4-mediated recruitment of type 2 cytokine-producing ILC2 and effector and memory Th2 cells (Fig. 6.1, 2b). In addition to CCR4 ligands, alarmins induced the secretion of a range of other chemokines by ILC2, of which some, including the skin-homing factor CCL27, may contribute to increased ILC2 and T cell chemotaxis into inflamed skin. Furthermore, through production of chemotactic factors including IL-5, eotaxins, CXCL8, CCL1 and CCL2, ILC2 may be involved in the accumulation of eosinophils (260), basophils (252), neutrophils (240) and myeloid cells (378, 379) in AD lesions (Fig. 6.1, 2c). Strikingly, ILC2 were identified as inducers of monocyte

differentiation into CD1a$^+$ CD11c$^+$ DC-SIGN$^+$ moDC through production of high GM-CSF levels (Fig. 6.1, 3a). Increased frequencies of “inflammatory” DC, characterised by co-expression of CD1a, CD11c and DC-SIGN, have been detected in AD skin (343). Thus, ILC2 may be involved in the differentiation of skin-infiltrating monocytes into inflammatory CD1a$^+$ moDC within the cutaneous microenvironment. ILC2-induced moDC were demonstrated to activate CD1a-autoreactive IFN-γ-secreting T cell clones (Fig. 6.1, 3b). CD1a-reactive T cells are resident in healthy skin (349, 352), with increased frequencies detected in the skin of individuals with AD (214), and secrete pro-inflammatory cytokines including IFN-γ, IL-13, IL-22, IL-17A/F, TNF-α and GM-CSF in response to lipid antigens (214, 349, 374). The altered lipid profile in lesional AD skin (350) combined with the generation of CD1a neolipid antigens by allergens such as HDM (214) is believed to result in increased cutaneous CD1a-reactive T cell activation in the context of AD. In addition to direct CD1a-mediated lipid antigen presentation by ILC2 (10) (Fig. 6.1, 3c), the findings of this study, showing activation of CD1a-autoreactive T cells by ILC2-induced moDC, further implicate ILC2 in the amplification of lipid-mediated responses in the skin. IFN-γ production by CD1a-reactive T cells has implications for AD pathogenesis. IFN-γ is particularly relevant during the chronic phase of AD, which is associated with increased infiltration of Th1 cells (262, 380). Consistent with increased IFN-γ expression in lesional AD skin (381), I detected elevated serum IFN-γ levels in individuals with AD. In the context of chronic AD, IFN-γ has been proposed to contribute to cutaneous inflammation and formation of eczematous lesions by acting on keratinocytes, stimulating the secretion of proinflammatory cytokines (382) and chemokines (383), upregulating MHCII surface expression (367) and inducing apoptosis (383, 384) (Fig. 6.1, 3d). Whether such ILC2-induced moDC would be

able to migrate from the skin to draining lymph nodes to activate naïve T cells is currently unknown (Fig. 6.1, 4). In a mouse model of allergic airway inflammation, ILC2-derived IL-13 was found to be critical for lung DC lymph node homing, Th2 cell priming and the induction of a robust airway Th2 response (211). Within the cutaneous microenvironment, ILC2 engage in soluble factor- and cell-contact-dependent crosstalks with both innate and adaptive immune cells that collectively mediate AD immunopathology (385). The findings of this study add to our understanding of ILC2 effector functions, demonstrating further mechanisms by which ILC2 can influence and link innate and adaptive immune responses.

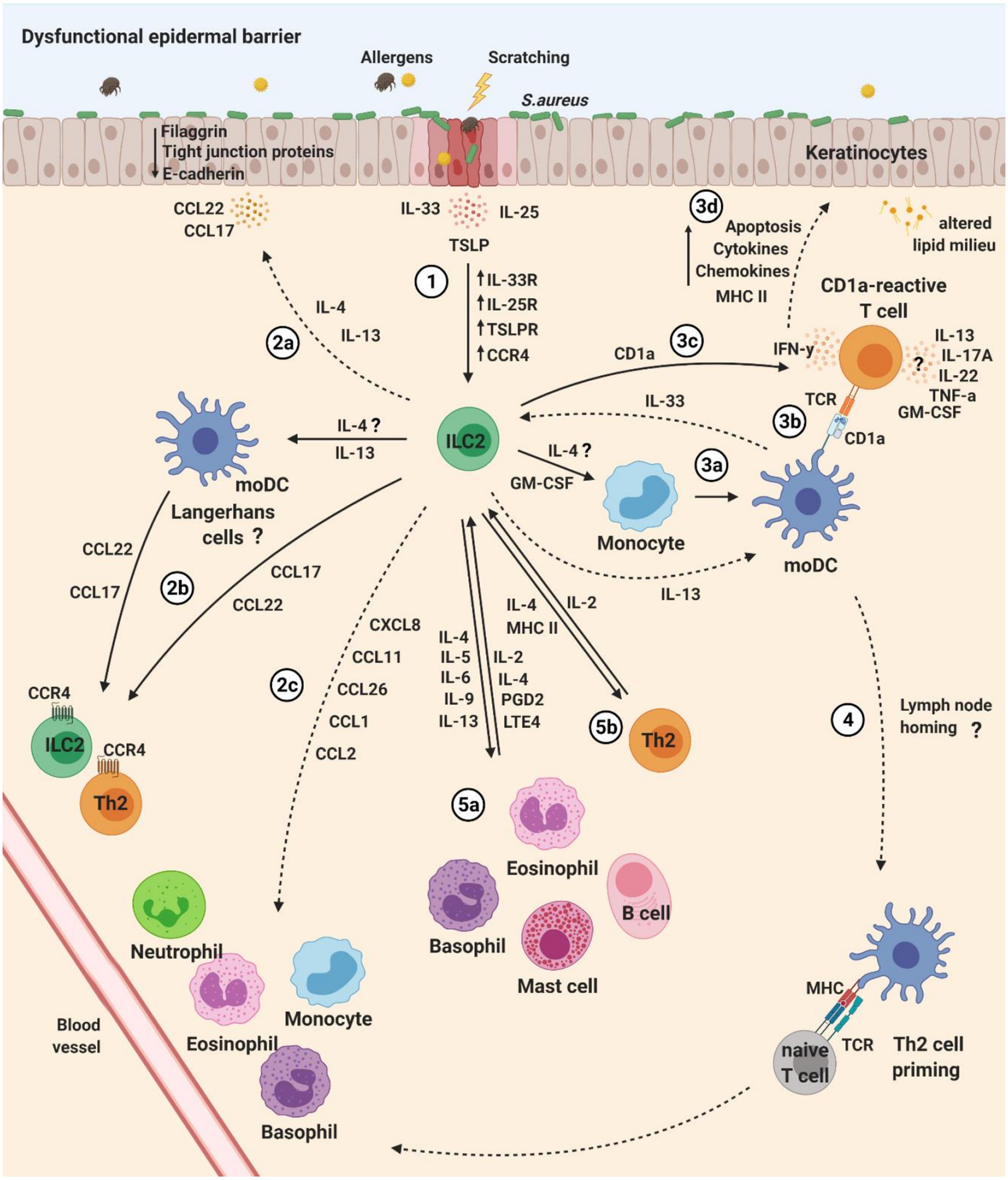


Figure 6.1 Proposed model of ILC2 involvement in AD skin inflammation.

(**1**) Epidermal barrier disruption leads to release of alarmins. Alarmins activate cutaneous ILC2 and upregulate expression of stimulatory receptors and CCR4 on ILC2. (**2a**) ILC2-derived IL-4 and/or IL-13 exacerbate epidermal barrier dysfunction and induce release of CCL22 and CCL17 by keratinocytes. (**2b**) ILC2 secrete CCL22 and CCL17 and induce CCL22 and CCL17 production by dermal DC/Langerhans cells leading to skin homing of $CCR4^{+}$ ILC2 and Th2 cells. (**2c**) ILC2 induce recruitment of inflammatory innate cells. (**3a**) ILC2-derived GM-CSF induces monocyte differentiation into inflammatory $CD1a^{+}$ moDC.

MoDC-derived IL-33 may in turn promote ILC2 activation. (**3b**) ILC2-induced moDC present permissive/stimulatory lipid antigens to cutaneous CD1a-reactive T cells that produce IFN-γ and other pro-inflammatory cytokines following activation. (**3c**) $CD1a^+$ ILC2 directly present lipid antigens to CD1a-reactive T cells. (**3d**) CD1a-reactive T cell-derived IFN-γ modulates keratinocyte survival and activity. (**4**) ILC2-derived moDC and/or dermal DC/Langerhans cells migrate to draining lymph nodes where they present peptide antigens to naïve T cells, inducing Th2 differentiation. Th2 cells are recruited to inflamed skin mediated by CCR4 and CCR10. (**5a**) Within inflamed skin, ILC2-derived type 2 cytokines promote activity of eosinophils, basophils, mast cells and B cells. In turn, basophils and mast cells promote ILC2 activity by release of IL-2, IL-4, PGD2 and LTE4. (**5b**) ILC2 can present peptide antigens to T cells, inducing Th2 differentiation. Collectively, these pathways amplify type 2 inflammation, leading to AD exacerbation and development of AD lesions.

6.2 Final conclusion and future directions

Prior to this study, relatively little was known about the protein profile of AD skin. Our *in vivo* human skin blister model enabled the characterisation of the skin proteome and the detection of skin-specific cytokine and chemokine levels. The cutaneous protein profile of individuals with AD showed significant overall differences compared to healthy skin, especially in the expression of pro-inflammatory cytokines and chemokines. However, limited donor numbers complicated the comparison of changes in protein expression in response to intradermal challenge with common environmental allergens or between lesional and non-lesional AD skin. Extending this study to a larger number of participants will enable the characterisation of allergen-induced cutaneous immune responses. Increased ILC2 frequency and activity in AD skin (93, 141) and the secretion of a broad range of cytokines and chemokines relevant to AD by human ILC2 *in vitro*, as demonstrated in this study, implicate ILC2 in AD pathogenesis. Analysis of *ex* vivo ILC2 from individuals with AD and healthy controls will allow investigation of inherent

differences. To study the role ILC2 occupy in the cutaneous immune network in the context of health and inflammation, and to profile the cellular and protein composition of healthy and AD skin *ex vivo*, imaging mass cytometry will be performed on skin tissue from individuals with AD and healthy controls. *In vivo* mouse experiments may help to decipher the involvement of ILC2 in leukocyte recruitment and lipid-mediated responses during steady state and inflammation and in the context of specific tissue microenvironments. Such *in vivo* work would have challenges due to the lack of a single unique identifying marker for ILC2 and mice not expressing CD1a, however, our collaborators have generated and characterised ILC2 depletion mouse models (183) and our lab has recently generated a CD1a transgenic mouse model. While the capacity of ILC2 to recruit T cells was demonstrated *in vitro*, questions remain regarding the recruitment of specific T cell subsets as well as the recruitment of innate immune cells including granulocytes and myeloid cells. This study demonstrated the production of IFN-γ by CD1a-reactive T cells induced by ILC2-induced moDC. Further experiments will be performed to assess the production of other cytokines, including IL-22 and IL-13, by CD1a-reactive T cell clones in response to co-culture with ILC2-induced moDC.

To conclude, the findings of this thesis add significantly to our understanding of human ILC2 biology. The identification of ILC2 as inducers of $CD1a^+$ moDC differentiation and as chemokine producers that mediate recruitment of both ILC2 and T cells, supports the notion that ILC2 effector functions go far beyond the production of type 2 cytokines. Given the important role of ILC2 in type 2 inflammation, reinforced by the data presented herein, ILC2 represent promising therapeutic targets.

Approximate Word Count**:** 50 000

References

1. Bonilla, F. A., and H. C. Oettgen. 2010. Adaptive immunity. *J. Allergy Clin. Immunol.* 125: S33–S40.

2. Iwasaki, A., and R. Medzhitov. 2015. Control of adaptive immunity by the innate immune system. *Nat. Immunol.* 16: 343–353.

3. Medzhitov, R., and C. A. Janeway. 1998. Innate immune recognition and control of adaptive immune responses. *Semin. Immunol.* 10: 351–353.

4. Pasparakis, M., I. Haase, and F. O. Nestle. 2014. Mechanisms regulating skin immunity and inflammation. *Nat. Rev. Immunol.* 14: 289–301.

5. Menon, G. K. 2002. New insights into skin structure: Scratching the surface. In *Adv. Drug Deliv. Rev.* vol. 54. Elsevier. S3–S17.

6. Egawa, G., and K. Kabashima. 2016. Multifactorial skin barrier deficiency and atopic dermatitis: Essential topics to prevent the atopic march. *J. Allergy Clin. Immunol.* 138: 350-358.e1.

7. Baroni, A., E. Buommino, V. De Gregorio, E. Ruocco, V. Ruocco, and R. Wolf. 2012. Structure and function of the epidermis related to barrier properties. *Clin. Dermatol.* 30: 257–262.

8. Deckers, J., H. Hammad, and E. Hoste. 2018. Langerhans cells: Sensing the environment in health and disease. *Front. Immunol.* 9: 93.

9. Foster, C. A., H. Yokozeki, K. Rappersberger, F. Koning, B. Volc-Platzer, A. Rieger, J. E. Coligan, K. Wolff, and G. Stingl. 1990. Human epidermal T cells predominately belong to the lineage expressing α/β T cell receptor. *J. Exp. Med.* 171: 997–1013.

10. Hardman, C. S., Y. L. Chen, M. Salimi, R. Jarrett, D. Johnson, V. J. Järvinen, R. J. Owens, E. Repapi, D. J. Cousins, J. L. Barlow, A. N. J. McKenzie, and G. Ogg. 2017. CD1a presentation of endogenous antigens by group 2 innate lymphoid cells. *Sci. Immunol.* 2: eaan5918.

11. Roediger, B., R. Kyle, K. H. Yip, N. Sumaria, T. V Guy, B. S. Kim, A. J. Mitchell, S. S. Tay, R. Jain, E. Forbes-Blom, X. Chen, P. L. Tong, H. A. Bolton, D. Artis, W. E. Paul, B. F. De St Groth, M. A. Grimbaldeston, G. Le Gros, and W. Weninger. 2013. Cutaneous immunosurveillance and regulation of inflammation by group 2 innate lymphoid cells. *Nat. Immunol.* 14: 564–573.

12. Kabashima, K., T. Honda, F. Ginhoux, and G. Egawa. 2019. The immunological anatomy of the skin. *Nat. Rev. Immunol.* 19: 19–30.

13. Orkin, S. H. 2000. Diversification of haematopoietic stem cells to specific lineages. *Nat. Rev. Genet.* 1: 57–64.

14. Doulatov, S., F. Notta, E. Laurenti, and J. E. Dick. 2012. Hematopoiesis: A human perspective. *Cell Stem Cell* 10: 120–136.

15. Orkin, S. H., and L. I. Zon. 2008. Hematopoiesis: An evolving paradigm for stem cell biology. *Cell* 132: 631–644.

16. Hoebe, K., E. Janssen, and B. Beutler. 2004. The interface between innate and adaptive immunity. *Nat. Immunol.* 5: 971–974.

17. Bianchi, M. E. 2007. DAMPs, PAMPs and alarmins: all we need to know about danger. *J. Leukoc. Biol.* 81: 1–5.

18. Medzhitov, R., and C. A. Janeway. 2002. Decoding the patterns of self and nonself by the innate immune system. *Science* 296: 298–300.

19. Eisenbarth, S. C. 2019. Dendritic cell subsets in T cell programming: location dictates function. *Nat. Rev. Immunol.* 19: 89–103.

20. Swiecki, M., and M. Colonna. 2015. The multifaceted biology of plasmacytoid dendritic cells. *Nat. Rev. Immunol.* 15: 471–485.

21. Collin, M., and V. Bigley. 2018. Human dendritic cell subsets: an update. *Immunology* 154: 3–20.

22. Slifka, M. K., R. Antia, J. K. Whitmire, and R. Ahmed. 1998. Humoral immunity due to long-lived plasma cells. *Immunity* 8: 363–372.

23. Farber, D. L., M. G. Netea, A. Radbruch, K. Rajewsky, and R. M. Zinkernagel. 2016. Immunological memory: Lessons from the past and a look to the future. *Nat. Rev. Immunol.* 16: 124–128.

24. Germain, R. N. 2002. T-cell development and the CD4-CD8 lineage decision. *Nat. Rev. Immunol.* 2: 309–322.

25. Mosmann, T. R., H. Cherwinski, M. W. Bond, M. A. Giedlin, and R. L. Coffman. 1986. Two types of murine helper T cell clone. I. Definition according to profiles of lymphokine activities and secreted proteins. *J. Immunol.* 136: 2348–57.

26. Mills, K. H. G., A. Barnard, J. Watkins, and K. Redhead. 1993. Cell-mediated immunity

to Bordetella pertussis: Role of Th1 cells in bacterial clearance in a murine respiratory infection model. *Infect. Immun.* 61: 399–410.

27. Street, N. E., J. H. Schumacher, T. A. T. Fong, H. Bass, D. F. Fiorentino, J. A. Leverah, and T. R. Mosmann. 1990. Heterogeneity of mouse helper T cells. Evidence from bulk cultures and limiting dilution cloning for precursors of Th1 and Th2 cells. *J. Immunol.* 144: 1629–1639.

28. Park, H., Z. Li, X. O. Yang, S. H. Chang, R. Nurieva, Y. H. Wang, Y. Wang, L. Hood, Z. Zhu, Q. Tian, and C. Dong. 2005. A distinct lineage of CD4 T cells regulates tissue inflammation by producing interleukin 17. *Nat. Immunol.* 6: 1133–1141.

29. Harrington, L. E., R. D. Hatton, P. R. Mangan, H. Turner, T. L. Murphy, K. M. Murphy, and C. T. Weaver. 2005. Interleukin 17-producing CD4+ effector T cells develop via a lineage distinct from the T helper type 1 and 2 lineages. *Nat. Immunol.* 6: 1123–1132.

30. Sakaguchi, S., N. Sakaguchi, M. Asano, M. Itoh, and M. Toda. 1995. Immunologic self-tolerance maintained by activated T cells expressing IL-2 receptor alpha-chains (CD25). Breakdown of a single mechanism of self-tolerance causes various autoimmune diseases. *J. Immunol.* 155: 1151–64.

31. Lee, Y. K., H. Turner, C. L. Maynard, J. R. Oliver, D. Chen, C. O. Elson, and C. T. Weaver. 2009. Late developmental plasticity in the T helper 17 lineage. *Immunity* 30: 92–107.

32. O'Shea, J., and W. E. Paul. 2010. Mechanisms underlying lineage commitment and plasticity of helper CD4 + T cells. *Science* 327: 1098–1102.

33. Lanier, L. L. 2013. Shades of grey-the blurring view of innate and adaptive immunity. *Nat. Rev. Immunol.* 13: 73–74.

34. Brennan, P. J., M. Brigl, and M. B. Brenner. 2013. Invariant natural killer T cells: An innate activation scheme linked to diverse effector functions. *Nat. Rev. Immunol.* 13: 101–117.

35. Gold, M. C., and D. M. Lewinsohn. 2013. Co-dependents: MR1-restricted MAIT cells and their antimicrobial function. *Nat. Rev. Microbiol.* 11: 14–19.

36. Vantourout, P., and A. Hayday. 2013. Six-of-the-best: Unique contributions of γδ T cells to immunology. *Nat. Rev. Immunol.* 13: 88–100.

37. Van Rhijn, I., D. I. Godfrey, J. Rossjohn, and D. B. Moody. 2015. Lipid and small-molecule display by CD1 and MR1. *Nat. Rev. Immunol.* 15: 643–654.

38. Gause, W. C., T. A. Wynn, and J. E. Allen. 2013. Type 2 immunity and wound healing: Evolutionary refinement of adaptive immunity by helminths. *Nat. Rev. Immunol.* 13: 607–614.

39. Paul, W. E., and J. Zhu. 2010. How are TH2-type immune responses initiated and amplified? *Nat. Rev. Immunol.* 10: 225–235.

40. Oliphant, C. J., J. L. Barlow, and A. N. J. McKenzie. 2011. Insights into the initiation of type 2 immune responses. *Immunology* 134: 378–385.

41. Lloyd, C. M., and R. J. Snelgrove. 2018. Type 2 immunity: Expanding our view. *Sci. Immunol.* 3: eaat1604.

42. Allen, J. E., and T. E. Sutherland. 2014. Host protective roles of type 2 immunity: Parasite killing and tissue repair, flip sides of the same coin. *Semin. Immunol.* 26: 329–340.

43. Humphreys, N. E., D. Xu, M. R. Hepworth, F. Y. Liew, and R. K. Grencis. 2008. IL-33, a potent inducer of adaptive immunity to intestinal nematodes. *J. Immunol.* 180: 2443–2449.

44. Gerbe, F., E. Sidot, D. J. Smyth, M. Ohmoto, I. Matsumoto, V. Dardalhon, P. Cesses, L. Garnier, M. Pouzolles, B. Brulin, M. Bruschi, Y. Harcus, V. S. Zimmermann, N. Taylor, R. M. Maizels, and P. Jay. 2016. Intestinal epithelial tuft cells initiate type 2 mucosal immunity to helminth parasites. *Nature* 529: 226–230.

45. Zhao, A., J. F. Urban, R. Sun, J. Stiltz, M. Morimoto, L. Notari, K. B. Madden, Z. Yang, V. Grinchuk, T. R. Ramalingam, T. A. Wynn, and T. Shea-Donohue. 2010. Critical role of IL-25 in nematode infection-induced alterations in intestinal function. *J. Immunol.* 185: 6921–6929.

46. Taylor, B. C., C. Zaph, A. E. Troy, Y. Du, K. J. Guild, M. R. Comeau, and D. Artis. 2009. TSLP regulates intestinal immunity and inflammation in mouse models of helminth infection and colitis. *J. Exp. Med.* 206: 655–667.

47. Owyang, A. M., C. Zaph, E. H. Wilson, K. J. Guild, T. McClanahan, H. R. P. Miller, D. J. Cua, M. Goldschmidt, C. A. Hunter, R. A. Kastelein, and D. Artis. 2006. Interleukin 25 regulates type 2 cytokine-dependent immunity and limits chronic inflammation in the gastrointestinal tract. *J. Exp. Med.* 203: 843–849.

48. Hung, L. Y., I. P. Lewkowich, L. A. Dawson, J. Downey, Y. Yang, D. E. Smith, and D. R. Herbert. 2013. IL-33 drives biphasic IL-13 production for noncanonical Type 2 immunity against hookworms. *Proc. Natl. Acad. Sci. U. S. A.* 110: 282–287.

49. Wan, H., H. L. Winton, C. Soeller, E. R. Tovey, D. C. Gruenert, P. J. Thompson, G. A.

Stewart, G. W. Taylor, D. R. Garrod, M. B. Cannell, and C. Robinson. 1999. Der p 1 facilitates transepithelial allergen delivery by disruption of tight junctions. *J. Clin. Invest.* 104: 123–133.

50. Trompette, A., S. Divanovic, A. Visintin, C. Blanchard, R. S. Hegde, R. Madan, P. S. Thorne, M. Wills-Karp, T. L. Gioannini, J. P. Weiss, and C. L. Karp. 2009. Allergenicity resulting from functional mimicry of a Toll-like receptor complex protein. *Nature* 457: 585–588.

51. Kouzaki, H., S. M. O'Grady, C. B. Lawrence, and H. Kita. 2009. Proteases induce production of thymic stromal lymphopoietin by airway epithelial cells through protease-activated receptor-2. *J. Immunol.* 183: 1427–1434.

52. Snelgrove, R. J., L. G. Gregory, T. Peiró, S. Akthar, G. A. Campbell, S. A. Walker, and C. M. Lloyd. 2014. Alternaria-derived serine protease activity drives IL-33-mediated asthma exacerbations. *J. Allergy Clin. Immunol.* 134: 583-592.e6.

53. Angkasekwinai, P., H. Park, Y. H. Wang, Y. H. Wang, H. C. Seon, D. B. Corry, Y. J. Liu, Z. Zhu, and C. Dong. 2007. Interleukin 25 promotes the initiation of proallergic type 2 responses. *J. Exp. Med.* 204: 1509–1517.

54. Zhou, B., M. R. Comeau, T. De Smedt, H. D. Liggitt, M. E. Dahl, D. B. Lewis, D. Gyarmati, T. Aye, D. J. Campbell, and S. F. Ziegler. 2005. Thymic stromal lymphopoietin as a key initiator of allergic airway inflammation in mice. *Nat. Immunol.* 6: 1047–1053.

55. Ballantyne, S. J., J. L. Barlow, H. E. Jolin, P. Nath, A. S. Williams, K. F. Chung, G. Sturton, S. H. Wong, and A. N. J. McKenzie. 2007. Blocking IL-25 prevents airway hyperresponsiveness in allergic asthma. *J. Allergy Clin. Immunol.* 120: 1324–1331.

56. Kearley, J., K. F. Buckland, S. A. Mathie, and C. M. Lloyd. 2009. Resolution of allergic inflammation and airway hyperreactivity is dependent upon disruption of the T1/ST2-IL-33 pathway. *Am. J. Respir. Crit. Care Med.* 179: 772–781.

57. van Panhuys, N., M. Prout, E. Forbes, B. Min, W. E. Paul, and G. Le Gros. 2011. Basophils are the major producers of IL-4 during primary helminth infection. *J. Immunol.* 186: 2719–2728.

58. Perrigoue, J. G., S. A. Saenz, M. C. Siracusa, E. J. Allenspach, B. C. Taylor, P. R. Giacomin, M. G. Nair, Y. Du, C. Zaph, N. van Rooijen, M. R. Comeau, E. J. Pearce, T. M. Laufer, and D. Artis. 2009. MHC class II-dependent basophil-CD4+ T cell interactions promote TH2 cytokine-dependent immunity. *Nat. Immunol.* 10: 697–705.

59. Sokol, C. L., N. Q. Chu, S. Yu, S. A. Nish, T. M. Laufer, and R. Medzhitov. 2009. Basophils function as antigen-presenting cells for an allergen-induced T helper type 2 response. *Nat. Immunol.* 10: 713–720.

60. Allakhverdi, Z., M. R. Comeau, H. K. Jessup, B. R. P. Yoon, A. Brewer, S. Chartier, N. Paquette, S. F. Ziegler, M. Sarfati, and G. Delespesse. 2007. Thymic stromal lymphopoietin is released by human epithelial cells in response to microbes, trauma, or inflammation and potently activates mast cells. *J. Exp. Med.* 204: 253–258.

61. Allakhverdi, Z., D. E. Smith, M. R. Comeau, and G. Delespesse. 2007. Cutting Edge: The ST2 ligand IL-33 potently activates and drives maturation of human mast cells. *J. Immunol.* 179: 2051–2054.

62. Hepworth, M. R., E. Daniłowicz-Luebert, S. Rausch, M. Metz, C. Klotz, M. Maurer, and S. Hartmann. 2012. Mast cells orchestrate type 2 immunity to helminths through regulation of tissue-derived cytokines. *Proc. Natl. Acad. Sci. U. S. A.* 109: 6644–6649.

63. Shimokawa, C., T. Kanaya, M. Hachisuka, K. Ishiwata, H. Hisaeda, Y. Kurashima, H. Kiyono, T. Yoshimoto, T. Kaisho, and H. Ohno. 2017. Mast cells are crucial for induction of group 2 innate lymphoid cells and clearance of helminth infections. *Immunity* 46: 863-874.e4.

64. Hsu, C. L., C. V. Neilsen, and P. J. Bryce. 2010. IL-33 is produced by mast cells and regulates IgE-dependent inflammation. *PLoS One* 5: e11944.

65. Spencer, L. A., and P. F. Weller. 2010. Eosinophils and Th2 immunity: Contemporary insights. *Immunol. Cell Biol.* 88: 250–256.

66. Gonzalo, J. A., C. M. Lloyd, L. Kremer, E. Finger, C. Martinez-A., M. H. Siegelman, M. Cybulsky, and J. C. Gutierrez-Ramos. 1996. Eosinophil recruitment to the lung in a murine model of allergic inflammation: The role of T cells, chemokines, and adhesion receptors. *J. Clin. Invest.* 98: 2332–2345.

67. Pecaric-Petkovic, T., S. A. Didichenko, S. Kaempfer, N. Spiegl, and C. A. Dahinden. 2009. Human basophils and eosinophils are the direct target leukocytes of the novel IL-1 family member IL-33. *Blood* 113: 1526–1534.

68. Schmid-Grendelmeier, P., F. Altznauer, B. Fischer, C. Bizer, A. Straumann, G. Menz, K. Blaser, B. Wüthrich, and H.-U. Simon. 2002. Eosinophils express functional IL-13 in eosinophilic inflammatory diseases. *J. Immunol.* 169: 1021–1027.

69. Duez, C., A. Dakhama, A. Tomkinson, P. Marquillies, A. Balhorn, A. B. Tonnel, D. L.

Bratton, and E. W. Gelfand. 2004. Migration and accumulation of eosinophils toward regional lymph nodes after airway allergen challenge. *J. Allergy Clin. Immunol.* 114: 820–825.

70. Shi, H. Z., A. Humbles, C. Gerard, Z. Jin, and P. F. Weller. 2000. Lymph node trafficking and antigen presentation by endobronchial eosinophils. *J. Clin. Invest.* 105: 945–953.

71. Padigel, U. M., J. J. Lee, T. J. Nolan, G. A. Schad, and D. Abraham. 2006. Eosinophils can function as antigen-presenting cells to induce primary and secondary immune responses to Strongyloides stercoralis. *Infect. Immun.* 74: 3232–3238.

72. Ohnmacht, C., C. Schwartz, M. Panzer, I. Schiedewitz, R. Naumann, and D. Voehringer. 2010. Basophils orchestrate chronic allergic dermatitis and protective immunity against helminths. *Immunity* 33: 364–374.

73. Phythian-Adams, A. T., P. C. Cook, R. J. Lundie, L. H. Jones, K. A. Smith, T. A. Barr, K. Hochweller, S. M. Anderton, G. J. Hämmerling, R. M. Maizels, and A. S. MacDonald. 2010. CD11c depletion severely disrupts Th2 induction and development in vivo. *J. Exp. Med.* 207: 2089–2096.

74. Van Rijt, L. S., S. Jung, A. KleinJan, N. Vos, M. Willart, C. Duez, H. C. Hoogsteden, and B. N. Lambrecht. 2005. In vivo depletion of lung CD11c+ dendritic cells during allergen challenge abrogates the characteristic features of asthma. *J. Exp. Med.* 201: 981–991.

75. Whelan, M., M. M. Harnett, K. M. Houston, V. Patel, W. Harnett, and K. P. Rigley. 2000. A filarial nematode-secreted product signals dendritic cells to acquire a phenotype that drives development of Th2 Cells. *J. Immunol.* 164: 6453–6460.

76. Traidl-Hoffmann, C., V. Mariani, H. Hochrein, K. Karg, H. Wagner, J. Ring, M. J. Mueller, T. Jakob, and H. Behrendt. 2005. Pollen-associated phytoprostanes inhibit dendritic cell interleukin-12 production and augment T helper type 2 cell polarization. *J. Exp. Med.* 201: 627–635.

77. Klechevsky, E., R. Morita, M. Liu, Y. Cao, S. Coquery, L. A. Thompson-Snipes, F. Briere, D. Chaussabel, G. Zurawski, A. K. Palucka, Y. Reiter, J. Banchereau, and H. Ueno. 2008. Functional specializations of human epidermal Langerhans cells and CD14+ dermal dendritic cells. *Immunity* 29: 497–510.

78. Galli, S. J., and M. Tsai. 2012. IgE and mast cells in allergic disease. *Nat. Med.* 18: 693–704.

79. Dahlgren, M. W., and A. B. Molofsky. 2018. All along the watchtower: group 2 innate

lymphoid cells in allergic responses. *Curr. Opin. Immunol.* 54: 13–19.

80. Allen, J. E., and R. M. Maizels. 2011. Diversity and dialogue in immunity to helminths. *Nat. Rev. Immunol.* 11: 375–388.

81. Loke, P., I. Gallagher, M. G. Nair, X. Zang, F. Brombacher, M. Mohrs, J. P. Allison, and J. E. Allen. 2007. Alternative activation is an innate response to injury that requires CD4 + T Cells to be sustained during chronic infection. *J. Immunol.* 179: 3926–3936.

82. Campbell, L., C. R. Saville, P. J. Murray, S. M. Cruickshank, and M. J. Hardman. 2013. Local arginase 1 activity is required for cutaneous wound healing. *J. Invest. Dermatol.* 133: 2461–2470.

83. Nair, M. G., I. J. Gallagher, M. D. Taylor, P. Loke, P. S. Coulson, R. A. Wilson, R. M. Maizels, and J. E. Allen. 2005. Chitinase and Fizz family members are a generalized feature of nematode infection with selective upregulation of Ym1 and Fizz1 by antigen-presenting cells. *Infect. Immun.* 73: 385–394.

84. Chen, F., Z. Liu, W. Wu, C. Rozo, S. Bowdridge, A. Millman, N. Van Rooijen, J. F. Urban, T. A. Wynn, and W. C. Gause. 2012. An essential role for T H 2-type responses in limiting acute tissue damage during experimental helminth infection. *Nat. Med.* 18: 260–266.

85. Artis, D., and H. Spits. 2015. The biology of innate lymphoid cells. *Nature* 517: 293–301.

86. Cella, M., A. Fuchs, W. Vermi, F. Facchetti, K. Otero, J. K. M. Lennerz, J. M. Doherty, J. C. Mills, and M. Colonna. 2009. A human natural killer cell subset provides an innate source of IL-22 for mucosal immunity. *Nature* 457: 722–725.

87. Neill, D. R., S. H. Wong, A. Bellosi, R. J. Flynn, M. Daly, T. K. A. Langford, C. Bucks, C. M. Kane, P. G. Fallon, R. Pannell, H. E. Jolin, and A. N. J. McKenzie. 2010. Nuocytes represent a new innate effector leukocyte that mediates type-2 immunity. *Nature* 464: 1367–1370.

88. Monticelli, L. A., G. F. Sonnenberg, M. C. Abt, T. Alenghat, C. G. K. Ziegler, T. A. Doering, J. M. Angelosanto, B. J. Laidlaw, C. Y. Yang, T. Sathaliyawala, M. Kubota, D. Turner, J. M. Diamond, A. W. Goldrath, D. L. Farber, R. G. Collman, E. J. Wherry, and D. Artis. 2011. Innate lymphoid cells promote lung-tissue homeostasis after infection with influenza virus. *Nat. Immunol.* 12: 1045–1054.

89. Scandella, E., B. Bolinger, E. Lattmann, S. Miller, S. Favre, D. R. Littman, D. Finke, S. A. Luther, T. Junt, and B. Ludewig. 2008. Restoration of lymphoid organ integrity through

the interaction of lymphoid tissue-inducer cells with stroma of the T cell zone. *Nat. Immunol.* 9: 667–675.

90. Rak, G. D., L. C. Osborne, M. C. Siracusa, B. S. Kim, K. Wang, A. Bayat, D. Artis, and S. W. Volk. 2016. IL-33-dependent group 2 innate lymphoid cells promote cutaneous wound healing. *J. Invest. Dermatol.* 136: 487–496.

91. Molofsky, A. B., J. C. Nussbaum, H. E. Liang, S. J. V. Dyken, L. E. Cheng, A. Mohapatra, A. Chawla, and R. M. Locksley. 2013. Innate lymphoid type 2 cells sustain visceral adipose tissue eosinophils and alternatively activated macrophages. *J. Exp. Med.* 210: 535–549.

92. Bernink, J. H., C. P. Peters, M. Munneke, A. A. Te Velde, S. L. Meijer, K. Weijer, H. S. Hreggvidsdottir, S. E. Heinsbroek, N. Legrand, C. J. Buskens, W. A. Bemelman, J. M. Mjösberg, and H. Spits. 2013. Human type 1 innate lymphoid cells accumulate in inflamed mucosal tissues. *Nat. Immunol.* 14: 221–229.

93. Salimi, M., J. L. Barlow, S. P. Saunders, L. Xue, D. Gutowska-Owsiak, X. Wang, L. C. Huang, D. Johnson, S. T. Scanlon, A. N. J. McKenzie, P. G. Fallon, and G. S. Ogg. 2013. A role for IL-25 and IL-33-driven type-2 innate lymphoid cells in atopic dermatitis. *J. Exp. Med.* 210: 2939–2950.

94. Mjösberg, J. M., S. Trifari, N. K. Crellin, C. P. Peters, C. M. Van Drunen, B. Piet, W. J. Fokkens, T. Cupedo, and H. Spits. 2011. Human IL-25-and IL-33-responsive type 2 innate lymphoid cells are defined by expression of CRTH2 and CD161. *Nat. Immunol.* 12: 1055–1062.

95. Perry, J. S. A., S. Han, Q. Xu, M. L. Herman, L. B. Kennedy, G. Csako, and B. Bielekova. 2012. Inhibition of LTi cell development by CD25 blockade is associated with decreased intrathecal inflammation in multiple sclerosis. *Sci. Transl. Med.* 4: 145ra106-145ra106.

96. Spits, H., D. Artis, M. Colonna, A. Diefenbach, J. P. Di Santo, G. Eberl, S. Koyasu, R. M. Locksley, A. N. J. McKenzie, R. E. Mebius, F. Powrie, and E. Vivier. 2013. Innate lymphoid cells-a proposal for uniform nomenclature. *Nat. Rev. Immunol.* 13: 145–149.

97. Fuchs, A., W. Vermi, J. S. Lee, S. Lonardi, S. Gilfillan, R. D. Newberry, M. Cella, and M. Colonna. 2013. Intraepithelial type 1 innate lymphoid cells are a unique subset of il-12- and il-15-responsive ifn-γ-producing cells. *Immunity* 38: 769–781.

98. Price, A. E., H. E. Liang, B. M. Sullivan, R. L. Reinhardt, C. J. Eisley, D. J. Erle, and R. M. Locksley. 2010. Systemically dispersed innate IL-13-expressing cells in type 2 immunity. *Proc. Natl. Acad. Sci. U. S. A.* 107: 11489–11494.

99. Moro, K., T. Yamada, M. Tanabe, T. Takeuchi, T. Ikawa, H. Kawamoto, J. I. Furusawa, M. Ohtani, H. Fujii, and S. Koyasu. 2010. Innate production of TH 2 cytokines by adipose tissue-associated c-Kit+ Sca-1+ lymphoid cells. *Nature* 463: 540–544.

100. Fallon, P. G., S. J. Ballantyne, N. E. Mangan, J. L. Barlow, A. Dasvarma, D. R. Hewett, A. McIlgorm, H. E. Jolin, A. N. J. McKenzie. 2006. Identification of an interleukin (IL)-25–dependent cell population that provides IL-4, IL-5, and IL-13 at the onset of helminth expulsion. *J. Exp. Med.* 203: 1105-1116.

101. Hoyler, T., C. S. N. Klose, A. Souabni, A. Turqueti-Neves, D. Pfeifer, E. L. Rawlins, D. Voehringer, M. Busslinger, and A. Diefenbach. 2012. The transcription factor GATA-3 controls cell fate and maintenance of type 2 innate lymphoid cells. *Immunity* 37: 634–648.

102. Cupedo, T., N. K. Crellin, N. Papazian, E. J. Rombouts, K. Weijer, J. L. Grogan, W. E. Fibbe, J. J. Cornelissen, and H. Spits. 2009. Human fetal lymphoid tissue-inducer cells are interleukin 17-producing precursors to RORC+ CD127+ natural killer-like cells. *Nat. Immunol.* 10: 66–74.

103. Melo-Gonzalez, F., and M. R. Hepworth. 2017. Functional and phenotypic heterogeneity of group 3 innate lymphoid cells. *Immunology* 150: 265–275.

104. Zeng, B., S. Shi, G. Ashworth, C. Dong, J. Liu, and F. Xing. 2019. ILC3 function as a double-edged sword in inflammatory bowel diseases. *Cell Death Dis.* 10: 1–12.

105. Teunissen, M. B. M., J. M. Munneke, J. H. Bernink, P. I. Spuls, P. C. M. Res, A. Te Velde, S. Cheuk, M. W. D. Brouwer, S. P. Menting, L. Eidsmo, H. Spits, M. D. Hazenberg, and J. Mjösberg. 2014. Composition of innate lymphoid cell subsets in the human skin: Enrichment of NCR + ILC3 in lesional skin and blood of psoriasis patients. *J. Invest. Dermatol.* 134: 2351–2360.

106. Klose, C. S. N., M. Flach, L. Möhle, L. Rogell, T. Hoyler, K. Ebert, C. Fabiunke, D. Pfeifer, V. Sexl, D. Fonseca-Pereira, R. G. Domingues, H. Veiga-Fernandes, S. J. Arnold, M. Busslinger, I. R. Dunay, Y. Tanriver, and A. Diefenbach. 2014. Differentiation of type 1 ILCs from a common progenitor to all helper-like innate lymphoid cell lineages. *Cell* 157: 340–356.

107. Satoh-Takayama, N., C. A. J. Vosshenrich, S. Lesjean-Pottier, S. Sawa, M. Lochner, F. Rattis, J. J. Mention, K. Thiam, N. Cerf-Bensussan, O. Mandelboim, G. Eberl, and J. P. Di Santo. 2008. Microbial flora drives interleukin 22 production in intestinal NKp46+ cells that provide innate mucosal immune defense. *Immunity* 29: 958–970.

108. Gladiator, A., N. Wangler, K. Trautwein-Weidner, and S. LeibundGut-Landmann. 2013.

Cutting edge: IL-17–secreting innate lymphoid cells are essential for host defense against fungal infection. *J. Immunol.* 190: 521–525.

109. Ardain, A., R. Domingo-Gonzalez, S. Das, S. W. Kazer, N. C. Howard, A. Singh, M. Ahmed, S. Nhamoyebonde, J. Rangel-Moreno, P. Ogongo, L. Lu, D. Ramsuran, M. de la Luz Garcia-Hernandez, T. K. Ulland, M. Darby, E. Park, F. Karim, L. Melocchi, R. Madansein, K. J. Dullabh, M. Dunlap, N. Marin-Agudelo, T. Ebihara, T. Ndung'u, D. Kaushal, A. S. Pym, J. K. Kolls, A. Steyn, J. Zúñiga, W. Horsnell, W. M. Yokoyama, A. K. Shalek, H. N. Kløverpris, M. Colonna, A. Leslie, and S. A. Khader. 2019. Group 3 innate lymphoid cells mediate early protective immunity against tuberculosis. *Nature* 570: 528–532.

110. Seehus, C. R., A. Kadavallore, B. D. La Torre, A. R. Yeckes, Y. Wang, J. Tang, and J. Kaye. 2017. Alternative activation generates IL-10 producing type 2 innate lymphoid cells. *Nat. Commun.* 8: 1–13.

111. Wang, S., P. Xia, Y. Chen, Z. Yin, Z. Xu, Z. F. Correspondence, Y. Qu, Z. Xiong, B. Ye, Y. Du, Y. Tian, and Z. Fan. 2017. Regulatory innate lymphoid cells control innate intestinal inflammation. *Cell* 171: 1–16.

112. Golebski, K., J. A. Layhadi, U. Sahiner, E. H. Steveling-Klein, M. M. Lenormand, R. C. Y. Li, S. M. Bal, B. A. Heesters, G. Vilà-Nadal, O. Hunewald, G. Montamat, F. Q. He, M. Ollert, O. Fedina, M. Lao-Araya, S. J. H. Vijverberg, A. H. Maitland-van der Zee, C. M. van Drunen, W. J. Fokkens, S. R. Durham, H. Spits, and M. H. Shamji. 2021. Induction of IL-10-producing type 2 innate lymphoid cells by allergen immunotherapy is associated with clinical response. *Immunity* 54: 291-307.e7.

113. Howard, E., G. Lewis, L. Galle-Treger, B. P. Hurrell, D. G. Helou, P. Shafiei-Jahani, J. D. Painter, G. A. Muench, P. Soroosh, and O. Akbari. 2021. IL-10 production by ILC2s requires Blimp-1 and cMaf, modulates cellular metabolism, and ameliorates airway hyperreactivity. *J. Allergy Clin. Immunol.* 147: 1281-1295.e5.

114. Cherrier, D. E., N. Serafini, and J. P. Di Santo. 2018. Innate Lymphoid Cell Development: A T Cell Perspective. *Immunity* 48: 1091–1103.

115. Vivier, E., D. Artis, M. Colonna, A. Diefenbach, J. P. Di Santo, G. Eberl, S. Koyasu, R. M. Locksley, A. N. J. McKenzie, R. E. Mebius, F. Powrie, and H. Spits. 2018. Innate lymphoid cells: 10 years on. *Cell* 174: 1054–1066.

116. Nagasawa, M., K. Germar, B. Blom, and H. Spits. 2017. Human CD5+ innate lymphoid cells are functionally immature and their development from CD34+ progenitor cells Is

regulated by Id2. *Front. Immunol.* 8: 1047.

117. Constantinides, M. G., B. D. McDonald, P. A. Verhoef, and A. Bendelac. 2014. A committed precursor to innate lymphoid cells. *Nature* 508: 397–401.

118. Wong, S. H., J. A. Walker, H. E. Jolin, L. F. Drynan, E. Hams, A. Camelo, J. L. Barlow, D. R. Neill, V. Panova, U. Koch, F. Radtke, C. S. Hardman, Y. Y. Hwang, P. G. Fallon, and A. N. J. McKenzie. 2012. Transcription factor RORα is critical for nuocyte development. *Nat. Immunol.* 13: 229–236.

119. Walker, J. A., C. J. Oliphant, A. Englezakis, Y. Yu, S. Clare, H. R. Rodewald, G. Belz, P. Liu, P. G. Fallon, and A. N. J. McKenzie. 2015. Bcl11b is essential for group 2 innate lymphoid cell development. *J. Exp. Med.* 212: 875–882.

120. Yu, Y., C. Wang, S. Clare, J. Wang, S. C. Lee, C. Brandt, S. Burke, L. Lu, D. He, N. A. Jenkins, N. G. Copeland, G. Dougan, and P. Liu. 2015. The transcription factor Bcl11b is specifically expressed in group 2 innate lymphoid cells and is essential for their development. *J. Exp. Med.* 212: 865–874.

121. Eberl, G., S. Marmon, M. J. Sunshine, P. D. Rennert, Y. Choi, and D. R. Littmann. 2004. An essential function for the nuclear receptor RORγt in the generation of fetal lymphoid tissue inducer cells. *Nat. Immunol.* 5: 64–73.

122. Lim, A. I., Y. Li, S. Lopez-Lastra, R. Stadhouders, F. Paul, A. Casrouge, N. Serafini, A. Puel, J. Bustamante, L. Surace, G. Masse-Ranson, E. David, H. Strick-Marchand, L. Le Bourhis, R. Cocchi, D. Topazio, P. Graziano, L. A. Muscarella, L. Rogge, X. Norel, J. M. Sallenave, M. Allez, T. Graf, R. W. Hendriks, J. L. Casanova, I. Amit, H. Yssel, and J. P. Di Santo. 2017. Systemic human ILC precursors provide a substrate for tissue ILC differentiation. *Cell* 168: 1086-1100.e10.

123. Lim, A. I., and J. P. Di Santo. 2019. ILC-poiesis: Ensuring tissue ILC differentiation at the right place and time. *Eur. J. Immunol.* 49: 11–18.

124. Ricardo-Gonzalez, R. R., S. J. Van Dyken, C. Schneider, J. Lee, J. C. Nussbaum, H.-E. Liang, D. Vaka, W. L. Eckalbar, A. B. Molofsky, D. J. Erle, and R. M. Locksley. 2018. Tissue signals imprint ILC2 identity with anticipatory function. *Nat. Immunol.* 19: 1093–1099.

125. Diefenbach, A., M. Colonna, and S. Koyasu. 2014. Development, differentiation, and diversity of innate lymphoid cells. *Immunity* 41: 354–365.

126. Gasteiger, G., X. Fan, S. Dikiy, S. Y. Lee, and A. Y. Rudensky. 2015. Tissue residency of innate lymphoid cells in lymphoid and nonlymphoid organs. *Science* 350: 981–985.

127. Huang, Y., K. Mao, X. Chen, M. A. Sun, T. Kawabe, W. Li, N. Usher, J. Zhu, J. F. Urban, W. E. Paul, and R. N. Germain. 2018. S1P-dependent interorgan trafficking of group 2 innate lymphoid cells supports host defense. *Science* 359: 114–119.

128. Kim, M. H., E. J. Taparowsky, and C. H. Kim. 2015. RetinOic Acid Differentially Regulates The Migration Of Innate Lymphoid Cell Subsets To The Gut. *Immunity* 43: 107–119.

129. Mackley, E. C., S. Houston, C. L. Marriott, E. E. Halford, B. Lucas, V. Cerovic, K. J. Filbey, R. M. Maizels, M. R. Hepworth, G. F. Sonnenberg, S. Milling, and D. R. Withers. 2015. CCR7-dependent trafficking of RORγ+ ILCs creates a unique microenvironment within mucosal draining lymph nodes. *Nat. Commun.* 6: 1–13.

130. Bernink, J. H., L. Krabbendam, K. Germar, E. de Jong, K. Gronke, M. Kofoed-Nielsen, J. M. Munneke, M. D. Hazenberg, J. Villaudy, C. J. Buskens, W. A. Bemelman, A. Diefenbach, B. Blom, and H. Spits. 2015. Interleukin-12 and -23 control plasticity Of CD127+ group 1 and group 3 innate lymphoid cells in the intestinal lamina propria. *Immunity* 43: 146–160.

131. Ohne, Y., J. S. Silver, L. A. Thompson-Snipes, M. A. Collet, J. P. Blanck, B. L. Cantarel, A. M. Copenhaver, A. A. Humbles, and Y. J. Liu. 2016. IL-1 is a critical regulator of group 2 innate lymphoid cell function and plasticity. *Nat. Immunol.* 17: 646–655.

132. Bal, S. M., J. H. Bernink, M. Nagasawa, J. Groot, M. M. Shikhagaie, K. Golebski, C. M. Van Drunen, R. Lutter, R. E. Jonkers, P. Hombrink, M. Bruchard, J. Villaudy, J. M. Munneke, W. Fokkens, J. S. Erjeflt, H. Spits, and X. R. Ros. 2016. IL-1β, IL-4 and IL-12 control the fate of group 2 innate lymphoid cells in human airway inflammation in the lungs. *Nat. Immunol.* 17: 636–645.

133. Silver, J. S., J. Kearley, A. M. Copenhaver, C. Sanden, M. Mori, L. Yu, G. H. Pritchard, A. A. Berlin, C. A. Hunter, R. Bowler, J. S. Erjefalt, R. Kolbeck, and A. A. Humbles. 2016. Inflammatory triggers associated with exacerbations of COPD orchestrate plasticity of group 2 innate lymphoid cells in the lungs. *Nat. Immunol.* 17: 626–635.

134. Mjösberg, J., J. Bernink, K. Golebski, J. J. Karrich, C. P. Peters, B. Blom, A. A. te Velde, W. J. Fokkens, C. M. van Drunen, and H. Spits. 2012. The transcription factor GATA3 is essential for the function of human type 2 innate lymphoid cells. *Immunity* 37: 649–659.

135. Hardman, C. S., Y.-L. Chen, M. Salimi, J. Nahler, D. Corridoni, M. Jagielowicz, C. L. Fonseka, D. Johnson, E. Repapi, D. J. Cousins, J. L. Barlow, A. N. J. McKenzie, A. Simmons, and G. Ogg. 2021. IL-6 effector function of group 2 innate lymphoid cells (ILC2)

is NOD2 dependent. *Sci. Immunol.* 6: eabe5084.

136. Xue, L., M. Salimi, I. Panse, J. M. Mjösberg, A. N. J. McKenzie, H. Spits, P. Klenerman, and G. Ogg. 2014. Prostaglandin D2 activates group 2 innate lymphoid cells through chemoattractant receptor-homologous molecule expressed on TH2 cells. *J. Allergy Clin. Immunol.* 133: 1184-1194.e7.

137. Denney, L., A. J. Byrne, T. J. Shea, J. S. Buckley, J. E. Pease, G. M. F. Herledan, S. A. Walker, L. G. Gregory, and C. M. Lloyd. 2015. Pulmonary epithelial cell-derived cytokine TGF-β1 Is a critical cofactor for enhanced innate lymphoid cell function. *Immunity* 43: 945–958.

138. Von Moltke, J., M. Ji, H. E. Liang, and R. M. Locksley. 2016. Tuft-cell-derived IL-25 regulates an intestinal ILC2-epithelial response circuit. *Nature* 529: 221–225.

139. Kabata, H., K. Moro, and S. Koyasu. 2018. The group 2 innate lymphoid cell (ILC2) regulatory network and its underlying mechanisms. *Immunol. Rev.* 286: 37–52.

140. Barlow, J. L., S. Peel, J. Fox, V. Panova, C. S. Hardman, A. Camelo, C. Bucks, X. Wu, C. M. Kane, D. R. Neill, R. J. Flynn, I. Sayers, I. P. Hall, and A. N. J. McKenzie. 2013. IL-33 is more potent than IL-25 in provoking IL-13-producing nuocytes (type 2 innate lymphoid cells) and airway contraction. *J. Allergy Clin. Immunol.* 132: 933–941.

141. Kim, B. S., M. C. Siracusa, S. A. Saenz, M. Noti, L. A. Monticelli, G. F. Sonnenberg, M. R. Hepworth, A. S. Van Voorhees, M. R. Comeau, and D. Artis. 2013. TSLP elicits IL-33-independent innate lymphoid cell responses to promote skin inflammation. *Sci. Transl. Med.* 5: 170ra16-170ra16.

142. Entwistle, L. J., L. G. Gregory, R. A. Oliver, W. J. Branchett, F. Puttur, and C. M. Lloyd. 2020. Pulmonary group 2 innate lymphoid cell phenotype is context specific: determining the effect of strain, location, and stimuli. *Front. Immunol.* 10: 3114.

143. Huang, Y., L. Guo, J. Qiu, X. Chen, J. Hu-Li, U. Siebenlist, P. R. Williamson, J. F. Urban, and W. E. Paul. 2015. IL-25-responsive, lineage-negative KLRG1 hi cells are multipotential “inflammatory” type 2 innate lymphoid cells. *Nat. Immunol.* 16: 161–169.

144. Camelo, A., G. Rosignoli, Y. Ohne, R. A. Stewart, C. Overed-Sayer, M. A. Sleeman, and R. D. May. 2017. IL-33, IL-25, and TSLP induce a distinct phenotypic and activation profile in human type 2 innate lymphoid cells. *Blood Adv.* 1: 577–589.

145. Halim, T. Y. F., R. H. Krauß, A. C. Sun, and F. Takei. 2012. Lung natural helper cells are a critical source of Th2 cell-type cytokines in protease allergen-induced airway

inflammation. *Immunity* 36: 451–463.

146. Mohapatra, A., S. J. Van Dyken, C. Schneider, J. C. Nussbaum, H. E. Liang, and R. M. Locksley. 2016. Group 2 innate lymphoid cells utilize the IRF4-IL-9 module to coordinate epithelial cell maintenance of lung homeostasis. *Mucosal Immunol.* 9: 275–286.

147. Toki, S., K. Goleniewska, J. Zhang, W. Zhou, D. C. Newcomb, B. Zhou, H. Kita, K. L. Boyd, and R. S. Peebles. 2020. TSLP and IL-33 reciprocally promote each other's lung protein expression and ILC2 receptor expression to enhance innate type-2 airway inflammation. *Allergy Eur. J. Allergy Clin. Immunol.* 75: 1606–1617.

148. Simoni, Y., M. Fehlings, H. N. Kløverpris, N. McGovern, S. L. Koo, C. Y. Loh, S. Lim, A. Kurioka, J. R. Fergusson, C. L. Tang, M. H. Kam, K. Dennis, T. K. H. Lim, A. C. Y. Fui, C. W. Hoong, J. K. Y. Chan, M. Curotto de Lafaille, S. Narayanan, S. Baig, M. Shabeer, S. A. E. S. Toh, H. K. K. Tan, R. Anicete, E. H. Tan, A. Takano, P. Klenerman, A. Leslie, D. S. W. Tan, I. B. Tan, F. Ginhoux, and E. W. Newell. 2017. Human innate lymphoid cell subsets possess tissue-type based heterogeneity in phenotype and frequency. *Immunity* 46: 148–161.

149. Lewis, R. A., N. A. Soter, P. T. Diamond, K. F. Austen, J. A. Oates, and L. J. Roberts. 1982. Prostaglandin D2 generation after activation of rat and human mast cells with anti-IgE. *J. Immunol.* 129: 1627–31.

150. Barnig, C., M. Cernadas, S. Dutile, X. Liu, M. A. Perrella, S. Kazani, M. E. Wechsler, E. Israel, and B. D. Levy. 2013. Lipoxin A4 regulates natural killer cell and type 2 innate lymphoid cell activation in asthma. *Sci. Transl. Med.* 5: 174ra26-174ra26.

151. Tait Wojno, E. D., L. A. Monticelli, S. V. Tran, T. Alenghat, L. C. Osborne, J. J. Thome, C. Willis, A. Budelsky, D. L. Farber, and D. Artis. 2015. The prostaglandin D2 receptor CRTH2 regulates accumulation of group 2 innate lymphoid cells in the inflamed lung. *Mucosal Immunol.* 8: 1313–1323.

152. Doherty, T. A., N. Khorram, S. Lund, A. K. Mehta, M. Croft, and D. H. Broide. 2013. Lung type 2 innate lymphoid cells express cysteinyl leukotriene receptor 1, which regulates TH2 cytokine production. *J. Allergy Clin. Immunol.* 132: 205–213.

153. Lund, S. J., A. Portillo, K. Cavagnero, R. E. Baum, L. H. Naji, J. H. Badrani, A. Mehta, M. Croft, D. H. Broide, and T. A. Doherty. 2017. Leukotriene C4 potentiates IL-33–induced group 2 innate lymphoid cell activation and lung inflammation. *J. Immunol.* 199: 1096–1104.

154. von Moltke, J., C. E. O'Leary, N. A. Barrett, Y. Kanaoka, K. F. Austen, and R. M. Locksley. 2017. Leukotrienes provide an NFAT-dependent signal that synergizes with IL-

33 to activate ILC2s. *J. Exp. Med.* 214: 27–37.

155. Salimi, M., L. Stöger, W. Liu, S. Go, I. Pavord, P. Klenerman, G. Ogg, and L. Xue. 2017. Cysteinyl leukotriene E4 activates human group 2 innate lymphoid cells and enhances the effect of prostaglandin D2 and epithelial cytokines. *J. Allergy Clin. Immunol.* 140: 1090-1100.e11.

156. Cardoso, V., J. Chesné, H. Ribeiro, B. Garcia-Cassani, T. Carvalho, T. Bouchery, K. Shah, N. L. Barbosa-Morais, N. Harris, and H. Veiga-Fernandes. 2017. Neuronal regulation of type 2 innate lymphoid cells via neuromedin U. *Nature* 549: 277–281.

157. Klose, C. S. N., T. Mahlakõiv, J. B. Moeller, L. C. Rankin, A. L. Flamar, H. Kabata, L. A. Monticelli, S. Moriyama, G. G. Putzel, N. Rakhilin, X. Shen, E. Kostenis, G. M. König, T. Senda, D. Carpenter, D. L. Farber, and D. Artis. 2017. The neuropeptide neuromedin U stimulates innate lymphoid cells and type 2 inflammation. *Nature* 549: 282–286.

158. Wallrapp, A., S. J. Riesenfeld, P. R. Burkett, R. E. E. Abdulnour, J. Nyman, D. Dionne, M. Hofree, M. S. Cuoco, C. Rodman, D. Farouq, B. J. Haas, T. L. Tickle, J. J. Trombetta, P. Baral, C. S. N. Klose, T. Mahlakõiv, D. Artis, O. Rozenblatt-Rosen, I. M. Chiu, B. D. Levy, M. S. Kowalczyk, A. Regev, and V. K. Kuchroo. 2017. The neuropeptide NMU amplifies ILC2-driven allergic lung inflammation. *Nature* 549: 351–356.

159. Nussbaum, J. C., S. J. Van Dyken, J. Von Moltke, L. E. Cheng, A. Mohapatra, A. B. Molofsky, E. E. Thornton, M. F. Krummel, A. Chawla, H. E. Liang, and R. M. Locksley. 2013. Type 2 innate lymphoid cells control eosinophil homeostasis. *Nature* 502: 245–248.

160. Talbot, S., R. E. E. Abdulnour, P. R. Burkett, S. Lee, S. J. F. Cronin, M. A. Pascal, C. Laedermann, S. L. Foster, J. V. Tran, N. Lai, I. M. Chiu, N. Ghasemlou, M. DiBiase, D. Roberson, C. Von Hehn, B. Agac, O. Haworth, H. Seki, J. M. Penninger, V. K. Kuchroo, B. P. Bean, B. D. Levy, and C. J. Woolf. 2015. Silencing nociceptor neurons reduces allergic airway inflammation. *Neuron* 87: 341–354.

161. Maazi, H., N. Patel, I. Sankaranarayanan, Y. Suzuki, D. Rigas, P. Soroosh, G. J. Freeman, A. H. Sharpe, and O. Akbari. 2015. ICOS: ICOS-Ligand interaction is required for type 2 innate lymphoid cell function, homeostasis, and induction of airway hyperreactivity. *Immunity* 42: 538–551.

162. Paclik, D., C. Stehle, A. Lahmann, A. Hutloff, and C. Romagnani. 2015. ICOS regulates the pool of group 2 innate lymphoid cells under homeostatic and inflammatory conditions in mice. *Eur. J. Immunol.* 45: 2766–2772.

163. Lei, A. H., Q. Xiao, G. Y. Liu, K. Shi, Q. Yang, X. Li, Y. F. Liu, H. K. Wang, W. P. Cai,

Y. J. Guan, D. I. Gabrilovich, and J. Zhou. 2018. ICAM-1 controls development and function of ILC2. *J. Exp. Med.* 215: 2157–2174.

164. Salimi, M., L. Xue, H. Jolin, C. Hardman, D. J. Cousins, A. N. J. McKenzie, and G. S. Ogg. 2016. Group 2 innate lymphoid cells express functional NKp30 receptor inducing type 2 cytokine production. *J. Immunol.* 196: 45–54.

165. Trabanelli, S., M. F. Chevalier, A. Martinez-Usatorre, A. Gomez-Cadena, B. Salomé, M. Lecciso, V. Salvestrini, G. Verdeil, J. Racle, C. Papayannidis, H. Morita, I. Pizzitola, C. Grandclément, P. Bohner, E. Bruni, M. Girotra, R. Pallavi, P. Falvo, E. O. Leibundgut, G. M. Baerlocher, C. Carlo-Stella, D. Taurino, A. Santoro, O. Spinelli, A. Rambaldi, E. Giarin, G. Basso, C. Tresoldi, F. Ciceri, D. Gfeller, C. A. Akdis, L. Mazzarella, S. Minucci, P. G. Pelicci, E. Marcenaro, A. N. J. McKenzie, D. Vanhecke, G. Coukos, D. Mavilio, A. Curti, L. Derré, and C. Jandus. 2017. Tumour-derived PGD2 and NKp30-B7H6 engagement drives an immunosuppressive ILC2-MDSC axis. *Nat. Commun.* 8: 1–14.

166. Yu, X., R. Pappu, V. Ramirez-Carrozzi, N. Ota, P. Caplazi, J. Zhang, D. Yan, M. Xu, W. P. Lee, and J. L. Grogan. 2014. TNF superfamily member TL1A elicits type 2 innate lymphoid cells at mucosal barriers. *Mucosal Immunol.* 7: 730–740.

167. Meylan, F., E. T. Hawley, L. Barron, J. L. J. Barlow, P. Penumetcha, M. Pelletier, G. Sciumè, A. C. Richard, E. T. Hayes, J. Gomez-Rodriguez, X. Chen, W. E. W. Paul, T. A. Wynn, A. N. J. McKenzie, and R. M. R. Siegel. 2014. The TNF-family cytokine TL1A promotes allergic immunopathology through group 2 innate lymphoid cells. *Mucosal Immunol.* 7: 958–968.

168. Nagashima, H., Y. Okuyama, T. Fujita, T. Takeda, Y. Motomura, K. Moro, T. Hidaka, K. Omori, T. Sakurai, T. Machiyama, L. C. Ndhlovu, C. Riccardi, T. So, and N. Ishii. 2018. GITR cosignal in ILC2s controls allergic lung inflammation. *J. Allergy Clin. Immunol.* 141: 1939-1943.e8.

169. Salimi, M., R. Wang, X. Yao, X. Li, X. Wang, Y. Hu, X. Chang, P. Fan, T. Dong, and G. Ogg. 2018. Activated innate lymphoid cell populations accumulate in human tumour tissues. *BMC Cancer* 18: 1–10.

170. Moral, J. A., J. Leung, L. A. Rojas, J. Ruan, J. Zhao, Z. Sethna, A. Ramnarain, B. Gasmi, M. Gururajan, D. Redmond, G. Askan, U. Bhanot, E. Elyada, Y. Park, D. A. Tuveson, M. Gönen, S. D. Leach, J. D. Wolchok, R. P. DeMatteo, T. Merghoub, and V. P. Balachandran. 2020. ILC2s amplify PD-1 blockade by activating tissue-specific cancer immunity. *Nature* 579: 130–135.

171. Wynn, T. A. 2015. Type 2 cytokines: Mechanisms and therapeutic strategies. *Nat. Rev. Immunol.* 15: 271–282.

172. Duerr, C. U., C. D. A. Mccarthy, B. C. Mindt, M. Rubio, A. P. Meli, J. Pothlichet, M. M. Eva, J. F. Gauchat, S. T. Qureshi, B. D. Mazer, K. L. Mossman, D. Malo, A. M. Gamero, S. M. Vidal, I. L. King, M. Sarfati, and J. H. Fritz. 2016. Type I interferon restricts type 2 immunopathology through the regulation of group 2 innate lymphoid cells. *Nat. Immunol.* 17: 65–75.

173. Moro, K., H. Kabata, M. Tanabe, S. Koga, N. Takeno, M. Mochizuki, K. Fukunaga, K. Asano, T. Betsuyaku, and S. Koyasu. 2016. Interferon and IL-27 antagonize the function of group 2 innate lymphoid cells and type 2 innate immune responses. *Nat. Immunol.* 17: 76–86.

174. Ogasawara, N., J. A. Poposki, A. I. Klingler, B. K. Tan, A. R. Weibman, K. E. Hulse, W. W. Stevens, A. T. Peters, L. C. Grammer, R. P. Schleimer, K. C. Welch, S. S. Smith, D. B. Conley, J. R. Raviv, P. Soroosh, O. Akbari, T. Himi, R. C. Kern, and A. Kato. 2018. IL-10, TGF-β and glucocorticoid prevent the production of type 2 cytokines in human group 2 innate lymphoid cells. *J. Allergy Clin. Immunol.* 141: 1147-1151.e8.

175. Maric, J., A. Ravindran, L. Mazzurana, Å. K. Björklund, A. Van Acker, A. Rao, D. Friberg, S. E. Dahlén, A. Heinemann, V. Konya, and J. Mjösberg. 2018. Prostaglandin E2 suppresses human group 2 innate lymphoid cell function. *J. Allergy Clin. Immunol.* 141: 1761-1773.e6.

176. Zhou, Y., W. Wang, C. Zhao, Y. Wang, H. Wu, X. Sun, Y. Guan, and Y. Zhang. 2018. Prostaglandin E2 inhibits group 2 innate lymphoid cell activation and allergic airway inflammation through E-prostanoid 4-cyclic adenosine monophosphate signaling. *Front. Immunol.* 9: 501.

177. Zhou, W., S. Toki, J. Zhang, K. Goleniewksa, D. C. Newcomb, J. Y. Cephus, D. E. Dulek, M. H. Bloodworth, M. T. Stier, V. Polosuhkin, R. D. Gangula, S. A. Mallal, D. H. Broide, and R. S. Peebles. 2016. Prostaglandin I2 signaling and inhibition of group 2 innate lymphoid cell responses. *Am. J. Respir. Crit. Care Med.* 193: 31–42.

178. Rigas, D., G. Lewis, J. L. Aron, B. Wang, H. Banie, I. Sankaranarayanan, L. Galle-Treger, H. Maazi, R. Lo, G. J. Freeman, A. H. Sharpe, P. Soroosh, and O. Akbari. 2017. Type 2 innate lymphoid cell suppression by regulatory T cells attenuates airway hyperreactivity and requires inducible T-cell costimulator–inducible T-cell costimulator ligand interaction. *J. Allergy Clin. Immunol.* 139: 1468-1477.e2.

179. Taylor, S., Y. Huang, G. Mallett, C. Stathopoulou, T. C. Felizardo, M. A. Sun, E. L. Martin, N. Zhu, E. L. Woodward, M. S. Elias, J. Scott, N. J. Reynolds, W. E. Paul, D. H. Fowler, and S. Amarnath. 2017. PD-1 regulates KLRG1+ group 2 innate lymphoid cells. *J. Exp. Med.* 214: 1663–1678.

180. Helou, D. G., P. Shafiei-Jahani, R. Lo, E. Howard, B. P. Hurrell, L. Galle-Treger, J. D. Painter, G. Lewis, P. Soroosh, A. H. Sharpe, and O. Akbari. 2020. PD-1 pathway regulates ILC2 metabolism and PD-1 agonist treatment ameliorates airway hyperreactivity. *Nat. Commun.* 11: 1–15.

181. Walker, J. A., J. L. Barlow, and A. N. J. McKenzie. 2013. Innate lymphoid cells-how did we miss them? *Nat. Rev. Immunol.* 13: 75–87.

182. McKenzie, G. J., A. Bancroft, R. K. Grencis, and A. N. J. McKenzie. 1998. A distinct role for interleukin-13 in Th2-cell-mediated immune responses. *Curr. Biol.* 8: 339–342.

183. Oliphant, C. J., Y. Y. Hwang, J. A. Walker, M. Salimi, S. H. Wong, J. M. Brewer, A. Englezakis, J. L. Barlow, E. Hams, S. T. Scanlon, G. S. Ogg, P. G. Fallon, and A. N. McKenzie. 2014. MHCII-mediated dialog between group 2 innate lymphoid cells and CD4+ T cells potentiates type 2 immunity and promotes parasitic helminth expulsion. *Immunity* 41: 283–295.

184. Turner, J. E., P. J. Morrison, C. Wilhelm, M. Wilson, H. Ahlfors, J. C. Renauld, U. Panzer, H. Helmby, and B. Stockinger. 2013. IL-9-mediated survival of type 2 innate lymphoid cells promotes damage control in helminth-induced lung inflammation. *J. Exp. Med.* 210: 2951–2965.

185. Nausch, N., L. J. Appleby, A. M. Sparks, N. Midzi, T. Mduluza, and F. Mutapi. 2015. Group 2 innate lymphoid cell proportions are diminished in young helminth infected children and restored by curative anti-helminthic treatment. *PLoS Negl. Trop. Dis.* 9: e0003627.

186. Eming, S. A., T. Krieg, and J. M. Davidson. 2007. Inflammation in wound repair: Molecular and cellular mechanisms. *J. Invest. Dermatol.* 127: 514–525.

187. Zaiss, D. M. W., W. C. Gause, L. C. Osborne, and D. Artis. 2015. Emerging functions of amphiregulin in orchestrating immunity, inflammation, and tissue repair. *Immunity* 42: 216–226.

188. Monticelli, L. A., L. C. Osborne, M. Noti, S. V. Tran, D. M. W. Zaiss, and D. Artis. 2015. IL-33 promotes an innate immune pathway of intestinal tissue protection dependent on amphiregulin-EGFR interactions. *Proc. Natl. Acad. Sci. U. S. A.* 112: 10762–10767.

189. Lucas, T., A. Waisman, R. Ranjan, J. Roes, T. Krieg, W. Müller, A. Roers, and S. A. Eming. 2010. Differential roles of macrophages in diverse phases of skin repair. *J. Immunol.* 184: 3964–3977.

190. Gorski, S. A., Y. S. Hahn, and T. J. Braciale. 2013. Group 2 innate lymphoid cell production of IL-5 Is regulated by NKT cells during influenza virus infection. *PLoS Pathog.* 9: e1002615.

191. Todd, R., B. R. Donoff, T. Chiang, M. Y. Chou, A. Elovic, G. T. Gallagher, and D. T. W. Wong. 1991. The eosinophil as a cellular source of transforming growth factor alpha in healing cutaneous wounds. *Am. J. Pathol.* 138: 1307–1313.

192. Li, D., R. Guabiraba, A. G. Besnard, M. Komai-Koma, M. S. Jabir, L. Zhang, G. J. Graham, M. Kurowska-Stolarska, F. Y. Liew, C. McSharry, and D. Xu. 2014. IL-33 promotes ST2-dependent lung fibrosis by the induction of alternatively activated macrophages and innate lymphoid cells in mice. *J. Allergy Clin. Immunol.* 134: 1422-1432.e11.

193. Mchedlidze, T., M. Waldner, S. Zopf, J. Walker, A. L. Rankin, M. Schuchmann, D. Voehringer, A. N. J. McKenzie, M. F. Neurath, S. Pflanz, and S. Wirtz. 2013. Interleukin-33-dependent innate lymphoid cells mediate hepatic fibrosis. *Immunity* 39: 357–371.

194. Poposki, J. A., A. I. Klingler, B. K. Tan, P. Soroosh, H. Banie, G. Lewis, K. E. Hulse, W. W. Stevens, A. T. Peters, L. C. Grammer, R. P. Schleimer, K. C. Welch, S. S. Smith, D. B. Conley, J. R. Raviv, J. G. Karras, O. Akbari, R. C. Kern, and A. Kato. 2017. Group 2 innate lymphoid cells are elevated and activated in chronic rhinosinusitis with nasal polyps. *Immunity, Inflamm. Dis.* 5: 233–243.

195. Smith, S. G., R. Chen, M. Kjarsgaard, C. Huang, J. P. Oliveria, P. M. O'Byrne, G. M. Gauvreau, L. P. Boulet, C. Lemiere, J. Martin, P. Nair, and R. Sehmi. 2016. Increased numbers of activated group 2 innate lymphoid cells in the airways of patients with severe asthma and persistent airway eosinophilia. *J. Allergy Clin. Immunol.* 137: 75-86.e8.

196. Christianson, C. A., N. P. Goplen, I. Zafar, C. Irvin, J. T. Good, D. R. Rollins, B. Gorentla, W. Liu, M. M. Gorska, H. W. Chu, R. J. Martin, and R. Alam. 2015. Persistence of asthma requires multiple feedback circuits involving type 2 innate lymphoid cells and IL-33. *J. Allergy Clin. Immunol.* 136: 59-68.e14.

197. Winkler, C., T. Hochdörfer, E. Israelsson, A. Hasselberg, A. Cavallin, K. Thörn, D. Muthas, S. Shojaee, K. Lüer, M. Müller, J. Mjösberg, O. Vaarala, J. Hohlfeld, and K. Pardali. 2019. Activation of group 2 innate lymphoid cells after allergen challenge in asthmatic patients. *J. Allergy Clin. Immunol.* 144: 61-69.e7.

198. Nagakumar, P., F. Puttur, L. G. Gregory, L. Denney, L. Fleming, A. Bush, C. M. Lloyd, and S. Saglani. 2019. Pulmonary type-2 innate lymphoid cells in paediatric severe asthma: phenotype and response to steroids. *Eur. Respir. J.* 54: 1801809.

199. Tamari, M., S. Tanaka, and T. Hirota. 2013. Genome-wide association studies of allergic diseases. *Allergol. Int.* 62: 21–28.

200. Préfontaine, D., S. Lajoie-Kadoch, S. Foley, S. Audusseau, R. Olivenstein, A. J. Halayko, C. Lemière, J. G. Martin, and Q. Hamid. 2009. Increased expression of IL-33 in severe asthma: Evidence of expression by airway smooth muscle cells. *J. Immunol.* 183: 5094–5103.

201. Fajt, M. L., S. L. Gelhaus, B. Freeman, C. E. Uvalle, J. B. Trudeau, F. Holguin, and S. E. Wenzel. 2013. Prostaglandin D2 pathway upregulation: Relation to asthma severity, control, and TH2 inflammation. *J. Allergy Clin. Immunol.* 131: 1504-1512.e12.

202. Wenzel, S. E., G. L. Larsen, K. Johnston, N. F. Voelkel, and J. Y. Westcott. 1990. Elevated levels of leukotriene C4 in bronchoalveolar lavage fluid from atopic asthmatics after endobronchial allergen challenge. *Am. Rev. Respir. Dis.* 142: 112–119.

203. Planagumà, A., S. Kazani, G. Marigowda, O. Haworth, T. J. Mariani, E. Israel, E. R. Bleecker, D. Curran-Everett, S. C. Erzurum, W. J. Calhoun, M. Castro, F. C. Kian, B. Gaston, N. N. Jarjour, W. W. Busse, S. E. Wenzel, and B. D. Levy. 2008. Airway lipoxin A4 generation and lipoxin A4 receptor expression are decreased in severe asthma. *Am. J. Respir. Crit. Care Med.* 178: 574–582.

204. Su, X., J. Pan, F. Bai, H. Yuan, N. Dong, D. Li, X. Wang, and Z. Chen. 2016. IL-27 attenuates airway inflammation in a mouse asthma model via the STAT1 and GADD45γ/p38 MAPK pathways. *J. Transl. Med.* 14: 1-12.

205. Barlow, J. L., A. Bellosi, C. S. Hardman, L. F. Drynan, S. H. Wong, J. P. Cruickshank, and A. N. J. McKenzie. 2012. Innate IL-13-producing nuocytes arise during allergic lung inflammation and contribute to airways hyperreactivity. *J. Allergy Clin. Immunol.* 129: 191-198.e4.

206. Bartemes, K. R., K. Iijima, T. Kobayashi, G. M. Kephart, A. N. McKenzie, and H. Kita. 2012. IL-33–responsive lineage − CD25 + CD44 hi lymphoid cells mediate innate type 2 immunity and allergic inflammation in the lungs. *J. Immunol.* 188: 1503–1513.

207. Kim, H. Y., Y. J. Chang, S. Subramanian, H. H. Lee, L. A. Albacker, P. Matangkasombut, P. B. Savage, A. N. J. McKenzie, D. E. Smith, J. B. Rottman, R. H. Dekruyff, and D. T. Umetsu. 2012. Innate lymphoid cells responding to IL-33 mediate airway

hyperreactivity independently of adaptive immunity. *J. Allergy Clin. Immunol.* 129: 216-227.e6.

208. Van Dyken, S. J., A. Mohapatra, J. C. Nussbaum, A. B. Molofsky, E. E. Thornton, S. F. Ziegler, A. N. J. McKenzie, M. F. Krummel, H. E. Liang, and R. M. Locksley. 2014. Chitin activates parallel immune modules that direct distinct inflammatory responses via innate lymphoid type 2 and γδ T cells. *Immunity* 40: 414–424.

209. Motomura, Y., H. Morita, K. Moro, S. Nakae, D. Artis, T. A. Endo, Y. Kuroki, O. Ohara, S. Koyasu, and M. Kubo. 2014. Basophil-derived interleukin-4 controls the function of natural helper cells, a member of ILC2s, in lung inflammation. *Immunity* 40: 758–771.

210. Moretti, S., G. Renga, V. Oikonomou, C. Galosi, M. Pariano, R. G. Iannitti, M. Borghi, M. Puccetti, M. De Zuani, C. E. Pucillo, G. Paolicelli, T. Zelante, J. C. Renauld, O. Bereshchenko, P. Sportoletti, V. Lucidi, M. C. Russo, C. Colombo, E. Fiscarelli, C. Lass-Flörl, F. Majo, G. Ricciotti, H. Ellemunter, L. Ratclif, V. N. Talesa, V. Napolioni, and L. Romani. 2017. A mast cell-ILC2-Th9 pathway promotes lung inflammation in cystic fibrosis. *Nat. Commun.* 8: 1–13.

211. Halim, T. Y. F., C. A. Steer, L. Mathä, M. J. Gold, I. Martinez-Gonzalez, K. M. Mcnagny, A. N. J. Mckenzie, and F. Takei. 2014. Group 2 innate lymphoid cells are critical for the initiation of adaptive T helper 2 cell-mediated allergic lung inflammation. *Immunity* 40: 425–435.

212. Halim, T. Y. F., Y. Y. Hwang, S. T. Scanlon, H. Zaghouani, N. Garbi, P. G. Fallon, and A. N. J. Mckenzie. 2016. Group 2 innate lymphoid cells license dendritic cells to potentiate memory TH2 cell responses. *Nat. Immunol.* 17: 57–64.

213. Eichenfield, L. F., A. W. Lucky, M. Boguniewicz, R. G. B. Langley, R. Cherill, K. Marshall, C. Bush, and M. Graeber. 2002. Safety and efficacy of pimecrolimus (ASM 981) cream 1% in the treatment of mild and moderate atopic dermatitis in children and adolescents. *J. Am. Acad. Dermatol.* 46: 495–504.

214. Jarrett, R., M. Salio, A. Lloyd-Lavery, S. Subramaniam, E. Bourgeois, C. Archer, K. L. Cheung, C. Hardman, D. Chandler, M. Salimi, D. Gutowska-Owsiak, J. B. De La Serna, P. G. Fallon, H. Jolin, A. McKenzie, A. Dziembowski, E. I. Podobas, W. Bal, D. Johnson, D. B. Moody, V. Cerundolo, and G. Ogg. 2016. Filaggrin inhibits generation of CD1a neolipid antigens by house dust mite-derived phospholipase. *Sci. Transl. Med.* 8: 325ra18-325ra18.

215. Candia, J., F. Cheung, Y. Kotliarov, G. Fantoni, B. Sellers, T. Griesman, J. Huang, S. Stuccio, A. Zingone, B. M. Ryan, J. S. Tsang, and A. Biancotto. 2017. Assessment of

variability in the SOMAscan assay. *Sci. Rep.* 7: 1–13.

216. Benjamini, Y., and Y. Hochberg. 1995. Controlling the false discovery rate: A practical and powerful approach to multiple testing. *J. R. Stat. Soc. Ser. B* 57: 289–300.

217. Banchereau, J., V. Pascual, and A. O'Garra. 2012. From IL-2 to IL-37: The expanding spectrum of anti-inflammatory cytokines. *Nat. Immunol.* 13: 925–931.

218. Turner, M. D., B. Nedjai, T. Hurst, and D. J. Pennington. 2014. Cytokines and chemokines: At the crossroads of cell signalling and inflammatory disease. *Biochim. Biophys. Acta - Mol. Cell Res.* 1843: 2563–2582.

219. O'Shea, J. J., A. Ma, and P. Lipsky. 2002. Cytokines and autoimmunity. *Nat. Rev. Immunol.* 2: 37–45.

220. Agace, W. W. 2006. Tissue-tropic effector T cells: Generation and targeting opportunities. *Nat. Rev. Immunol.* 6: 682–692.

221. Schall, T. J., and A. E. I. Proudfoot. 2011. Overcoming hurdles in developing successful drugs targeting chemokine receptors. *Nat. Rev. Immunol.* 11: 355–363.

222. Mantovani, A. 1999. The chemokine system: Redundancy for robust outputs. *Immunol. Today* 20: 254–257.

223. Proudfoot, A. E. I. 2002. Chemokine receptors: Multifaceted therapeutic targets. *Nat. Rev. Immunol.* 2: 106–115.

224. Charo, I. F., and R. M. Ransohoff. 2006. The many roles of chemokines and chemokine receptors in inflammation. *N. Engl. J. Med.* 354: 610–621.

225. Bromley, S. K., T. R. Mempel, and A. D. Luster. 2008. Orchestrating the orchestrators: Chemokines in control of T cell traffic. *Nat. Immunol.* 9: 970–980.

226. Cork, M. J., S. G. Danby, and G. S. Ogg. 2020. Atopic dermatitis epidemiology and unmet need in the United Kingdom. *J. Dermatolog. Treat.* 31: 801–809.

227. Proksch, E., R. Fölster-Holst, and J. M. Jensen. 2006. Skin barrier function, epidermal proliferation and differentiation in eczema. *J. Dermatol. Sci.* 43: 159–169.

228. De Benedetto, A., N. M. Rafaels, L. Y. McGirt, A. I. Ivanov, S. N. Georas, C. Cheadle, A. E. Berger, K. Zhang, S. Vidyasagar, T. Yoshida, M. Boguniewicz, T. Hata, L. C. Schneider, J. M. Hanifin, R. L. Gallo, N. Novak, S. Weidinger, T. H. Beaty, D. Y. M. Leung, K. C. Barnes, and L. A. Beck. 2011. Tight junction defects in patients with atopic dermatitis. *J. Allergy Clin. Immunol.* 127: 773-786.e7.

229. Palmer, C. N. A., A. D. Irvine, A. Terron-Kwiatkowski, Y. Zhao, H. Liao, S. P. Lee, D. R. Goudie, A. Sandilands, L. E. Campbell, F.J.D. Smith, G. M. O'Regan, R. M. Watson, J. E. Cecil, S. J. Bale, J. G. Compton, J. J. DiGiovanna, P. Fleckman, S. Lewis-Jones, G. Arseculeratne, A. Sergeant, C. S. Munro, B. El Houate, K. McElreavey, L. B. Halkjaer, H. Bisgaard, S. Mukhopadhyay and W. H. I. McLean. 2006. Common loss-of-function variants of the epidermal barrier protein filaggrin are a major predisposing factor for atopic dermatitis. *Nat. Genet.* 38: 441–446.

230. Seguchi, T., C. Chang-Yi, S. Kusuda, M. Takahashi, K. Aisu, and T. Tezuka. 1996. Decreased expression of filaggrin in atonic skin. *Arch. Dermatol. Res.* 288: 442–446.

231. Kawasaki, H., K. Nagao, A. Kubo, T. Hata, A. Shimizu, H. Mizuno, T. Yamada, and M. Amagai. 2012. Altered stratum corneum barrier and enhanced percutaneous immune responses in filaggrin-null mice. *J. Allergy Clin. Immunol.* 129: 1538-1546.e6.

232. Scharschmidt, T. C., M. Q. Man, Y. Hatano, D. Crumrine, R. Gunathilake, J. P. Sundberg, K. A. Silva, T. M. Mauro, M. Hupe, S. Cho, Y. Wu, A. Celli, M. Schmuth, K. R. Feingold, and P. M. Elias. 2009. Filaggrin deficiency confers a paracellular barrier abnormality that reduces inflammatory thresholds to irritants and haptens. *J. Allergy Clin. Immunol.* 124: 496-506.e6.

233. Brown, S. J., C. L. Relton, H. Liao, Y. Zhao, A. Sandilands, I. J. Wilson, J. Burn, N. J. Reynolds, W. H. I. McLean, and H. J. Cordell. 2008. Filaggrin null mutations and childhood atopic eczema: A population-based case-control study. *J. Allergy Clin. Immunol.* 121: 940-946.e3.

234. Guzik, T. J., M. Bzowska, A. Kasprowicz, G. Czerniawska-Mysik, K. Wójcik, D. Szmyd, T. Adamek-Guzik, and J. Pryjma. 2005. Persistent skin colonization with Staphylococcus aureus in atopic dermatitis: Relationship to clinical and immunological parameters. *Clin. Exp. Allergy* 35: 448–455.

235. Boguniewicz, M., and D. Y. M. Leung. 2011. Atopic dermatitis: A disease of altered skin barrier and immune dysregulation. *Immunol. Rev.* 242: 233–246.

236. Savinko, T., S. Matikainen, U. Saarialho-Kere, M. Lehto, G. Wang, S. Lehtimäki, P. Karisola, T. Reunala, H. Wolff, A. Lauerma, and H. Alenius. 2012. IL-33 and ST2 in atopic dermatitis: Expression profiles and modulation by triggering factors. *J. Invest. Dermatol.* 132: 1392–1400.

237. Hvid, M., C. Vestergaard, K. Kemp, G. B. Christensen, B. Deleuran, and M. Deleuran. 2011. IL-25 in atopic dermatitis: A possible link between inflammation and skin barrier

dysfunction. *J. Invest. Dermatol.* 131: 150–157.

238. Soumelis, V., P. A. Reche, H. Kanzler, W. Yuan, G. Edward, B. Homey, M. Gilliet, S. Ho, S. Antonenko, A. Lauerma, K. Smith, D. Gorman, S. Zurawski, J. Abrams, S. Menon, T. McClanahan, R. De Waal-Malefyt, F. Bazan, R. A. Kastelein, and Y. J. Liu. 2002. Human epithelial cells trigger dendritic cell-mediated allergic inflammation by producing TSLP. *Nat. Immunol.* 3: 673–680.

239. Imai, Y., K. Yasuda, Y. Sakaguchi, T. Haneda, H. Mizutani, T. Yoshimoto, K. Nakanishi, and K. Yamanishi. 2013. Skin-specific expression of IL-33 activates group 2 innate lymphoid cells and elicits atopic dermatitis-like inflammation in mice. *Proc. Natl. Acad. Sci. U. S. A.* 110: 13921–13926.

240. Chen, Y. L., D. Gutowska-Owsiak, C. S. Hardman, M. Westmoreland, T. MacKenzie, L. Cifuentes, D. Waithe, A. Lloyd-Lavery, A. Marquette, M. Londei, and G. Ogg. 2019. Proof-of-concept clinical trial of etokimab shows a key role for IL-33 in atopic dermatitis pathogenesis. *Sci. Transl. Med.* 11: eaax2945.

241. Simpson, E. L., J. R. Parnes, D. She, S. Crouch, W. Rees, M. Mo, and R. van der Merwe. 2019. Tezepelumab, an anti–thymic stromal lymphopoietin monoclonal antibody, in the treatment of moderate to severe atopic dermatitis: A randomized phase 2a clinical trial. *J. Am. Acad. Dermatol.* 80: 1013–1021.

242. Hamid, Q., M. Boguniewicz, and D. Y. M. Leung. 1994. Differential in situ cytokine gene expression in acute versus chronic atopic dermatitis. *J. Clin. Invest.* 94: 870–876.

243. Hamid, Q., T. Naseer, E. M. Minshall, Y. L. Song, M. Boguniewicz, and D. Y. M. Leung. 1996. In vivo expression of IL-12 and IL-13 in atopic dermatitis. *J. Allergy Clin. Immunol.* 98: 225–231.

244. Simpson, E. L., T. Bieber, E. Guttman-Yassky, L. A. Beck, A. Blauvelt, M. J. Cork, J. I. Silverberg, M. Deleuran, Y. Kataoka, J.-P. Lacour, K. Kingo, M. Worm, Y. Poulin, A. Wollenberg, Y. Soo, N. M. H. Graham, G. Pirozzi, B. Akinlade, H. Staudinger, V. Mastey, L. Eckert, A. Gadkari, N. Stahl, G. D. Yancopoulos, and M. Ardeleanu. 2016. Two phase 3 trials of dupilumab versus placebo in atopic dermatitis. *N. Engl. J. Med.* 375: 2335–2348.

245. Cesare, A. Di, P. Di Meglio, and F. O. Nestle. 2008. A role for Th17 cells in the immunopathogenesis of atopic dermatitis? *J. Invest. Dermatol.* 128: 2569–2571.

246. Gittler, J. K., A. Shemer, M. Suárez-Fariñas, J. Fuentes-Duculan, K. J. Gulewicz, C. Q. F. Wang, H. Mitsui, I. Cardinale, C. De Guzman Strong, J. G. Krueger, and E. Guttman-Yassky. 2012. Progressive activation of TH2/TH22 cytokines and selective epidermal

proteins characterizes acute and chronic atopic dermatitis. *J. Allergy Clin. Immunol.* 130: 1344–1354.

247. Seltmann, J., L. M. Roesner, F. W. Von Hesler, M. Wittmann, and T. Werfel. 2015. IL-33 impacts on the skin barrier by downregulating the expression of filaggrin. *J. Allergy Clin. Immunol.* 135: 1659-1661.e4.

248. Howell, M. D., B. E. Kim, P. Gao, A. V. Grant, M. Boguniewicz, A. DeBenedetto, L. Schneider, L. A. Beck, K. C. Barnes, and D. Y. M. Leung. 2009. Cytokine modulation of atopic dermatitis filaggrin skin expression. *J. Allergy Clin. Immunol.* 124: R7–R12.

249. Kim, B. E., D. Y. M. Leung, M. Boguniewicz, and M. D. Howell. 2008. Loricrin and involucrin expression is down-regulated by Th2 cytokines through STAT-6. *Clin. Immunol.* 126: 332–337.

250. Guttman-Yassky, E., R. Bissonnette, B. Ungar, M. Suárez-Fariñas, M. Ardeleanu, H. Esaki, M. Suprun, Y. Estrada, H. Xu, X. Peng, J. I. Silverberg, A. Menter, J. G. Krueger, R. Zhang, U. Chaudhry, B. Swanson, N. M. H. Graham, G. Pirozzi, G. D. Yancopoulos, and J. D. Jennifer. 2019. Dupilumab progressively improves systemic and cutaneous abnormalities in patients with atopic dermatitis. *J. Allergy Clin. Immunol.* 143: 155–172.

251. Sullivan, M., and N. B. Silverberg. 2017. Current and emerging concepts in atopic dermatitis pathogenesis. *Clin. Dermatol.* 35: 349–353.

252. Mashiko, S., H. Mehta, R. Bissonnette, and M. Sarfati. 2017. Increased frequencies of basophils, type 2 innate lymphoid cells and Th2 cells in skin of patients with atopic dermatitis but not psoriasis. *J. Dermatol. Sci.* 88: 167–174.

253. Saunders, S. P., T. Moran, A. Floudas, F. Wurlod, A. Kaszlikowska, M. Salimi, E. M. Quinn, C. J. Oliphant, G. Núñez, R. McManus, E. Hams, A. D. Irvine, A. N. J. McKenzie, G. S. Ogg, and P. G. Fallon. 2016. Spontaneous atopic dermatitis is mediated by innate immunity, with the secondary lung inflammation of the atopic March requiring adaptive immunity. *J. Allergy Clin. Immunol.* 137: 482–491.

254. Imai, Y., K. Yasuda, M. Nagai, M. Kusakabe, M. Kubo, K. Nakanishi, and K. Yamanishi. 2019. IL-33–induced atopic dermatitis–like inflammation in mice is mediated by group 2 innate lymphoid cells in concert with basophils. *J. Invest. Dermatol.* 139: 2185-2194.e3.

255. Wilhelm, C., K. Hirota, B. Stieglitz, J. Van Snick, M. Tolaini, K. Lahl, T. Sparwasser, H. Helmby, and B. Stockinger. 2011. An IL-9 fate reporter demonstrates the induction of an innate IL-9 response in lung inflammation. *Nat. Immunol.* 12: 1071–1077.

256. Stenderup, K., C. Rosada, A. Worsaae, J. T. Clausen, and T. N. Dam. 2007. Interleukin-20 as a target in psoriasis treatment. *Ann. N. Y. Acad. Sci.* 1110: 368–381.

257. Khalifian, S., G. Raimondi, and G. Brandacher. 2015. The use of Luminex assays to measure cytokines. *J. Invest. Dermatol.* 135: e31.

258. Möbus, L., E. Rodriguez, I. Harder, D. Stölzl, N. Boraczynski, S. Gerdes, A. Kleinheinz, S. Abraham, A. Heratizadeh, C. Handrick, E. Haufe, T. Werfel, J. Schmitt, and S. Weidinger. 2021. Atopic dermatitis displays stable and dynamic skin transcriptome signatures. *J. Allergy Clin. Immunol.* 147: 213–223.

259. Hamilton, J. D., M. Suárez-Fariñas, N. Dhingra, I. Cardinale, X. Li, A. Kostic, J. E. Ming, A. R. Radin, J. G. Krueger, N. Graham, G. D. Yancopoulos, G. Pirozzi, and E. Guttman-Yassky. 2014. Dupilumab improves the molecular signature in skin of patients with moderate-to-severe atopic dermatitis. *J. Allergy Clin. Immunol.* 134: 1293–1300.

260. Kiehl, P., K. Falkenberg, M. Vogelbruch, and A. Kapp. 2001. Tissue eosinophilia in acute and chronic atopic dermatitis: A morphometric approach using quantitative image analysis of immunostaining. *Br. J. Dermatol.* 145: 720–729.

261. Menzies-Gow, A., S. Ying, I. Sabroe, V. L. Stubbs, D. Soler, T. J. Williams, and A. B. Kay. 2002. Eotaxin (CCL11) and eotaxin-2 (CCL24) induce recruitment of eosinophils, basophils, neutrophils, and macrophages as well as features of early- and late-phase allergic reactions following cutaneous injection in human atopic and nonatopic volunteers. *J. Immunol.* 169: 2712–2718.

262. Werfel, T., A. Morita, M. Grewe, H. Renz, U. Wahn, J. Krutmann, and A. Kapp. 1996. Allergen specificity of skin-infiltrating T cells is not restricted to a type-2 cytokine pattern in chronic skin lesions of atopic dermatitis. *J. Invest. Dermatol.* 107: 871–876.

263. Boniface, K., F.-X. Bernard, M. Garcia, A. L. Gurney, J.-C. Lecron, and F. Morel. 2005. IL-22 inhibits epidermal differentiation and induces proinflammatory gene expression and migration of human keratinocytes. *J. Immunol.* 174: 3695–3702.

264. Zheng, T., M. H. Oh, S. Y. Oh, J. T. Schroeder, A. B. Glick, and Z. Zhu. 2009. Transgenic expression of interleukin-13 in the skin induces a pruritic dermatitis and skin remodeling. *J. Invest. Dermatol.* 129: 742–751.

265. Schmid, P., D. Simon, H. U. Simon, C. A. Akdis, and B. Wüthrich. 2001. Epidemiology, clinical features, and immunology of the “intrinsic” (non-IgE-mediated) type of atopic dermatitis (constitutional dermatitis). *Allergy Eur. J. Allergy Clin. Immunol.* 56: 841–849.

266. Xue, L., S. L. Gyles, F. R. Wettey, L. Gazi, E. Townsend, M. G. Hunter, and R. Pettipher. 2005. Prostaglandin D 2 causes preferential induction of proinflammatory Th2 cytokine production through an action on chemoattractant receptor-like molecule expressed on Th2 cells. *J. Immunol.* 175: 6531–6536.

267. Kakinuma, T., K. Nakamura, M. Wakugawa, H. Mitsui, Y. Tada, H. Saeki, H. Torii, A. Asahina, N. Onai, K. Matsushima, and K. Tamaki. 2001. Thymus and activation-regulated chemokine in atopic dermatitis: Serum thymus and activation-regulated chemokine level is closely related with disease activity. *J. Allergy Clin. Immunol.* 107: 535–541.

268. Kakinuma, T., K. Nakamura, M. Wakugawa, H. Mitsui, Y. Tada, H. Saeki, H. Torii, M. Komine, A. Asahina, and K. Tamaki. 2002. Serum macrophage-derived chemokine (MDC) levels are closely related with the disease activity of atopic dermatitis. *Clin. Exp. Immunol.* 127: 270–273.

269. Novak, H., A. Müller, N. Harrer, C. Günther, J. M. Carballido, and M. Woisetschläger. 2007. CCL23 expression is induced by IL-4 in a STAT6-dependent fashion. *J. Immunol.* 178: 4335–4341.

270. Lloyd, C. M., T. Delaney, T. Nguyen, J. Tian, C. Martinez-A, A. J. Coyle, and J. C. Gutierrez-Ramos. 2000. CC chemokine receptor (CCR)3/eotaxin is followed by CCR4/monocyte- derived chemokine in mediating pulmonary T helper lymphocyte type 2 recruitment after serial antigen challenge in vivo. *J. Exp. Med.* 191: 265–273.

271. Kagami, S., T. Kakinuma, H. Saeki, Y. Tsunemi, H. Fujita, K. Nakamura, T. Takekoshi, M. Kishimoto, H. Mitsui, H. Torii, M. Komine, A. Asahina, and K. Tamaki. 2003. Significant elevation of serum levels of eotaxin-3/CCL26, but not of eotaxin-2/CCL24, in patients with atopic dermatitis: Serum eotaxin-3/CCL26 levels reflect the disease activity of atopic dermatitis. *Clin. Exp. Immunol.* 134: 309–313.

272. Kakinuma, T., H. Saeki, Y. Tsunemi, H. Fujita, N. Asano, H. Mitsui, Y. Tada, M. Wakugawa, T. Watanabe, H. Torii, M. Komine, A. Asahina, K. Nakamura, and K. Tamaki. 2003. Increased serum cutaneous T cell-attracting chemokine (CCL27) levels in patients with atopic dermatitis and psoriasis vulgaris. *J. Allergy Clin. Immunol.* 111: 592–597.

273. Nakazato, J., M. Kishida, R. Kuroiwa, J. Fujiwara, M. Shimoda, and N. Shinomiya. 2008. Serum levels of Th2 chemokines, CCL17, CCL22, and CCL27, were the important markers of severity in infantile atopic dermatitis. *Pediatr. Allergy Immunol.* 19: 605–613.

274. Pavel, A. B., L. Zhou, A. Diaz, B. Ungar, J. Dan, H. He, Y. D. Estrada, H. Xu, M. Fernandes, Y. Renert-Yuval, J. G. Krueger, and E. Guttman-Yassky. 2020. The proteomic

skin profile of moderate-to-severe atopic dermatitis patients shows an inflammatory signature. *J. Am. Acad. Dermatol.* 82: 690–699.

275. Morales, J., B. Homey, A. P. Vicari, S. Hudak, E. Oldham, J. Hedrick, R. Orozco, N. G. Copeland, N. A. Jenkins, L. M. McEvoy, and A. Zlotnik. 1999. CTACK, a skin-associated chemokine that preferentially attracts skin-homing memory T cells. *Proc. Natl. Acad. Sci. U. S. A.* 96: 14470–14475.

276. Snelgrove, R. J., D. F. Patel, T. Patel, and C. M. Lloyd. 2018. The enigmatic role of the neutrophil in asthma: Friend, foe or indifferent? *Clin. Exp. Allergy* 48: 1275–1285.

277. Cosmi, L., and F. Annunziato. 2017. Group 2 innate lymphoid cells are the earliest recruiters of eosinophils in lungs of patients with allergic asthma. *Am. J. Respir. Crit. Care Med.* 196: 666–668.

278. Kopf, M., H. Baumann, G. Freer, M. Freudenberg, M. Lamers, T. Kishimoto, R. Zinkernagel, H. Bluethmann, and G. Köhler. 1994. Impaired immune and acute-phase responses in interleukin-6-deficient mice. *Nature* 368: 339–342.

279. Lin, Z.-Q., T. Kondo, Y. Ishida, T. Takayasu, and N. Mukaida. 2003. Essential involvement of IL-6 in the skin wound-healing process as evidenced by delayed wound healing in IL-6-deficient mice. *J. Leukoc. Biol.* 73: 713–721.

280. Maggi, L., M. Capone, A. Mazzoni, F. Liotta, L. Cosmi, and F. Annunziato. 2020. Plasticity and regulatory mechanisms of human ILC2 functions. *Immunol. Lett.* 227: 109–116.

281. Jackson, D. J., H. Makrinioti, B. M. J. Rana, B. W. H. Shamji, M. B. Trujillo-Torralbo, J. Footitt, J. Del-Rosario, A. G. Telcian, A. Nikonova, J. Zhu, J. Aniscenko, L. Gogsadze, E. Bakhsoliani, S. Traub, J. Dhariwal, J. Porter, D. Hunt, T. Hunt, T. Hunt, L. A. Stanciu, M. Khaitov, N. W. Bartlett, M. R. Edwards, O. M. Kon, P. Mallia, N. G. Papadopoulos, C. A. Akdis, J. Westwick, M. J. Edwards, D. J. Cousins, R. P. Walton, and S. L. Johnston. 2014. IL-33-Dependent type 2 inflammation during rhinovirus-induced asthma exacerbations in vivo. *Am. J. Respir. Crit. Care Med.* 190: 1373–1382.

282. Rabin, R. L., M. K. Park, F. Liao, R. Swofford, D. Stephany, and J. M. Farber. 1999. Chemokine receptor responses on T cells are achieved through regulation of both receptor expression and signaling. *J. Immunol.* 162: 3840–50.

283. Colantonio, L., H. Recalde, F. Sinigaglia, and D. D'Ambrosio. 2002. Modulation of chemokine receptor expression and chemotactic responsiveness during differentiation of human naive T cells into Th1 or Th2 cells. *Eur. J. Immunol.* 32: 1264–1273.

284. Hirai, H., K. Tanaka, O. Yoshie, K. Ogawa, K. Kenmotsu, Y. Takamori, M. Ichimasa, K. Sugamura, M. Nakamura, S. Takano, and K. Nagata. 2001. Prostaglandin D2 selectively induces chemotaxis in T helper type 2 cells, eosinophils, and basophils via seven-transmembrane receptor CRTH2. *J. Exp. Med.* 193: 255–261.

285. Collins, C., F. W. L. Tsui, and M. J. Shulman. 2002. Induction of the chemokine receptor CXCR3 on TCR-stimulated T cells: Dependence on the release from persistent TCR-triggering and requirement for IFN-γ stimulation. *Eur. J. Immunol.* 32: 1792–1801.

286. Sundrud, M. S., S. M. Grill, D. Ni, K. Nagata, S. S. Alkan, A. Subramaniam, and D. Unutmaz. 2003. Genetic reprogramming of primary human T cells reveals functional plasticity in Th cell differentiation. *J. Immunol.* 171: 3542–3549.

287. Morimoto, Y., Y. Bian, P. Gao, Y. Yashiro-Ohtani, X.-Y. Zhou, S. Ono, H. Nakahara, M. Kogo, T. Hamaoka, and H. Fujiwara. 2005. Induction of surface CCR4 and its functionality in mouse Th2 cells is regulated differently during Th2 development. *J. Leukoc. Biol.* 78: 753–761.

288. Yamazaki, T., X. O. Yang, Y. Chung, A. Fukunaga, R. Nurieva, B. Pappu, N. Martin-Orozco, H. S. Kang, L. Ma, A. D. Panopoulos, S. Craig, S. S. Watowich, A. M. Jetten, Q. Tian, and C. Dong. 2008. CCR6 regulates the migration of inflammatory and regulatory T cells. *J. Immunol.* 181: 8391–8401.

289. Singh, S. P., H. H. Zhang, J. F. Foley, M. N. Hedrick, and J. M. Farber. 2008. Human T Cells that are able to produce IL-17 express the chemokine receptor CCR6. *J. Immunol.* 180: 214–221.

290. Stenstad, H., A. Ericsson, B. Johansson-Lindbom, M. Svensson, J. Marsal, M. Mack, D. Picarella, D. Soler, G. Marquez, M. Briskin, and W. W. Agace. 2006. Gut-associated lymphoid tissue-primed CD4+ T cells display CCR9-dependent and -independent homing to the small intestine. *Blood* 107: 3447–3454.

291. Reiss, Y., A. E. Proudfoot, C. A. Power, J. J. Campbell, and E. C. Butcher. 2002. CC chemokine receptor (CCR)4 and the CCR10 ligand cutaneous T cell–attracting chemokine (CTACK) in lymphocyte trafficking to inflamed skin. *J. Exp. Med.* 194: 1541–1547.

292. Lee, J. H., S. G. Kang, and C. H. Kim. 2007. FoxP3 + T cells undergo conventional first switch to lymphoid tissue homing receptors in thymus but accelerated second switch to nonlymphoid tissue homing receptors in secondary lymphoid tissues. *J. Immunol.* 178: 301–311.

293. Castan, L., A. Magnan, and G. Bouchaud. 2017. Chemokine receptors in allergic

diseases. *Allergy Eur. J. Allergy Clin. Immunol.* 72: 682–690.

294. Masopust, D., and J. M. Schenkel. 2013. The integration of T cell migration, differentiation and function. *Nat. Rev. Immunol.* 13: 309–320.

295. Imai, T., M. Nagira, S. Takagi, M. Kakizaki, M. Nishimura, J. Wang, P. W. Gray, K. Matsushima, and O. Yoshie. 1999. Selective recruitment of CCR4-bearing T(h)2 cells toward antigen-presenting cells by the CC chemokines thymus and activation-regulated chemokine and macrophage-derived chemokine. *Int. Immunol.* 11: 81–88.

296. Yamamoto, J., Y. Adachi, Y. Onoue, Y. S. Adachi, Y. Okabe, T. Itazawa, M. Toyoda, T. Seki, M. Morohashi, K. Matsushima, and T. Miyawaki. 2000. Differential expression of the chemokine receptors by the Th1- and Th2-type effector populations within circulating CD4+ T cells. *J. Leukoc. Biol.* 68: 568–74.

297. Campbell, J. J., G. Haraldsen, J. Pan, J. Rottman, S. Qin, P. Ponath, D. P. Andrew, R. Warnke, N. Ruffing, N. Kassam, L. Wu, and E. C. Butcher. 1999. The chemokine receptor CCR4 in vascular recognition by cutaneous but not intestinal memory T cells. *Nature* 400: 776–780.

298. Soler, D., T. L. Humphreys, S. M. Spinola, and J. J. Campbell. 2003. CCR4 versus CCR10 in human cutaneous TH lymphocyte trafficking. *Blood* 101: 1677–1683.

299. Baatar, D., P. Olkhanud, K. Sumitomo, D. Taub, R. Gress, and A. Biragyn. 2007. Human peripheral blood T regulatory cells (Tregs), functionally primed CCR4 + Tregs and unprimed CCR4 − Tregs, regulate effector T cells using FasL. *J. Immunol.* 178: 4891–4900.

300. Lim, H. W., J. Lee, P. Hillsamer, and C. H. Kim. 2008. Human Th17 cells share major trafficking receptors with both polarized effector T cells and Foxp3 + regulatory T Cells. *J. Immunol.* 180: 122–129.

301. Horikawa, T., T. Nakayama, I. Hikita, H. Yamada, R. Fujisawa, T. Bito, S. Harada, A. Fukunaga, D. Chantry, P. W. Gray, A. Morita, R. Suzuki, T. Tezuka, M. Ichihashi, and O. Yoshie. 2002. IFN-g-inducible expression of thymus and activation-regulated chemokine/CCL17 and macrophage-derived chemokine/CCL22 in epidermal keratinocytes and their roles in atopic dermatitis. *Int. J. Immunol.* 7: 767-773.

302. Purwar, R., T. Werfel, and M. Wittmann. 2006. IL-13-stimulated human keratinocytes preferentially attract CD4+ CCR4+ T cells: Possible role in atopic dermatitis. *J. Invest. Dermatol.* 126: 1043–1051.

303. Panina-Bordignon, P., A. Papi, M. Mariani, P. Di Lucia, G. Casoni, C. Bellettato, C.

Buonsanti, D. Miotto, C. Mapp, A. Villa, G. Arrigoni, L. M. Fabbri, and F. Sinigaglia. 2001. The C-C chemokine receptors CCR4 and CCR8 identify airway T cells of allergen-challenged atopic asthmatics. *J. Clin. Invest.* 107: 1357–1364.

304. Godiska, R., D. Chantry, C. J. Raport, S. Sozzani, P. Allavena, D. Leviten, A. Mantovani, and P. W. Gray. 1997. Human macrophage-derived chemokine (MDC), a novel chemoattractant for monocytes, monocyte-derived dendritic cells, and natural killer cells. *J. Exp. Med.* 185: 1595–1604.

305. Vulcano, M., C. Albanesi, A. Stoppacciaro, R. Bagnati, G. D'Amico, S. Struyf, P. Transidico, R. Bonecchi, A. Del Prete, P. Allavena, L. P. Ruco, C. Chiabrando, G. Girolomoni, A. Mantovani, and S. Sozzani. 2001. Dendritic cells as a major source of macrophage-derived chemokine/CCL22 in vitro and in vivo. *Eur. J. Immunol.* 31: 812–822.

306. Hashimoto, S., K. Nakamura, N. Oyama, F. Kaneko, Y. Tsunemi, H. Saeki, and K. Tamaki. 2006. Macrophage-derived chemokine (MDC)/CCL22 produced by monocyte derived dendritic cells reflects the disease activity in patients with atopic dermatitis. *J. Dermatol. Sci.* 44: 93–99.

307. D'Ambrosio, D., C. Albanesi, R. Lang, G. Girolomoni, F. Sinigaglia, and C. Laudanna. 2002. Quantitative differences in chemokine receptor engagement generate diversity in integrin-dependent lymphocyte adhesion. *J. Immunol.* 169: 2303–2312.

308. Mariani, M., R. Lang, E. Binda, P. Panina-Bordignon, and D. D'Ambrosio. 2004. Dominance of CCL22 over CCL17 in induction of chemokine receptor CCR4 desensitization and internalization on human Th2 cells. *Eur. J. Immunol.* 34: 231–240.

309. Ying, S., B. O'Connor, J. Ratoff, Q. Meng, C. Fang, D. Cousins, G. Zhang, S. Gu, Z. Gao, B. Shamji, M. J. Edwards, T. H. Lee, and C. J. Corrigan. 2008. Expression and cellular provenance of thymic stromal lymphopoietin and chemokines in patients with severe asthma and chronic obstructive pulmonary disease. *J. Immunol.* 181: 2790–2798.

310. Perros, F., H. C. Hoogsteden, A. J. Coyle, B. N. Lambrecht, and H. Hammad. 2009. Blockade of CCR4 in a humanized model of asthma reveals a critical role for DC-derived CCL17 and CCL22 in attracting Th2 cells and inducing airway inflammation. *Allergy* 64: 995–1002.

311. Kunkel, J. E., J. Boisvert, K. Murphy, M. A. Vierra, M. C. Genovese, A. J. Wardlaw, H. B. Greenberg, M. R. Hodge, L. Wu, E. C. Butcher, J. J. Campbell, J. K. Eric, J. Boisvert, K. Murphy, M. A. Vierra, M. C. Genovese, A. J. Wardlaw, H. B. Greenberg, M. R. Hodge, L. Wu, E. C. Butcher, and J. J. Campbell. 2002. Expression of the chemokine receptors CCR4,

CCR5, and CXCR3 by human tissue-infiltrating lymphocytes. *Am. J. Pathol.* 160: 347–355.

312. Chong, B. F., J.-E. Murphy, T. S. Kupper, and R. C. Fuhlbrigge. 2004. E-selectin, thymus- and activation-regulated chemokine/CCL17, and intercellular adhesion molecule-1 are constitutively coexpressed in dermal microvessels: A foundation for a cutaneous immunosurveillance system. *J. Immunol.* 172: 1575–1581.

313. Sather, B. D., P. Treuting, N. Perdue, M. Miazgowicz, J. D. Fontenot, A. Y. Rudensky, and D. J. Campbell. 2007. Altering the distribution of Foxp3+ regulatory T cells results in tissue-specific inflammatory disease. *J. Exp. Med.* 204: 1335–1347.

314. Ishida, T., A. Ito, F. Sato, S. Kusumoto, S. Iida, H. Inagaki, A. Morita, S. Akinaga, and R. Ueda. 2013. Stevens-Johnson Syndrome associated with mogamulizumab treatment of adult T-cell leukemia/lymphoma. *Cancer Sci.* 104: 647–650.

315. Shimada, Y., K. Takehara, and S. Sato. 2004. Both Th2 and Th1 chemokines (TARC/CCL17, MDC/CCL22, and Mig/CXCL9) are elevated in sera from patients with atopic dermatitis. *J. Dermatol. Sci.* 34: 201–208.

316. Zheng, X., K. Nakamura, H. Furukawa, A. Nishibu, M. Takahashi, M. Tojo, F. Kaneko, T. Kakinuma, K. Tamaki, T. Kakinuma, M. Takahashi, K. Nakamura, H. Furukawa, A. Nishibu, and F. Kaneko. 2015. Demonstration of TARC and CCR4 mRNA expression and distribution using in situ RT-PCR in the lesional skin of atopic dermatitis. *J. Dermatol.* 30: 26–32.

317. Wakugawa, M., K. Nakamura, T. Kakinuma, N. Onai, K. Matsushima, and K. Tamaki. 2001. CC chemokine receptor 4 expression on peripheral blood CD4+ T cells reflects disease activity of atopic dermatitis. *J. Invest. Dermatol.* 117: 188–196.

318. Tsunemi, Y., H. Saeki, K. Nakamura, D. Nagakubo, T. Nakayama, O. Yoshie, S. Kagami, K. Shimazu, T. Kadono, M. Sugaya, M. Komine, K. Matsushima, and K. Tamaki. 2006. CCL17 transgenic mice show an enhanced Th2-type response to both allergic and non-allergic stimuli. *Eur. J. Immunol.* 36: 2116–2127.

319. Gong, J. Q., L. Lin, T. Lin, F. Hao, F. Q. Zeng, Z. G. Bi, D. Yi, and B. Zhao. 2006. Skin colonization by Staphylococcus aureus in patients with eczema and atopic dermatitis and relevant combined topical therapy: A double-blind multicentre randomized controlled trial. *Br. J. Dermatol.* 155: 680–687.

320. Miyano, K., S. Matsushita, T. Tsuchida, and K. Nakamura. 2016. Inhibitory effect of a histamine 4 receptor antagonist on CCL17 and CCL22 production by monocyte-derived Langerhans cells in patients with atopic dermatitis. *J. Dermatol.* 43: 1024–1029.

321. Matsuo, K., S. Hatanaka, Y. Kimura, Y. Hara, K. Nishiwaki, Y. S. Quan, F. Kamiyama, N. Oiso, A. Kawada, K. Kabashima, and T. Nakayama. 2019. A CCR4 antagonist ameliorates atopic dermatitis-like skin lesions induced by dibutyl phthalate and a hydrogel patch containing ovalbumin. *Biomed. Pharmacother.* 109: 1437–1444.

322. Matsuo, K., D. Nagakubo, Y. Komori, S. Fujisato, N. Takeda, M. Kitamatsu, K. Nishiwaki, Y. S. Quan, F. Kamiyama, N. Oiso, A. Kawada, O. Yoshie, and T. Nakayama. 2018. CCR4 Is critically involved in skin allergic inflammation of BALB/c mice. *J. Invest. Dermatol.* 138: 1764–1773.

323. Kim, C. H., S. Hashimoto-Hill, and M. Kim. 2016. Migration and tissue tropism of innate lymphoid cells. *Trends Immunol.* 37: 68–79.

324. Puttur, F., L. Denney, L. G. Gregory, J. Vuononvirta, R. Oliver, L. J. Entwistle, S. A. Walker, M. B. Headley, E. J. McGhee, J. E. Pease, M. F. Krummel, L. M. Carlin, and C. M. Lloyd. 2019. Pulmonary environmental cues drive group 2 innate lymphoid cell dynamics in mice and humans. *Sci. Immunol.* 4: 7638.

325. Stier, M. T., J. Zhang, K. Goleniewska, J. Y. Cephus, M. Rusznak, L. Wu, L. Van Kaer, B. Zhou, D. C. Newcomb, and R. S. Peebles. 2018. IL-33 promotes the egress of group 2 innate lymphoid cells from the bone marrow. 215: 263–281.

326. Crapster-Pregont, M., J. Yeo, R. L. Sanchez, and D. A. Kuperman. 2012. Dendritic cells and alveolar macrophages mediate IL-13-induced airway inflammation and chemokine production. *J. Allergy Clin. Immunol.* 129: 1621-1627.e3.

327. Yoshie, O., and K. Matsushima. 2015. CCR4 and its ligands: From bench to bedside. *Int. Immunol.* 27: 11–20.

328. Bartemes, K. R., G. M. Kephart, S. J. Fox, and H. Kita. 2014. Enhanced innate type 2 immune response in peripheral blood from patients with asthma. *J. Allergy Clin. Immunol.* 134: 671-678.e4.

329. Su, Z., J. Lin, F. Lu, X. Zhang, L. Zhang, N. B. Gandhi, C. S. De Paiva, S. C. Pflugfelder, and D. Q. Li. 2013. Potential autocrine regulation of interleukin-33/ST2 signaling of dendritic cells in allergic inflammation. *Mucosal Immunol.* 6: 921–930.

330. Claudio, E., I. Tassi, H. Wang, W. Tang, H. Ha, and U. Siebenlist. 2015. Cutting edge: IL-25 targets dendritic cells To attract IL-9–producing T cells in acute allergic lung inflammation. *J. Immunol.* 195: 3525–3529.

331. Clark, R. A., B. Chong, N. Mirchandani, N. K. Brinster, K. Yamanaka, R. K. Dowgiert,

and T. S. Kupper. 2006. The vast majority of CLA + T cells are resident in normal skin. *J. Immunol.* 176: 4431–4439.

332. Shih, H. Y., G. Sciumè, Y. Mikami, L. Guo, H. W. Sun, S. R. Brooks, J. F. Urban, F. P. Davis, Y. Kanno, and J. J. O'Shea. 2016. Developmental acquisition of regulomes underlies innate lymphoid cell functionality. *Cell* 165: 1120–1133.

333. Drake, L. Y., K. Iijima, and H. Kita. 2014. Group 2 innate lymphoid cells and CD4+ T cells cooperate to mediate type 2 immune response in mice. *Allergy Eur. J. Allergy Clin. Immunol.* 69: 1300–1307.

334. Halim, T. Y. F., B. M. J. Rana, J. A. Walker, B. Kerscher, M. D. Knolle, H. E. Jolin, E. M. Serrao, L. Haim-Vilmovsky, S. A. Teichmann, H. R. Rodewald, M. Botto, T. J. Vyse, P. G. Fallon, Z. Li, D. R. Withers, and A. N. J. McKenzie. 2018. Tissue-restricted adaptive Type 2 immunity Is orchestrated by expression of the costimulatory molecule OX40L on group 2 innate lymphoid cells. *Immunity* 48: 1195-1207.e6.

335. Sallusto, F., and A. Lanzavecchi. 1994. Efficient presentation of soluble antigen by cultured human dendritic cells is maintained by granulocyte/macrophage colony-stimulating factor plus iuterleukin 4 and downregulated by tumor necrosis factor α. *J. Exp. Med.* 179: 1109–1118.

336. Menetrier-Caux, C., M. C. Thomachot, L. Alberti, G. Montmain, and J. Y. Blay. 2001. Il-4 prevents the blockade of dendritic cell differentiation induced by tumor cells. *Cancer Res.* 61: 3096–3104.

337. Chapuis, F., M. Rosenzwajg, M. Yagello, M. Ekman, P. Biberfeld, and J. C. Gluckman. 1997. Differentiation of human dendritic cells from monocytes in vitro. *Eur. J. Immunol.* 27: 431–441.

338. Palucka, K. A., N. Taquet, F. Sanchez-Chapuis, and J. C. Gluckman. 1998. Dendritic cells as the terminal stage of monocyte differentiation. *J. Immunol.* 160: 4587–95.

339. Romani, N., D. Reider, M. Heuer, S. Ebner, E. Kämpgen, B. Eibl, D. Niederwieser, and G. Schuler. 1996. Generation of mature dendritic cells from human blood An improved method with special regard to clinical applicability. *J. Immunol. Methods* 196: 137–151.

340. Beitnes, A. C. R., M. Ráki, M. Brottveit, K. E. A. Lundin, F. L. Jahnsen, and L. M. Sollid. 2012. Rapid accumulation of CD14 +CD11c + dendritic cells in gut mucosa of celiac disease after in vivo gluten challenge. *PLoS One* 7: e33556.

341. Randolph, G. J., K. Inaba, D. F. Robbiani, R. M. Steinman, and W. A. Muller. 1999.

Differentiation of phagocytic monocytes into lymph node dendritic cells in vivo. *Immunity* 11: 753–761.

342. Plantinga, M., M. Guilliams, M. Vanheerswynghels, K. Deswarte, F. Branco-Madeira, W. Toussaint, L. Vanhoutte, K. Neyt, N. Killeen, B. Malissen, H. Hammad, and B. N. Lambrecht. 2013. Conventional and monocyte-derived CD11b+ dendritic cells initiate and maintain T helper 2 cell-mediated immunity to house dust mite allergen. *Immunity* 38: 322–335.

343. Guttman-Yassky, E., M. A. Lowes, J. Fuentes-Duculan, J. Whynot, I. Novitskaya, I. Cardinale, A. Haider, A. Khatcherian, J. A. Carucci, R. Bergman, and J. G. Krueger. 2007. Major differences in inflammatory dendritic cells and their products distinguish atopic dermatitis from psoriasis. *J. Allergy Clin. Immunol.* 119: 1210–1217.

344. Barral, D. C., and M. B. Brenner. 2007. CD1 antigen presentation: How it works. *Nat. Rev. Immunol.* 7: 929–941.

345. Van Kaer, L., L. Wu, and S. Joyce. 2016. Mechanisms and consequences of antigen presentation by CD1. *Trends Immunol.* 37: 738–754.

346. de Jong, A., and G. Ogg. 2021. CD1a function in human skin disease. *Mol. Immunol.* 130: 14–19.

347. Zajonc, D. M., M. A. Elsliger, L. Teyton, and I. A. Wilson. 2003. Crystal structure of CD1a in complex with a sulfatide self antigen at a resolution of 2.15 Å. *Nat. Immunol.* 4: 808–815.

348. Cernadas, M., M. Cavallari, G. Watts, L. Mori, G. De Libero, and M. B. Brenner. 2010. Early recycling compartment trafficking of CD1a is essential for its intersection and presentation of lipid antigens. *J. Immunol.* 184: 1235–1241.

349. De Jong, A., V. Peña-Cruz, T. Y. Cheng, R. A. Clark, I. Van Rhijn, and D. B. Moody. 2010. CD1a-autoreactive T cells are a normal component of the human αβ T cell repertoire. *Nat. Immunol.* 11: 1102–1109.

350. De Jong, A., T. Y. Cheng, S. Huang, S. Gras, R. W. Birkinshaw, A. G. Kasmar, I. Van Rhijn, V. Peña-Cruz, D. T. Ruan, J. D. Altman, J. Rossjohn, and D. B. Moody. 2014. CD1a-autoreactive T cells recognize natural skin oils that function as headless antigens. *Nat. Immunol.* 15: 177–185.

351. Birkinshaw, R. W., D. G. Pellicci, T. Y. Cheng, A. N. Keller, M. Sandoval-Romero, S. Gras, A. De Jong, A. P. Uldrich, D. B. Moody, D. I. Godfrey, and J. Rossjohn. 2015. αβ T

cell antigen receptor recognition of CD1a presenting self lipid ligands. *Nat. Immunol.* 16: 258–266.

352. Cotton, R. N., T. Y. Cheng, M. Wegrecki, J. Le Nours, D. P. Orgill, B. Pomahac, S. G. Talbot, R. A. Willis, J. D. Altman, A. de Jong, G. Ogg, I. Van Rhijn, J. Rossjohn, R. A. Clark, and D. B. Moody. 2021. Human skin is colonized by T cells that recognize CD1a independently of lipid. *J. Clin. Invest.* 131.

353. Zajonc, D. M., M. D. M. Crispin, T. A. Bowden, D. C. Young, T. Y. Cheng, J. Hu, C. E. Costello, P. M. Rudd, R. A. Dwek, M. J. Miller, M. B. Brenner, D. B. Moody, and I. A. Wilson. 2005. Molecular mechanism of lipopeptide presentation by CD1a. *Immunity* 22: 209–219.

354. Moody, D. B., D. C. Young, T. Y. Cheng, J. P. Rosat, C. Roura-Mir, P. B. O'Connor, D. M. Zajonc, A. Walz, M. J. Miller, S. B. Levery, I. A. Wilson, C. E. Costello, and M. B. Brenner. 2004. T Cell activation by lipopeptide antigens. *Science* 303: 527–531.

355. Peña-Cruz, V., S. Ito, C. C. Dascher, M. B. Brenner, and M. Sugita. 2003. Epidermal Langerhans cells efficiently mediate CD1a-dependent presentation of microbial lipid antigens to T cells. *J. Invest. Dermatol.* 121: 517–521.

356. Angel, C. E., E. George, A. E. S. Brooks, L. L. Ostrovsky, T. L. H. Brown, and P. R. Dunbar. 2006. Cutting edge: CD1a+ antigen-presenting cells in human dermis respond rapidly to CCR7 ligands. *J. Immunol.* 176: 5730–5734.

357. Chen, Y.-L., T. Gomes, C. S. Hardman, F. A. Vieira Braga, D. Gutowska-Owsiak, M. Salimi, N. Gray, D. A. Duncan, G. Reynolds, D. Johnson, M. Salio, V. Cerundolo, J. L. Barlow, A. N. J. McKenzie, S. A. Teichmann, M. Haniffa, and G. Ogg. 2020. Re-evaluation of human BDCA-2+ DC during acute sterile skin inflammation. *J. Exp. Med.* 217: e20190811.

358. Shi, C., and E. G. Pamer. 2011. Monocyte recruitment during infection and inflammation. *Nat. Rev. Immunol.* 11: 762–774.

359. Leslie, D. S., C. C. Dascher, K. Cembrola, M. A. Townes, D. L. Hava, L. C. Hugendubler, E. Mueller, L. Fox, C. Roura-Mir, D. B. Moody, M. S. Vincent, J. E. Gumperz, P. A. Illarionov, G. S. Besra, C. G. Reynolds, and M. B. Brenner. 2008. Serum lipids regulate dendritic cell CD1 expression and function. *Immunology* 125: 289–301.

360. Geijtenbeek, T. B. H., R. Torensma, S. J. Van Vliet, G. C. F. Van Duijnhoven, G. J. Adema, Y. Van Kooyk, and C. G. Figdor. 2000. Identification of DC-SIGN, a novel dendritic cell-specific ICAM-3 receptor that supports primary immune responses. *Cell* 100: 575–585.

361. Dauer, M., B. Obermaier, J. Herten, C. Haerle, K. Pohl, S. Rothenfusser, M. Schnurr, S. Endres, and A. Eigler. 2003. Mature dendritic cells derived from human monocytes within 48 hours: A novel strategy for dendritic cell differentiation from blood precursors. *J. Immunol.* 170: 4069–4076.

362. Hubo, M., B. Trinschek, F. Kryczanowsky, A. Tuettenberg, K. Steinbrink, and H. Jonuleit. 2013. Costimulatory molecules on immunogenic versus tolerogenic human dendritic cells. *Front. Immunol.* 4: 82.

363. Coillard, A., and E. Segura. 2019. In vivo differentiation of human monocytes. *Front. Immunol.* 10: 1907.

364. Patel, A. A., Y. Zhang, J. N. Fullerton, L. Boelen, A. Rongvaux, A. A. Maini, V. Bigley, R. A. Flavell, D. W. Gilroy, B. Asquith, D. Macallan, and S. Yona. 2017. The fate and lifespan of human monocyte subsets in steady state and systemic inflammation. *J. Exp. Med.* 214: 1913–1923.

365. Mortha, A., and K. Burrows. 2018. Cytokine networks between innate lymphoid cells and myeloid cells. *Front. Immunol.* 9: 1.

366. Sander, J., S. V. Schmidt, B. Cirovic, N. McGovern, O. Papantonopoulou, A. L. Hardt, A. C. Aschenbrenner, C. Kreer, T. Quast, A. M. Xu, L. M. Schmidleithner, H. Theis, L. Do Thi Huong, H. R. Bin Sumatoh, M. A. R. Lauterbach, J. Schulte-Schrepping, P. Günther, J. Xue, K. Baßler, T. Ulas, K. Klee, N. Katzmarski, S. Herresthal, W. Krebs, B. Martin, E. Latz, K. Händler, M. Kraut, W. Kolanus, M. Beyer, C. S. Falk, B. Wiegmann, S. Burgdorf, N. A. Melosh, E. W. Newell, F. Ginhoux, A. Schlitzer, and J. L. Schultze. 2017. Cellular differentiation of human monocytes Is regulated by time-dependent interleukin-4 signaling and the transcriptional regulator NCOR2. *Immunity* 47: 1051-1066.e12.

367. Albanesi, C., A. Cavani, and G. Girolomoni. 1998. Interferon-γ-stimulated human keratinocytes express the genes necessary for the production of peptide-loaded MHC class II molecules. *J. Invest. Dermatol.* 110: 138–142.

368. Callard, R. E., and J. I. Harper. 2007. The skin barrier, atopic dermatitis and allergy: a role for Langerhans cells? *Trends Immunol.* 28: 294–298.

369. Larregina, A. T., A. E. Morelli, L. A. Spencer, A. J. Logar, S. C. Watkins, A. W. Thomson, and L. D. Falo. 2001. Dermal-resident CD14+ cells differentiate into Langerhans cells. *Nat. Immunol.* 2: 1151–1158.

370. Bellmann, L., C. Zelle-Rieser, P. Milne, A. Resteu, C. H. Tripp, N. Hermann-Kleiter, V. Zaderer, D. Wilflingseder, P. Hörtnagl, M. Theochari, J. Schulze, M. Rentzsch, B. Del Frari,

M. Collin, C. Rademacher, N. Romani, and P. Stoitzner. 2021. Notch-mediated generation of monocyte-derived Langerhans cells: Phenotype and function. *J. Invest. Dermatol.* 141: 84-94.e6.

371. Raker, V. K., M. P. Domogalla, and K. Steinbrink. 2015. Tolerogenic dendritic cells for regulatory T cell induction in man. *Front. Immunol.* 6: 569.

372. Jenner, W., M. Motwani, K. Veighey, J. Newson, T. Audzevich, A. Nicolaou, S. Murphy, R. MacAllister, and D. W. Gilroy. 2014. Characterisation of leukocytes in a human skin blister model of acute inflammation and resolution. *PLoS One* 9: e89375.

373. Eguíluz-Gracia, I., A. Bosco, R. Dollner, G. R. Melum, M. H. Lexberg, A. C. Jones, S. A. Dheyauldeen, P. G. Holt, E. S. Bækkevold, and F. L. Jahnsen. 2016. Rapid recruitment of CD14+ monocytes in experimentally induced allergic rhinitis in human subjects. *J. Allergy Clin. Immunol.* 137: 1872-1881.e12.

374. Cheung, K. L., R. Jarrett, S. Subramaniam, M. Salimi, D. Gutowska-Owsiak, Y. L. Chen, C. Hardman, L. Xue, V. Cerundolo, and G. Ogg. 2016. Psoriatic T cells recognize neolipid antigens generated by mast cell phospholipase delivered by exosomes and presented by CD1a. *J. Exp. Med.* 213: 2399–2412.

375. Peng, Y. Q., Z. L. Qin, S. Bin Fang, Z. Bin Xu, H. Y. Zhang, D. Chen, Z. Liu, J. A. Bellanti, S. G. Zheng, and Q. L. Fu. 2020. Effects of myeloid and plasmacytoid dendritic cells on ILC2s in patients with allergic rhinitis. *J. Allergy Clin. Immunol.* 145: 855-867.e8.

376. Sallusto, F., P. Schaerli, P. Loetscher, C. Schaniel, D. Lenig, C. R. Mackay, S. Qin, and A. Lanzavecchia. 1998. Rapid and coordinated switch in chemokine receptor expression during dendritic cell maturation. *Eur. J. Immunol.* 28: 2760–2769.

377. Xiao, T., H. Fujita, H. Saeki, H. Mitsui, M. Sugaya, Y. Tada, T. Kakinuma, H. Torii, K. Nakamura, A. Asahina, and K. Tamaki. 2003. Thymus and activation-regulated chemokine (TARC/CCL17) produced by mouse epidermal Langerhans cells is upregulated by TNF-α and IL-4 and downregulated by IFN-γ. *Cytokine* 23: 126–132.

378. Vestergaard, C., H. Just, J. Baumgartner Nielsen, K. Thestrup-Pedersen, and M. Deleuran. 2004. Expression of CCR2 on monocytes and macrophages in chronically inflamed skin in atopic dermatitis and psoriasis. *Acta Derm. Venereol.* 84: 353–358.

379. Gros, E., C. Bussmann, T. Bieber, I. Förster, and N. Novak. 2009. Expression of chemokines and chemokine receptors in lesional and nonlesional upper skin of patients with atopic dermatitis. *J. Allergy Clin. Immunol.* 124: 753-760.e1.

380. Thepen, T., E. G. Langeveld-Wildschut, I. C. Bihari, D. F. Van Wichen, F. C. Van Reijsen, G. C. Mudde, and C. A. F. M. Bruijnzeel-Koomen. 1996. Biphasic response against aeroallergen in atopic dermatitis showing a switch from an initial T(H2) response to a T(H1) response in situ: An immunocytochemical study. *J. Allergy Clin. Immunol.* 97: 828–837.

381. Grewe, M., K. Gyufko, E. Schöpf, and J. Krutmann. 1994. Lesional expression of interferon-γ in atopic eczema. *Lancet* 343: 25–26.

382. Pastore, S., S. Corinti, M. La Placa, B. Didona, and G. Girolomoni. 1998. Interferon-γ promotes exaggerated cytokine production in keratinocytes cultured from patients with atopic dermatitis. *J. Allergy Clin. Immunol.* 101: 538–544.

383. Klunker, S., A. Trautmann, M. Akdis, J. Verhagen, P. Schmid-Grendelmeier, K. Blaser, and C. A. Akdis. 2003. A second step of chemotaxis after transendothelial migration: Keratinocytes undergoing apoptosis release IFN-γ-inducible protein 10, monokine induced by IFN-γ, and IFN-γ-inducible α-chemoattractant for T cell chemotaxis toward epidermis in atopic dermatit. *J. Immunol.* 171: 1078–1084.

384. Rebane, A., M. Zimmermann, A. Aab, H. Baurecht, A. Koreck, M. Karelson, K. Abram, T. Metsalu, M. Pihlap, N. Meyer, R. Fölster-Holst, N. Nagy, L. Kemeny, K. Kingo, J. Vilo, T. Illig, M. Akdis, A. Franke, N. Novak, S. Weidinger, and C. A. Akdis. 2012. Mechanisms of IFN-γ-induced apoptosis of human skin keratinocytes in patients with atopic dermatitis. *J. Allergy Clin. Immunol.* 129: 1297–1306.

385. Kim, B. S. 2015. Innate lymphoid cells in the skin. *J. Invest. Dermatol.* 135: 673–678.

Appendix

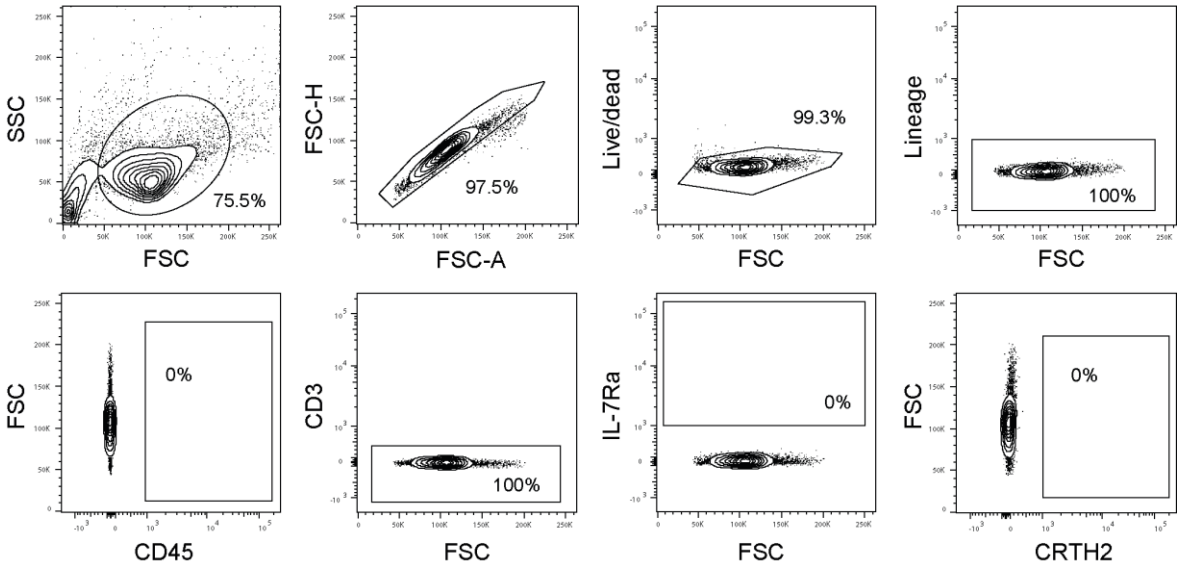


Figure A. 1 FMO controls for gating strategy of ILC2 analysis.

ILC2 were identified as Lin^{-} $CD45^{+}$ $CD3^{-}$ IL-7Rα^{+} $CRTH2^{+}$ cells.

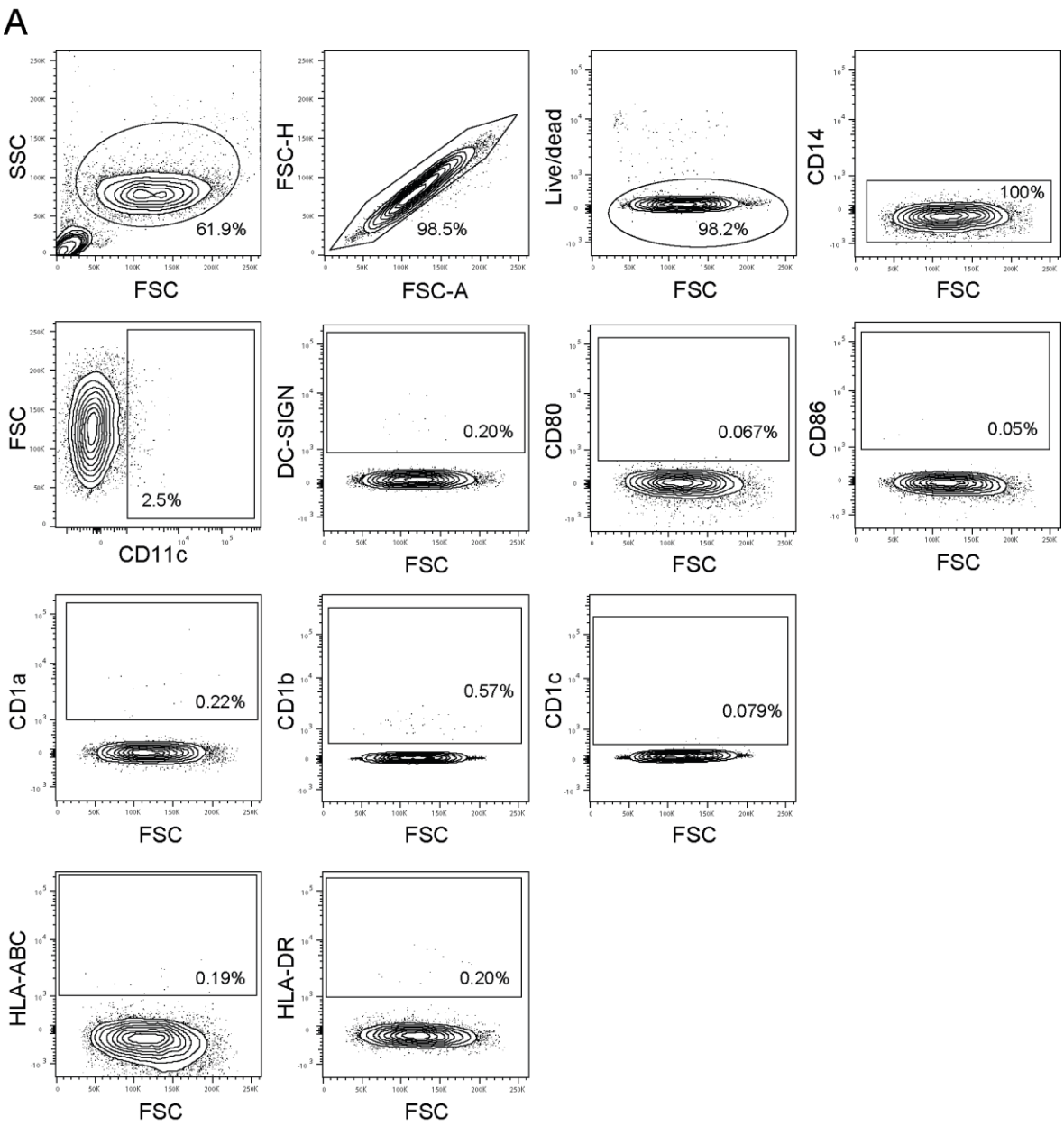


Figure A. 2 FMO controls for gating strategy of moDC analysis.

MoDC were identified as $CD14^{-}$ $CD11c^{+}$ and expression of cell surface markers (DC-SIGN, CD80, CD86, CD1a, CD1b, CD1c, HLA-ABC, HLA-DR) analysed.

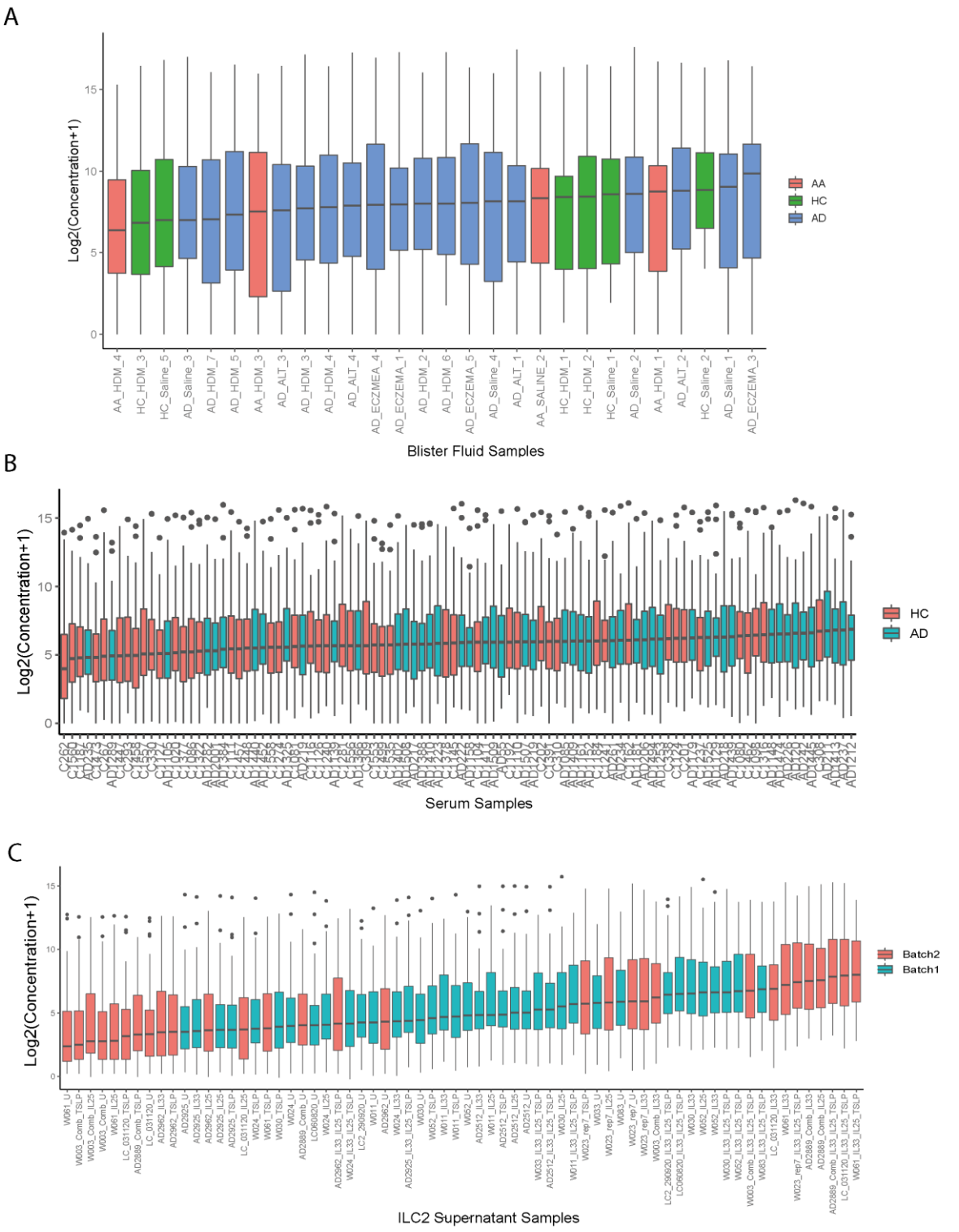
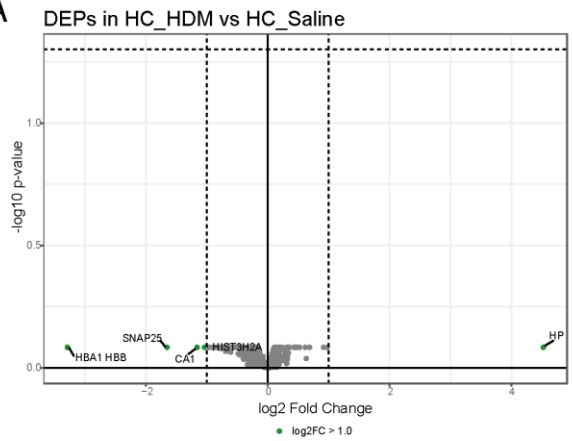
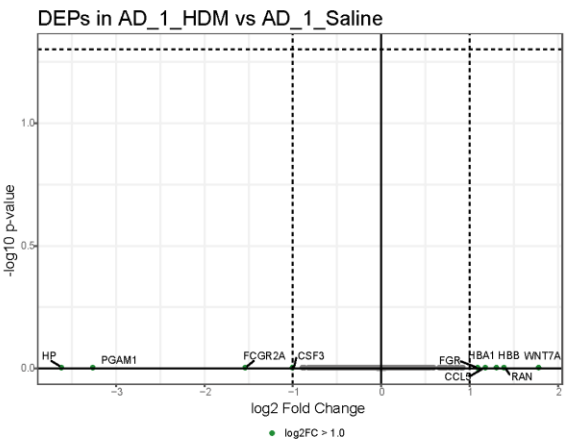


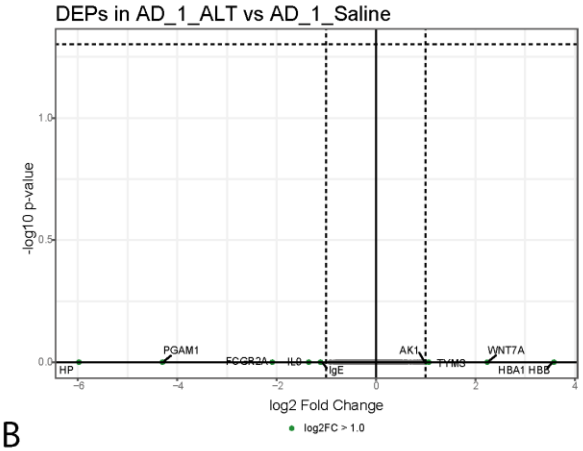
Figure A. 3 Luminex data distribution.

(**A-C**) Luminex data was pre-processed by log2(concentration+1). Data distribution of Luminex results on skin suction blister fluids (**A**), on serum samples (**B**) and ILC2 supernatants following batch correction (**C**). HC = healthy controls; AA = atopic asymptomatic; AD = individuals with atopic dermatitis;

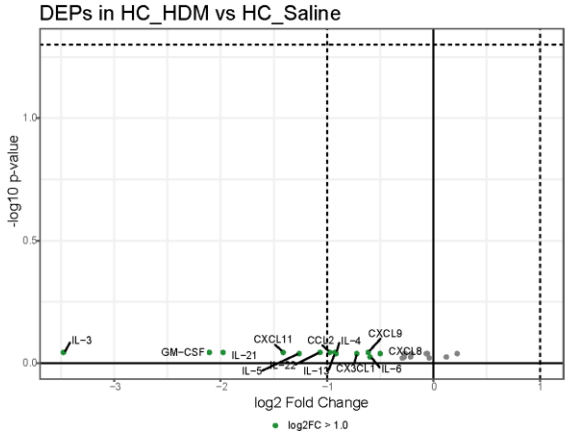
A

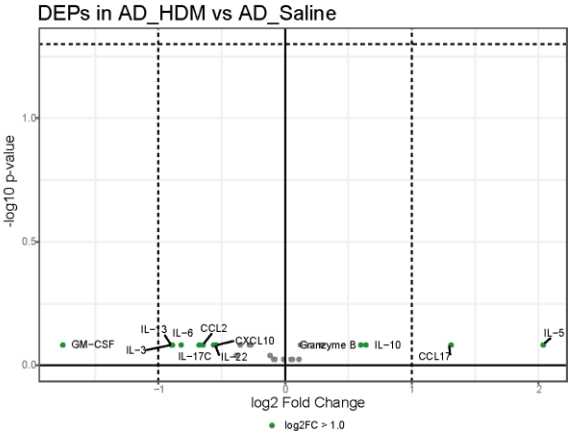

DEPs in HC_HDM vs HC_Saline
-log10 p-value
log2 Fold Change
log2FC > 1.0
SNAP25
HBA1 HBB
CA1
HIST3H2A
HP

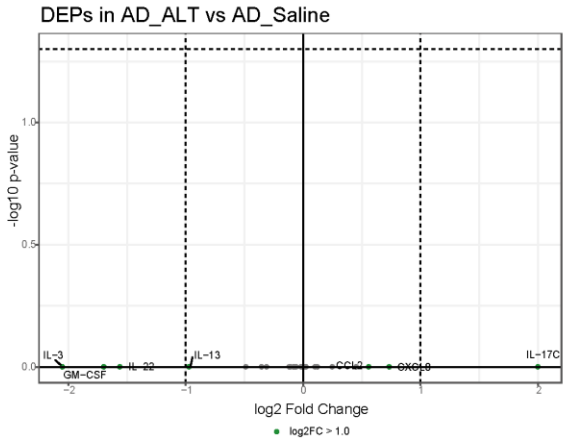

DEPs in AD_1_HDM vs AD_1_Saline
-log10 p-value
log2 Fold Change
log2FC > 1.0
HP
PGAM1
FCGR2A
CSF3
FGR
HBA1 HBB
WNT7A
CCL5
RAN


DEPs in AD_1_ALT vs AD_1_Saline
-log10 p-value
log2 Fold Change
log2FC > 1.0
HP
PGAM1
FCGR2A
IL6
IgE
AK1
TYMS
WNT7A
HBA1 HBB

B


DEPs in HC_HDM vs HC_Saline
-log10 p-value
log2 Fold Change
log2FC > 1.0
IL-3
GM-CSF
IL-21
CXCL11
CCL2
IL-4
CXCL9
CXCL8
IL-5
IL-22
IL-17
CX3CL1
IL-6


DEPs in AD_HDM vs AD_Saline
-log10 p-value
log2 Fold Change
log2FC > 1.0
GM-CSF
IL-13
IL-6
CCL2
IL-3
CXCL10
IL-17C
IL-22
Granzyme B
IL-10
CCL17
IL-5


DEPs in AD_ALT vs AD_Saline
-log10 p-value
log2 Fold Change
log2FC > 1.0
IL-3
GM-CSF
IL-22
IL-13
CCL2
CXCL8
IL-17C

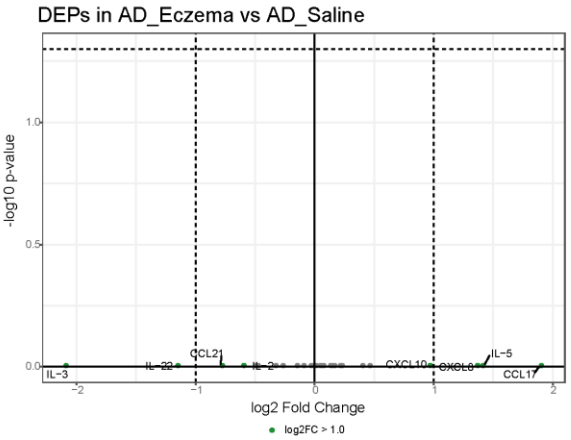

DEPs in AD_Eczema vs AD_Saline
-log10 p-value
log2 Fold Change
log2FC > 1.0
IL-3
IL-22
CCL21
IL-2
CXCL10
CXCL8
IL-5
CCL17

Figure A. 4 Comparison of cutaneous protein expression profiles of AD and HC subjects following intradermal allergen challenge measured by SOMAscan and Luminex.

(**A-B**) Volcano plots visualising blister fluid protein expression differences following intradermal injection of saline, HDM and ALT and differences between lesional and non-lesional saline-treated AD skin as measured by SOMAscan (**A**) and Luminex assay (**B**). DEPs were identified by limma (**A**) or Student's *t*-test (**B**) followed by BH-multiple testing correction (BH-adjusted p-value <0.05; log2FC >1.0).

Table A. 1 Skin suction blister fluids analysed by Luminex multianalyte profiling.

Participants (Disease status)	Intradermal Challenge	Number of Participants
Healthy control (HC)	Saline (Nil)	3
	House dust mite (HDM)	4
Atopic asymptomatic (AA)	Saline (Nil)	1
	House dust mite (HDM)	2
Atopic dermatitis (AD)	Saline (Nil)	4
	House dust mite (HDM)	6
	Alternaria alternata (ALT)	4
	Lesional skin (Eczema)	4

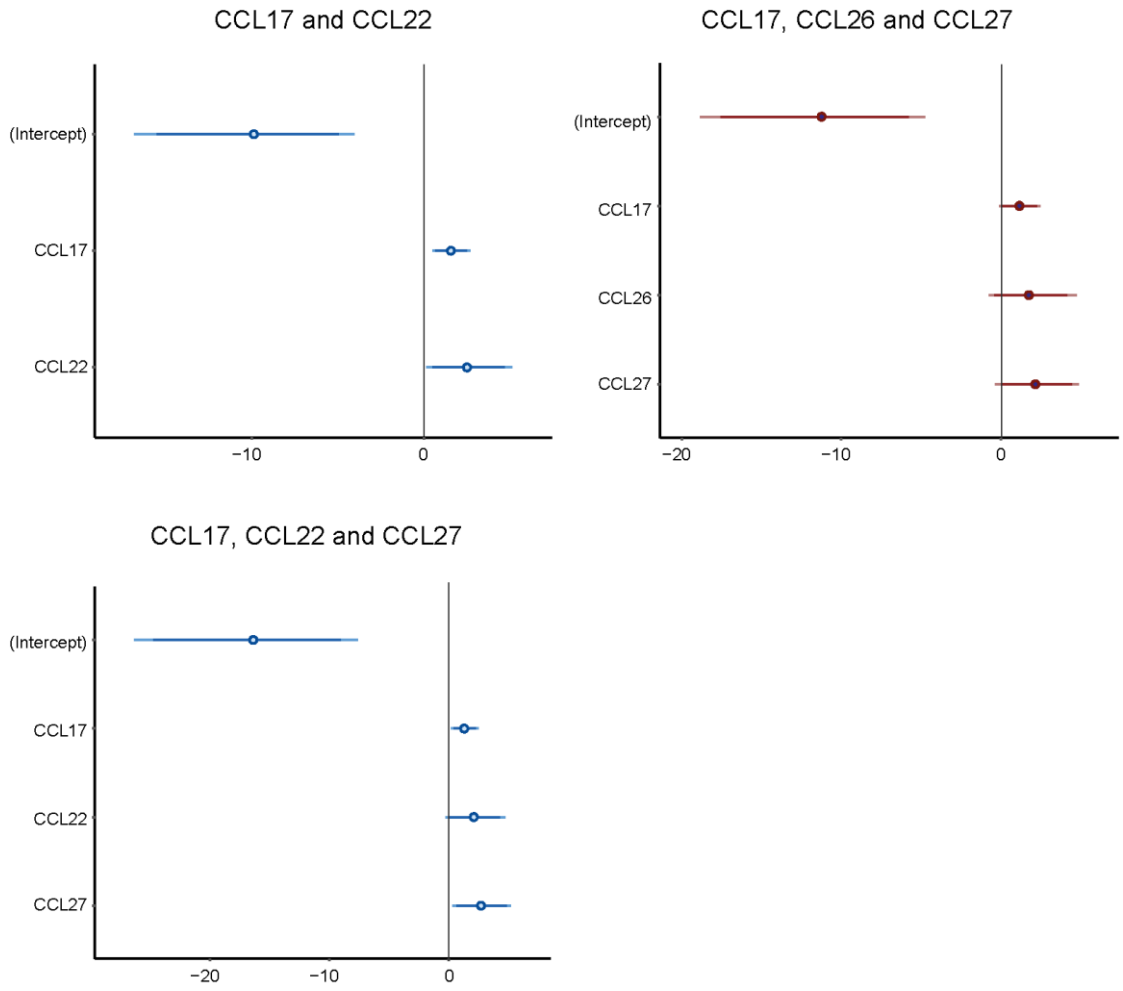


Figure A. 5 Posterior distribution of multivariate logistic regression model.
Multivariate logistic regression modelling was performed on Luminex serum data to test serum levels of CCL17, CCL22, CCL26 and CCL17 as predictors of AD. Posterior distribution with 95% high density credible intervals.

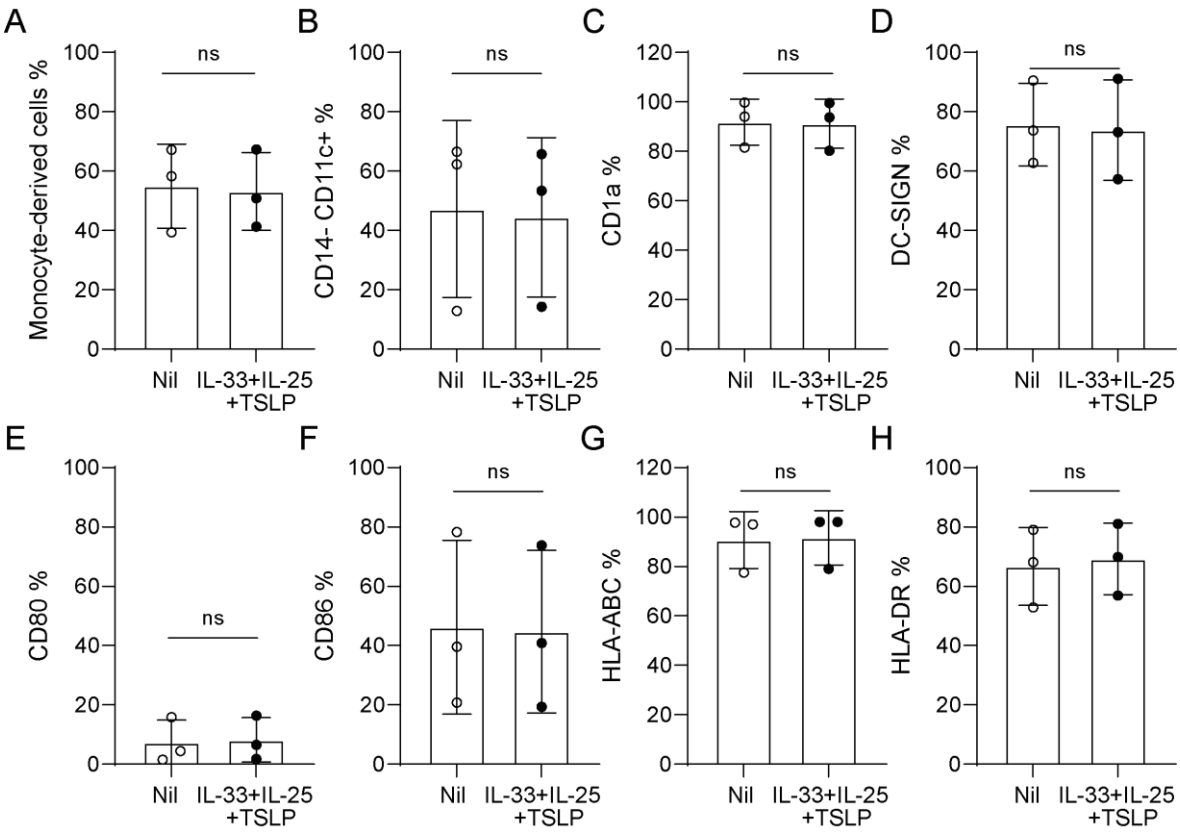


Figure A. 6 Effect of ILC2 stimulants on the phenotype on moDC.

(**A-H**) Medium containing IL-33, IL-25 and TSLP (50 ng/ml each) was incubated for 72h in parallel with ILC2. *In vitro* differentiated moDC were cultured for 48h in medium alone (Nil) or medium containing IL-33, IL-25, TSLP and analysed by flow cytometry. (**A**) Percentage of viable moDC. **(B)** Percentage of $CD14^{-}CD11c^{+}$ cell population. (**C-F**) Surface expression of CD1a (**C**), DC-SIGN (**D**), CD80 (**E**), CD86 (**F**), MHCI (HLA-ABC) (**G**) and MHCII (HLA-DR) (**H**), as percentage of live monocyte-derived cells. (n=3; data representative of ≥ 3 independent experiments). ns with paired Student's *t*-test.

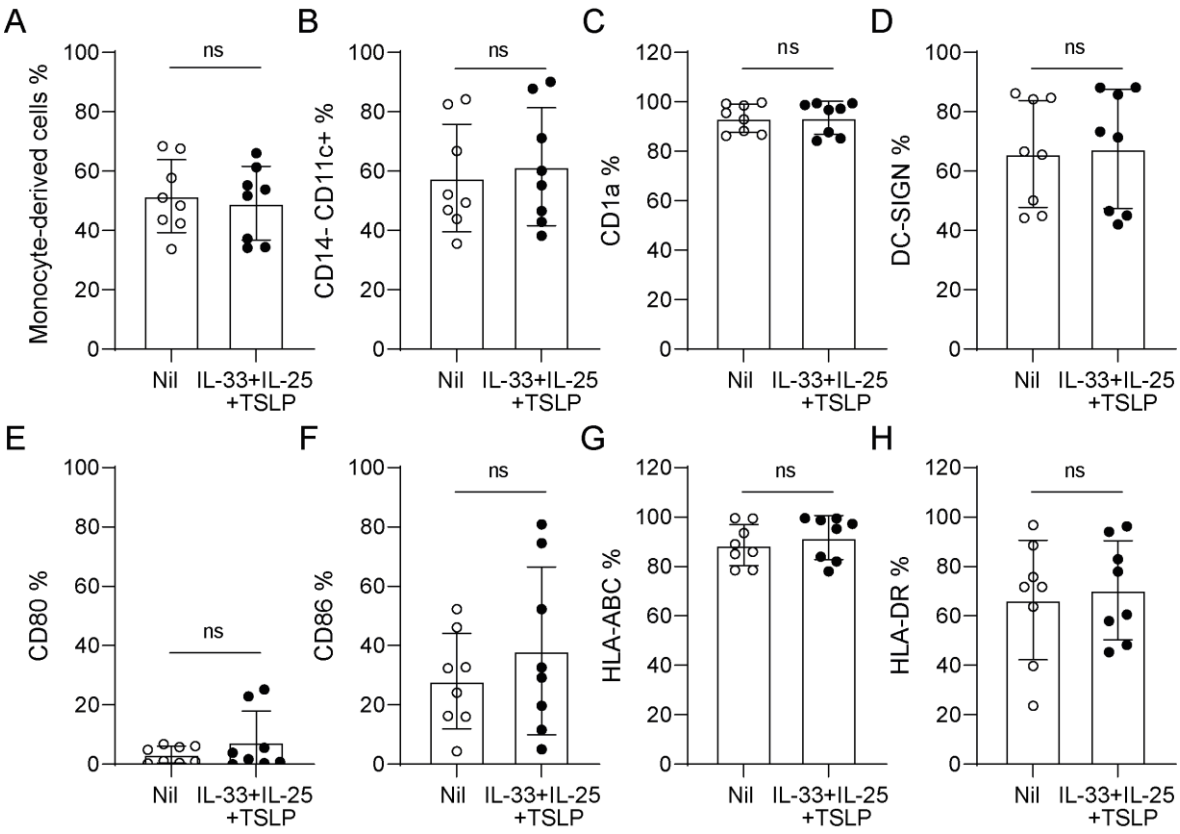


Figure A. 7 Effect of ILC2 stimulants on the differentiation process of moDC.

(**A-H**) Medium containing IL-33, IL-25 and TSLP (50 ng/ml each) was incubated for 72h in parallel with ILC2. MoDC differentiation was induced by culturing monocytes in IL-4 (10 ng/ml) and GM-CSF (100 ng/ml) for 3 days. On d3, differentiating moDC were washed and cultured for 48h in medium alone (Nil) or medium containing IL-33, IL-25 and TSLP, before being analysed by flow cytometry. (**A**) Percentage of viable monocyte-derived cells. **(B)** Percentage of $CD14^{-}CD11c^{+}$ cell population. (**C-F**) Surface expression of CD1a (**C**), DC-SIGN (**D**), CD80 (**E**), CD86 (**F**), MHCI (HLA-ABC) (**G**) and MHCII (HLA-DR) (**H**), as percentage of live monocyte-derived cells. (n=8; data representative of ≥ 3 independent experiments). ns with paired Student's *t*-test.

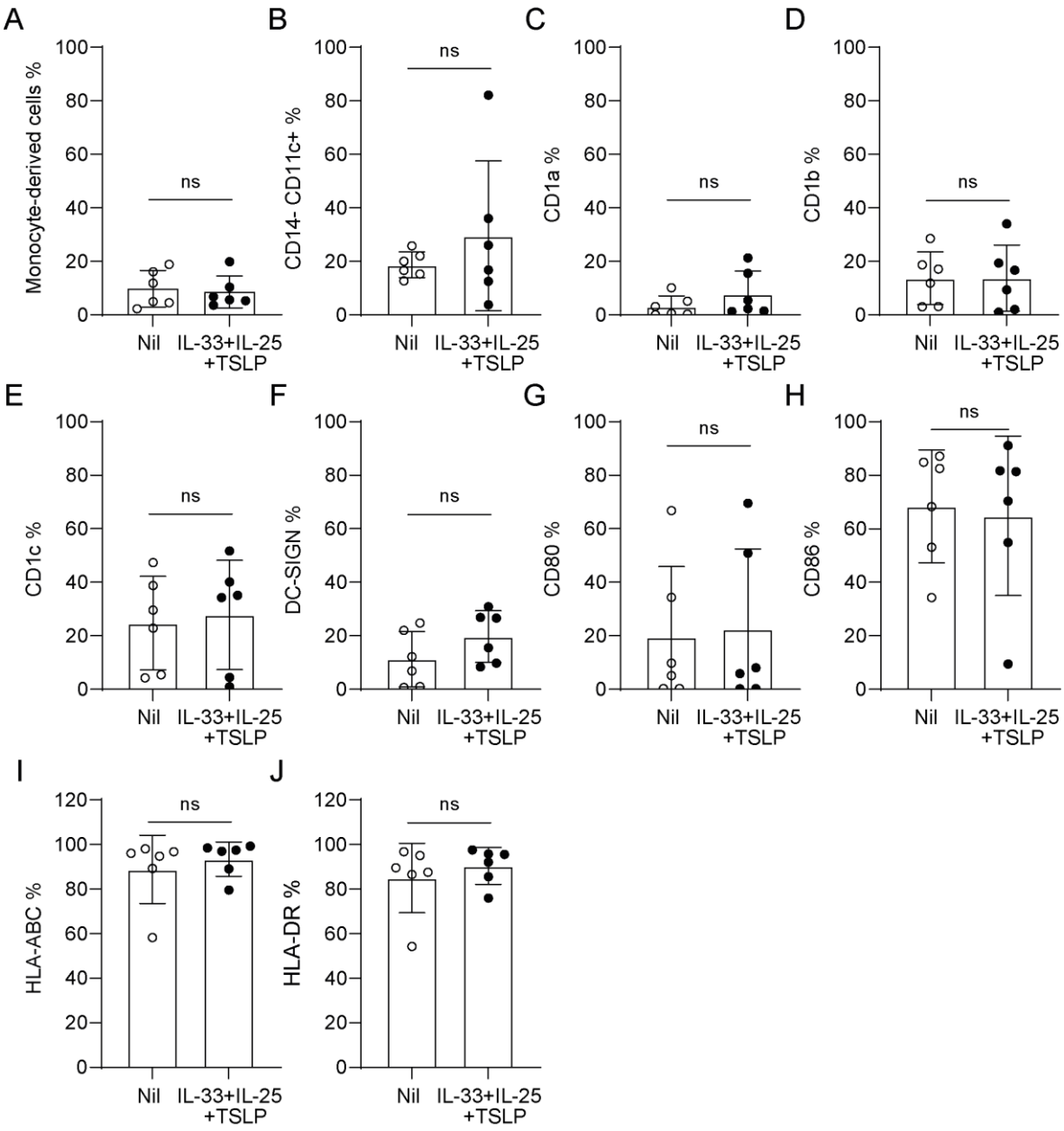


Figure A. 8 Effect of ILC2 stimulants on monocytes.

(**A-J**) Medium containing IL-33, IL-25 and TSLP (50 ng/ml each) was incubated for 72h in parallel with ILC2. Monocytes were incubated for 5 days in medium alone (Nil) or medium containing IL-33, IL-25 and TSLP, before being analysed by flow cytometry. (**A**) Percentage of viable monocyte-derived cells. **(B)** Percentage of $CD14^{-}CD11c^{+}$ cell population. (**C-J**) Surface expression of CD1a (**C**), CD1b (**D**), CD1c (**E**), DC-SIGN (**F**), CD80 (**G**), CD86 (**H**), MHCI (HLA-ABC) (**I**) and MHCII (HLA-DR) (**J**), as percentage of live monocyte-derived cells. (n=6; data representative of ≥ 3 independent experiments). ns with paired Student's *t*-test.

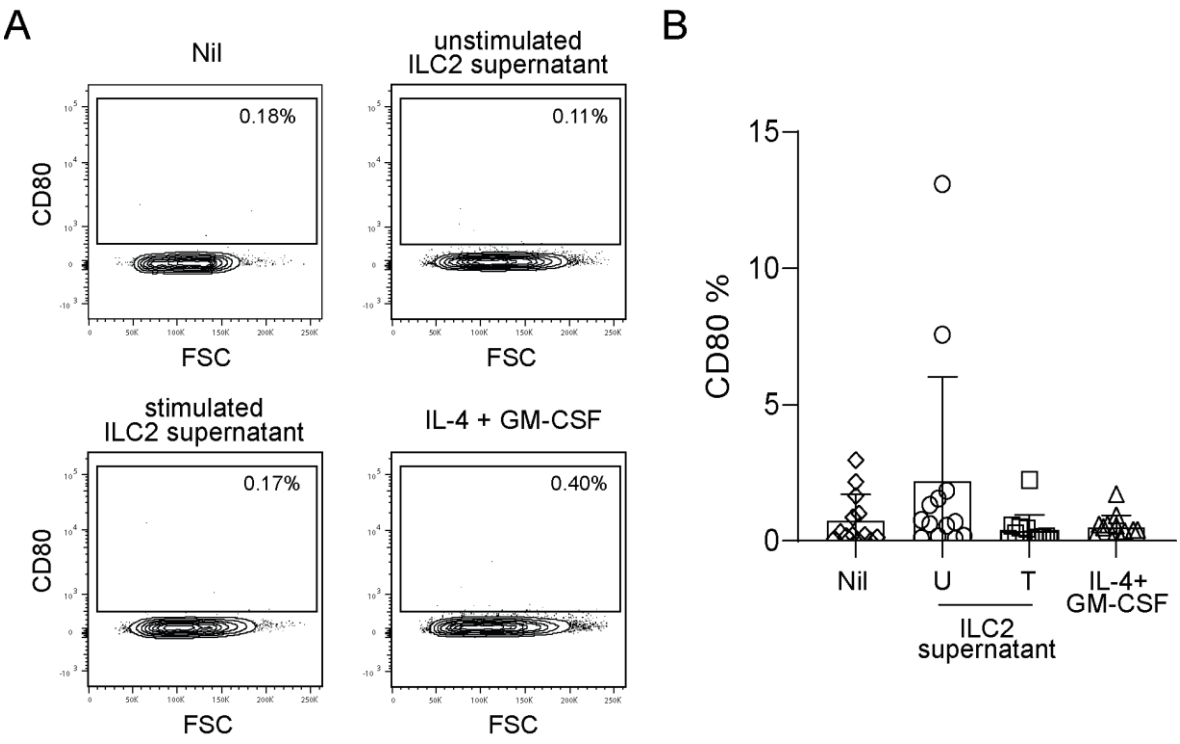


Figure A. 9 CD80 expression on ILC2-induced moDC.

(**A-B**) CD80 surface expression on monocyte-derived cells was analysed by flow cytometry following 5 day culture in medium alone (Nil), supernatants from unstimulated (U) and stimulated (T) ILC2 or recombinant IL-4 (10 ng/ml) plus GM-CSF (100 ng/ml). (**A**) Flow cytometry plots of CD80 expression. (**B**) Summary of CD80 expression, as percentage of live monocyte-derived cells. (n=13; data representative of ≥ 3 independent experiments). ns with RM one-way ANOVA with Turkey's post hoc multiple comparisons test (mean ± SD).

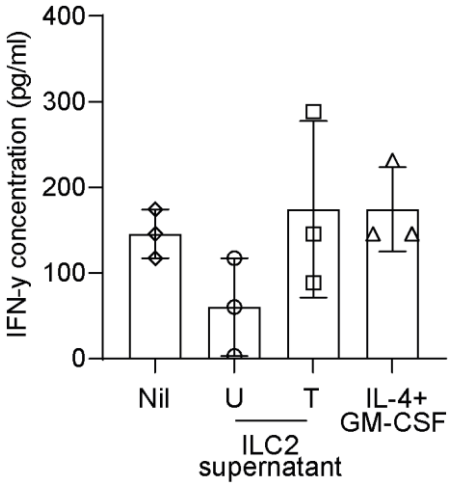


Figure A. 10 IFN-γ levels in ILC2-induced moDC.

Following 5 day culture of monocytes in medium alone (Nil), supernatants from unstimulated (U) and stimulated (T) ILC2 or recombinant IL-4 (10 ng/ml) plus GM-CSF (100 ng/ml), IFN-γ levels in culture supernatants was measured by ELISA. ns with RM one-way ANOVA with Turkey's post hoc multiple comparisons test (mean ± SD).